AD NUMBER
AD880949
LIMITATION CHANGES
TO: **Approved for public release; distribution is unlimited.**
FROM: **Distribution authorized to U.S. Gov't. agencies and their contractors; Critical Technology; DEC 1978. Other requests shall be referred to Army Air Mobility Research and Development Laboratory, Fort Eustis, VA 23604. This document contains export-controlled technical data.**
AUTHORITY
usaamrdl ltr, 30 jul 1971

20

AD

AD880949

USAAVLABS TECHNICAL REPORT 70-64

THE LAMINAR BOUNDARY LAYER ON A ROTATING BLADE OF SYMMETRICAL AIRFOIL SHAPE

By

J. C. Williams, III
Warren H. Young, Jr.

December 1970

EUSTIS DIRECTORATE
U. S. ARMY AIR MOBILITY RESEARCH AND DEVELOPMENT LABORATORY
FORT EUSTIS, VIRGINIA

CONTRACT DAAJ02-69-C-0086
NORTH CAROLINA STATE UNIVERSITY AT RALEIGH
RALEIGH, NORTH CAROLINA

156

Disclaimers

The findings in this report are not to be construed as an official Department of the Army position unless so designated by other authorized documents.

When Government drawings, specifications, or other data are used for any purpose other than in connection with a definitely related Government procurement operation, the United States Government thereby incurs no responsibility nor any obligation whatsoever; and the fact that the Government may have formulated, furnished, or in any way supplied the said drawings, specifications, or other data is not to be regarded by implication or otherwise as in any manner licensing the holder or any other person or corporation, or conveying any rights or permission, to manufacture, use, or sell any patented invention that may in any way be related thereto.

Disposition Instructions

Destroy this report when no longer needed. Do not return it to the originator.

DEPARTMENT OF THE ARMY
EUSTIS DIRECTORATE
U. S. ARMY AIR MOBILITY RESEARCH AND DEVELOPMENT LABORATORY
FORT EUSTIS, VIRGINIA 23604

This report has been reviewed by the Eustis Directorate, U. S. Army Air Mobility Research and Development Laboratory and is considered to be technically sound. The report is published to disseminate information which will provide a stimulant for technical exchange and the advancement of rotary-wing technology.

Task 1F162204A13903
Contract DAAJ02-69-C-0086
USAAVLABS Technical Report 70-64
December 1970

THE LAMINAR BOUNDARY LAYER ON A ROTATING BLADE OF SYMMETRICAL AIRFOIL SHAPE

Final Report

By

J. C. Williams, III
and
Warren H. Young, Jr.

Prepared by

North Carolina State University at Raleigh
Raleigh, North Carolina

for

Eustis Directorate
U. S. Army Air Mobility Research and Development Laboratory
Fort Eustis, Virginia

ABSTRACT

A theoretical study has been conducted to determine the effects of rotation, inflow, and forward flight on the development of the laminar boundary layer on a helicopter blade. Particular emphasis was placed on the determination of the separation line. In order to facilitate the computation of the inviscid flow about the blade, an 11.9%-thick symmetrical Joukowski airfoil was used. The essential feature of the analysis was the scaling of the chordwise coordinate so that the separation line is invariant with span and time in the transformed coordinate system. The transformed boundary layer equations were expanded in an asymptotic series in span, and the resulting equations were solved by the method of Smith and Clutter.

The major effect of rotation is a delay in separation. The separation line delay is most pronounced near the axis of rotation. Forward flight causes an oscillation about this separation line, so that the delay is greatest in the first and fourth quadrants. The oscillations are affected by the blade angle of attack and the inflow due to lift. The phase advance between the wall shear and the free-stream velocity is in qualitative agreement with the results of Lighthill.

Rotation alone does not influence the separation line greatly. However, its combination with forward flight and inflow contribute, at least in part, to the increase in maximum lift observed on helicopter blades.

TABLE OF CONTENTS

LIST OF ILLUSTRATIONS

Figure		Page

LIST OF TABLES

LIST OF SYMBOLS

In the following list, all quantities for which dimensions are not given have been nondimensionalized by the angular velocity Ω (units of time^{-1}) and/or the chord c (units of length).

A_R	the aspect ratio of the blade
a_0	the slope of the lift curve
B	a function of σ that defines $dx/d\sigma$, given by Equation (6)
C_t	the coefficient of thrust
c	the chord of the airfoil; units of length
f, g, $\bar{w}$	stream functions for u, v, and w
F_{nj}, G_{nj}	terms in the series for f and g
$\vec{i}$, $\vec{j}$, $\vec{k}$	unit vectors in the X, Y, Z coordinate system
K_n, K_{nj}	terms in the series for q
Q	the velocity vector in the X, Y, and Z coordinate system; units of length/time
M_t	Mach number at the tip of the blade in an azimuthal angle of 90 degrees
N_b	the number of blades in the rotor disk
q	a factor in the transformation of x into ξ
R	radius of the rotor disk
S_g	denotes the upper surface of the blade by +1, the lower surface by -1
S_H	the speed of forward flight; units of length/time
s_H	the speed of forward flight
s_s	the resultant of induced and forward flight speeds

T	the thrust generated by the entire rotor disk; units of force
T_j	a function of time and forward flight speed
t	time; units of time
$\bar{t}$	time
U, V, W	velocities in the X, Y, Z system; units of length/time
$\bar{U}, \bar{V}, \bar{W}$	velocities in the X, Y, Z coordinate system
U_0	the value of U far from the blade; defined in Equation (3); units of length/time
$\bar{U}_0$	the value of $\bar{U}$ far from the blade
u, v, w	velocities in the x, y, z coordinate system
u_δ, v_δ	velocities at the edge of the boundary layer
$\hat{u}_a, \hat{u}_c, \hat{u}_e$	the derivatives, with respect to x, of ϕa, ϕc, and ϕe
V_a	the constant part of the inflow, units of length/time
v_a	the constant part of the inflow
V_i	the inflow induced by the combined action of all the blades; units of length/time
v_i	the inflow induced by all the blades
$\bar{X}, \bar{Y}, \bar{Z}$	the Cartesian coordinate system that rotates with the blade
X_{NS}	a value of X_σ chosen to be near the separation point
X_R, Z_R	the Cartesian coordinate system that is fixed on the blade
X_σ, Z_σ	the coordinates of the surface of the blade in the X_R, Z_R coordinate system

x_0	the distance of the axis of rotation from the leading edge, measured along the chord line
x	the distance from the leading edge of the blade, measured in the chordwise direction along the surface of the blade
y	the distance from the axis of rotation, measured along the span of the blade
z	the distance from the surface of the blade, measured along a normal to the surface
α	the angle between the normal to the surface of the blade and a normal to the chord line of the blade
α_a	the aerodynamic angle of attack of the blade
α_b	the geometric blade angle of attack; the angle between a normal to the chord line and the axis of rotation
β	the skew angle of the flow on the blade surface
γ	phase angle between the maximums of shear stress and chordwise velocity
δ_x, δ_y	the displacement thickness multiplied by $\sqrt{\Omega / \nu}$
θ_x, θ_y	the momentum thickness multiplied by $\sqrt{\Omega / \nu}$
Δ_h	the spacing between ξ_h and ξ_{h-1}
ϵ	a parameter determing the maximum thickness of the Joukowski
ν	the kinematic viscosity; units of length^2/time
ρ	the density of the fluid; units of mass/length^3
ξ, ζ, η	the transform of the x, y, z coordinates
σ	a parametric variable for x in the potential flow
σ_r	the solidity of the rotor disk
ϕ	the potential function for a unit velocity; units of length

ϕ	the potential function for a unit velocity
ϕ_a, ϕ_c, ϕ_e	potential functions that depend on ω_i and α_b, defined by Equation (5)
ϕ_σ	the potential for a unit velocity parallel to the chord
ϕ_ρ	the potential for a unit velocity normal to the chord
ψ	time; the azimuthal angle measured as shown in Figure 1
Ω	the rotational velocity; units of time^{-1}
Ω_i	the constant of proportionality for nonuniform inflow; units of time^{-1}
ω_i	the constant of proportionality for nonuniform inflow

The following variables are defined for the hover case only:

C^c	$2 \cos (\alpha / \alpha_b) / \tilde{u}_a$
C^s	$\omega_i(x - x_I) \sin (\alpha - \alpha_b) / \tilde{u}_a$
H	$(x - x_I)\ \tilde{u}_a$
M	$(x - x_I)(d\tilde{u}_a / dx) / \tilde{u}_a$
P	$(x - x_I) / \tilde{u}_a$
C_n^c, C_n^s, h_n, m_n, P_n	terms in the series expansion for C_n^c, C_n^s, H, M, and P

The following variables are defined for the forward flight case only:

c_n	a term in the series expansion for $2 \cos (\alpha - \alpha_b)$
m_n, m_{nj}	functions defined in Equations (51) through (54)
P_0	ξ / μ_0^δ

$\tilde{v}$	the part of v_δ that does not depend on time
χ_n	a term in the series for x_I
μ_n^a, μ_n^c, μ_n^δ	terms in the series for $\tilde{u}_a$, $\tilde{u}_c$, and u_δ
$\tilde{\nu}_n$	a term in the series for $\tilde{v}$

The following symbols are used as subscripts:

c	K_n is not a coefficient of the subscripted function
I	at the stagnation point
i	induced; concerned with the induced downflow
k	K_n is a coefficient of the subscripted function
j	the subscripted function is to be multiplied by T_j where $j = 0, 1, 2 \ldots$
n	a coefficient of ζ^{-n} where $n = 0, 1, 2 \ldots$
r	neither v_a nor T_j is a coefficient of the subscripted function
s	at the separation point
δ	at the edge of the boundary layer

The following symbols are used as superscripts:

'	the derivative with respect to η
*	the asymptotic value for large values of span
-	nondimensionalized with respect to Ω and/or c

In the forward flight case, terms in the series expansion for ζ are denoted by the first numeral subscript. For example, p_{21}, m_1, and G_{nj} are coefficients of ζ^{-2}, ζ^{-1}, and ζ^{-n}, respectively. The second numeral subscript (often denoted in general by j) indicates that the function is a coefficient of T_j, where $T_0 = 1$, $T_1 = s_H \sin\psi$, $T_2 = s_H \cos\psi$.

The double numerical subscript (often denoted by nj), or a single 0 subscript, also indicates that the function is independent of v_a, s_H, ζ, and ψ; the single exception is G_0, which has the components

$$G_0 = G_{00} + T_1 G_{01}$$

BLANK PAGE

INTRODUCTION

The separation of the boundary layer near the leading edge of an airfoil in two-dimensional flow produces well defined and easily interpretable symptoms. As the aerodynamic angle of attack increases beyond a certain point, the lift of the airfoil does not increase, the drag increases more rapidly, and the pitching moment becomes large and negative. These three symptoms characterize the two-dimensional stall of an airfoil. Experimental measurements have shown that helicopter rotors do not experience this type of stall.[1] The lift does not decrease at the expected angle of attack,[2] but the drag and pitching moment are more nearly predicted by the two-dimensional situation.[3,4]

The helicopter rotor in forward flight (translation perpendicular to the axis of rotation) has a constantly changing angle of yaw. Spanwise flow is also generated by centrifugal and Coriolis forces. Both the angle of attack and the chordwise velocity vary periodically as the blade rotates. Additional time dependence is introduced by feathering, flapping, and lead-lag motions of the blade. Each of these effects may contribute to the peculiarities of stall on helicopter blades, but no single effect has been identified as the cause. Examinations of the lift, drag, and pitching moment in three-dimensional (yawed) steady-state flow[3] and in unsteady two-dimensional flows[4] have shown trends that suggest that yaw and time variation of the flow are important. Such investigations have outlined the effects of unsteady and three-dimensional behavior on helicopter rotors, but the cause of stall is to be found in the boundary layer. This suggests the approach of the present work: an analysis of the boundary layer on a blade that is simultaneously undergoing rotation, inflow due to lift, and forward flight. It is not yet feasible to include, in one analysis, every factor that influences the boundary layer. The present work is valuable in evaluating some of the factors that influence the boundary layer, and since separation is the most important feature of the boundary layer, the primary interest of this work will be the determination of the position of the separation line. Most experimental work has been concerned with such aerodynamic characteristics as the lift, drag, and pitching moment. There is a need for experimental measurements in the boundary layer. Except for some measurements of surface streamlines,[5,6] the investigation of the boundary layer has been analytical.

The consideration of rotational effects on blades began after the discovery by Sears[7] of a simple but powerful potential flow transformation for the flow about rotating blades. The application of this transformation to the rotating cylindrical nonlifting blade reduced the potential flow problem to an easily solved two-dimensional problem. By utilizing this potential flow solution, several solutions to the boundary layer problem on rotating blades have been found for the special case where the span is large compared to the chord. The solutions of Rott and Smith[8] for wedge-type flows, and of McCroskey and Yaggy[9] for the linearly decelerating flow, are of this type. The assumption of a large span-to-chord ratio simplifies the boundary layer equations by uncoupling the equations which govern the chordwise and spanwise flows. The chordwise equation then becomes the equation for two-dimensional flow and may be solved by standard techniques. Once the chordwise flow is known, it is a straightforward procedure to determine the spanwise boundary layer flow. These solutions give no information on the effect of the spanwise flow on the chordwise flow, and they are not valid as separation is approached.

S. W. Liu[10] removed the restriction of large span-to-chord ratio by expanding the velocities in a series in the spanwise coordinate and then using a Blasius series technique to investigate the boundary layer on a cubic cylinder for several positions of the axis of rotation. Although this solution presents many interesting features of the boundary layers on rotating blades, expecially at small spans, it is limited in that the equations solved have been simplified by the assumption of thin blade sections. The solutions are not valid, therefore, in the vicinity of the stagnation point. Furthermore, it does not seem reasonable that the procedure used by Liu could be extended for use on a realistic airfoil (blade) section, since it is well known that the Blasius series technique requires a large number of terms to represent the boundary layer on practical airfoil sections. McCroskey and Yaggy applied Liu's method to a flat blade in forward flight. Forward flight solutions for linearly decelerating flows at large span-to-chord ratios were also obtained. This work gives considerable insight into the simultaneous action of forward flight and rotation, as well as establishes the method for including forward flight in the analysis.

A solution for a symmetric Joukowski airfoil with forward flight and rotation was found by Young and Williams.[11] By utilizing a series in the spanwise coordinate similar to that of Liu, a solution that was valid for small values of span, and from the stagnation point to near separation, was found. The variation of the separation point with time and span was found for several positions of the axis of rotation, but only the zero angle of attack (no lift) case was considered. Centrifugal and Coriolis effects were found to be most important in the strong adverse pressure gradients near separation. Forward flight caused the separation line to oscillate about the hover (no forward flight) separation line. Separation was delayed most on the downstream side of the rotor disk because of the predominance of the time derivatives of the nonsteady flow. The effects of forward flight, in general, were greater than the rotational effects. By examining the order of magnitude of the terms in the boundary layer equations, Dwyer and McCroskey[6] confirmed this conclusion. From series solutions on a rotating flat plate in forward flight, from finite difference solutions on airfoils in hover, and from unsteady two-dimensional solutions, it was concluded that the unsteady effects and rotational effects are larger at smaller blade angles of attack. It was also suggested that the chordwise dimension should be nondimensionalized by the span.

Beyond the preceding investigations, little if anything has been done to answer pressing questions regarding the effects of blade shape, blade lift (angle of attack), forward flight velocity, and rotation on the boundary layer development and separation on a blade of practical airfoil shape. The present investigation considers these factors analytically. The boundary layer equations are expanded in an asymptotic series in span, and then in a finite series in time by utilizing the principle of superposition. The chordwise and spanwise stream functions are governed by a series of two-dimensional differential equations. These equations are solved numerically. The velocities at any point, and for any time, in the unseparated boundary layer are now calculable. The equation for the separation line may also be found. The effects of the inflow due to the lift of the rotor disk, the angle of attack of the blade, and the speed of forward flight are assessed.

THEORY

ASSUMPTIONS

The axis of rotation is taken to be the Z axis in the rotating coordinate system shown in Figures 1 and 2. The blade rotates about the Z axis with constant rotational speed Ω so that there is no lead-lag motion. The blade is assumed to be straight and rigid and to have no twist or taper. This restricts the blade from any flapping motion. It is further assumed that the blade remains normal to the axis of rotation (without coning), so that the Y axis remains fixed in the blade. Both the X and Y axes rotate with the blade so as to define a plane of rotation which is normal to the axis of rotation. Translation due to forward flight results in a velocity S_H which lies in this plane of rotation. The azimuthal angle ψ is the angle between the vector S_H and the Y axis. The blade under consideration is only one of several blades that make up the rotor disk. The entire disk will induce an inflow V_i. This inflow velocity is assumed to be parallel to the axis of rotation and may be a function of the span, but not of the azimuthal angle. The inflow may be proportional to span, or it may be constant over the rotor disk. That is, it has the functional form

$$V_i = - V_a - \Omega_i Y$$

Both V_a and Ω_i are constants; for a lifting rotor they will be greater than or equal to zero. If Ω_i is not zero, the potential flow is no longer irrotational.

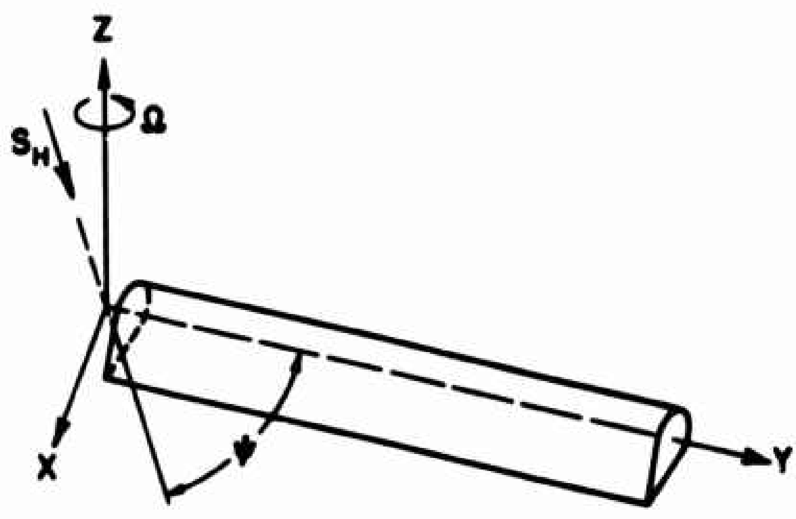

Figure 1. Rotating Coordinates.

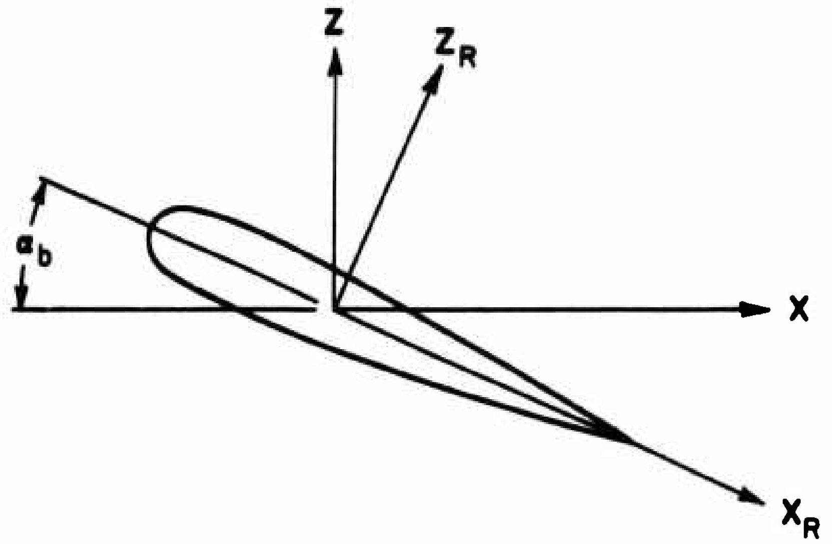

Figure 2. Blade Coordinates.

No attempt will be made to account for end effects or tip vortices. This is equivalent to assuming that the blade is infinitely long. The blade length R cannot be neglected entirely, however, since it must be used when finding a relation between the thrust of the rotor disk, the inflow, and the angle of attack of the blade (see APPENDIX I). The boundary layer solution must not be applied to the region of the blade near the tip. The reverse flow region must also be excluded from consideration. This is the region on the retreating blade where the flow is from the trailing edge to the leading edge. It is a circular region in the plane of rotation represented mathematically by

$$\Omega Y + S_H \sin \psi < 0$$

A cross section of the blade is shown in Figure 2. The geometric angle of attack α_b is the angle between the chord line of the blade and the X axis. It is assumed that this geometric angle of attack does not vary along the span (the Y direction), nor does it vary with azimuthal angle. This precludes any consideration of feathering of the blade. When there is no inflow, only the forward flight velocity and the velocity due to rotation are present. Both of these velocities lie in the plane of rotation, and thus the geometric angle of attack coincides with the aerodynamic angle of attack. If inflow is present, as it must be if lift is generated, the aerodynamic angle of attack will be the angle between the chord line and the resultant of the inflow, forward flight, and rotational velocities. The component of forward flight in the chordwise direction is $S_H \cos \psi$. This results in an aerodynamic angle of attack which varies with azimuthal angle. The velocity due to rotation, given by ΩY, gives rise to a spanwise variation.

In order to define a tractable problem, the variation of the aerodynamic angle of attack due to blade twist, flapping, feathering, nonuniform inflow, and lead-lag motion has been neglected. The neglect of the spanwise variation can be assessed, and justified, from the results. The change with azimuthal angle presents more difficulty. The change of angle of attack with time is a difficult problem even in two-dimensional flow. The present method of solution can account for the time dependence introduced by forward flight very well, but this effect is usually small compared to the effects of flapping or feathering. The failure to account fully for the change of the aerodynamic angle of attack with azimuthal angle is probably the most restrictive assumption in the present analysis. The forward tilt of the rotor disk in forward flight can be easily included in the present mathematical formulation, but the results obtained would not be realistic. The effects of tilt are partially cancelled out by blade twist and by feathering or flapping. Since it is not practicable to include the cancelling effects, tilt was omitted, hence the assumption that the forward flight velocity lies in the plane of rotation.

Assumptions have been made that would not be justified if the performance of the helicopter were to be calculated. The tip vortices have a definite effect on helicopter performance, but since this is not a boundary layer effect, their neglect is justified. The flow outside the boundary layer is assumed to be incompressible and inviscid, and the circulation in this potential flow is calculated by the Kutta condition. The Kutta condition is chosen for convenience. If a more accurate determination of the circulation were desired, the present method of solution for the boundary would still be valid.

With regard to the Kutta-Joukowski trailing edge condition, one should recognize that this condition is only an approximate condition which accounts for the viscous origin of the airfoil circulation. When separation occurs on the airfoil, this approximation is poor. Unfortunately, there has not been established, as yet, an appropriate condition to replace the Kutta-Joukowski condition when the separation is extensive or when the separation line is time dependent.

The assumptions that have been made lead to equations that are solvable, and the results will contain several effects that have not been considered in the previous solutions for the boundary layer on rotating blades. It has not been possible to include all the factors that influence the development of the boundary layer, but the importance of some of the omitted factors can be better assessed from the results.

POTENTIAL FLOW SOLUTION

Before solving the boundary layer equations, it is necessary to furnish the boundary conditions at the edge of the boundary layer from a potential flow solution. This solution has been chosen to present the features of the potential flow that significantly influence the boundary layer. The circulation will be calculated from the Kutta condition, but the thickness of the boundary layer will not be taken into account. As in the boundary layer, the flow is assumed incompressible. For ease of calculations, results will be found for a symmetrical Joukowski airfoil. Interest in this investigation is focused on the boundary layer itself, although the method of solution could be applied to a more precise determination of the potential flow.

The inviscid flow over a rotating cylindrical blade was found by Sears and Fogarty[12] for a constant inflow. In the rotating coordinate system, the velocity vector Q must obey

$$\nabla \cdot Q = 0 \qquad \nabla X Q = -2\Omega\vec{k} - \Omega_i\vec{i}$$

The first of these equations is an expression of conservation of mass (continuity equation) in the fluid flow; the second defines the rotation of the external flow. It is possible to write Q in terms of a potential function Φ and a two-dimensional stream function Ψ,

$$\vec{Q} = \vec{\nabla}\Phi + \vec{\nabla} X \Psi \vec{k} \tag{1}$$

The equation for the rotation of the flow is then satisfied if Ψ is chosen as

$$\Psi = \Omega(X^2 + Y^2)/2 - \Omega_i XZ \tag{2}$$

To include the effects of forward flight, Φ is written as

$$\Phi = U_0 \Phi_1 + V_i \Phi_2 + Y(-\Omega X + S_H \cos \Omega t) \tag{3}$$

where $U_0 = \Omega Y + S_H \sin \Omega t$.

The boundary conditions on Φ_1 and Φ_2 are

at $X^2 + Z^2 = \infty$ $\quad \Phi_1 = X, \quad \Phi_2 = Z$

on the surface of the airfoil:

$$\frac{\partial\phi_1}{\partial X} \tan\,(\alpha - \alpha_b) = \frac{\partial\phi_1}{\partial Z}$$

$$\frac{\partial\phi_2}{\partial X} \tan\,(\alpha - \alpha_b) = \frac{\partial\phi_2}{\partial Z}$$

where $(\alpha - \alpha_b)$ is the angle between the Z axis and the normal to the surface of the blade.

The equation of continuity is satisfied if ϕ_1 and ϕ_2 are two dimensional (in X and Z), and if they satisfy

$$\frac{\partial^2\phi_1}{\partial X^2} + \frac{\partial^2\phi_1}{\partial X^2} = 0$$

$$\frac{\partial^2\phi_2}{\partial X^2} + \frac{\partial^2\phi_2}{\partial Z^2} = 0$$

Thus, ϕ_1 and ϕ_2 are the two-dimensional potentials for flow around the rotor blade section in a unit stream. If the rotor blade generates lift, there will be a circulation included in the potential.

Nondimensionalizing the lengths by the chord of the airfoil c and the velocities by Ωc, the velocities become

$$\bar{U} = \bar{U}_0 \frac{\partial\phi_1}{\partial\bar{X}} + V_i \frac{\partial\phi_2}{\partial\bar{X}}$$

$$\bar{V} = \phi_1 - 2\bar{X} + s_H \cos\bar{t} + \omega_i(\bar{Z} - \phi_2)$$

$$\bar{W} = \bar{U}_0 \frac{\partial\phi_1}{\partial\bar{Z}} + V_i \frac{\partial\phi_2}{\partial\bar{Z}}$$

In order to find the velocities at the edge of the boundary layer, the velocities must be written in a coordinate system fixed on the body. The distance along the surface of the blade x is measured from the leading edge. The z dimension is measured normal to the surface. The spanwise dimension y is measured in the spanwise direction from the axis of rotation.

It is also convenient to define a Cartesian coordinate system that is fixed with respect to the blade, as shown in Figure 2. The X_R axis will lie along the chord line of the blade. The angle between the X axis and the X_R axis will be the blade angle of attack α_b. The Z_R axis is perpendicular to X_R, and is at angle α_b to the Z axis (the axis of rotation). The origin of the X_R, Z_R coordinate system is the point where the Z axis intersects the chord line of the blade. This intersection is at a distance X_0 from the leading edge of the blade.

Finally, it is convenient to define two new potential functions in the new X_R, Z_R coordinate system. In this system, ϕ_σ is the two-dimensional potential, on the surface, for a unit stream in the chordwise direction, and ϕ_ρ is the two-dimensional potential, evaluated on the surface, for a unit stream normal to the chord. There is no circulation in ϕ_σ, but matching the Kutta condition requires a circulation in ϕ_ρ. The velocities at the edge of the boundary layer, u_δ and v_δ, are now given by

$$u_\delta = y\tilde{u}_a + v_a \tilde{u}_c + T_2 \tilde{u}_e \tag{4}$$

$$v_\delta = \phi_a + T_1 - X_R(2 \cos \alpha_b + \omega_i \sin \alpha_b) + Z_R(-2 \sin \alpha_b + \omega_i \cos \alpha_b) \tag{5}$$

where $T_0 = 1, \quad T_1 = S_H \cos \bar{t}, \quad T_2 = S_H \sin \bar{t}$

$$v_i = - v_a - \omega_i y$$

$$\tilde{u}_a = \partial\phi_a/\partial x, \quad \tilde{u}_c = \partial\phi_c/\partial x, \quad \tilde{u}_e = \partial\phi_e/\partial x$$

$$\phi_a = (\cos \alpha_b + \omega_i \sin \alpha_b)\ \phi_\sigma + (\sin \alpha_b - \omega_i \cos \alpha_b)\ \phi_\rho$$

$$\phi_c = \phi_\sigma \sin \alpha_b - \phi_\rho \cos \alpha_b$$

$$\phi_e = \phi_\sigma \cos \alpha_b + \phi_\rho \sin \alpha_b$$

Once ϕ_σ and ϕ_ρ are found as functions of the body coordinate x, the velocities at the edge of the boundary layer can be evaluated. All velocities and lengths in the remainder of this section, and in the following sections, are nondimensional.

For ease of calculating ϕ_σ and ϕ_ρ, a symmetrical Joukowski airfoil will be used. The parameter ε is related to the thickness of the airfoil; the value $\varepsilon = 0.092$ gives an 11.9%-thick airfoil. This thickness was chosen so that the airfoil would closely resemble an NACA 0012 airfoil. The NACA 0012 is widely used for helicopters. It is less blunt near the leading edge and is flatter near the quarter chord than a Joukowski airfoil. To lessen these differences, the Joukowski airfoil was chosen to be thinner (11.9% thick as compared to the 12%-thick NACA 0012). In terms of the parameter σ, the potentials are

$$\phi_\sigma = (1 + \varepsilon)\ \sigma/2$$

$$\phi_\rho = (1 + \varepsilon)[S_g\sqrt{1 - \sigma^2} - \tan^{-1}\ (S_g\sqrt{1 - \sigma^2}/\sigma)]/2$$

where $S_g = +1$ denotes the upper surface of the airfoil

$S_g = -1$ denotes the lower surface of the airfoil

The parameter σ is given as a function of x by

$$\frac{dx}{d\sigma} = B(\sigma) \quad , \quad x = \int_{-1}^{\sigma} B\ d\sigma \tag{6}$$

where $B = \frac{dX_\sigma}{d\sigma} / \cos\alpha$

$$\tan\alpha = \frac{dZ_\sigma}{dX_\sigma}$$

$$X_\sigma = \frac{1 + \varepsilon}{4}(\sigma - \varepsilon)[1 + \frac{(1 - \varepsilon)^2}{1 + \varepsilon^2 - 2\varepsilon\sigma}] + \frac{1 + \varepsilon^2}{2} - X_0$$

$$Z_\sigma = \frac{1 + \varepsilon}{4} S_g \sqrt{1 - \sigma^2}\ [1 + \frac{(1 - \varepsilon)^2}{1 + \varepsilon^2 - 2\varepsilon\sigma}]$$

The angle α is the angle between the normal to the surface and the Z_R axis. X_σ and Z_σ are the coordinates of the airfoil surface in the X_R, Z_R coordinate system.

Considerable simplification can be obtained for certain special cases. A solution is available for the rotor blade at zero angle of attack and no induced flow ($\alpha_b = 0$, $v_i = 0$) in Young and Williams.[11] For this case, the velocities at the edge of the boundary layer are

$$u_\delta = (y + T_2)\ \Omega_\sigma \tag{7}$$

$$v_\delta = \phi_\sigma + T_1 - 2X_\sigma \tag{8}$$

This, in turn, is contained within the special case of forward flight with constant induced velocity ($\omega_i = 0$), for which

$$u_\delta = y\Omega_a + v_a\Omega_c + T_2\Omega_a \tag{9}$$

$$v_\delta = \phi_\sigma + T_1 - 2X_\sigma \cos \alpha_b - 2Z_\sigma \sin \alpha_b \tag{10}$$

$$\phi_a = \phi_\sigma \cos \alpha_b + \phi_\rho \sin \alpha_b$$

$$\phi_c = \phi_\sigma \sin \alpha_b - \phi_\rho \cos \alpha_b$$

In the case of hover ($s_H = 0$), it is more convenient to allow the induced velocity to be proportional to the span ($v_a = 0$). In this case,

$$u_\delta = y\Omega_a \tag{11}$$

$$v_\delta = \phi_a - X_\sigma\ (2 \cos \alpha_b + \omega_i \sin \alpha_b) + Z_\sigma(-2 \sin \alpha_b + \omega_i \cos \alpha_b) \tag{12}$$

In order to calculate X_σ, Z_σ, ϕ_σ and ϕ_ρ, it is necessary to specify the airfoil shape (in all examples herein, a Joukowski airfoil) and the airfoil thickness (always 11.9%). The only purpose of finding the potential flow is to furnish the boundary conditions on the velocities u_δ and v_δ. These depend on the choices made for the constants α_b, ω_i and ℓ_0; once these are specified, the boundary layer equations may be solved. The general theory in the next section is applicable to both the hover case and the forward flight case. In succeeding sections, advantage is taken of the simplifications in u_δ and v_δ that occur in the above two cases.

BOUNDARY LAYER EQUATIONS

By making the usual boundary layer assumptions, the Navier-Stokes equations can be reduced to the simplified equations for the boundary layer on a rotating blade:[9]

$$\frac{\partial u}{\partial x} + \frac{\partial v}{\partial y} + \frac{\partial w}{\partial z} = 0 \tag{13}$$

$$\frac{\partial u}{\partial \bar{t}} + u\frac{\partial u}{\partial x} + v\frac{\partial u}{\partial y} + w\frac{\partial u}{\partial z} - 2(v - v_\delta)\cos(\alpha - \alpha_b) - \nu\frac{\partial^2 u}{\partial z^2} / \Omega c^2$$

$$= \frac{\partial u_\delta}{\partial \bar{t}} + u_\delta\frac{\partial u_\delta}{x} + v_\delta\frac{\partial u_\delta}{y} \tag{14}$$

$$\frac{\partial v}{\partial \bar{t}} + u\frac{\partial v}{\partial x} + v\frac{\partial v}{\partial y} + w\frac{\partial v}{\partial z} + 2(u - u_\delta)\cos(\alpha - \alpha_b) - \nu\frac{\partial^2 v}{\partial z^2} / \Omega c^2$$

$$= \frac{\partial v_\delta}{\partial \bar{t}} + u_\delta\frac{\partial v_\delta}{\partial x} + v_\delta\frac{\partial v_\delta}{\partial y} \tag{15}$$

The boundary conditions for these equations are:

at $z = 0$ $\quad u = v = w = 0$

at $z = \infty$ $\quad u = u_\delta, \; v = v_\delta$

These equations differ from the usual unsteady, three-dimensional boundary layer equations in the terms that give the Coriolis acceleration. These terms, involving the product of velocity and $\cos(\alpha - \alpha_b)$, appear explicitly because the equations are written in a rotating coordinate system.

As the span increases, there is little change in the spanwise flow. The potential flow in the spanwise direction u_δ is independent of span. Time dependence is introduced into the equations by the forward flight speed, which is also independent of span. However, the chordwise velocity due to rotation is proportional to span. Thus, at large values of span, the chordwise flow is dominated entirely by the flow due to rotation, and both time dependence and the spanwise flow become negligible in the chordwise momentum equation. It is not that the spanwise flow and time dependence have become so small, but that the chordwise flow due to rotation has become so large when the span is large, that the effects of spanwise flow and time dependence are relatively small. The underlined terms in the equations may be neglected at large values of span. Typically, the effect of spanwise flow is negligible in the chordwise equation at values of span greater than three to ten chord lengths and at time dependence from five to fifteen chord lengths. Over a significant portion of a typical helicopter rotor, the boundary layer flow is governed by the asymptotic solution at large span. The chordwise flow in such an asymptotic solution is given by the steady, two-dimensional equations, and thus separation occurs at the same point as in two-dimensional, steady-state flow. Figure 3 shows the separation line approaching the two-dimensional value at large span.

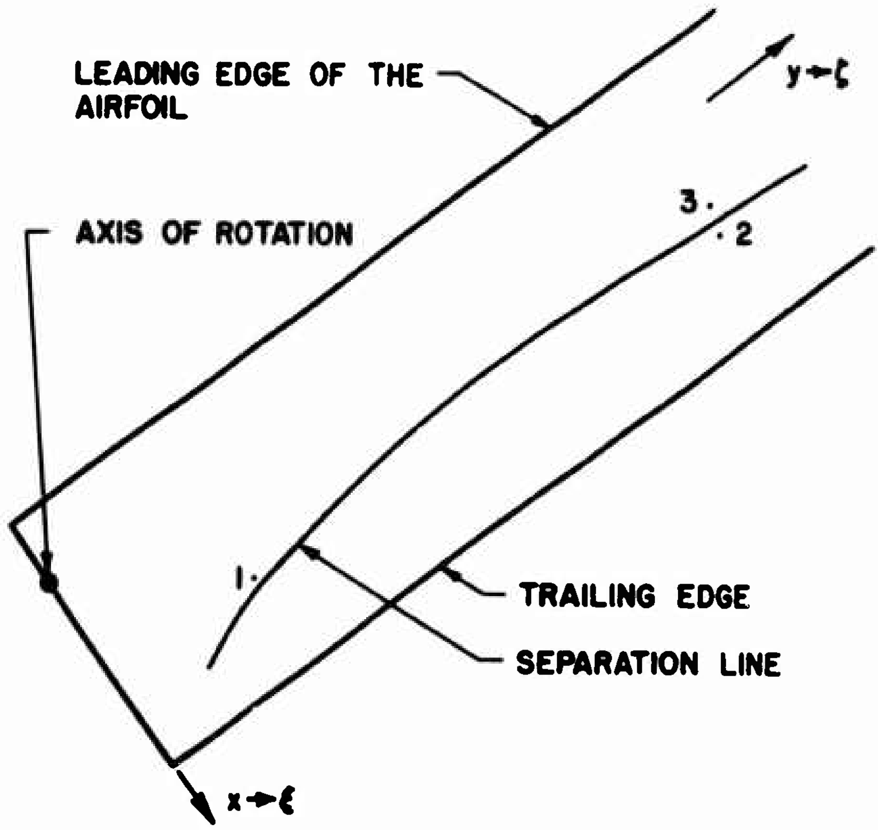

Figure 3. The Separation Line.

The solution at smaller values of span is found by expanding the stream functions in an asymptotic series in the span. This may be done most simply by allowing the first term in the series (or the first approximation to the solution) to be the two-dimensional solution at the same chordwise position. In Figure 3, if this technique is used, the first approximation to the velocity profile at point 1 is the profile at point 2. The profile at point 2 is in the separated region. The profile at point 2 is difficult to obtain, and once it is found, it will be a poor first approximation to the profile at point 1.

A superior technique for finding a first approximation to point 1 has been devised. The X coordinate may be transformed into the ξ coordinate. The ξ coordinate is stretched as span decreases so that point 1 has the same ξ coordinate as point 3. Point 3, like point 1, is in the unseparated region. The ξ coordinate, if chosen so that the separation line always occurs at the same value of ξ, say ξ_s, will give a much better solution near separation. If time dependence is introduced by forward flight, then the ξ coordinate will expand and contract with time as well as be dependent on the span. The transform from x to ξ is accompanied by a complete coordinate transform, which is given by

$$\xi = [x - x_I\ (y, \bar{t})]\ q\ (y, \bar{t}) \quad , \quad \zeta = y \tag{16}$$

$$\eta = cz\sqrt{\Omega u_\delta/\nu(x - x_I)} \quad , \quad \psi = \bar{t}$$

$$u = u_\delta\ f'(\xi,\zeta,\eta,\psi) \quad , \quad v = g'(\xi,\zeta,\eta,\psi) \tag{17}$$

$$w = \sqrt{\nu(x - x_I)/\Omega u_\delta}\ \bar{w}(\xi,\zeta,\eta,\psi)/c$$

In the transformed system, the boundary conditions become

at $\eta = 0$ $\quad f = f' = g = g' = \bar{w} = 0$

at $\eta = \infty$ $\quad f' = 1 \quad , \quad g' = v_\delta$

The primes denote differentiation with respect to η. The ξ, ζ, η coordinate system has the same orientation as the x, y, z system, but the dimensions are stretched. For example, the η direction is the same as the z direction; it is normal to the body. The η coordinate, however, is stretched by the familiar Falkner-Skan factor $\sqrt{u_\delta/\nu x}$. This factor accounts for the dependence of the boundary layer height on u_δ, ν, and x. The stretching of the ξ coordinate to account for the position of the separation line is accomplished by including the factor q. If q is chosen correctly, the separation line will have the constant location ξ_s for all values of ζ and ψ. Since the separation line is not yet known, q cannot be found immediately. Instead, q will be written in the form of a series in $1/\zeta$, with the coefficients in the series still undetermined. After solving a series of differential equations, these coefficients will be determined from the condition that the separation line be invariant with ζ and ψ.

The choice of x_I determined the origin of the ξ coordinate. It is most convenient to let x_I be the position of the stagnation point in the x coordinate system. It will usually be a negative number; it is defined as the value of x at which

$$u_\delta = 0$$

For this choice of x_I, the stagnation line will be given by $\xi = 0$.

The velocities have been written in terms of stream functions. The stream function for flow normal to the surface $\bar{w}$ can be eliminated through the continuity equation. The stream functions for chordwise flow (f) and for spanwise flow (g) are given as functions of ξ, ζ, η and ψ by the simultaneous equations

$$u_\delta^2 \left(-f''' - \frac{1}{2} ff'' + \xi f' \frac{\partial f'}{\partial \xi} - \xi f'' \frac{\partial f}{\partial \xi}\right) + \xi u_\delta \frac{\partial u_\delta}{\partial \xi} \left(f'^2 - \frac{1}{2} ff'' - 1\right)$$

$$+ \frac{\xi u_\delta}{q\zeta} \left[\left(\zeta \frac{\partial q}{\partial \bar{t}} - \frac{\zeta q^2}{\xi} \frac{\partial x_I}{\partial \bar{t}}\right) \frac{\xi}{q} \frac{\partial f'}{\partial \xi} + \frac{\eta q \zeta}{2\xi} f'' \frac{\partial x_I}{\partial \bar{t}} + \zeta \frac{\partial f'}{\partial \psi}\right.$$

$$+ \zeta \left(g' \frac{\partial f'}{\partial \zeta} - f'' \frac{\partial g}{\partial \zeta}\right) + \left(\frac{\zeta}{q} \frac{\partial q}{\partial y} - \frac{\zeta q}{\xi} \frac{\partial x_I}{\partial y}\right) \xi \left(g' \frac{\partial f'}{\partial \xi} - f'' \frac{\partial g}{\partial \xi}\right)$$

$$\left. + \frac{q\zeta}{2\xi} f''g \frac{\partial x_I}{\partial y}\right] + \frac{\xi \Omega_e}{q} T_1\left(f' + \frac{\eta}{2} f'' - 1\right) + \frac{\xi \Omega_a}{q} \left(g'f' + \frac{1}{2} f''g - v_\delta\right)$$

$$- 2 \frac{\xi}{q} (g' - v_\delta) \cos (\alpha - \alpha_b) = 0 \qquad (18)$$

$$u_\delta^2 \left[-g''' - \frac{1}{2} fg' + \xi\left(f' \frac{\partial g'}{\partial \xi} - g'' \frac{\partial f}{\partial \xi}\right) - \frac{\xi \Omega_a}{q} - \omega_i \frac{\xi}{q} \sin (\alpha - \alpha_b)\right.$$

$$\left. + 2f' \frac{\xi}{q} \cos (\alpha - \alpha_b)\right] + \frac{\xi}{q} u_\delta T_2 - \frac{1}{2} \xi u_\delta \frac{\partial u_\delta}{\partial \xi} fg''$$

$$+ \frac{\xi u_\delta}{q\zeta} \left[\zeta \frac{\partial g'}{\partial \psi} + \left(\frac{\zeta}{q} \frac{\partial q}{\partial \bar{t}} - \frac{\zeta q}{\xi} \frac{\partial x_I}{\partial \bar{t}}\right) \xi \frac{\partial g'}{\partial \xi} + \zeta\eta \frac{q}{\xi} \frac{\partial x_I}{\partial \bar{t}} g'' + \zeta g' \frac{\partial g'}{\partial \zeta}\right.$$

$$+ \left(\frac{\zeta}{q}\frac{\partial q}{\partial y} - \frac{q\zeta}{\xi}\frac{\partial x_I}{\partial y}\right) \xi \left(g' \frac{\partial g'}{\partial \xi} - g'' \frac{\partial g}{\partial \xi}\right) - \zeta g'' \frac{\partial g}{\partial \zeta} + \frac{q\zeta}{2\xi}\frac{\partial x_I}{\partial y} g g'']$$

$$+ \frac{\xi \Omega_a}{q} g g'' + \frac{\xi \Omega_e}{q} \eta T_1 g'' = 0 \qquad (19)$$

From this point on, the developments of the hover case and the forward flight case differ, but the general method is the same. The stream functions are expanded in asymptotic series in $1/\zeta$. Also, functions such as Ω_a and q are converted to functions of ξ, ζ, and ψ and expanded in series. The boundary layer equations then become a series of equations. The details of these calculations are outlined in the following sections.

HOVER CASE

In the hover case, the forward flight speed s_H is zero. It will simplify the solution considerably if the constant part of the inflow is eliminated. For the hover case, therefore, the induced velocity is taken to be proportional to span, *i.e.*,

$$v_i = -\omega_i y$$

This case is considerably simplified by the elimination of time dependence and by having a constant aerodynamic angle of attack α_a. The geometric angle of attack of the blade α_b (the angle between the chord line and the plane of rotation) is constant by assumption. The aerodynamic angle of attack is then

$$\alpha_a = \alpha_b - v_i/\bar{U}_0 = \alpha_b - \omega_i \qquad (20)$$

for small values of ω_i. This makes the position of the stagnation point x_I constant. The value of x_I is found by determining the value of x at which u_δ is equal to zero. This gives a value of σ (σ is the parametric variable for x) at the stagnation point σ_I.

$$\sigma_I = (1 - L^2) \;/\; (1 + L^2)$$

$$L = -(1 + \omega_i \tan \alpha_b) \;/\; (\tan \alpha_b - \omega_i) \qquad (21)$$

If $L < 0$, the stagnation point is on the underside of the airfoil, and S_g is taken to be -1. In body coordinates, the stagnation point is

$$x_I = \int_{-1}^{\sigma_I} B \, d\sigma$$

with $S_g = L/|L|$.

It is convenient to define the following functions of x:

$$C^c = \frac{2 \cos (\alpha - \alpha_b)}{\hat{u}_a} \qquad H = (x - x_I) \, \hat{u}_a$$

$$C^s = \omega_i \, (x - x_I) \sin (\alpha - \alpha_b) \quad , \quad P = \frac{x - x_I}{\hat{u}_a}$$

$$M = \frac{x - x_I}{\hat{u}_a} \frac{d\hat{u}_a}{dx}$$

These functions appear in the boundary layer equations. Before solving the boundary layer equations, the functions of x, y, and z must be converted to functions of ξ, ζ, and η. Since the transform between the two coordinate systems contains the function q, this function must be chosen before solving the equations. The first step in preparing the equations for solution is to decrease the number of independent variables from three to two. The variable ζ will be eliminated from the equations by expanding the dependent variables in infinite series in $1/\zeta$. The coefficients in the series, in general, will be functions of ξ and η. First, the stream functions will be expressed as infinite series in ζ as follows:

$$f' = \sum_{n=0}^{\infty} F'_{2n} \, \zeta^{-2n} \tag{22}$$

$$g' = \sum_{n=0}^{\infty} G'_{2n} \, \zeta^{-2n} \tag{23}$$

where the F_n and G_n are functions of ξ and η. The series is infinite, so the accuracy of the solution will depend on the number of terms retained and the rapidity of convergence of the series. In order to expand the functions C^c, C^s, H, P, M, $\tilde{u}_a$ and v_q as functions of ζ, the form of the function q(y) must be chosen. The function q will stretch the chordwise dimension ξ so that separation will always occur at the same value of ξ, say ξ_s. The criterion for separation is taken to be

$$f''\big|_{\eta=0} = 0 = F''_0 + F''_2/\zeta^2 + \ldots$$

For the separation to be independent of ζ, it is required for all n that

$$F''_n\big|_{\eta=0} = 0 \qquad \text{at} \qquad \xi = \xi_s \tag{24}$$

This is not a requirement that separation occur at the same point along the chord or that it be independent of the span. The spanwise dependence of the separation will be removed from the equations and expressed explicitly in the function q. The relation between the physical chordwise dimension x and the transformed, stretched dimension ξ is

$$x = \xi/q(y) + x_I$$

Thus, since ξ_s is independent of ζ, the position of the separation line in physical dimensions is

$$x_s = \xi_s/q(y) + x_I \tag{25}$$

By intuition, and by trial and error, an appropriate form for the arbitrary function q has been found to be

$$q = 1 - K_2 y^2 + \ldots \tag{26}$$

The constant K_2 will be determined after the equations have been solved. The functions C^c, C^s, M, P, H, $\tilde{u}_a$, and v_δ are all functions of $(\xi/q + v_I)$, and they can be expanded in series in the following manner:

$$C^c = \sum_{n=0}^{\infty} c^c_{2n}\, \zeta^{-2n} \qquad\qquad H = \sum_{n=0}^{\infty} h_{2n}\, \zeta^{-2n} \tag{27),(28}$$

$$C^s = \sum_{n=0}^{\infty} c^s_{2n}\, \zeta^{-2n} \quad , \quad M = \sum_{n=0}^{\infty} m_{2n}\, \zeta^{-2n} \qquad (29),(30)$$

$$\nu_\delta = \sum_{n=0}^{\infty} \nu_{2n}\, \zeta^{-2n} \quad , \quad \Omega_a = \sum_{n=0}^{\infty} \omega^2_{2n}\, \zeta^{-2n} \qquad (31),(32)$$

$$P = \sum_{n=0}^{\infty} P_{2n}\, \zeta^{-2n} \qquad (33)$$

These functions depend on the values of α and ϕ_a obtained from the potential flow solutions. Once the constant parameters ω_1, α_b and X_0 are chosen, the techniques of a Taylor series can be applied; for example,

$$P(\xi q + x_I) = P(\xi + x_I) + K_2\, \xi\, \frac{dP(\xi + x_I)}{d(\xi + x_I)} \Big/ \zeta^2 + \ldots$$

Now that the ζ dependence has been expressed by an infinite series, the governing equations become an infinite set of equations in ξ and η. Retaining only the first two terms of the velocity series yields

$$-F_0''' - \frac{m_0 + 1}{2} F_0 F_0'' + m_0 F_0'^2 - m_0 + \xi\left(F_0' \frac{\partial F_0'}{\partial \xi} - F_0'' \frac{\partial F_0}{\partial \xi}\right) = 0 \qquad (34)$$

$$-G_0''' - \left(\frac{m_0 + 1}{2} F_0 + \xi \frac{\partial F_0}{\partial \xi}\right) G_0'' + \xi F_0' \frac{\partial G_0'}{\partial \xi} - h_0(1 - c_0^c F_0') - c_0^s = 0 \qquad (35)$$

$$-F_2''' - \left(\frac{m_0 + 1}{2} F_0 + \xi \frac{\partial F_0}{\partial \xi}\right) F_2'' + \left(2m_0 F_0' + \xi \frac{\partial F_0'}{\partial \xi}\right) F_2' - \frac{m_0 + 1}{2} F_0'' F_2$$

$$+ \xi\left(F_0' \frac{\partial F_2'}{\partial \xi} - F_0'' \frac{\partial F_2}{\partial \xi}\right) + m_2\left(F_0'^2 - 1 - \frac{1}{2} F_0'' F_0\right)$$

$$+ p_0\left[G_0' F_0' - \nu_0 + \frac{1}{2} F_0'' G_0 - c_0^c (G_0' - \nu_0)\right] = 0 \qquad (36)$$

$$- G_2''' - \left(\frac{m_0 + 1}{2} F_0 + \xi \frac{\partial F_0}{\partial \xi}\right) G_2'' + \xi F_0' \frac{\partial G_2'}{\partial \xi}$$

$$- \left[\frac{m_0 + 1}{2} F_2 + \xi \frac{\partial F_2}{\partial \xi} + \frac{m_2}{2} F_0 - \frac{p_0}{2} G_0\right] G_0'' + \xi F_2' \frac{\partial G_0'}{\partial \xi} - h_2(1 - c_0^c F_0')$$

$$+ h_0(c_2^c F_0' + c_0^c F_2') - c_2^s = 0 \qquad (37)$$

The boundary conditions are

at $\eta = 0 \qquad F_j = G_j = F_j' = G_j' = 0$

at $\eta = \infty \qquad F_0' = 1 \quad , \quad F_j' = 0 \quad$ for $\quad j > 1 \quad , \quad G_j' = \nu_j$

At $\xi = 0$, the product $\bar{U}_a F_2'$ has a finite, non-zero value. Since $\xi = 0$ is the stagnation point of the potential flow, $\bar{U}_a = 0$ there. However, rotational effects cause a small flow in the boundary layer there, and

$$f' = u/y\bar{U}_a$$

A singularity in the stream function is caused by the method of non-dimensionalization chosen. To avoid this, and to remove K_2 from the equations, let

$$F_2' \mu_0^a = K_2 F_{2k}' + F_{2c}' \qquad (38)$$

The equations for the stream functions can now be solved if the potential flow solution is known. This solution is fixed by the type of the airfoil (in this case, a symmetrical Joukowski airfoil); the maximum thickness (fixed by the parameter ϵ; in this case $\epsilon = .092$ for a maximum thickness of 11.9%); the position of the axis of rotation, X_0; the geometric angle of attack, α_b; and the induced velocity, which is proportional to ω_i. All these are nondimensional quantities; the lengths are nondimensional with respect to the chord and the velocities are nondimensional with respect to the product of chord and angular velocity. Once the equations for F_{2k} and F_{2c} are solved, K_2 is found from Equation (32), which may now be written, for $n = 2$, as

$$K_2 F_{2k}'' + F_{2c}'' = 0 \qquad \text{at} \qquad \eta = 0 \quad \text{and} \quad \xi = \xi_s \qquad (39)$$

and ξ_s is the value of ξ at which

$$F_0'' = 0 \quad \text{at} \quad \eta = 0$$

The velocities in the boundary layer are

$$u = y\Omega_a(x) \; [F_0' + (K_2F_{2k}' + F_{2c}')/\mu_0^a\zeta^2 + \ldots] \tag{40}$$

$$v = G_0' + G_2'/\zeta^2 + \ldots \tag{41}$$

Once the equations for F_0, G_0, F_{2k} and F_{2c} have been solved, and the value of K_2 is found, the chordwise and spanwise velocities are known.

FORWARD FLIGHT CASE

For this case, the analysis is simplified if the induced velocity is taken as constant ($\omega_i = 0$), so that

$$v_i = - v_a$$

For a lifting helicopter, v_a is a positive constant. Both the aerodynamic angle of attack and the stagnation point vary with time and position along the span. The stagnation point is found by setting u_δ equal to zero. This gives

$$\sigma_I = (1 - L^2)/(1 + L^2)$$

$$L = - [(y + T_2) \cos \alpha_b + v_a \sin \alpha_b] \; / \; [(y + T_2) \sin \alpha_b - v_a \cos \alpha_b]$$

$$S_g = L/|L|$$

In body coordinates, the value of x at the stagnation point is given by

$$x_I = \int_{-1}^{\sigma_I} B \, d\sigma \tag{42}$$

where B is the function of σ given by Equation (6). The dependence of x_I on y and $\bar{t}$ is complex, but x_I may be expanded in a series in y, *i.e.*,

$$x_I = \chi_0 + \chi_1/y + \chi_2/y^2$$

$$\chi_0 = \int_{-1}^{\sigma_I^*} B \, d\sigma$$

$$\chi_1 = v_a \chi_{10} = - v_a 4B_I^* \cos \alpha_b \sin \alpha_b$$

$$\chi_2 = v_a^2 \chi_{20} + v_a T_2 \chi_{22} \qquad \chi_{22} = - \chi_{10}$$

$$\chi_{20} = (\partial B/\partial \sigma)_I^* \, 8 \cos^2 \alpha_b \sin^2 \alpha_b$$

$$+ B_I^* [2 \sin^2 \alpha_b (3 \cot^2 \alpha_b - 1) - 4 \cos^2 \alpha_b] \tag{43}$$

The superscript * denotes "the asymptotic value for large values of y." For example, as y becomes large, x becomes ξ^*, where $\xi^* = \xi + \chi_0$. χ_0, χ_{10}, χ_{20} and χ_{22} are constants and are independent of v_a, ψ, and ζ. The equations will be made independent of v_a by a careful choice of the coefficients of the double subscripted terms. A variable with a single number as a subscript will be independent of ζ. A double subscript or the single subscript 0 (except for G_0) indicates independence of ζ, ψ, s_H, and v_a. This removal of induced velocity is possible because ω_i is zero and the flow at the edge of the boundary layer has been simplified to

$$\phi_e = \phi_a = \phi_\sigma \cos \alpha_b + \phi_\rho \sin \alpha_b$$

$$\phi_c = \phi_\sigma \sin \alpha_b - \phi_\rho \cos \alpha_b$$

$$u_\delta = (y + T_2) \, \tilde{u}_a + v_a \tilde{u}_c$$

$$v_\delta = T_1 + \tilde{v}$$

$$\tilde{v} = \phi_a - 2(X_\sigma \cos \alpha_b + Z_\sigma \sin \alpha_b)$$

The functions $\bar{u}_a$, $\bar{u}_c$, ϑ, and $\cos(\alpha - \alpha_b)$ are functions of x only. However, in the transformed coordinate system (ξ, ζ, η, ψ) they are functions of ζ and ψ (as well as ξ), because x_I and q depend on ζ and ψ. As in the hover case, q is chosen so that separation, given by

$$f''(\xi_s, \zeta, \eta = 0, \psi) = 0,$$

occurs at a fixed value of ξ, say ξ_s. An appropriate form for q has been found to be

$$q = 1 - K_1/\zeta - K_2/\zeta^2 \ldots \tag{44}$$

$$K_1 = v_a K_{10}$$

$$K_2 = K_{20r} + v_a^2 K_{20} + K_{21} T_1 + v_a K_{22} T_2$$

The double subscripted K's are constants.

This choice of q allows functions of x to be expanded in a Taylor series in $1/\zeta$:

$$\vartheta = \sum_{n=0}^{\infty} \nu_n \zeta^{-n} \qquad \cos(\alpha - \alpha_b) = \sum_{n=0}^{\infty} c_n \zeta^{-n} \tag{45),(46}$$

$$\bar{u}_a = \sum_{n=0}^{\infty} \mu_n^a \zeta^{-n} \qquad \bar{u}_c = \sum_{n=0}^{\infty} \mu_n^c \zeta^{-n} \tag{47),(48}$$

$$u_\delta = \zeta \sum_{n=0}^{\infty} \mu_n^\delta \zeta^{-n} = \zeta[\mu_0^a + \sum_{n=1}^{\infty} (\mu_n^a + v_a \mu_{n-1}^c + T_2 \mu_{n-1}^a) \zeta^{-n}] \tag{49}$$

As an example, the coefficients for ϑ are found to be

$$\nu_0 = \vartheta^*$$

$$\nu_1 = (\chi_1 + \xi K_1)(\partial\Phi/\partial x)^*$$

$$\nu_2 = (\chi_2 + \xi K_1^2 + \xi K_2)(\partial\Phi/\partial x)^* + (\chi_1 + \xi K_1)^2(\partial^2\Phi/\partial x^2)^*/2$$

The ν_n are still functions of ψ and v_a, so a further expansion is necessary:

$$\nu_1 = v_a\nu_{10} = v_a(\chi_{10} + \xi K_{10})(\partial\Phi/\partial x)^*$$

$$\nu_2 = v_a^2\nu_{20} + \nu_{20r} + T_1\nu_{21} + v_a T_2\nu_{22}$$

$$\nu_{20} = (\chi_{20} + \xi K_{10}^2 + K_{20})(\partial\Phi/\partial x)^* + (\chi_{10} + \xi K_{10})^2(\partial^2\Phi/\partial x^2)^2/2$$

$$\nu_{20r} = \xi K_{20r}\ (\partial\Phi/\partial x)^*$$

$$\nu_{21} = \xi K_{21}(\partial\Phi/\partial x)^*$$

$$\nu_{22} = (\chi_{22} + K_{22})(\partial\Phi/\partial x)^*$$

The other functions of x are handled in a similar manner. In order to express the coefficients of the stream functions in the boundary layer equations, it is convenient to define the following:

$$p_0 = \frac{\xi}{\mu_0^\delta} \qquad (50)$$

$$m_0 = \frac{\xi}{\mu_0^\delta}\frac{\partial\mu_0^\delta}{\partial\xi} \qquad (51)$$

$$m_1 = \frac{\partial\mu_1^\delta}{\partial\xi} - \frac{\mu_1^\delta}{\mu_0^\delta}\frac{\partial\mu_0^\delta}{\partial\xi} = v_a\, m_{10} \qquad (52)$$

$$m_{10} = K_{10}\, m_{1k} + m_{10c} \qquad (53)$$

$$m_2 = \frac{\partial \mu_2^\delta}{\partial \xi} - \frac{\mu_2^\delta}{\mu_0^\delta}\frac{\partial \mu_0^\delta}{\partial \xi}$$

$$= m_{2k} K_{20r} + v_a^2(m_{2k} K_{20} + m_{20c}) + T_1 m_{2k} K_{21}$$

$$+ v_a T_2 (m_{2k} K_{22} + m_{22c}) \qquad (54)$$

At this point, all the expressions in the boundary layer equations have been written in series form except for the stream functions. They are now written as

$$f = F_0(\xi,\eta) + F_1(\xi,\eta,\phi)/\zeta + F_2(\xi,\eta,\phi)/\zeta^2 + \ldots \qquad (55)$$

$$g = G_0(\xi,\eta,\phi) + G_1(\xi,\eta,\phi)/\zeta + \ldots \qquad (56)$$

$$F_1 = v_a F_{10} = v_a(K_{10}F_{1k} + F_{10c}) \qquad (57)$$

$$F_2 = [(F_{20r} + K_{20r} F_{2k}) + (F_{20c} + K_{20} F_{2k}) v_a^2 + T_1 (F_{21c} + K_{21} F_{2k})$$

$$+ v_a T_2(F_{22c} + K_{22} F_{2k})]/\mu_0^\delta \qquad (58)$$

$$G_0 = G_{00} + G_{01}T_1 \qquad (59)$$

$$G_1 = v_a G_{10} + v_a T_1 G_{11} + T_2 G_{12} \qquad (60)$$

Substituting all the infinite series into the boundary layer equations and neglecting the terms of higher order in $1/\zeta^2$ in the F series and $1/\zeta$ in the G series, the equations to be solved may be found. The equations for the first terms in the stream functions are

$$- F_0''' - \frac{m_0 + 1}{2} F_0 F_0'' + m_0 F_0'^2 - m_0 + \xi (F_0' \frac{\partial F_0'}{\partial \xi} - F_0'' \frac{\partial F_0}{\partial \xi}) = 0 \qquad (61)$$

$$D^G(G_{00}) = -\xi(F_0' c_0 - \mu_0^a) \tag{62}$$

$$D^G(G_{01}) = 0 \tag{63}$$

where $D^G(G_0) = -G_0''' - (\frac{m_0+1}{2} F_0 + \xi \frac{\partial F_0}{\partial \xi}) G_0'' + \xi F_0' \frac{\partial G_0'}{\partial \xi}$

The equations for the second terms in the series for the stream functions are

$$D_1^F(F_{1k}) = -p_0 m_{1k} (F_0'^2 - \frac{1}{2} F_0 F_0'' - 1) \tag{64}$$

$$D_1^F(F_{1c}) = -p_0 m_{10c} (F_0'^2 - \frac{1}{2} F_0 F_0'' - 1) \tag{65}$$

where
$$\begin{aligned} D_1^F(F_1) = &-F_1''' - (\frac{m_0+1}{2} F_0 + \xi \frac{\partial F_0}{\partial \xi}) F_1'' \\ &+ (2m_0 F_0' + \xi \frac{\partial F_0'}{\partial \xi}) F_1' - \frac{m_0+1}{2} F_0'' F_1) \\ &+ \xi (F_0' \frac{\partial F_1'}{\partial \xi} - F_0'' \frac{\partial F_1}{\partial \xi}) \end{aligned}$$

$$\begin{aligned} D^G(G_{10}) = &(\frac{m_0+1}{2} F_{10} + \xi \frac{\partial F_{10}}{\partial \xi} + \frac{1}{2} p_0 m_{10} F_0) G_{00}'' \\ &- F_{10}' \xi \frac{\partial G_{00}'}{\partial \xi} - \xi (F_{10}' c_0 + F_0' c_{10} - \mu_{10}^a) \\ &- K_{10} \xi (F_0' c_0 - \mu_0^a) \end{aligned} \tag{66}$$

$$\begin{aligned} D^G(G_{11}) = &(\frac{m_0+1}{2} F_{10} + \xi \frac{\partial F_{10}}{\partial \xi} + \frac{1}{2} p_0 m_{10} F_0) G_{01}'' \\ &- F_0' \xi \frac{\partial G_{01}'}{\partial \xi} \end{aligned} \tag{67}$$

$$D^G(G_{12}) = -\, p_0(1 - G'_{01})$$

The operator $D^G(G_0)$ is given above. The third term in the series for the chordwise stream function is given by

$$D_2^F(F_{2k}) = -\, \xi m_{2k}(F_0'^{\,2} - \frac{1}{2} F_0'' F_0 - 1) \tag{69}$$

$$D_2^F(F_{20r}) = -\, \xi(F_0' F_{00}' + \frac{1}{2} G_{00} F_0'' - \nu_0) - p_0 c_0(\nu_0 - G_{00}') \tag{70}$$

$$\begin{aligned} D_2^F(F_{20c}) = -\, \mu_0^\delta \Big(&- \frac{m_0 + 1}{2} F_{10}'' F_{10} - m_0 F_{10}'^{\,2} + \xi F_{10}' \frac{\partial F_{10}'}{\partial \xi} - \xi F_{10}'' \frac{\partial F_{10}}{\partial \xi}\Big) \\ &- \xi\, m_{10}\, (2F_0' F_{10}' - \frac{1}{2} F_{10}'' F_0 - \frac{1}{2} F_0'' F_{10}) \\ &- \xi(m_{20c} - \frac{\mu_{10}^\delta}{\mu_0^\delta} m_{10})(F_0'^{\,2} - \frac{1}{2} F_0 F_0'' - 1) \end{aligned} \tag{71}$$

$$\begin{aligned} D_2^F(F_{21c}) = -\, &\xi(F_0' - 2 + \frac{n}{2} F_0'') - p_0\, c_0(1 - G_{01}') \\ &- \xi(\frac{1}{2} F_0'' G_{01} + F_0' G_{01}') \end{aligned} \tag{72}$$

$$D_2(F_{22c}) = -\, \xi(m_{22c} - \frac{\mu_{12}^\delta}{\mu_0^\delta} m_{10})(F_0'^{\,2} - \frac{1}{2} F_0 F_0'' - 1) \tag{73}$$

where
$$\begin{aligned} D_2^F(F_2) = &- F_2''' - (\frac{m_0 + 1}{2} F_0 + \xi \frac{\partial F_0}{\partial \xi}) F_2'' \\ &+ (m_0 F_0' + \xi \frac{\partial F_0'}{\partial \xi}) F_2' + \frac{m_0 - 1}{2} F_0'' F_2 \\ &+ \xi(F_0' \frac{\partial F_2'}{\partial \xi} - F_0'' \frac{\partial F_2}{\partial \xi}) \end{aligned}$$

The variable ψ has been eliminated from the equation by applying the principle of superposition. The independent variables in the equations are ξ and η. The equations have the boundary conditions given by

At $\eta = 0$ $\quad F_{nj} = F'_{nj} = G_{nj} = G'_{nj} = 0$

at $\eta = \infty$ $\quad F'_0 = 1 \quad , \quad F'_{nj} = 0 \quad$ for $\quad n > 0$

$$G'_0 = \nu_0 \quad , \quad G'_{01} = 1 \quad , \quad G'_{nj} = \nu_{nj} \quad \text{for} \quad n > 0$$

These equations may be solved sequentially, once values have been fixed for the thickness of the airfoil (ε), the type of airfoil (symmetrical Joukowski), the geometric angle of attack (α_b), and the location of the axis of rotation (X_0). The separation point ξ_s is the point at which

$$F''_0(\xi_s, 0) = 0$$

The values of K_{nj} are found from the equations

$$F''_{nk}(\xi_s, 0)\, K_{nj} + F''_{njc}(\xi_s, 0) = 0 \tag{74}$$

The equation for the separation line is given by

$$x_s = X_0 + v_a X_{10}/y + (v_a^2 X_{20} + v_a X_{22}\, T_2)/y^2$$
$$+ \xi_s/[1 - v_a K_{10}/y - (K_{20r} + v_a^2 K_{20} + T_1 K_{21} + v_a T_2 K_{22})/y^2] \tag{75}$$

The velocities in the boundary layer are given by

$$u = (y\bar{u}_a(x) + v_a \bar{u}_c(x) + T_2 \bar{u}_a)\; f'(\xi, \zeta, \eta, \psi) \tag{76}$$

$$v = g'(\xi, \zeta, \eta, \psi) \tag{77}$$

The stream functions f and g are given by Equations (61) through (72).

METHOD OF SOLUTION

For both the hover case and the forward flight case, a series of equations for the stream functions must be solved. The dependent variables in these partial differential equations are the transformed chordwise coordinate ξ and the transformed coordinate normal to the surface of the airfoil η. By finite difference techniques, numerical solutions can be found from straightforward calculations. Special techniques are required to start the solution at the stagnation point, and some numerical experimentation is required to find the optimum spacing in the ξ direction. The calculations for the potential flow and the conversion from the transformed coordinates to the real coordinates involve considerable algebraic manipulation, but the computer programs, especially the one for forward flight, are simple and straightforward in logic. Both are shown in APPENDIX II.

The potential flow solution requires the solution of the differential equation

$$dx \,/\, d\sigma = B(\sigma) \tag{78}$$

where $x = 0$ at $\sigma = -1$. This equation must be solved to find the value of x at the stagnation point, and then for each value of x, the corresponding value of σ must be found. This was accomplished by the RK1 Runge-Kutta scheme in the IBM System 360 Scientific Subroutine Package. Since B becomes infinite at $\sigma = -1$, the value of x must be known at a value of σ greater than -1. For $(\sigma + 1) << 1$, $B(\sigma)$ can be simplified and integrated analytically. The relation between x and σ near $\sigma = -1$ is

$$x = \frac{\varepsilon \sqrt{2(1 + \sigma)}}{1 + \varepsilon}$$

Since the integration of the differential equation cannot begain at $\sigma = -1$, it begins at $(\sigma + 1) = 10^{-20}$.

A similar situation is encountered at the stagnation point, where several functions become indeterminate. The function m_0,

$$m_0 = \frac{\xi}{\mu_0^a} \frac{d\mu_0^a}{d\xi}$$

is indeterminate in that both the numerator and denominator are zero at $\xi = 0$. It is well known that the velocity μ_0^a is proportional to ξ at a stagnation point, and that m_0 should equal 1. To avoid exponent overflow (the computer, an IBM 360/75, is limited to exponents of about 75), the solution was started at values of ξ of 10^{-5} to 10^{-6}. For $\xi = 1.2 \times 10^{-6}$, the value $m_0 = 1.00004$ was found, and $F_0'' = 1.23259$. This is close enough to the stagnation point value of F_0'' of 1.2326 to ensure the desired accuracy. Varying the starting value of ξ by a factor of two produced insignificant changes in the solution.

A similar situation was encountered for $\alpha_b = 0$. Although negative angles of attack cause no problem, exponent overflow occurs for α_b much less than 0.005°. A solution at 0.005° was compared to a solution specifically designed for only zero angle of attack, and the results of this comparison indicate that 0.005° is a satisfactory approximation to zero degrees. The results for the hover case for zero angle of attack are found from Reference 11, and for forward flight, the 0.005° approximation was used.

Since all the functions of x, such as $\tilde{u}_a$ and $\cos(\alpha - \alpha_b)$, are actually known as analytic functions of the parametric variation σ, the determination of σ for the desired value of x allowed the functions of x, and their derivatives, to be found. This allows the functions of ξ, such as μ_2^a and c_0^c, to be found, and all the coefficients of the stream functions in the equations to be solved are determined. Each equation is a partial differential equation in ξ and η. If they are solved in the correct order, each equation will contain only one undetermined stream function. This allows the equations to be solved sequentially, and not simultaneously. The starting of the solution in the ξ direction is simplified by the form into which the ξ derivatives have been cast. Each derivative with respect to ξ is multiplied by ξ. Thus, at $\xi = 0$ the equations become ordinary differential equations in η. Once a solution is found at the stagnation point ($\xi = 0$), the solution proceeds in the ξ direction by the method of A. M. O. Smith.[13]

This method reduces each partial differential equation to an ordinary differential equation in η at each successive value of ξ, by expressing the ξ derivatives in terms of the values at the preceding stations by Lagrangian finite differences. When the solution is known at the stagnation point ($\xi = \xi_1$), ξ is incremented and a solution at $\xi = \xi_2$ is sought. The ξ derivatives are approximated by a two-point Lagrangian formula using values at ξ_1 and ξ_2. The equations are solved in η at ξ_2. At the next point, ξ_3, a three-point formula is used, and at each succeeding point a four-point formula is employed. The spacing of the points required some numerical experimentation. The two-point formula is considerably less accurate than the three point, so $\Delta_2 (\Delta_h = \xi_h - \xi_{h-1})$ is small, typically $.5 \times 10^{-3}$. A. M. O. Smith[13] has given several guidelines for the selection of ξ spacing. If the value of ξ_h / Δ_h is greater than 25, the equation for F_0 may become unstable. This instability is manifested in an inability to find a solution for the ordinary differential equation in η. If the value of Δ_h is too large, the ξ derivatives will be inaccurate. The accuracy can be checked in two ways. After finding a solution at point ξ_{h+1}, a central difference differentiation using ξ_{h-1}, ξ_h, and ξ_{h+1} can be compared to the backward formula (using ξ_h, ξ_{h-1}, ξ_{h-2}, ...) used in the solution. This method is not as complete a check as rerunning the entire solution with smaller values of Δ_h. Since the accuracy of the ξ derivatives depends strongly on Δ_h, this will reveal any inaccuracies that affect the results. From 30 to 60 stations in ξ were required for the case run, with values of ξ_h / Δ_h ranging from 8 to 25 away from the stagnation point. Near the stagnation point, Δ_h was varied from about 0.002 (at large angles of attack) to 0.005 (at small angles of attack). Near stagnation, Δ_h ranged from 0.01 to 0.02.

The equation for F_0 is the equation for a two-dimensional boundary layer. At the point of separation it has a singularity, and the solution cannot be carried to the separation point. Smith and Clutter[13] have shown that it may be accurately found by extrapolation. To approach the separation point closely enough to successfully extrapolate often required two or three attempts to find a suitable spacing. The instability in the ordinary differential equation near separation is similar to that caused by large values of ξ_h / Δ_h. In both cases, the scheme used to integrate the equation in η failed to converge. The conditions under which the η equation diverged depended partly on the integration scheme used.

For the hover case, a Runge-Kutta scheme, attributed to Kutta[14], was used to solve the ordinary differential equation in η. One of the boundary conditions on F_n' (or G_n') is given at $\eta = \infty$. This requires that guesses be made of a maximum value of η large enough to cause little error, and of the value of F_n'' at the wall that will match the boundary condition on F_n' at the maximum value of η. Little difficulty was experienced with the linear equations, but for the nonlinear equation for F_0, and error of 10^{-12} in F_0'' often caused appreciable error in F_0' at the maximum value of η. This problem was greatly accentuated if the maximum value of η was so large that F_0'' became much less than 10^{-3}. Near separation, or if ξ_h / Δ_h became too large, the equation would not converge. Since the computer retained only 15 significant digits, this could limit the accuracy of F_0'' to less than that needed to match the boundary condition in F_0' at the maximum η. This divergence of the Runge-Kutta integration made it difficult to approach the separation point closely, and required constant adjustment of the maximum value of η.

For the forward flight case, Lew's method of accelerated successive replacement[15] was used to solve the equation in η. This method has some of the features of quasi-linearization. For each equation, an estimate of F_n' (or G_n') at discrete values of $\eta(\eta_1, \eta_2 \ldots \eta_{\ell\ max})$ is required. The values of F_n, F_n'', and F_n''' at η_ℓ are found by finite differences from the current value of F_n' at $\eta_{\ell-1}$, η_ℓ and $\eta_{\ell+1}$. The error in the equation is used to find a new value of F_n', and the old value is immediately replaced. This procedure continues until the change in F_n' is less than 10^{-6} or 10^{-7}. Both the accuracy and speed of this method depend strongly on the spacing between the values of η. A spacing of .1 gives sufficient accuracy (3 to 4 places). The computer time required is greater than that of the

Runge-Kutta scheme, except near separation, where they are comparable. On an IBM Model 360/75, even the Runge-Kutta scheme required 5 to 8 minutes of computer time. For η greater than 4 or 5, the spacing in η was gradually increased, but the decrease in computer time is probably not worth the effort involved. Using Lew's method, the maximum value of η and the values of Δ_h are less critical, and separation can be approached more closely and easily than with the Runge-Kutta scheme. The method of Lew proved much simpler to program, but comparison with the results of the Runge-Kutta scheme were necessary to establish confidence in its accuracy.

Since neither the Runge-Kutta solution or the solution by Lew's method is clearly superior, the advantages of each are listed. First, for Lew's method:

1. Separation may be approached more easily.
2. Larger values of η, and smaller values of Δ_h, may be used.
3. The computer program is simpler.

The advantages of the Runge-Kutta scheme are:

1. Less computer time is required.
2. Greater accuracy is obtainable.

Other programmers have successfully used predictor-corrector methods and the method of quasi-linearization, in conjunction with A. M. O. Smith's method.

About one-half the storage required by the program (100 to 200 thousand bytes) is occupied by a matrix with four subscripts, $y_{m,\,j,\,l,\,i}$, that contains all the stream functions and their derivatives. The subscript j denotes the variable. In the hover case, for example, j = 1 denotes F_0, 2 denotes G_0, 3 denotes F_{2k}, and so on. The number of primes is given by m - 1. Thus, m = 1 denotes F_0, 2 denotes F_0', and 3 denotes F_0''. The value of η is η_ℓ, and the value of ξ is ξ_{h-i+1} where ξ_h is the current value of ξ. When a solution at ξ_h is sought, values at ξ_{h-1}, ξ_{h-2}, and ξ_{h-3} are needed to find the derivatives with respect to ξ. Thus $y_{2,2,6,3}$ denotes G_0' evaluated at η_6 and ξ_{h-2}. Much computer time was saved by evaluating the ξ derivatives only once at each ξ station and storing the result in a matrix $A_{m,j,l}$. When the value of ξ is incremented, the Y and A matrices must be revised.

Whatever method is used to solve the equations in ξ and η, the solution will be limited in accuracy by the truncation of the asymptotic series in span. Like any asymptotic series, the convergence of the series cannot be determined mathematically. It does appear that for values of span greater than 12 or 15 times the chord of the blade an adequate approximation is provided by the first term of the series, F_0. The spanwise series is taken to terms of the order $1 / \zeta^2$, which has a coefficient F_2. In the hover case, F_1 is zero and F_2' is smaller than F_0'. These terms may approximate the solution for values of span as small as 1 or 2. In the forward flight case, the magnitude of F_1' and F_2' depends on the magnitude of the inflow v_a and the forward flight speed s_H. Helicopters may have speeds to give values of s_H of 3 to 5, and the inflow may be in the range 0.05 to 0.2. The accuracy of the series is in doubt for values of span less than 5 to 10 and near the region of reverse flow where $s_H \sin \psi + y < 1$.

The spanwise series has been taken to terms of order $1 / \zeta$. Over most of the airfoil, the spanwise velocity is of the order of $1 / \zeta$ times the chordwise velocity. The primary interest in this investigation lies in the chordwise, not the spanwise, flow. Determination of the spanwise flow is primarily for evaluating its effect on the chordwise flow. Since terms of order $1 / \zeta^2$ in the spanwise flow affect the chordwise flow only to order $1 / \zeta^3$, the truncation of the spanwise series at $1 / \zeta$ is consistent with truncation of the chordwise series at $1 / \zeta^2$.

RESULTS

HOVER CASE

The computer program in APPENDIX II was run for four conditions, and a fifth condition, for zero angle of attack, was taken from a special computer program.[11] All conditions were for a symmetrical Joukowski airfoil with a thickness of 11.9% and for the axis of rotation at the quarter chord ($X_0 = 0.25$). For each condition, the geometric angle of attack α_b and the downflow constant ω_i must be chosen. These have not been selected arbitrarily, but have been chosen to be representative of conditions found in two specific helicopters. Values of thrust of 6000 lbf, 8000 lbf, and 10,000 lbf were given for a helicopter with a 24-foot radius rotor. For a 40-foot radius rotor, values of geometric angle of attack of zero and 6 degrees were given. The relationship of the inflow constant, geometric angle of attack, and thrust is described in APPENDIX I.

It has been found that the solution depends strongly on the aerodynamic angle of attack, which was found to be

$$\alpha_a = \alpha_b - \omega_i$$

For this reason, the conditions are identified by the aerodynamic angle of attack, and the corresponding values of α_b and ω_i are understood to be those in Table I. Table I also shows the position of the stagnation point x_I, the value of ξ at separation ξ_s, and the constant in the expression for q, *i.e.*, K_2.

TABLE I. SUMMARY OF CALCULATED RESULTS FOR THE HOVER CASE

α_a (deg)	α_b (deg)	ω_i	T (lbf)	R (ft)	x_I	ξ_s	K_2	X_{NS}
0	0	0	-	40	0	.440	.784	30.0
2.38	6.00	.0631	-	40	-.00721	.300	.450	24.2
3.12	6.01	.0504	6000	24	-.0096	.256	.365	20.1
4.16	7.50	.0582	8000	24	-.01323	.188	.226	13.3
5.21	8.94	.0651	10000	24	-.01718	.123	.081	6.48

The percent of chord called "near separation" is used only in constructing some of the figures. Its position depends mainly on how close to separation the solution was taken. The third digit in the values for ξ_s and K_2 is probably not accurate. No attempt was made to calculate the derivatives of the stream functions to more than three significant figures in order to conserve computer time. The instability of the Runge-Kutta solution near the separation point makes these values at separation less reliable than those obtained by Lew's method.

In examining the results for the hover case, it should be remembered that the ξ dimension is not a physical dimension. The x dimension is the distance along the surface of the airfoil, measured from the leading edge. The ξ^* dimension is the distance along the surface of the airfoil, measured from the stagnation point. For a given angle of attack, x and ξ^* differ only by a constant. However, for one value of ξ the distance along the surface of the airfoil will vary with span. Figure 4 shows that, for $\alpha_a = 3.12°$, a value of ξ of 0.15 corresponds to values of x ranging from 0.2266 at y = 1 to 0.1426 at y = 5. In every case, as y becomes very large, the value of ξ approaches ξ^*.

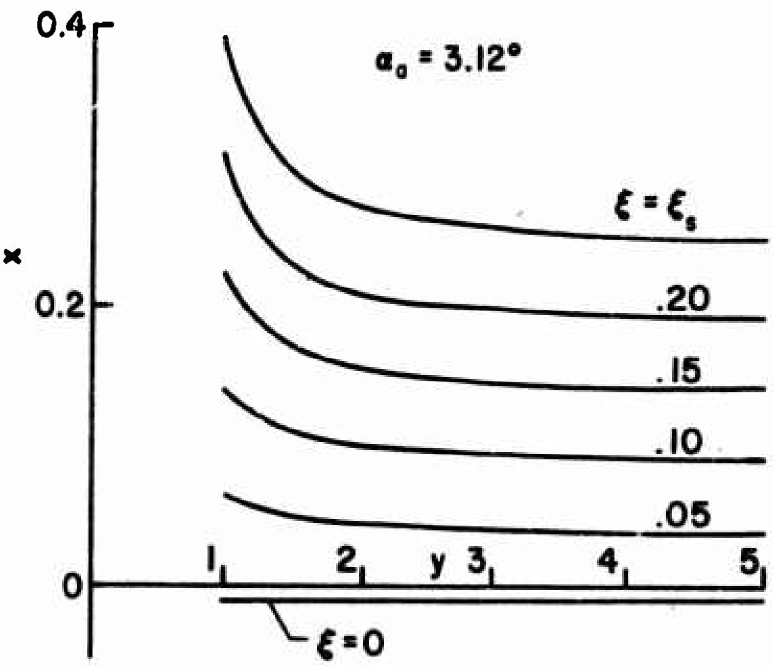

Figure 4. The ξ Coordinate.

Some of the results are more readily seen by examining the stream functions, and other results are made more apparent by considering the velocities. Both approaches will be used. A detailed examination of the stream functions, similar in approach to that of Young and Williams,[11] will evaluate the various effects that occur in the boundary layer for angles of attack greater than zero. Then, for conditions applicable to the two helicopers described in APPENDIX I, the results will be discussed in terms of such physically recognizable variables as velocity profiles, skew angles, and boundary layer thicknesses.

The effect of the angle of attack on the chordwise flow can be seen in Figures 5 and 6. The function F_0'' is just the result found on a two-dimensional airfoil. The function F_2'' reflects the rotational effects in the chordwise flow. These rotational effects cause a spanwise flow, which in turn gives rise to the function F_2 in the chordwise flow. The increase in F_2'' as the angle of attack decreases is reflected in the values of K_2 in Table I. At large angles of attack, the effect of rotation on the chordwise flow is much less than at small angles of attack. Experimental and analytical results with an NACA 0012 airfoil led Dwyer and McCroskey[6] to the same conclusion. The reason for this dependence on angle of attack can be seen by examining the spanwise flow. Positive values of spanwise velocity indicate flow away from the axis of rotation. For large values of η, G_0' is influenced primarily by the spanwise velocity in the potential flow v_δ. Figure 7 shows that v_δ is directed toward the axis of rotation, and, over most of the airfoil, its magnitude increases along the chord. At smaller values of η, the spanwise velocity is influenced by rotational effects which tend to cause flow away from the axis of rotation. This flow increases along the chord and is greatest near separation. As the blade slows the fluid flow through shear stress in the boundary layer, the fluid experiences Coriolis and centrifugal accelerations. These accelerations must act on the flow for some length of time, or equivalently, for some distance along the chord, before the velocity is affected. A convenient measure of the rotational effects is G_0'', shown in Figure 8. This shows a steady buildup of the cumulative effect of rotational accelerations along the chord, even though v_δ, which opposes this increase in G_0'', also increases in magnitude along the chord over most of the airfoil.

The spanwise flow affects the chordwise flow through the Coriolis acceleration of the fluid. This acceleration must act on the chordwise flow for some distance, or more precisely, for some time, before it affects the velocity. Figure 8 shows that the rate of increase of G_0'' at the wall increases with angle of attack, but the magnitude of G_0'' at the wall at separation depends more on the length of the boundary layer. The spanwise flow also experiences a Coriolis acceleration. When the spanwise flow is outward, this will delay separation. The spanwise inviscid flow is usually more important than the Coriolis acceleration. The terms in the chordwise boundary layer equation that involve the spanwise potential flow are written as $-2v_\delta \cos (\alpha - \alpha_b) + v_\delta \hat{u}_a(x)$. Figure 7 shows that the magnitude of v_δ depends upon the distance along the surface of the airfoil, and over the rear portion of the airfoil, v_δ increases along the chord. Thus, the greater the length of the boundary layer, the greater the magnitude of v_δ, resulting in a larger effect due to the Coriolis force terms.

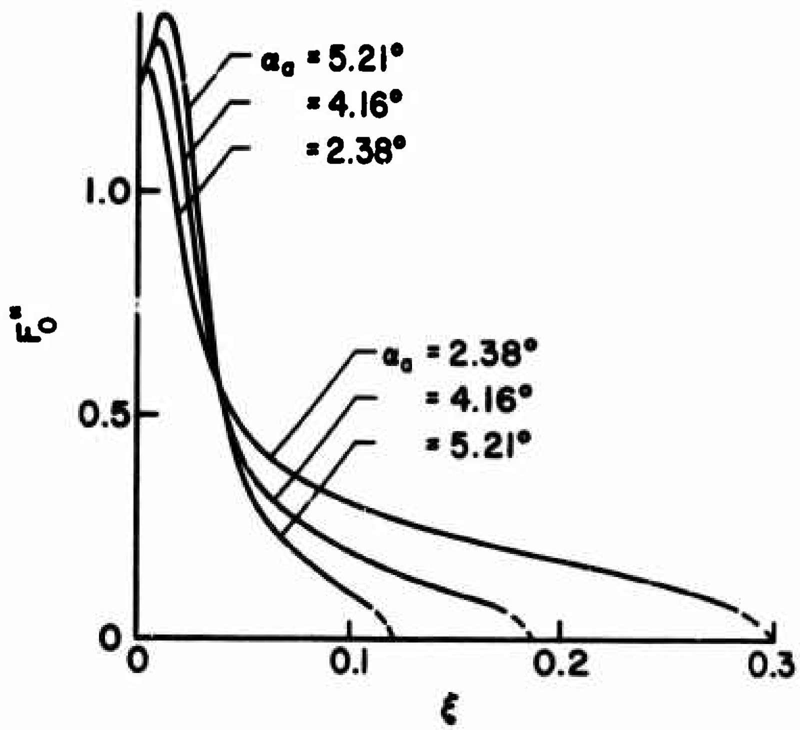

Figure 5. The Function F_0'' on the Surface of the Blade.

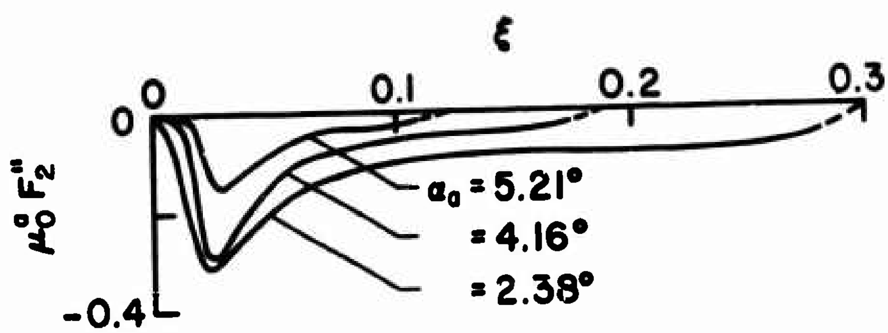

Figure 6. The Function $\mu_0^a F_2''$ on the Surface of the Blade.

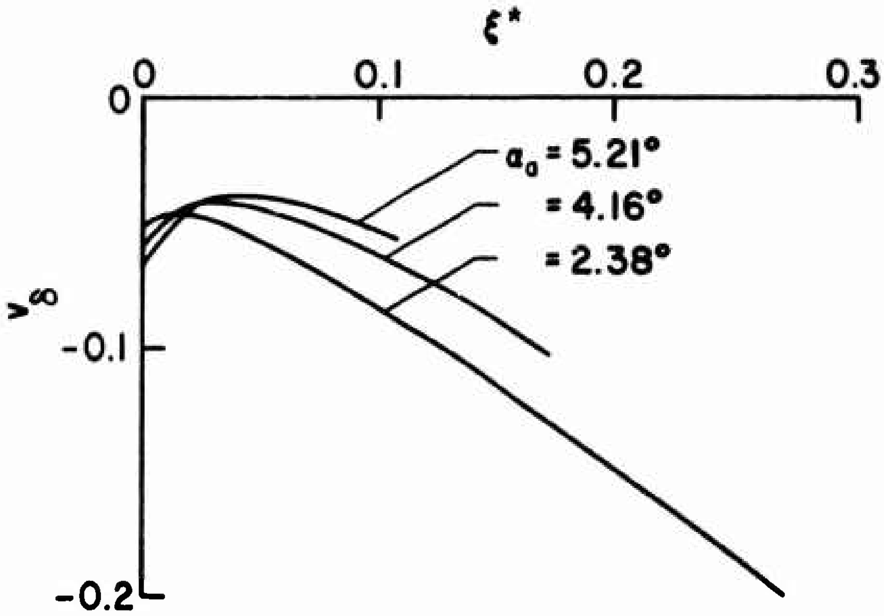

Figure 7. The Spanwise Velocity in the Potential Flow.

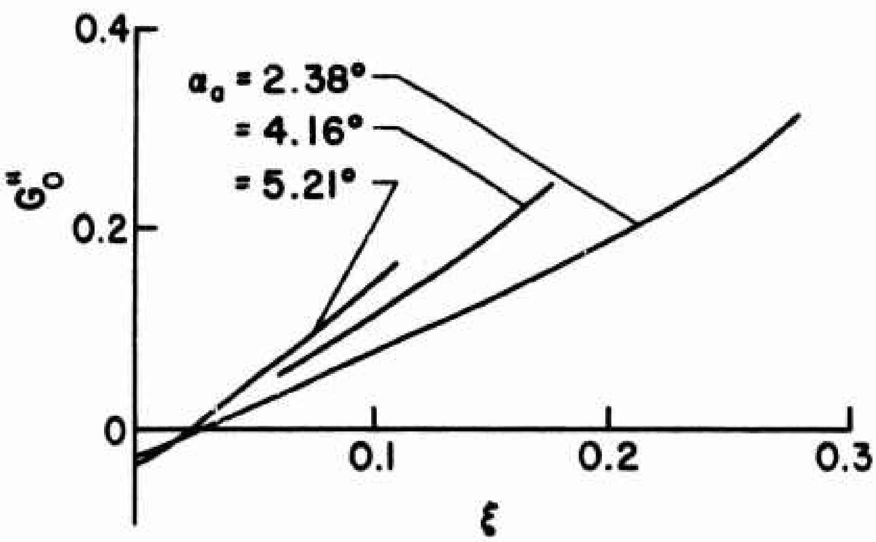

Figure 8. The Function G''_0 on the Surface of the Blade.

The length of the boundary layer, or the time the fluid spends in the boundary layer, not only allows the spanwise flow to grow but increases the chordwise velocity caused by accelerations in the spanwise flow. Since only one body shape has been considered, a real distinction between time and length of the boundary layer has not been found. However, this point of view seems to provide more understanding than an emphasis on chordwise pressure gradient.

A more familiar view of the boundary layer is provided by examination of velocity profiles calculated for specific applications. Figures 9 through 14 show the chordwise velocity profiles for two helicopters. One has a 24-foot radius rotor; the other has a 40-foot radius rotor; both are described in APPENDIX I. Figures 11 through 14 show that little spanwise variation occurs for values of span greater than 30%. The spanwise variation is not a function of the length of the blade, but the percent span can easily be converted back to the number of chord lengths from the axis of rotation. For the 24-foot rotor, 30% span is about 4 chord lengths from the axis of rotation (actually, $y = 4.113$). For the 40-foot rotor, 30% span is 6 chord lengths. Since such quantities as percent span, thrust in pounds force, percent chord, and forward flight speed in knots are usual and easily recognizable variables, they will be used in presenting the velocity profiles, boundary layer thicknesses, and skew angles. The notation "Near Separation" (or "NS") denotes the values of X_{NS} in Table I. Figures 10, 11, and 14 show that chordwise velocity profiles near separation have a shape like Falkner-Skan profiles near separation. Figure 13 shows that the profile is fuller at smaller values of chord. A small spanwise variation is seen at 24.4% chord, whereas none can be seen (in fact, none was seen on the original, computer-drawn graph) at 10% chord. This is related to the increase in rotational effects along the chord.

The spanwise velocity profiles, shown in Figures 15 through 20, show the characteristic S shape. The positive values of velocity (flow away from the axis of rotation) are caused by centrifugal forces in the boundary layer. The Coriolis force acting on the chordwise flow causes negative spanwise flow. The sum of the two effects is small and positive near the wall. In comparing spanwise and chordwise profiles, the magnitude of u_δ must be considered. The factor $\tilde{u}_a$ in u_δ is the velocity at the edge of the boundary layer on the airfoil in a two-dimensional flow where the impinging stream has unit velocity. Away from the stagnation point, $\tilde{u}_a$ is of the order of unity. The factor ΩY thus determines the order of magnitude of the chordwise potential flow. For comparison, the nondimensionalizing factor for the spanwise velocity is ΩR, the value of ΩY at the blade tip. This arrangement is dictated by the physical situation: the chordwise velocity is nearly proportional to span and the spanwise velocity is nearly independent of it. In both spanwise and chordwise velocity profiles, there is dependence on span through the variable η. A chordwise variation is expressed implicitly in η, and in addition, both v_δ and v near the wall increase along the chord. This is seen in Figures 18 and 19.

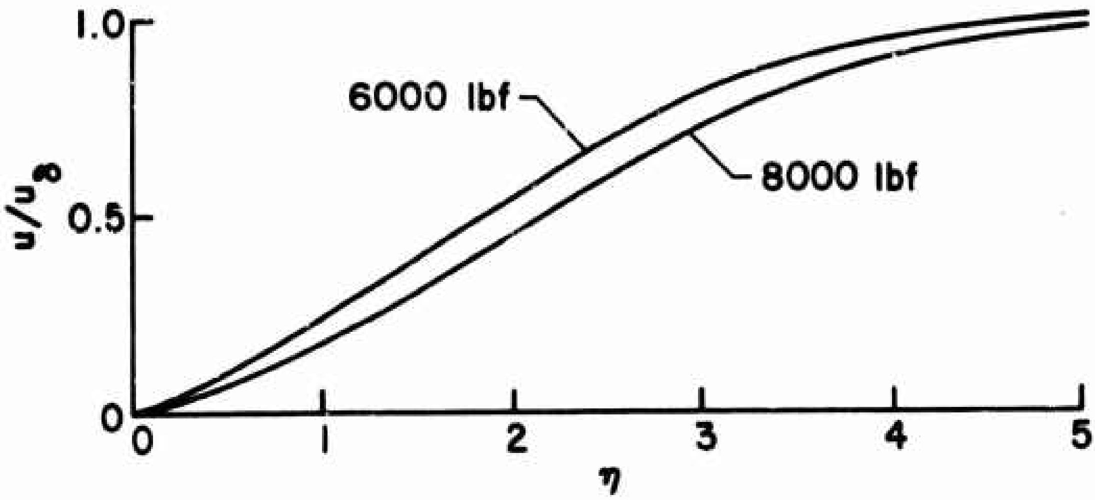

Figure 9. The Chordwise Velocity Profile for the 24-Foot Rotor (at 10% Chord and 60% Span) in Hover.

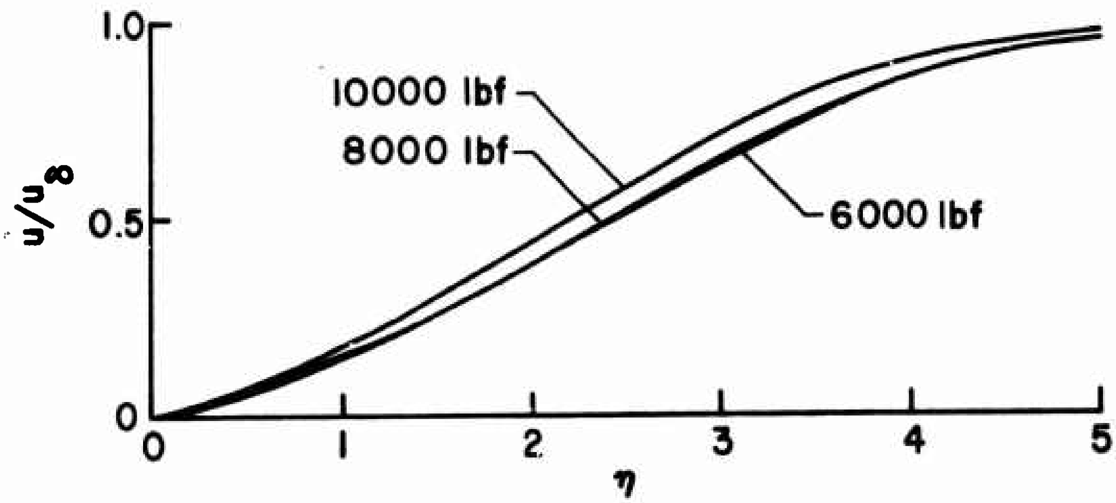

Figure 10. The Chordwise Velocity Profile for the 24-Foot Rotor (Near Separation and 60% Span) in Hover.

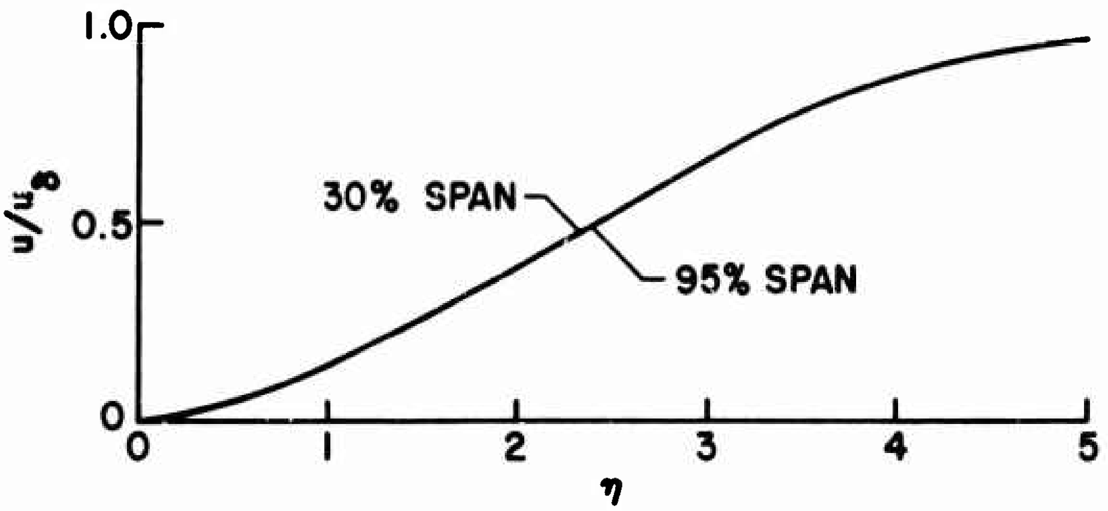

Figure 11. The Chordwise Velocity Profile for the 24-Foot Rotor (Near Separation and With 8000 lbf Thrust) in Hover.

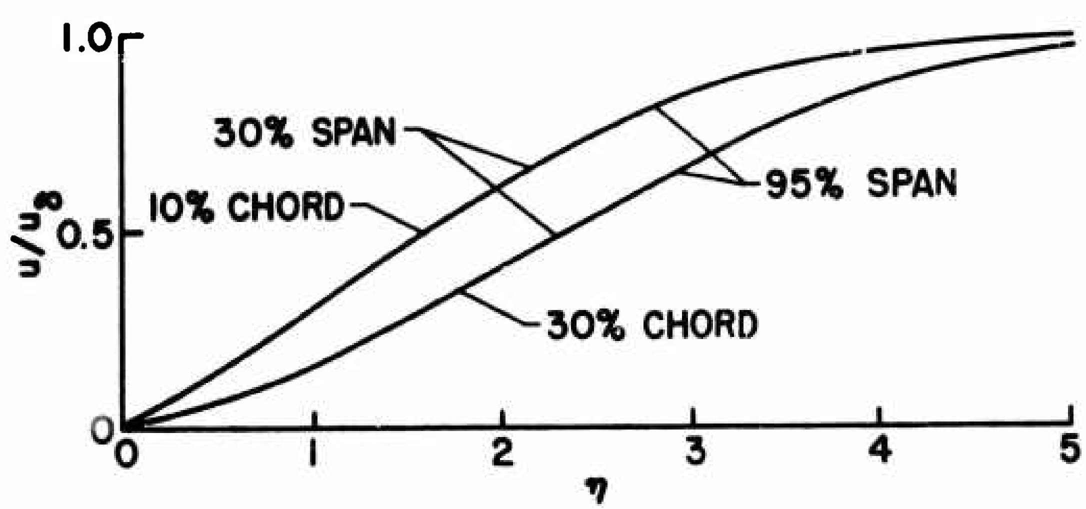

Figure 12. The Chordwise Velocity Profile for the 40-Foot Rotor (at Zero Degrees Blade Angle of Attack) in Hover.

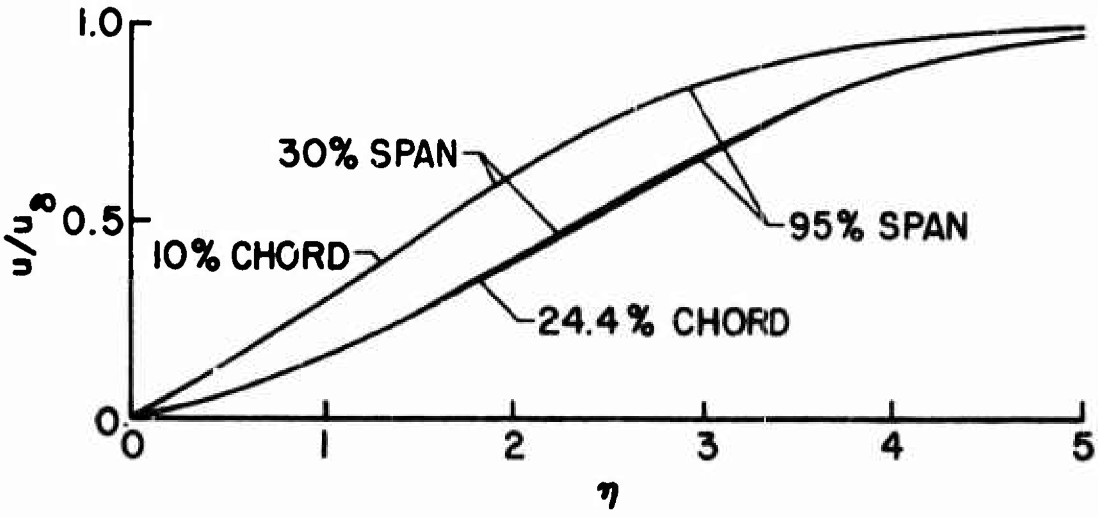

Figure 13. The Chordwise Velocity Profile for the 40-Foot Rotor (at 6 Degrees Blade Angle of Attack) in Hover.

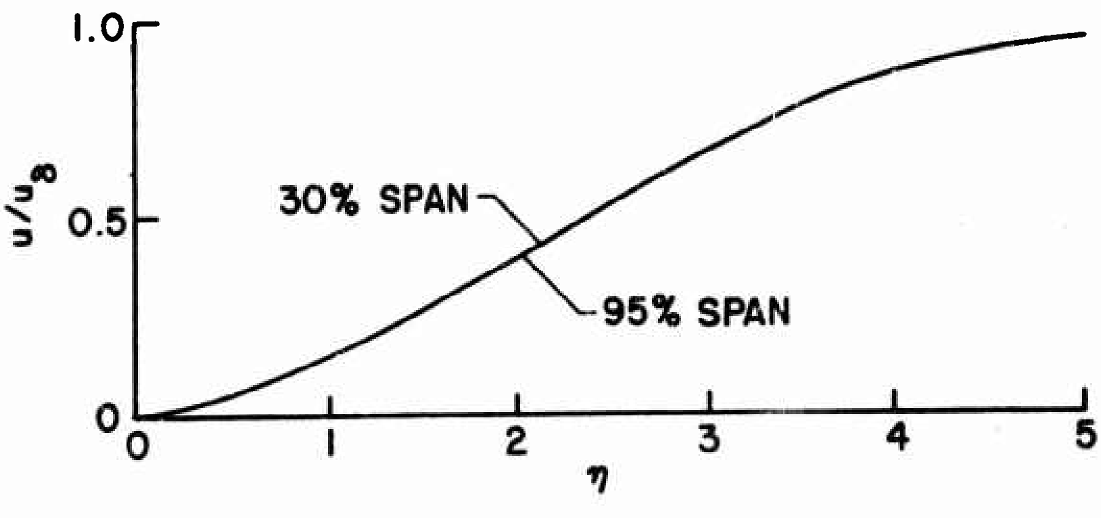

Figure 14. The Chordwise Velocity Profile for the 40-Foot Rotor (at 6 Degrees Blade Angle of Attack and 24.4% Chord) in Hover.

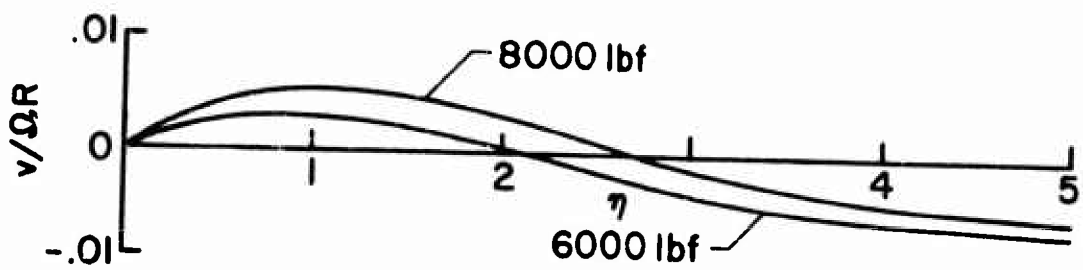

Figure 15. The Spanwise Velocity Profile for the 24-Foot Rotor (at 10% Chord and 60% Span) in Hover.

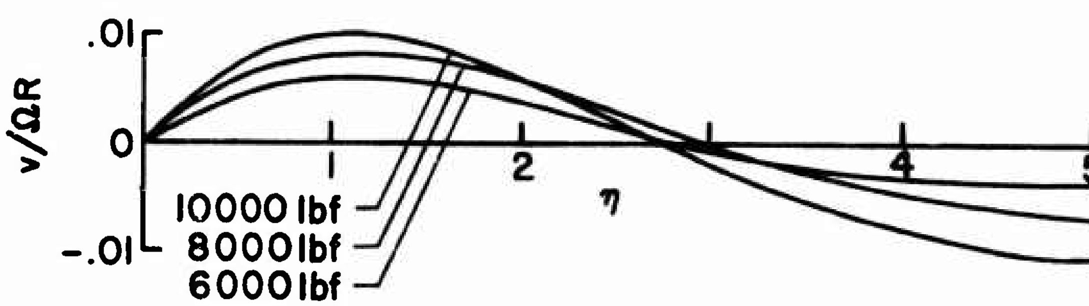

Figure 16. The Spanwise Velocity Profile for the 24-Foot Rotor (at 60% Span and Near Separation) in Hover.

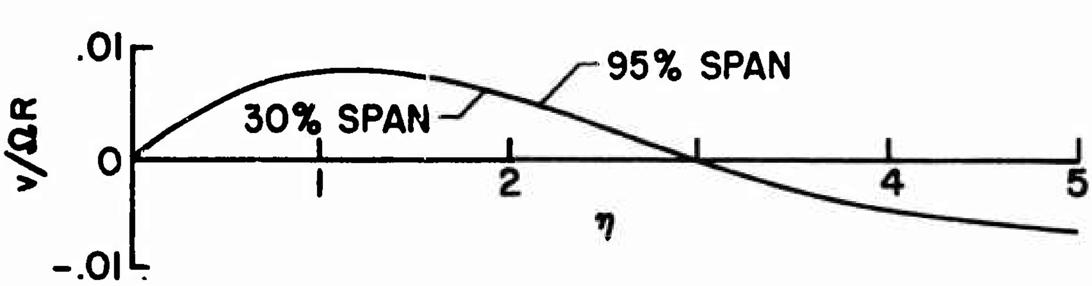

Figure 17. The Spanwise Velocity Profile for the 24-Foot Rotor (Near Separation and With 8000 lbf Thrust) in Hover.

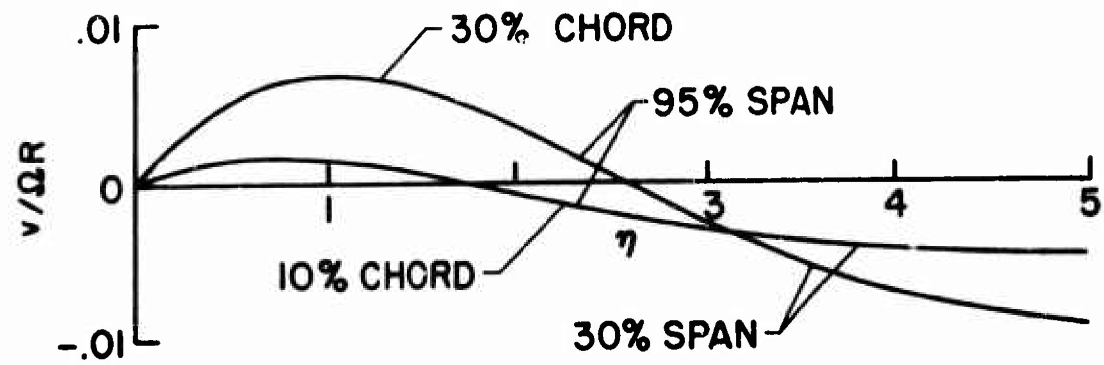

Figure 18. The Spanwise Velocity Profile for the 40-Foot Rotor (at Zero Degrees Blade Angle of Attack) in Hover.

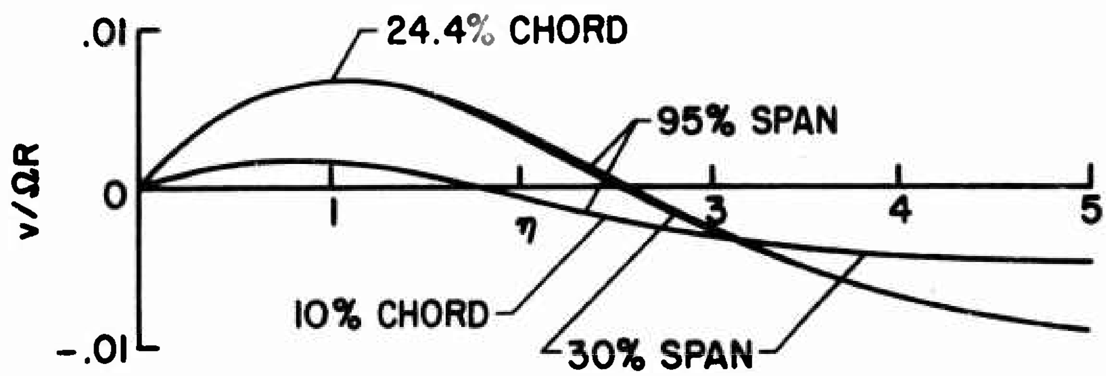

Figure 19. The Spanwise Velocity Profile for the 40-Foot Rotor (at 6 Degrees Blade Angle of Attack) in Hover.

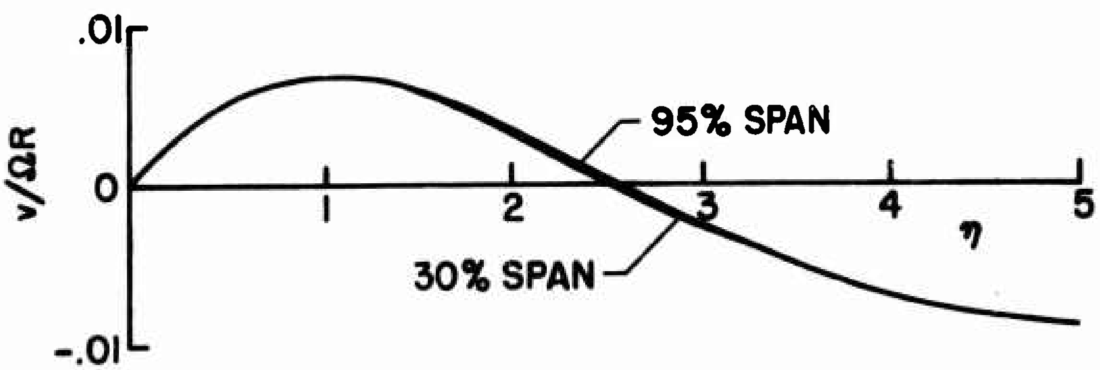

Figure 20. The Spanwise Velocity Profile for the 40-Foot Rotor (at 24.4% Chord and 6 Degrees Blade Angle of Attack) in Hover.

Figure 15 shows that an increase in thrust (a higher angle of attack) gives larger wall shear stress but smaller potential flow. Plotting velocity profiles as a function of η conceals some dependence on chord and span. The boundary layer displacement thicknesses δ_x (in the chordwise direction) and δ_y (in the spanwise direction) are nondimensionalized by a constant $\sqrt{\Omega/\nu}$. The equation for δ_y, for example, is

$$\delta_y = \sqrt{(x - x_I) / u_\delta}\, [\eta_{max} - \int_0^{\eta_{max}} (v / v_\delta)\, d\eta] \tag{78}$$

The term in brackets is very nearly independent of span,[16] but, through u_δ, the displacement thickness has the variation shown in Figures 21 through 28. The graphs begin at the leading edge of the airfoil ($x = 0$) in order to avoid the stagnation point. A true stagnation point occurs only in the chordwise potential flow. At the point where $u_\delta = 0$, rotational effects cause flow in the boundary layer. This was discussed in the arguments leading to Equation (38). Away from the stagnation point, the displacement thicknesses increase smoothly with chord. In some cases an upturn near separation can be detected. This is because the boundary layer thickness at separation becomes very large (in fact, the flow is not adequately described by a boundary layer there). The spanwise displacement thickness is larger than the chordwise, but the shape of the curves is similar. The spanwise graphs show a larger increase of thickness along the chord. In both cases the rate of increase along the chord increases with thrust (or angle of attack), but because of the greater length of the boundary layer, the final thickness is greater for smaller angles of attack (or lower thrust). The S shape of the spanwise velocity profiles can intuitively be seen to cause a greater displacement thickness than a chordwise profile, which has no reverse flow.

The chordwise momentum thicknesses (Figures 29 and 30) show much the same effects as the displacement thicknesses. The spanwise momentum thickness will decrease along the span and even become negative. Because of the S shape of the spanwise profile, the physical meaningfulness of the momentum thickness is lost.

To allow meaningful comparison between the two different rotors and to allow the implications of Equation (25) to be seen, the separation line in Figures 31 and 32 is plotted as a function of y (y is spanwise position/chord). The position of the separation line x_s is the distance along the surface measured from the leading edge of the airfoil. This separation line has the same criterion as in two-dimensional flow, but separation occurs in a different way. The description of separation that best fits the present case was given by Maskell[17] and is shown in Figure 33. The separation line is an asymptote of all the limiting streamlines (the streamlines on the surface of the blade).

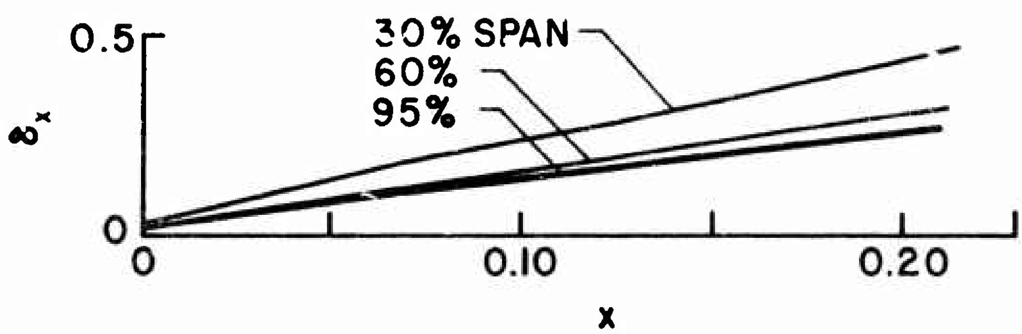

Figure 21. The Chordwise Displacement Thickness for the 24-Foot Rotor (at 6000 lbf Thrust) in Hover.

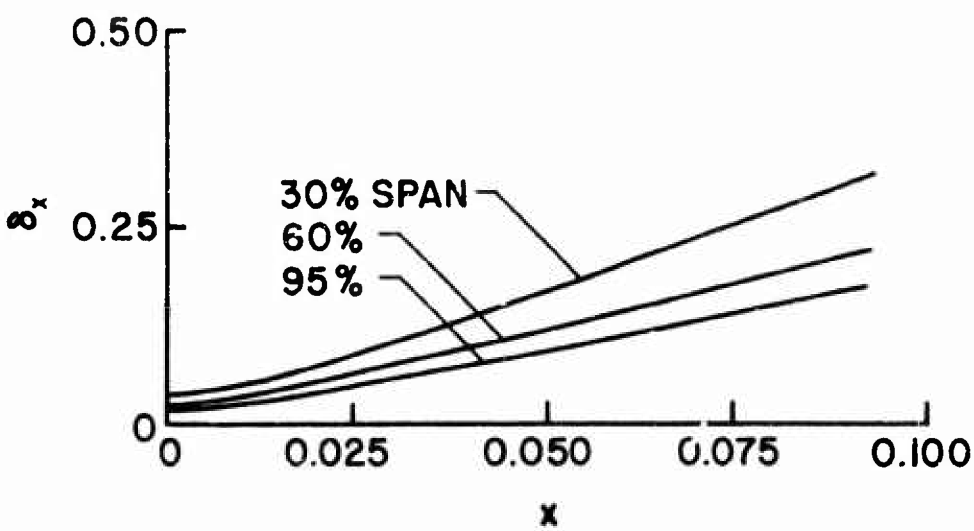

Figure 22. The Chordwise Displacement Thickness for the 24-Foot Rotor (at 10,000 lbf Thrust) in Hover.

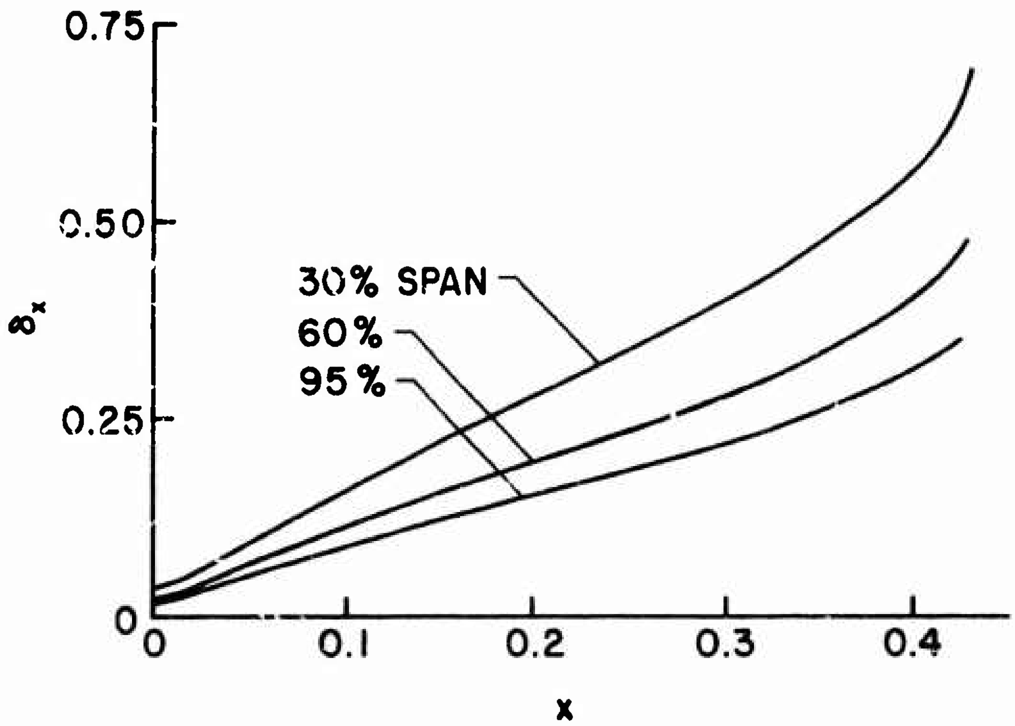

Figure 23. The Chordwise Displacement Thickness for the 40-Foot Rotor (at Zero Degrees Blade Angle of Attack) in Hover.

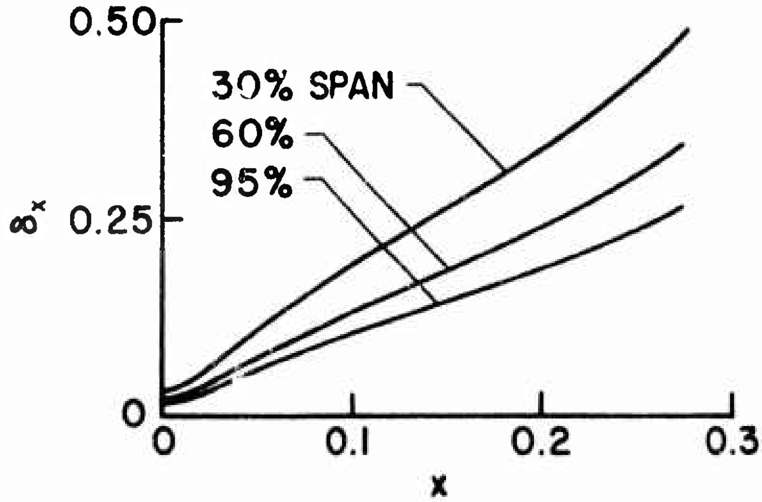

Figure 24. The Chordwise Displacement Thickness for the 40-Foot Rotor (at 6 Degrees Blade Angle of Attack) in Hover.

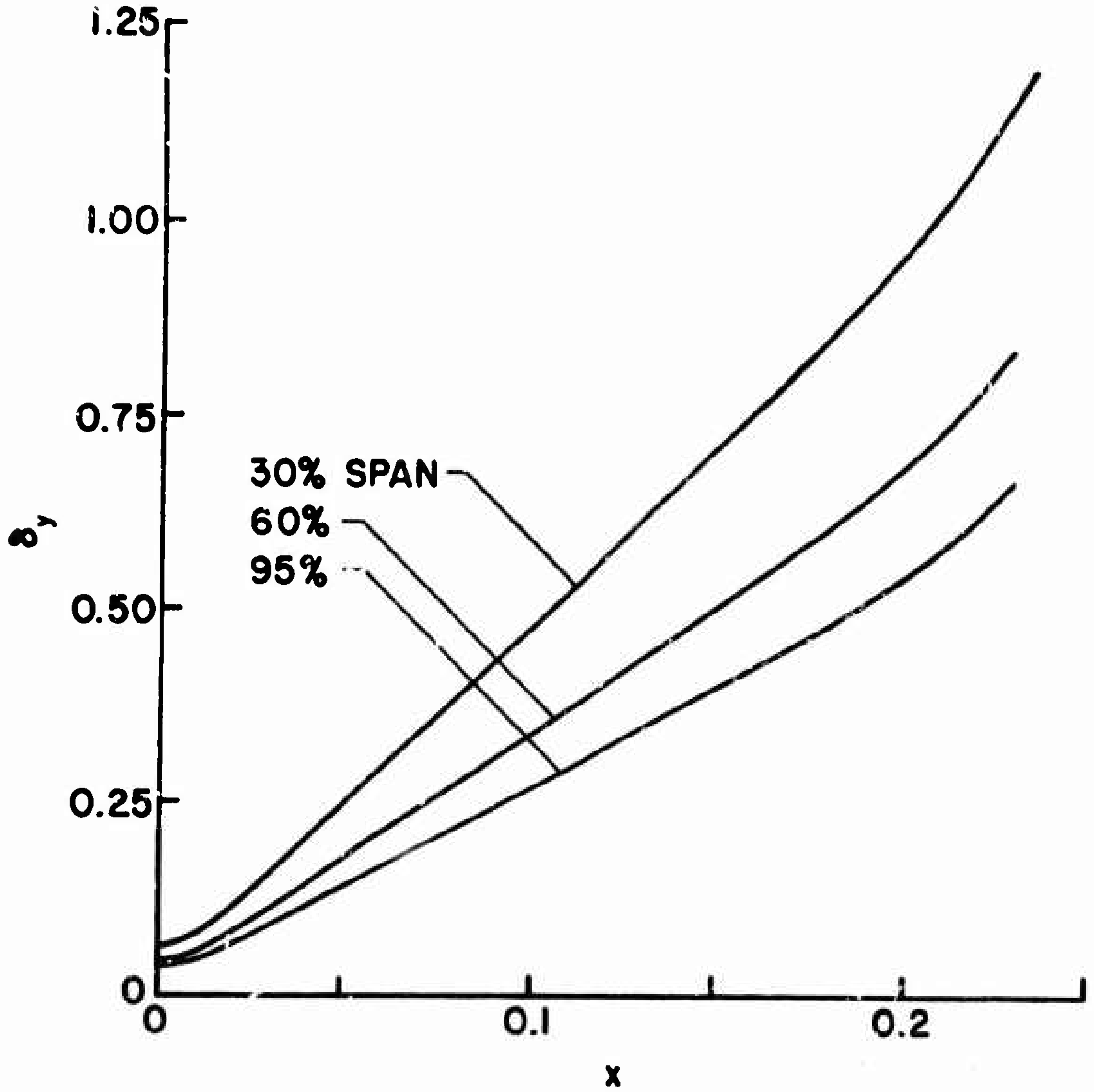

Figure 25. The Spanwise Displacement Thickness for the 24-Foot Rotor (for 6000 lbf Thrust) in Hover.

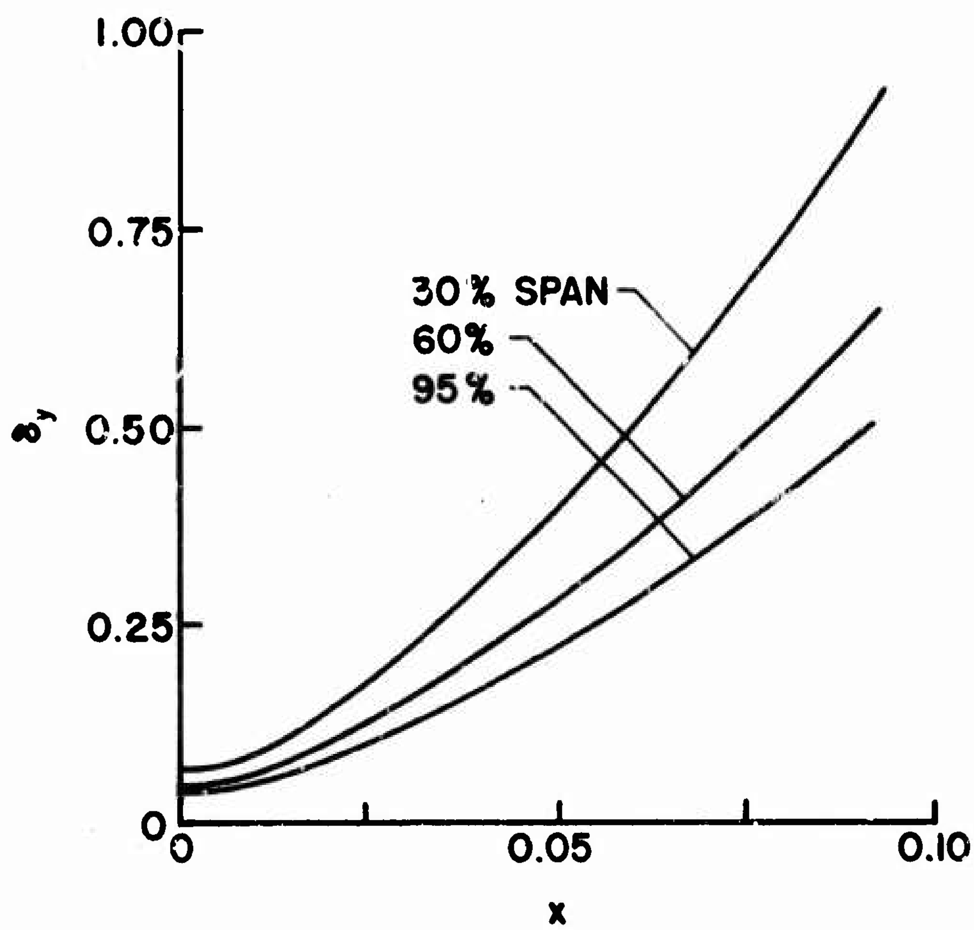

Figure 26. The Spanwise Displacement Thickness for the 24-Foot Rotor (for 10,000 lbf Thrust) in Hover.

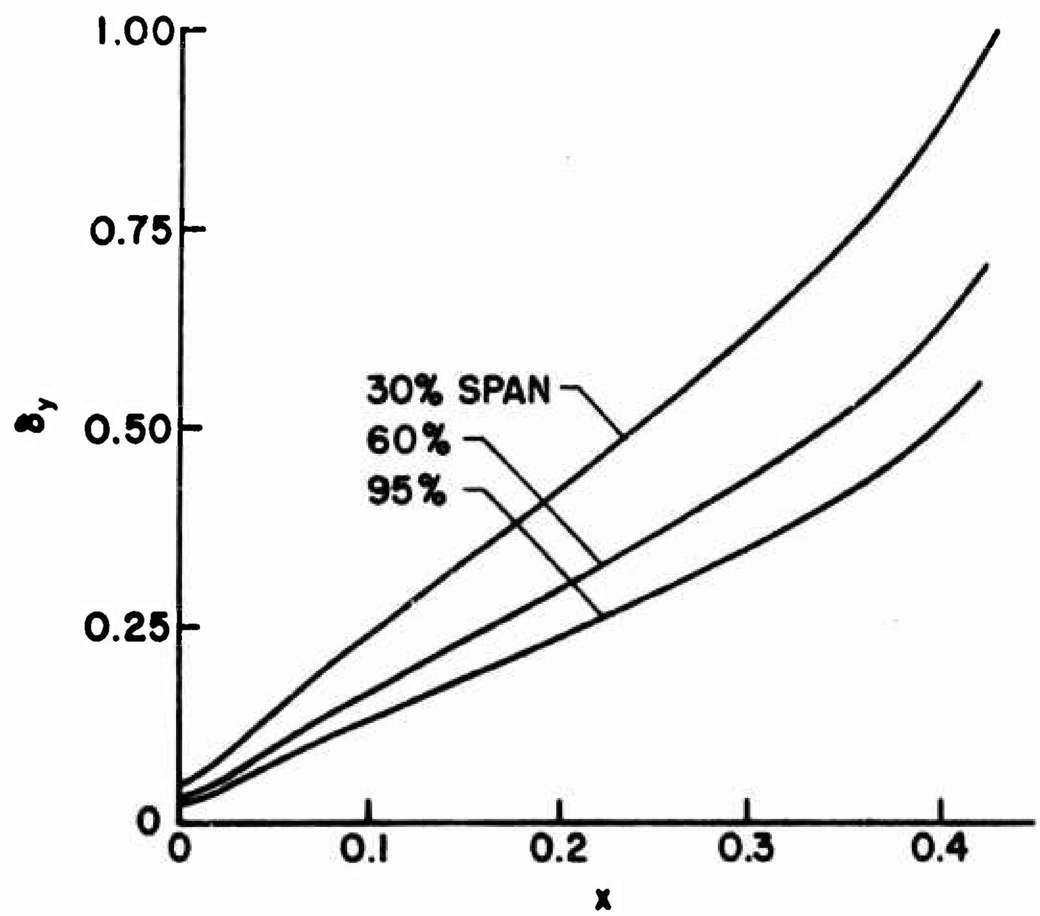

Figure 27. The Spanwise Displacement Thickness for the 40-Foot Rotor (at Zero Degrees Blade Angle of Attack) in Hover.

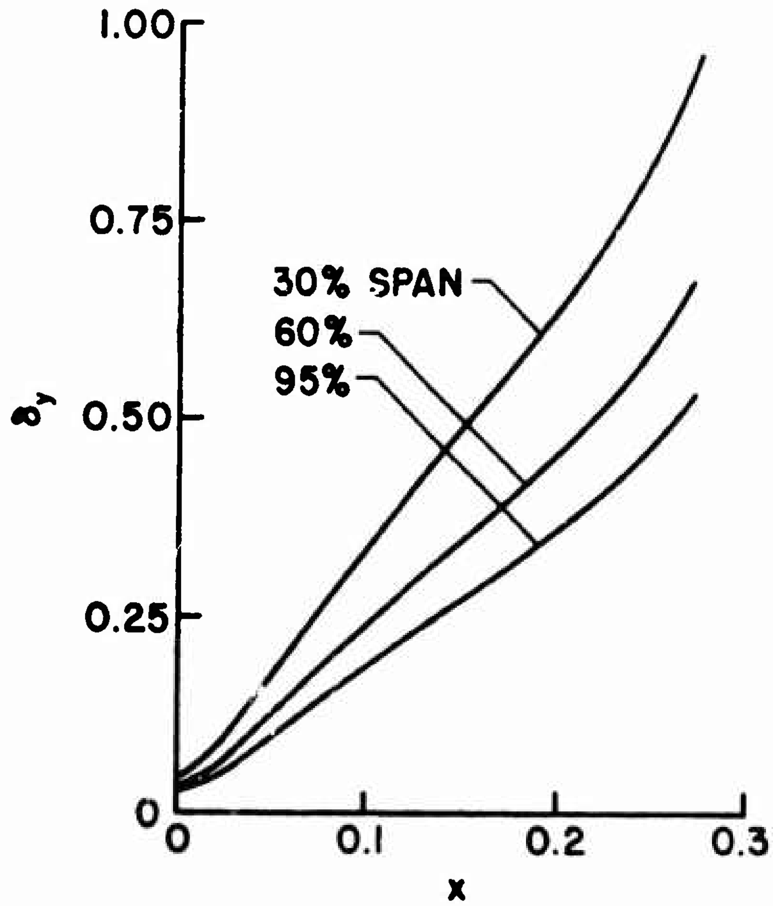

Figure 28. The Spanwise Displacement Thickness for the 40-Foot Rotor (at 6 Degrees Blade Angle of Attack) in Hover.

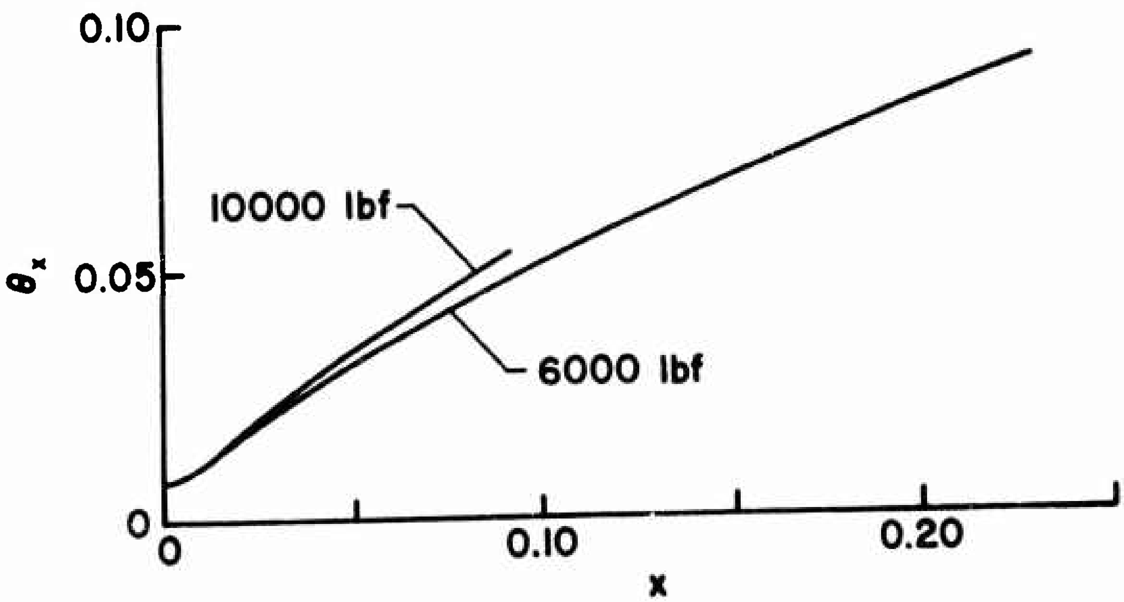

Figure 29. The Chordwise Momentum Thickness for the 24-Foot Rotor (at 60% Span) in Hover.

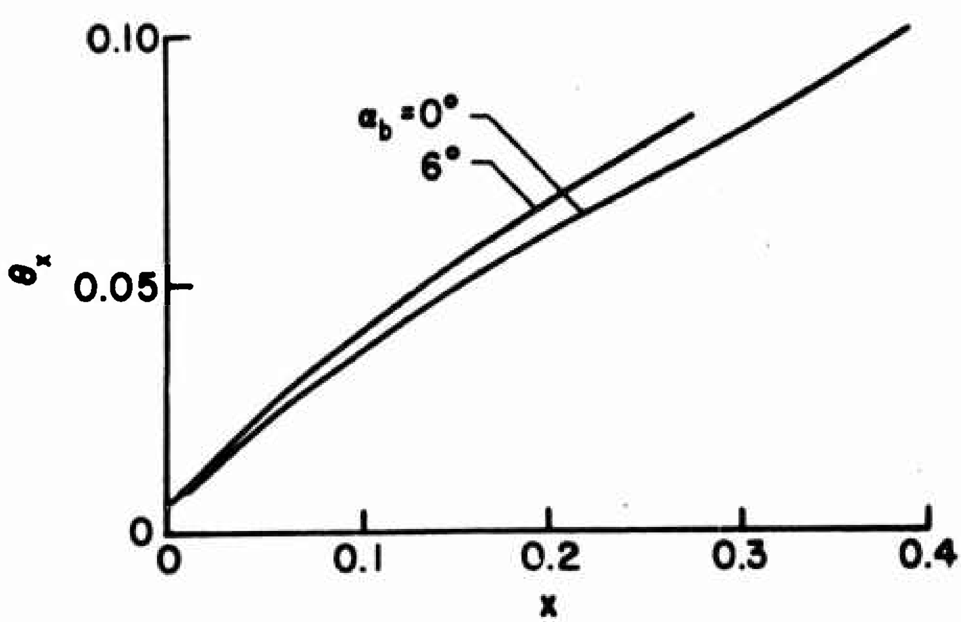

Figure 30. The Chordwise Momentum Thickness for the 40-Foot Rotor (at 60% Span) in Hover.

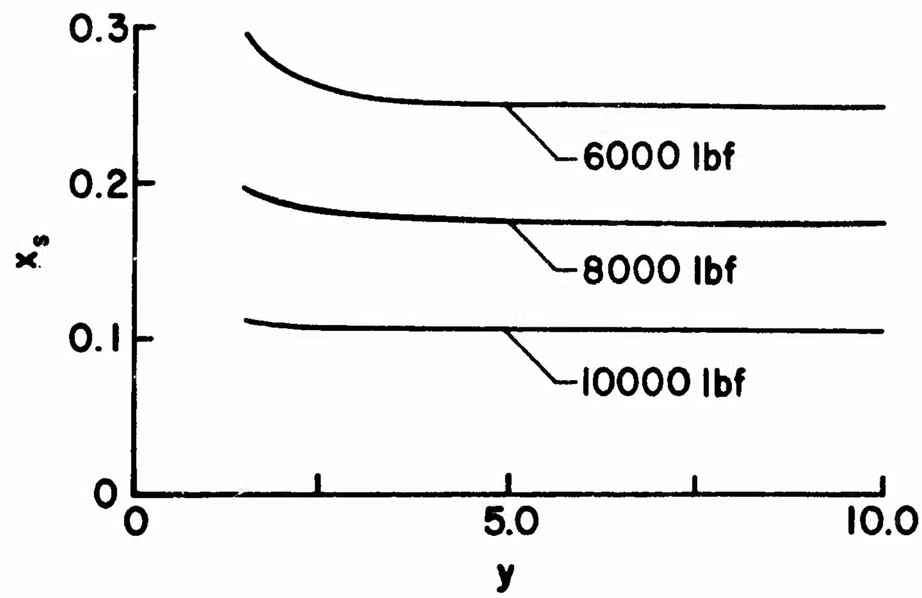

Figure 31. The Separation Line for the 24-Foot Rotor in Hover.

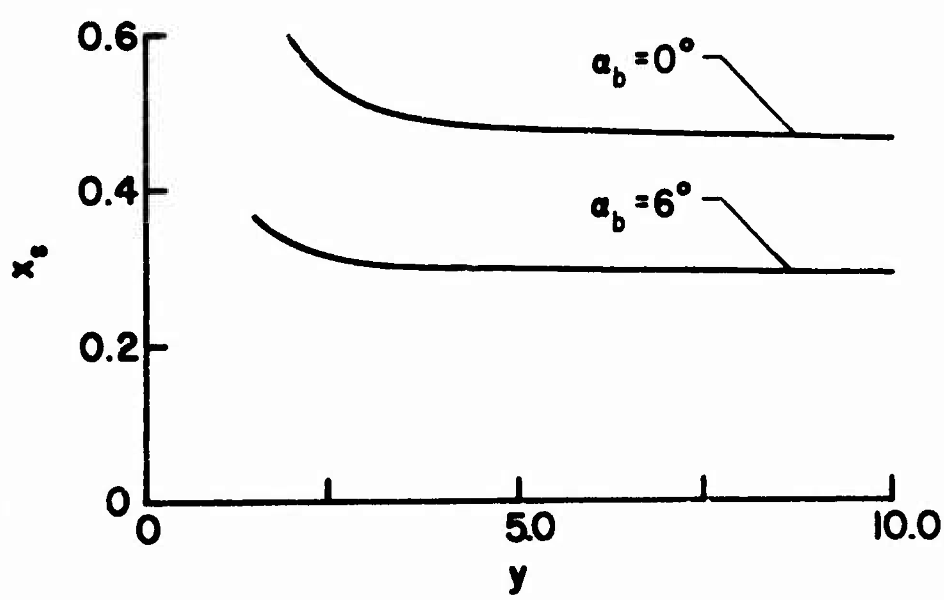

Figure 32. The Separation Line for the 40-Foot Rotor in Hover.

Because the streamline that lies on the separation line cannot carry an infinite amount of fluid (it is the asymptote for an infinite number of limiting streamlines), the limiting streamlines must leave the surface of the blade; *i.e.*, separation must occur. The skew angles (Figures 34 through 37) show how the streamline turn outward to approach the separation line. At smaller angles of attack the turn is more gradual, but in all cases an extension to separation would show the same type of approach to the separation line. The spanwise dependence can be better understood from the equation for skew angle:

$$\tan \beta = \lim_{\eta \to 0} \frac{v}{u} = \left. \frac{g''}{u_\delta f''} \right|_{\eta=0} \tag{79}$$

The y dependence in u_δ is the primary, but not the only, source of y dependence. A skew angle of 90° indicates outward flow parallel to the span. If the skew angle is zero, there is no spanwise flow at the surface.

The rotational effects are not large in the hover case, but much understanding of their effect can be gained. When forward flight is added to the problem, the complexity of the flow field obscures many of the basic phenomena.

FORWARD FLIGHT CASE

The results for the forward flight case are summarized in Table II. The aerodynamic angle of attack varies with span and time, so it may not be used to identify the conditions as in the hover case. If a graph is drawn with application to a specific helicopter, then the length of the rotor in feet R and either thrust in pounds force T or the geometric angle of attack in degrees α_b will be given. All results are understood to be for an 11.9%-thick symmetrical Joukowski airfoil with the axis of rotation at the quarter-chord point. The values for ξ_s and K_{nj} are more accurate than those in the hover case. This is due to the superior stability of Lew's method, which allows a closer approach to separation.

The results will be presented in parts. First, each factor that influences the separation line will be analyzed. A series of special cases will be used to investigate the various effects. The values of inflow and forward flight speed will be chosen for illustration and do not necessarily reflect realistic values. The second method of presentation of the results uses values of inflow, thrust, and forward flight speed for the two helicopters described in APPENDIX I. Plots of velocity profiles and the separation lines are presented in terms of parameters related to helicopters.

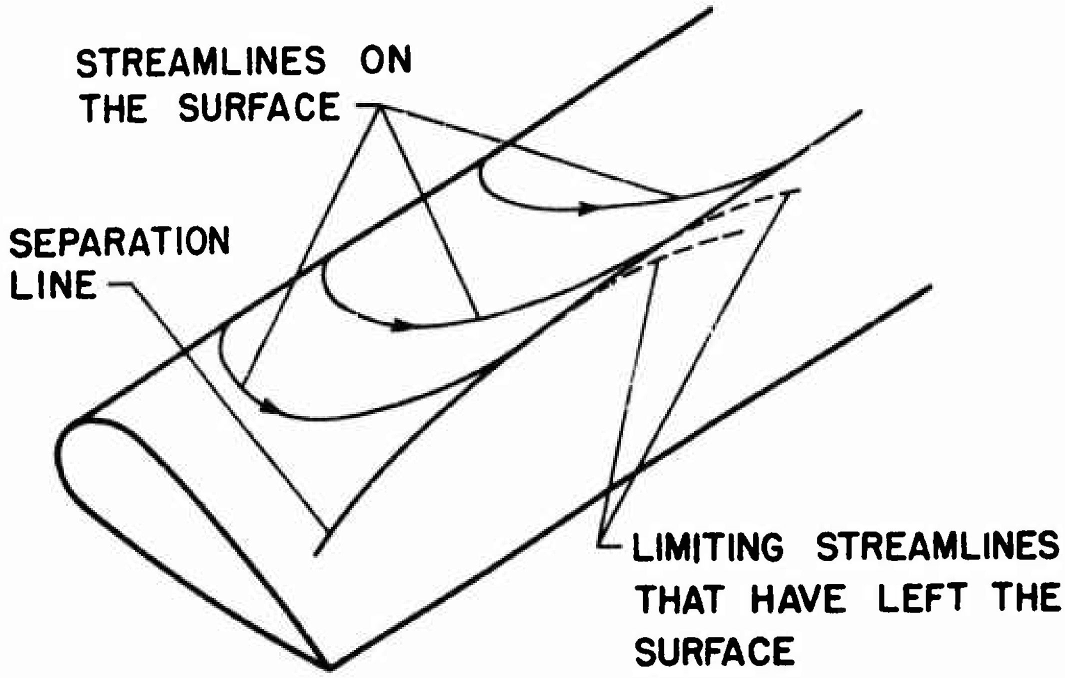

Figure 33. The Streamlines at Separation in the Hover Case.

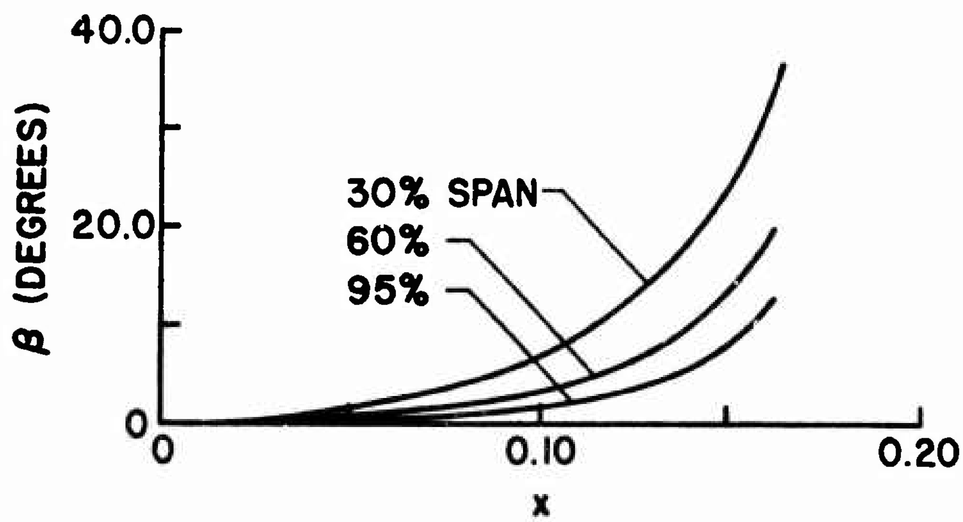

Figure 34. The Surface Skew Angle for the 24-Foot Rotor (at 8000 lbf Thrust) in Hover.

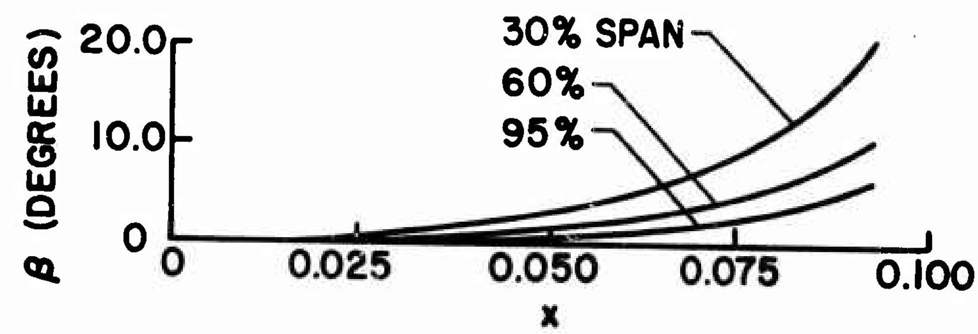

Figure 35. The Surface Skew Angle for the 24-Foot Rotor (at 10,000 lbf Thrust) in Hover.

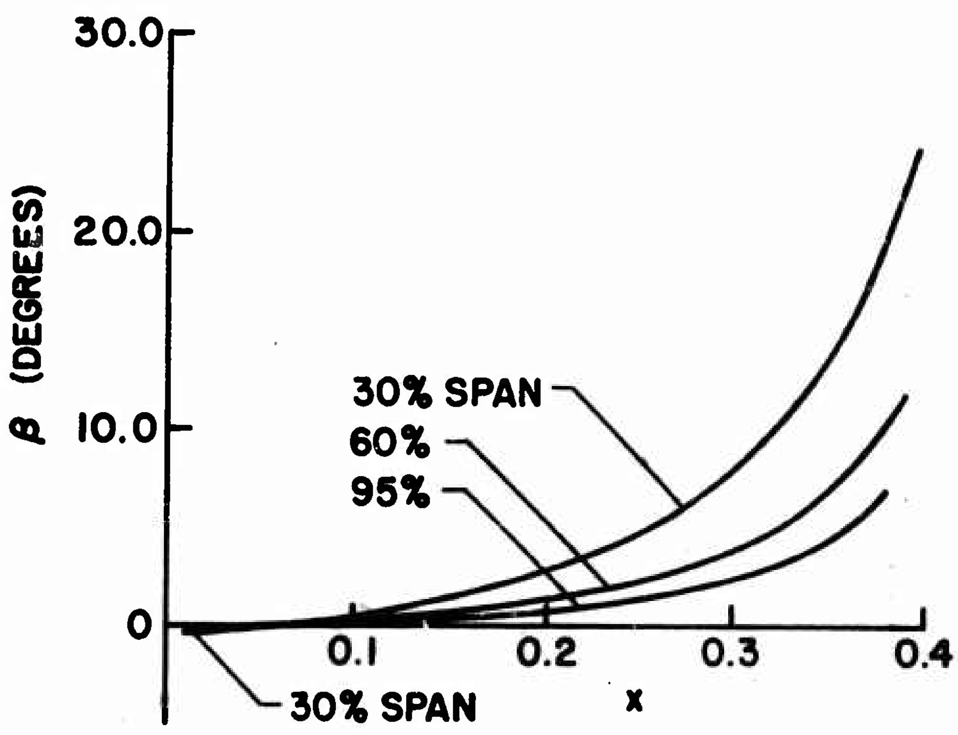

Figure 36. The Surface Skew Angle for the 40-Foot Rotor (at Zero Degrees Blade Angle of Attack) in Hover.

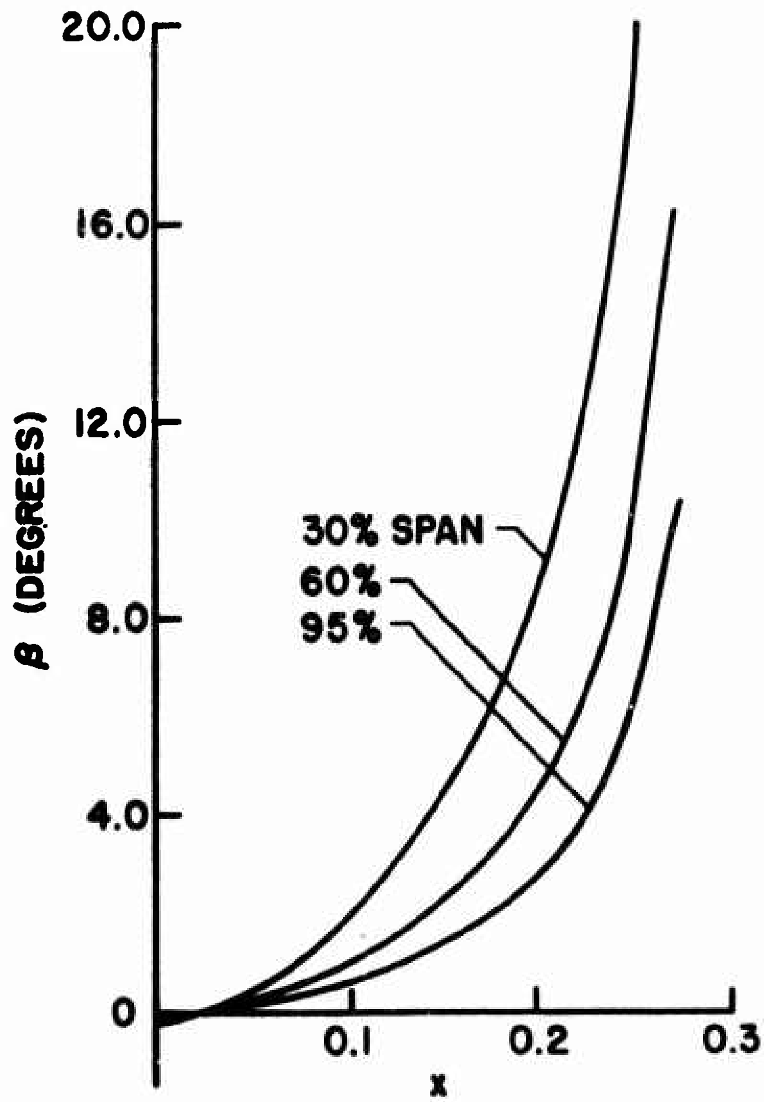

Figure 37. The Surface Skew Angle for the 40-Foot Rotor (at 6 Degrees Blade Angle of Attack) in Hover.

TABLE II. SUMMARY OF CALCULATED RESULTS FOR THE FORWARD FLIGHT CASE

α_b (deg)	R (ft)	χ_0	χ_{10}	χ_{20}	χ_{22}	ξ_s	K_{10}	K_{2Cr}	K_{2C}	K_{21}	K_{22}
.005	40	$-.161 \times 10^{-4}$	.1685	-.000706	-.1685	.440	7.18	.795	- 55.05	.423	- 7.19
2.0	-	-.00599	.1781	-.2667	-.1781	.323	10.4	.485	-122.4	.596	-10.46
3.349	24	-.01036	.1941	-.4084	-.1941	.244	15.01	.329	-252.6	.703	-15.05
4.0	40	-.01262	.2040	-.4631	-.2040	.201	18.80	.246	-368.7	.728	-18.82
4.465	24	-.01431	.2118	-.4971	-.2118	.170	22.15	.178	-447.5	.709	-22.15
5.581	24	-.0186	.2325	-.5631	-.2325	.1065	24.22	.0482	-86.0	.450	-24.13

Special Case of Zero Inflow and Forward Flight Speed

The solution for forward flight is particularly well suited to the evaluation of the effects of inflow and forward flight because both v_a and s_H appear explicitly in the equations. For example, if both s_H and v_a are set equal to zero, the separation line becomes

$$x_s = \chi_0 + \xi_s / (1 - K_{20r} / y^2) \tag{80}$$

However, this is not a physically realistic situation. In calculating the potential flow for the rotor blade under consideration, circulation sufficient to satisfy the Kutta condition was included. Yet by setting v_a equal to zero, the net sum of the inflow of all the blades in the rotor disk was made equal to zero. This situation is interesting, however, because of its similarity to the hover case. In the two cases, the equations for the separation line and F_0 have the same form. Also, F_{20} in the hover case is governed by the same equation as that for F_{20c} in the forward flight case. The two cases are not identical, however, because the spanwise flow due to G'_{00} is different.

In the forward flight case, the nonhomogeneous terms in Equation (62) for G'_{00} arise from both the pressure gradient terms and the Coriolis term. The term $\xi\mu_0^a$ comes from the product of u_δ and the x derivative of ϕ_a (v_δ depends on ϕ_a and X). The term $-\xi F'_0 c_0$ comes from both the Coriolis acceleration 2 $(u - u_\delta) \cos (\alpha - \alpha_b)$ and the product of u_δ and the x derivative of X. In the hover case an additional term, arising from $u_\delta \partial v_\delta / \partial x$, that depends on the inflow, appears. For the forward flight case, neither inflow nor forward flight speed appear explicitly in the reduced equations of motion. The nonhomogeneous terms in Equation (70) for F_{20r} (or F_{20} in the hover case) depend on the spanwise flow. The term $p_0\ c_0\ (\nu_0 - G'_{00})$ comes from the Coriolis acceleration of the spanwise flow due to rotation. The convective term $v\partial u / \partial y$ contributes the term $\xi F'_0 G'_0$, and the part of w due to G'_{00} gives rise to $\xi F''_0 G_{00} / 2$ through $w\partial u / \partial z$. The term $\xi\nu_0$ comes from $v_\delta \partial u_\delta / \partial y$.

For both v_a and s_H equal to zero, the aerodynamic angle of attack and the geometric angle of attack are identical and constant. Although the form of the separation line in this situation is the same as in the hover case, the values of K_2 and K_{20r} will not agree for the same geometric angle of attack because the inflow in the hover case will influence both the aerodynamic angle of attack (making it differ from the geometric) and the spanwise flow (through the part of $u_\delta \partial v_\delta / \partial x$ that arises from the inflow). However, if the values of K_2 are compared on the basis of aerodynamic angle of attack, it appears that separation is influenced more by the aerodynamic angle of attack than by the dependence of the inflow on the span.

Special Case of Zero Inflow

The present solution is formally valid for $v_a = 0$, even if s_H is not zero. This situation is as physically unrealistic as the previous one for blade angles of attack that give rise to lift. The zero blade angle of attack case was investigated by Young and Williams.[11] The present investigation is in agreement except for the value of ξ_s. Improvements in the computer program that allowed separation to be approached more closely, and improvements in the extrapolation technique, give better values for ξ_s and the constants for the separation line. The separation line for $v_a = 0$ is given by

$$x_s = \chi_0 + \xi_s / (1 - K_{20r} / y^2 - K_{21} T_1 / y^2) \tag{81}$$

In the present situation, the same effects operate to give the time dependence of the separation line as in Young and Williams[11], but α_b may be other than zero.

The spanwise flow contains an additional contribution, G_{01}', due to the yaw angle of the blade. This is the time dependent part of the spanwise flow, and it causes a Coriolis force which affects the chordwise flow. The nonhomogeneous terms in the equation for F_{21c} (Equation (72)) come from the Coriolis acceleration of the spanwise flow due to yaw ($-p_0c_0 + p_0c_0G_{\delta 1}'$); from the time dependent part of v in $v\partial u / \partial y$ ($-\xi F_0' G_{\delta 1}'$); from the time derivatives of the chordwise flow found in the terms $\partial u / \partial t$ and $\partial u_\delta / \partial t$ ($-\xi F_0'$ and ξ); from the time dependent part of the spanwise potential flow in $v_\delta \, \partial u_\delta / \partial y$ (ξ); and from the dependence of η on time in $\partial u / \partial t$ ($-\xi \eta F_0'' / 2$). Figure 38 shows that, as the angle of attack becomes larger than 2°, the magnitude of the oscillations of the separation line with azimuthal angle decreases. This is in agreement with a two-dimensional, time-dependent solution of Dwyer and McCroskey[6] on an NACA 0012 airfoil at 8° angle of attack which showed no time dependence of the separation line. The combined effects of rotation and forward flight, without inflow, seem to decrease in magnitude, but remain unchanged in character, as the angle of attack is increased.

The maximum displacement of the separation line occurs at $\psi = 0$. This is a 90° phase advance from the maximum of the velocity at the edge of the boundary layer, which occurs at $\psi = 90°$. The time dependence of the chordwise velocity resides partly in u_δ and partly in f'. Since separation occurs at the point where f" is zero, only the time dependence of the f' part appears in the equation for the separation line. At other points along the chord, the shear stress reflects the time dependence of both u_δ and f'. The phase advance (the angle γ between the maximum of the shear stress at the wall and the maximum of u_δ) has been calculated by Lighthill[18] for two-dimensional oscillatory flow. Lighthill based γ on the steady-state displacement thickness and shear stress, and specifically excluded the region near separation.

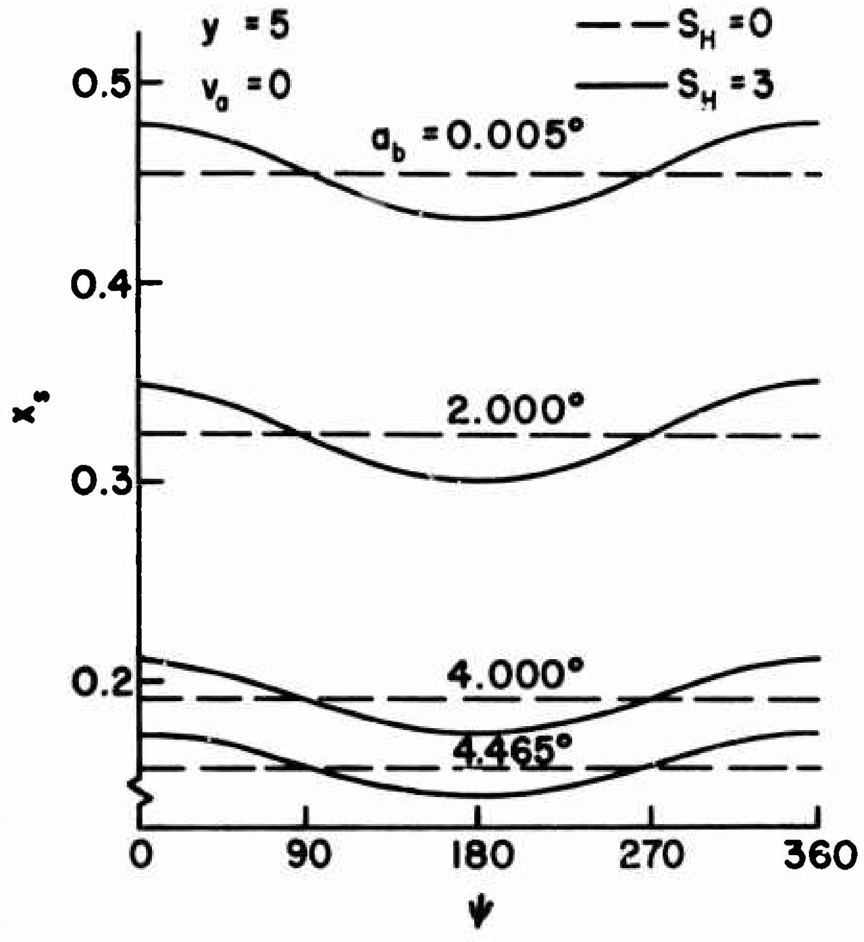

Figure 38. The Separation Line in Forward Flight for No Inflow.

Figure 39 shows that the trend of Lighthill's solution and the phase advance in the present solution are in general agreement for no inflow. A quantitative comparison is not justified because of the difference in the physical situation and the method of solution between the two cases. In the present solution, three-dimensional effects cause a phase shift in the chordwise pressure gradient, and the asymptotic series is formed quite differently from that of Lighthill.

Special Case of Zero Forward Flight Speed

Another special case may be isolated at this point; namely, the solution obtained by setting s_H equal to zero and retaining the inflow. This is basically a solution for hover but will differ from the previously presented hover case in that now the inflow is a constant. The constancy of the inflow causes the aerodynamic angle of attack to vary with span. The aerodynamic angle of attack is given in this case by

$$\alpha_a = \alpha_b - \tan^{-1} v_a / y \tag{82}$$

Relative to the chordwise flow, which increases with span, the downflow decreases as the span increases. This relative change is reflected in the potential flow both indirectly by a change in the position of the stagnation point and directly by a change in the importance of the potential flow function $\bar{u}_c$ relative to $\bar{u}_a$. Since the inflow was proportional to span in the previously considered hover case, these effects were not present.

The transform of the x coordinate into the ξ coordinate causes the terms in the series for f' of higher order than F_0' to be larger over most of the airfoil for the hover and forward flight cases. In the forward flight case, however, the function F_{10}' will be large even if the problem had been solved in the x, y, z coordinate system. The plot of F_{10}'' in Figure 40 demonstrates the behavior of the function. The large negative values behind the leading edge grow rapidly with angle of attack; for an α_b of 4.465, $F_{10}'' = -29.0$ at $\xi = .022$. At the large values of F_{10}'', the dominant effect is the change in the pressure gradient due to the change in the position of the stagnation point along the span. For the positive values of F_{10}'', the change in the pressure gradient due to the change in the importance of $\bar{u}_c$ relative to $\bar{u}_a$ becomes the largest influence on F_{10}''. In addition to F_{10}, the constant inflow gives rise to the function F_{20}. For comparison to F_{10}'', a plot of F_{20}'' is shown in Figure 41. The large magnitude of F_{20}'' is partly due to the nonhomogeneous terms in the equation for F_{20} being dependent on F_{10}. The magnitudes of F_{10}'' and F_{20}'' seem large in comparison to F_0''. The proper comparison, however, should be to $v_a F_{10}'' / \zeta$ and $v_a^2 F_{20}'' / \mu_0^a \zeta^2$.

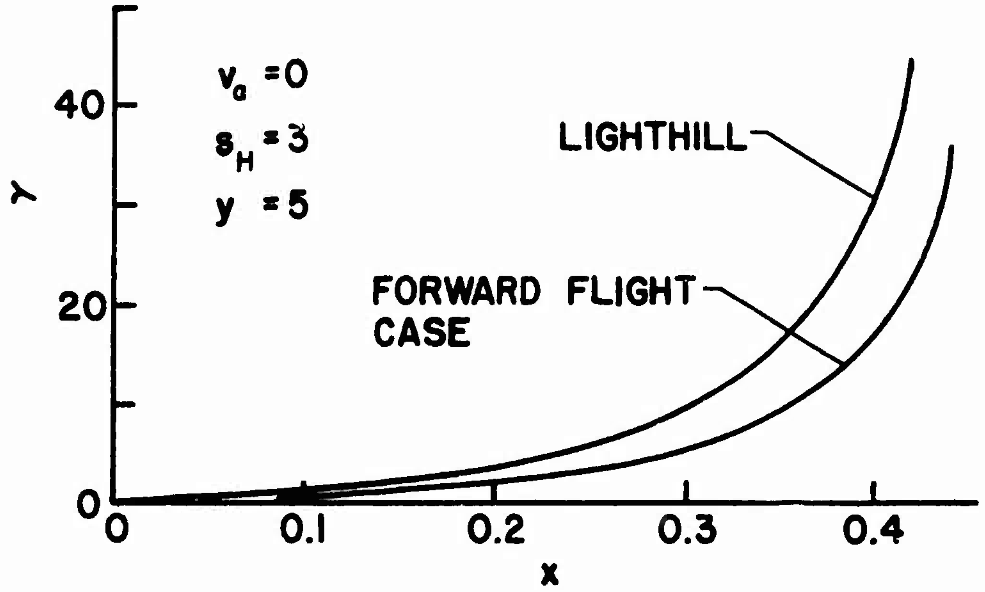

Figure 39. The Advance Angle (in Degrees) of the Shear Stress on the Surface.

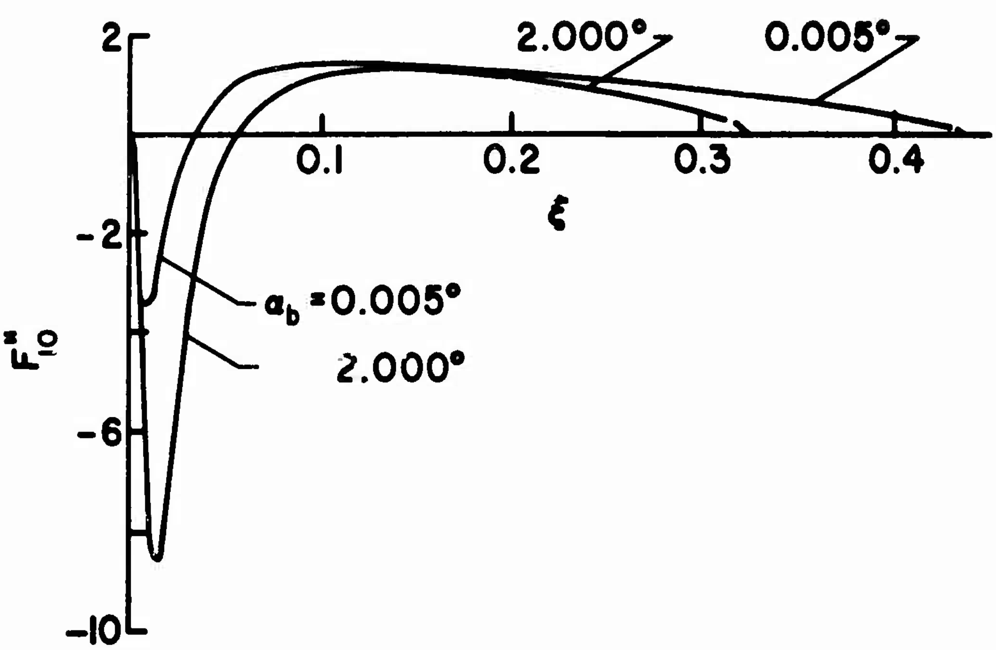

Figure 40. The Function F''_{10} on the Surface of the Blade.

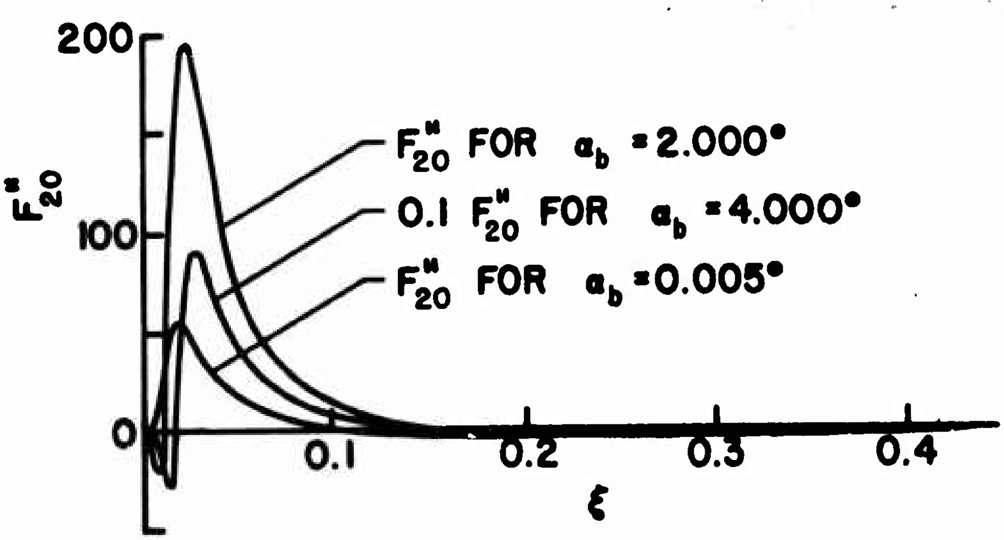

Figure 41. The Function F''_{20} on the Surface of the Blade.

Since v_a is small (typically .1), and since F''_{10} and F''_{20} are of opposite sign where they are largest, the infinite series for span may be accurate over the entire chord for values of span / chord as small as 3 or 4 for the present situation ($s_H = 0$). The functions F_{10} and F_{20}, through the constants K_{10} and K_{20}, affect the separation line through

$$x_s = \chi_0 + v_a\chi_{10}/y + v_a^2\chi_{20}/y^2 + \xi_s \,/\, (1 - v_aK_{10}/y - K_{20r}/y^2 - v_a^2K_{20}/y^2) \tag{83}$$

As shown in Table II, K_{10} and K_{20} are of opposite sign. Separation is delayed by K_{10} and advanced by K_{20}, so that their effect is to tend to cancel each other. Both increase in magnitude as the angle of attack increases in such a way that the net effect on separation is delay (except for values of span so small as to cast doubt on the accuracy of the series). Figure 42 shows the separation line as a function of span for $s_H = 0$. The situation of large inflow at near zero angle of attack is not realistic, but it is included for completeness.

The effect of the constant inflow is to delay separation, and this delay is increased as span decreases. At least part of this effect is due to the increase in aerodynamic angle of attack as span decreases. The importance of the aerodynamic angle of attack may be assessed from Figure 43. When the forward flight speed is zero, the results for the two different cases agree very well when compared on the basis of aerodynamic angle of attack. The inflow affects the separation line almost entirely through a change in the aerodynamic angle of attack in the hover case (with inflow proportional to span) and in the forward flight case (with $s_H = 0$), which has constant downflow.

General Case With Inflow and Forward Flight

Combining the effects of inflow and forward flight introduces one function that has not yet been considered, F_{22}. It has the value $-\mu_0^a F_{10}$ and arises from the combined action of the constant inflow and the time dependence due to forward flight. It is not present unless both are acting simultaneously. Its effect on the separation line is shown in Figure 44. As the inflow increases, the mean (with respect to time) position of the separation line is moved rearward on the airfoil. Also, the oscillations about this mean separation line increase in magnitude, and the maxima and minima occur at smaller values of azimuthal angle. For no inflow, the time dependence of the flow is dominated by time derivatives of the chordwise velocity.[6,11] This effect is represented by the function F_{21c}, which has the coefficient cos ψ. As the inflow increases, the function F_{22c}, with the coefficient sin ψ, becomes important.

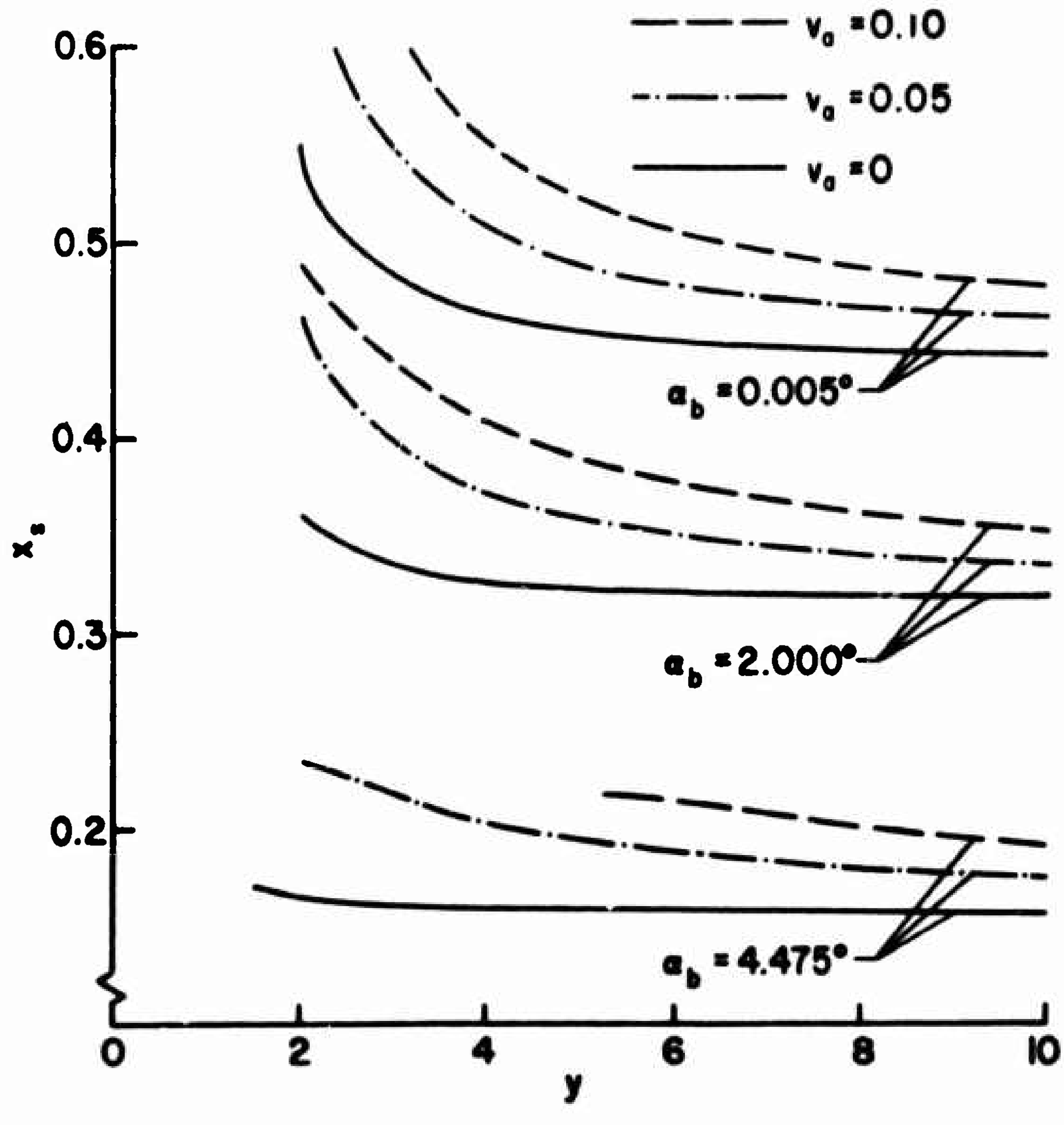

Figure 42. The Separation Line as a Function of Span and Inflow for No Forward Flight.

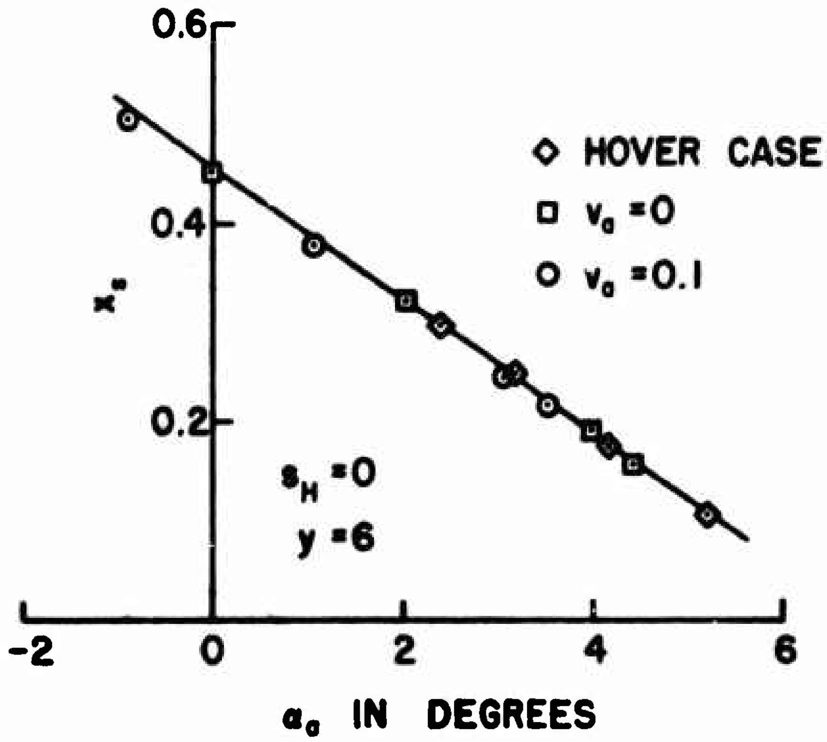

Figure 43. Separation Points With and Without Inflow for No Forward Flight.

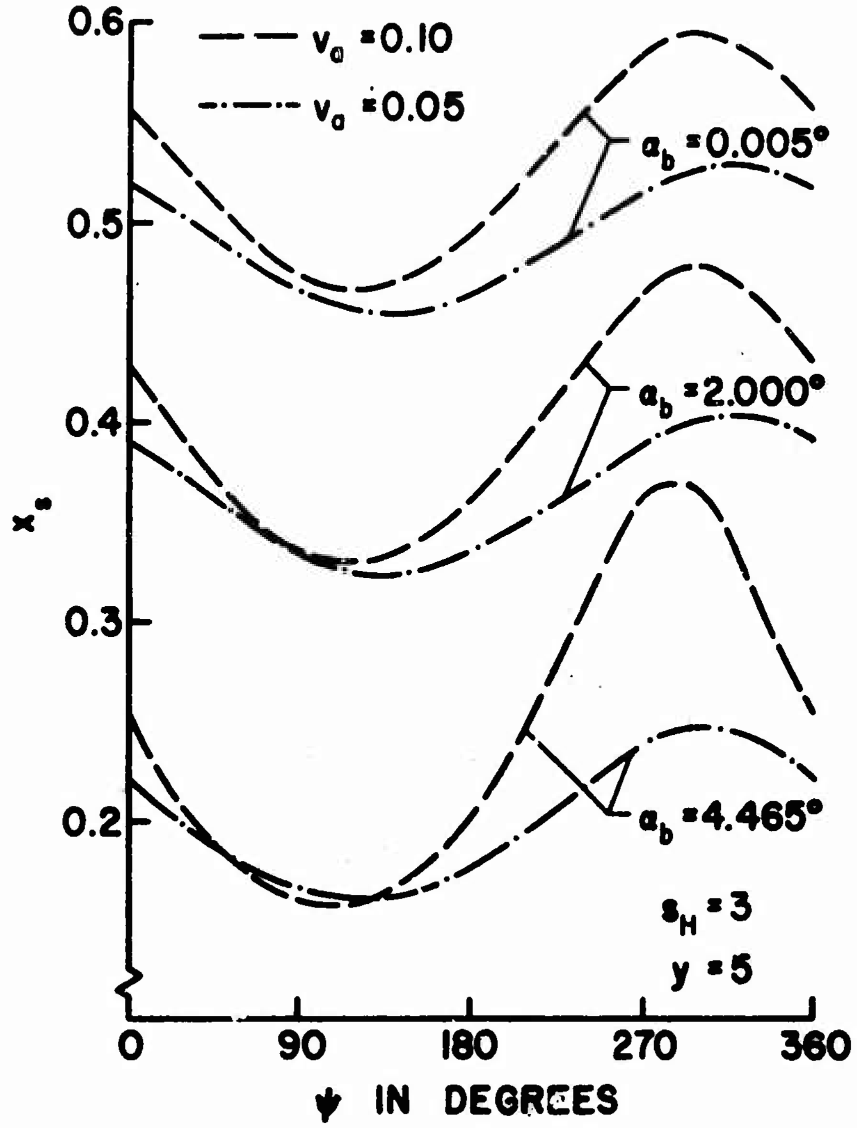

Figure 44. The Separation Line as a Function of Azimuthal Angle and Inflow.

This function increases the magnitude of the oscillations and causes the phase shift in the separation line. The forward flight speed and the inflow cause a change with time of the aerodynamic angle of attack which is given by

$$\alpha_a = \alpha_b - \tan^{-1}\left(v_a / (y + T_2)\right) \tag{84}$$

The aerodynamic angle of attack is a minimum at $\psi = 270°$. This is a result of the simplifying assumptions imposed to obtain a tractable solution. For an actual helicopter, the blade angle of attack is maximum at $\psi = 270°$ due to cyclic pitch. As the inflow increases, the maximum of the separation line moves away from 360° toward 270°. For zero forward flight speed, the inflow did not significantly affect the relationship between separation and aerodynamic angle of attack. From Figure 45, it can be seen that this is not true in forward flight. Going from $\psi = 0$ to $\psi = 360°$ is equivalent to traversing the closed curves in a clockwise direction. For no inflow, the aerodynamic angle of attack is constant, and the separation point is represented by a straight vertical line. This time-dependent behavior of the separation line could not be found except by considering rotation, inflow, and forward flight simultaneously. It must be ascribed to an interaction of all three.

General Case of Two Specific Helicopters

The values of inflow, thrust, and angle of attack have been calculated in APPENDIX I for two specific helicopters. There are, of course, other effects that are not included in the present analysis. Only special forms of time dependence, those due to forward flight, can be handled. The aerodynamic angle of attack has been calculated without taking into account blade twist or flapping. Due to these factors and others discussed in the theory, the results may not be applied directly to a helicopter rotor. For example, results are shown at various values of span. At 60% span, the assumption of no end effects is defensible. At 95% span, the results still properly represent the effects which the present work is investigating, but the end effects, which this theory cannot calculate, will have to be accounted for in some other way.

The chordwise velocity profiles are shown in Figures 46 through 55. The general shape is that of Falkner-Skan profiles. Figures 50 and 51 show that the effect of forward flight speed is small at $\psi = 90°$. Graphs of the separation line will show the effects of forward flight speed more clearly. The dependence of the chordwise velocity profiles on azimuthal angle shown in Figures 52 and 53 will grow larger if the span is decreased or the separation point is approached. At 45° and 135°, similar values are found for the aerodynamic angle of attack. The aerodynamic angle of attack at 225° is about the same as at 315°.

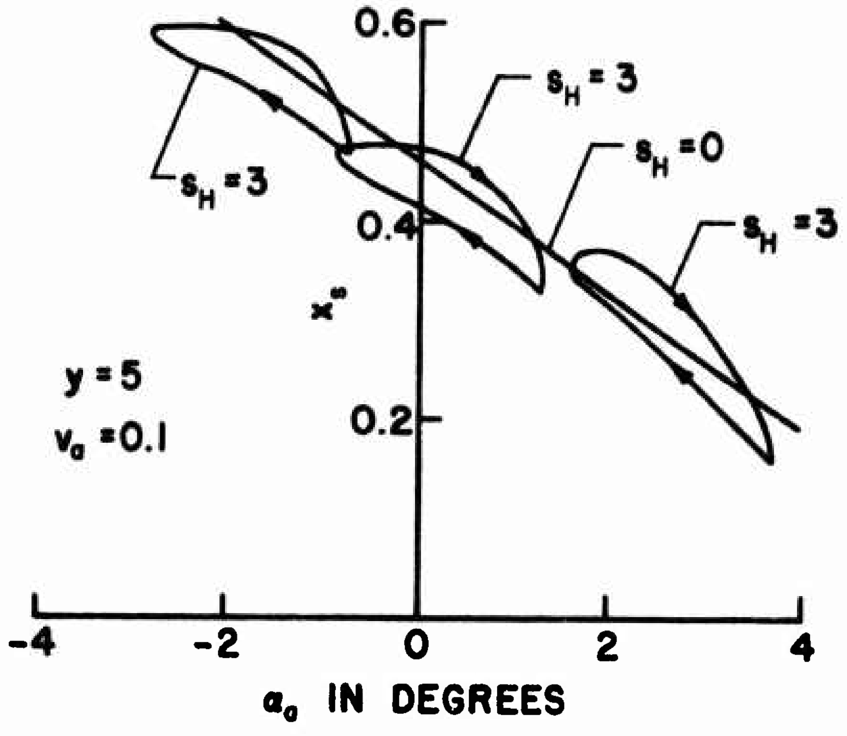

Figure 45. The Separation Line as a Function of Aerodynamic Angle of Attack in Forward Flight With Lift.

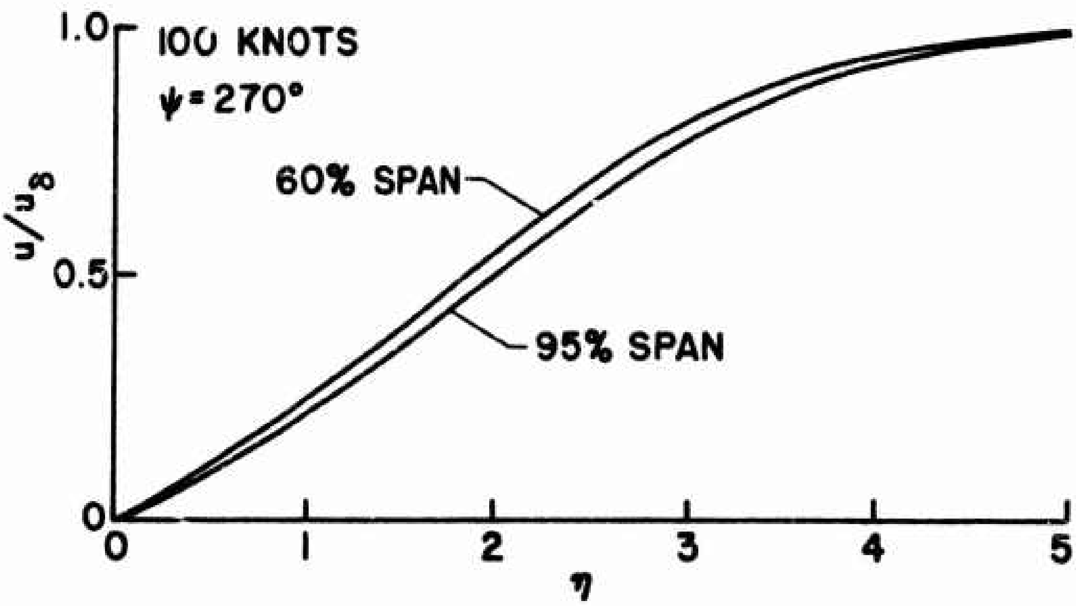

Figure 46. The Chordwise Velocity Profile for the 24-Foot Rotor (at 8000 lbf and 10% Chord).

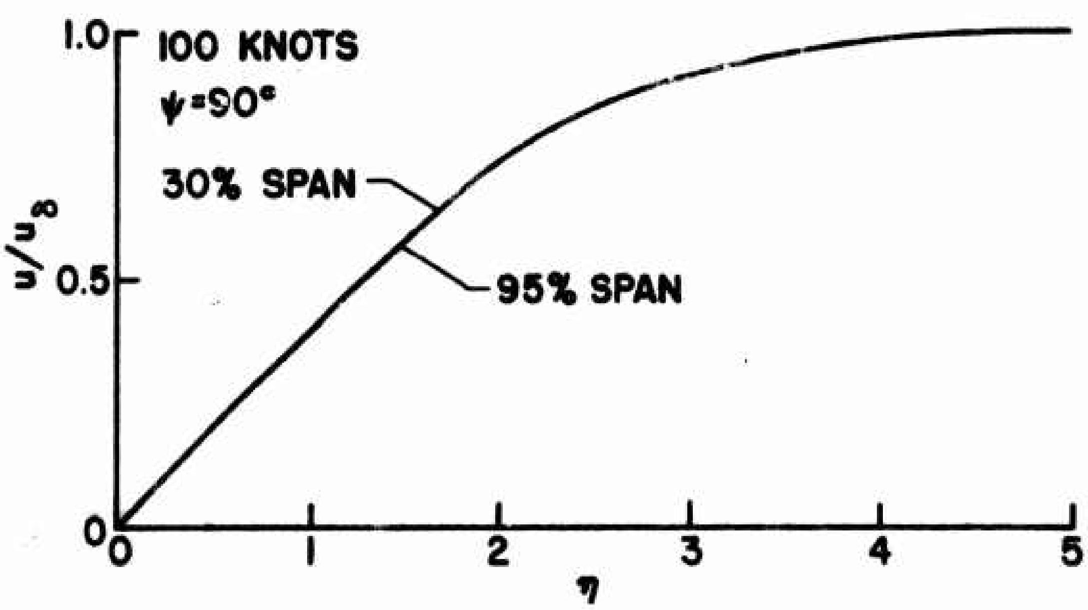

Figure 47. The Chordwise Velocity Profile for the 40-Foot Rotor (at Zero Degrees Blade Angle of Attack and 10% Chord).

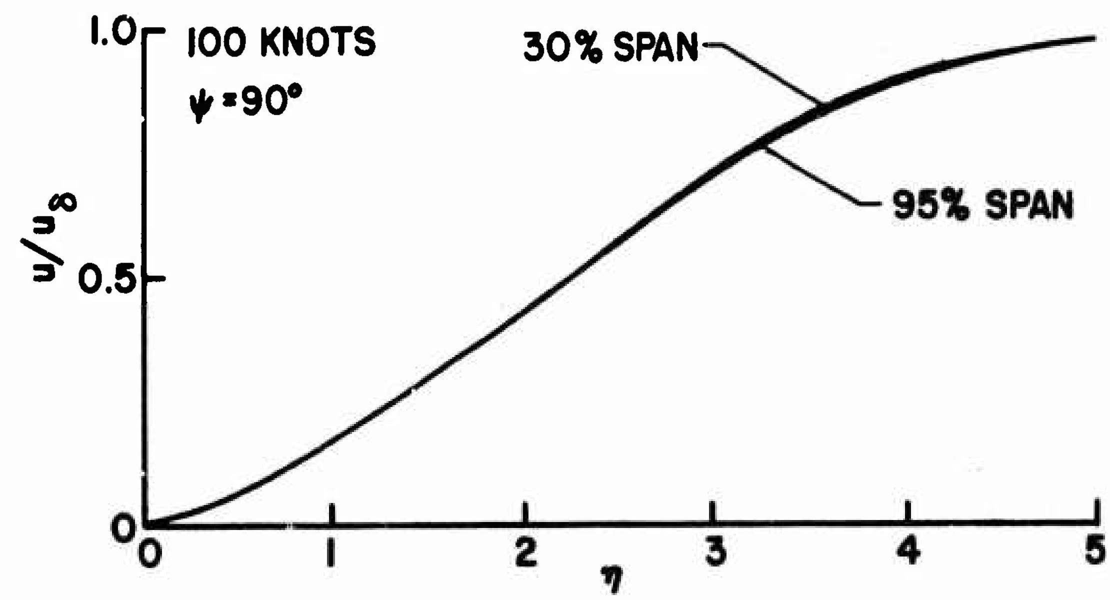

Figure 48. The Chordwise Velocity Profile for the 24-Foot Rotor (at 8000 lbf and 12% Chord).

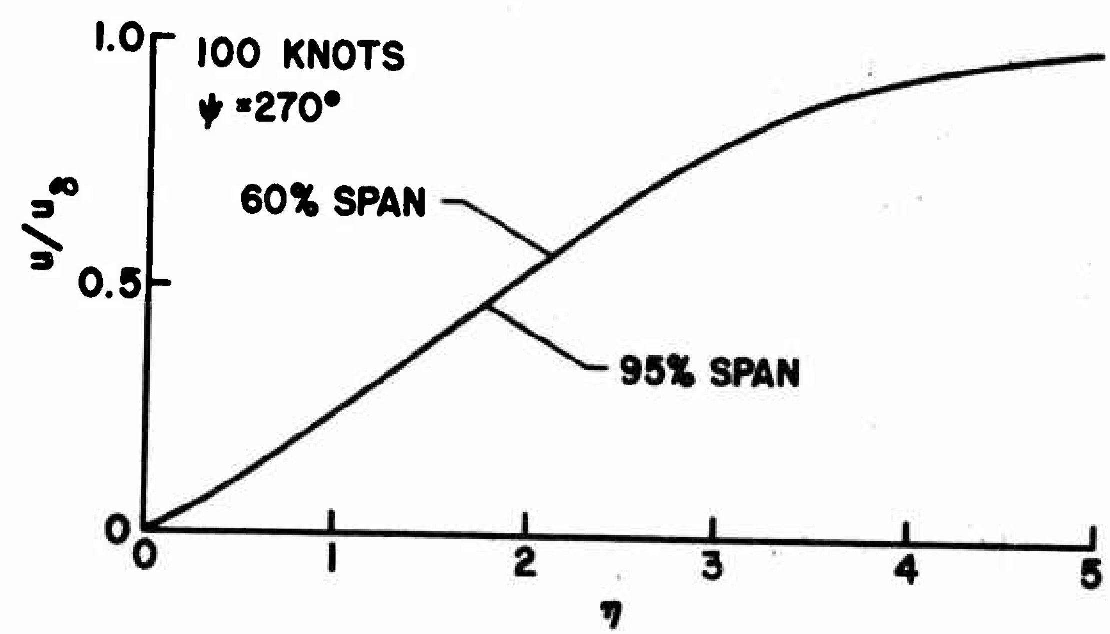

Figure 49. The Chordwise Velocity Profile for the 40-Foot Rotor (at Zero Degrees Blade Angle of Attack and 30% Chord).

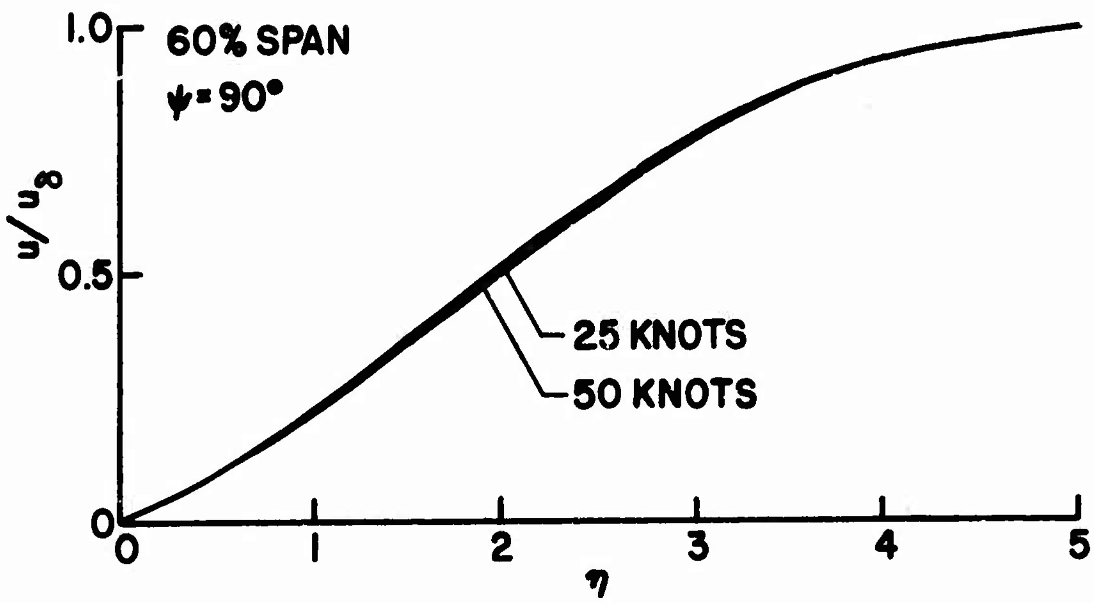

Figure 50. The Chordwise Velocity Profile for the 24-Foot Rotor (at 8000 lbf, 60% Span, and 10% Chord).

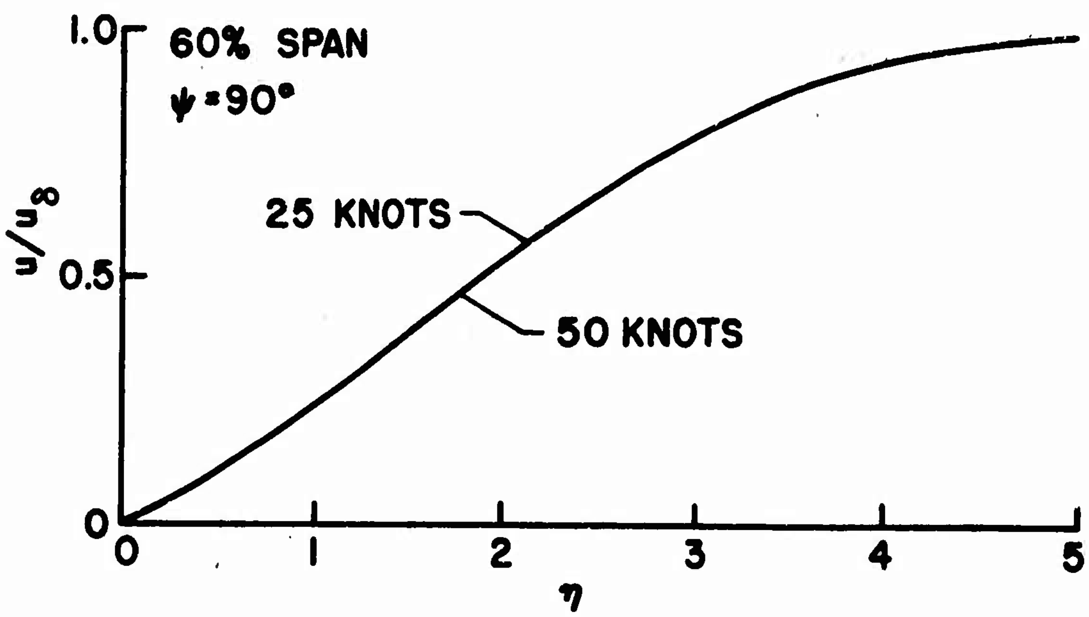

Figure 51. The Chordwise Velocity Profile for the 40-Foot Rotor (at Zero Degrees Blade Angle of Attack, 60% Span, and 30% Chord).

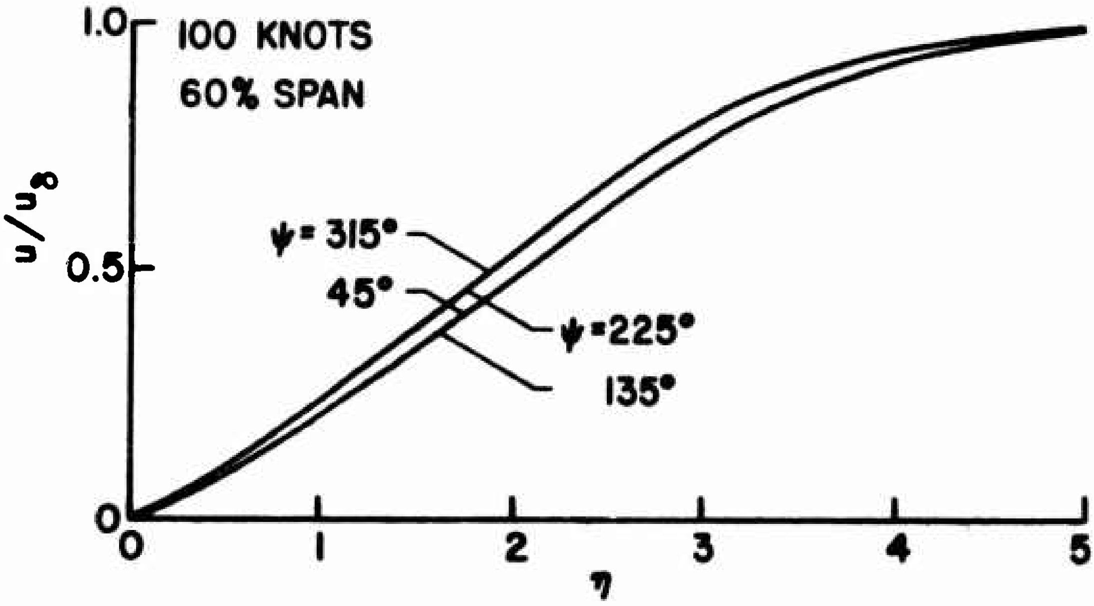

Figure 52. The Chordwise Velocity Profile for the 24-Foot Rotor (at 8000 lbf and 10% Chord) in Forward Flight.

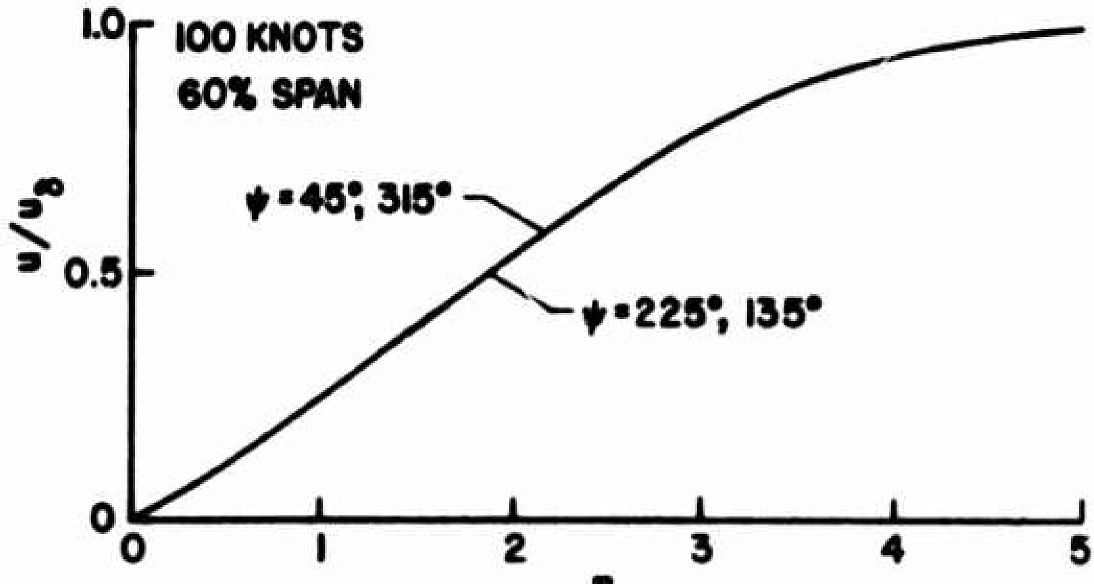

Figure 53. The Chordwise Velocity Profile for the 40-Foot Rotor (at Zero Degrees Blade Angle of Attack and 30% Chord) in Forward Flight.

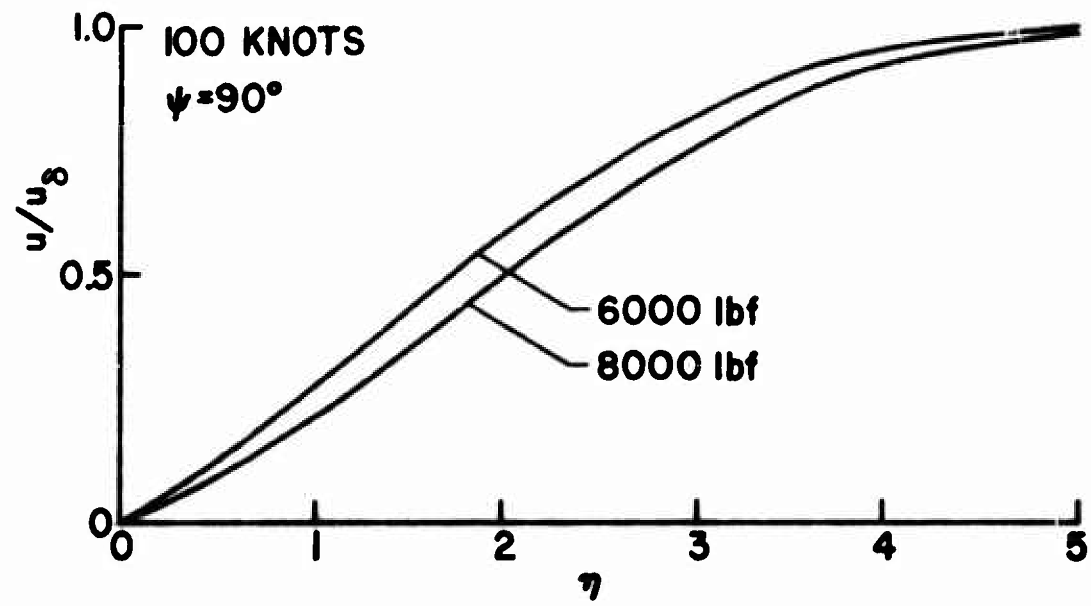

Figure 54. The Chordwise Velocity Profile for the 24-Foot Rotor (at 10% Chord and 60% Span) in Forward Flight.

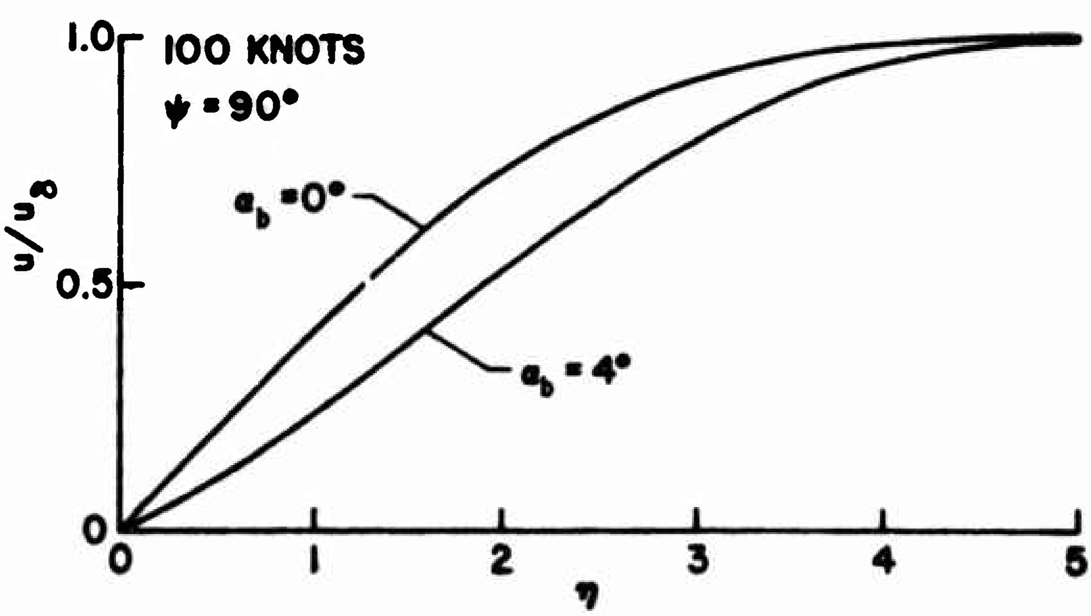

Figure 55. The Chordwise Velocity Profile for the 40-Foot Rotor (at 10% Chord and 60% Span) in Forward Flight.

The pattern of the aerodynamic angle of attack with azimuthal angle is reversed from normal helicopter operation (since flapping is not included), but the implication that time derivatives and spanwise flow are not dominant over angle of attack will apply. Figures 54 and 55 indicate that fuller profiles occur at smaller angles of attack for a given spanwise and chordwise position.

From Figures 56 through 64, the characteristics of the spanwise velocity profiles can be seen. Figures 56 through 59 show that the spanwise variation is greater at 270° than at 90°. Figure 57 does not have the characteristic S shape because the centrifugal forces have not yet caused positive values near the wall. The points $\psi = 90°$ and $\psi = 270°$ are not typical points; the spanwise flow due to yaw is zero there. Figures 60 and 61 show clearly that the flow due to forward flight dominates the flow due to rotational effects. At 45° and 315° there is outward spanwise flow, and at 135° and 225° there is inward spanwise flow. This flow is so much larger than the induced flow due to rotation that a larger scale is required. Near the wall, however, an asymmetry between the upper and lower curves can be detected. This is due to rotational effects; or more precisely, it is not due to the yaw angle. There is some dependence on forward flight at 90° or 270° due to the time derivative of spanwise velocity and due to the combination of inflow and forward flight (from Equations (67) and (68)). Figures 62 and 63 show that at 90°, these effects are small.

The dependence of the chordwise displacement thickness on azimuthal angle, shown in Figure 65, is much larger than that seen in the velocity profiles (Figures 52 and 53). In the velocity profiles, this time dependence (or dependence on azimuthal angle) is contained in the variable η, and so cannot be seen on the graph. In Figure 65, this time dependence is displayed. The large difference between the 225°, 315° pair and the 45°, 135° pair occurs because of the appearance of u_δ in the Falkner-Skan transform from z to η. A similar effect occurs in Figure 66; the forward flight speed also appears in u_δ. This dependence on forward flight speed will become more important at smaller values of span.

In examining the graphs of the separation line, the shape of the curves in Figures 67 and 68 should be understood. For no inflow ($\alpha_b = .005°$), there is a minimum in the separation line at 180° azimuthal angle and a maximum at 360° (or 0°). The separation line with inflow, shown in Figure 68, has a minimum near 90° and a maximum near 270°. The time derivatives of chordwise flow tend to cause a maximum at 360°. The inflow makes the aerodynamic angle of attack smallest at 270° (since flapping and cyclic pitch are not considered) and tends to cause a maximum in the separation line at 270°. The resultant maximum lies between 270° and 360° azimuthal angle. If the y (spanwise) dependence is examined near a minimum, the separation line will move forward on the blade as y decreases. Near the maximum, the opposite is true. However, the mean or time-averaged separation line will move backward as y decreases.

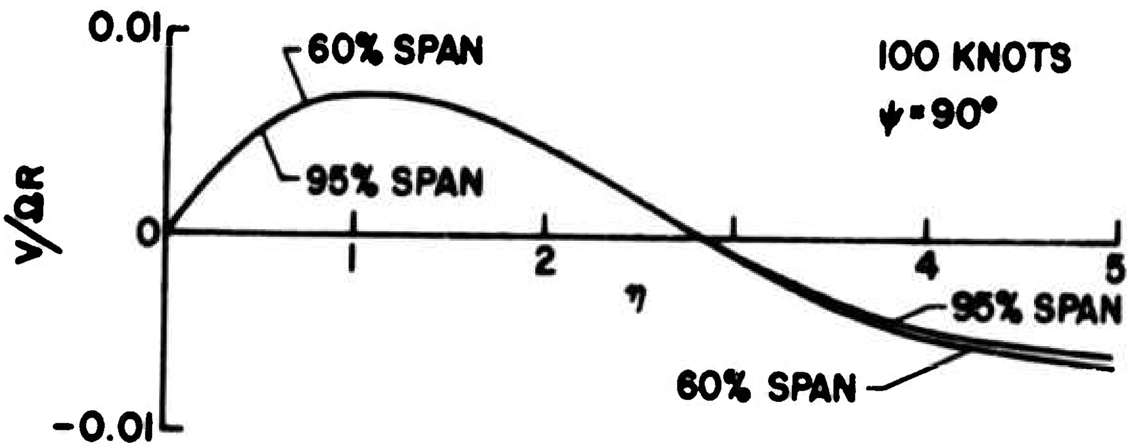

Figure 56. The Spanwise Velocity Profile for the 24-Foot Rotor (at 8000 lbf and 12% Chord) in Forward Flight.

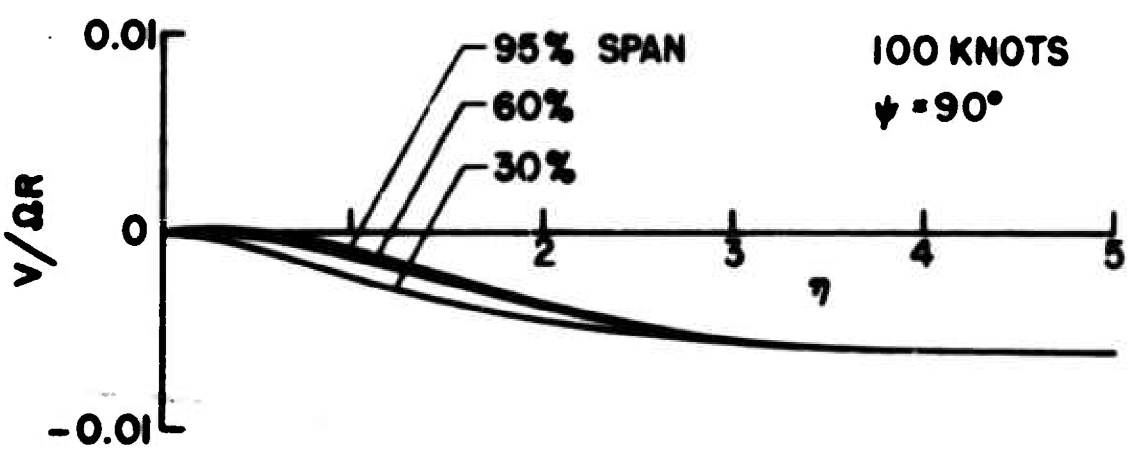

Figure 57. The Spanwise Velocity Profile for the 40-Foot Rotor (at Zero Degrees Blade Angle of Attack and 10% Chord) in Forward Flight.

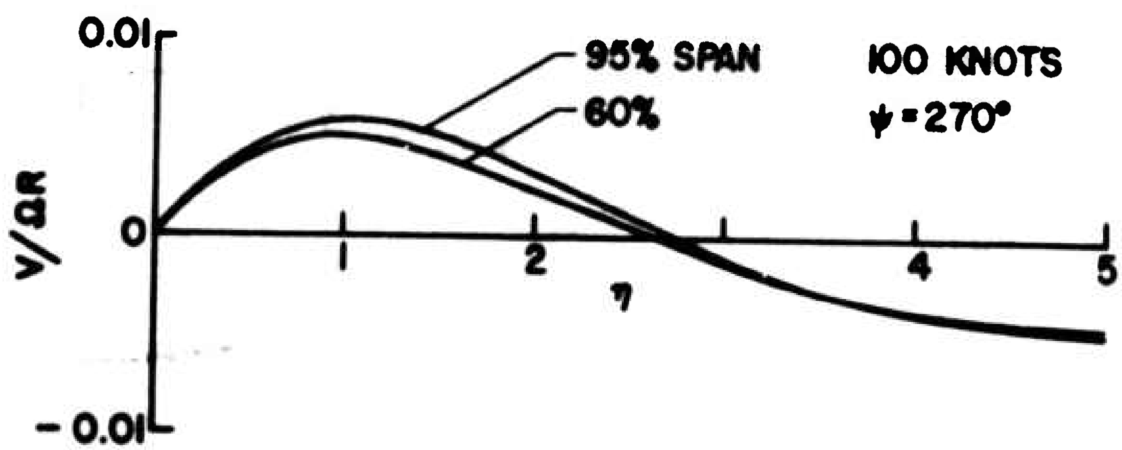

Figure 58. The Spanwise Velocity Profile for the 24-Foot Rotor (at 8000 lbf and 10% Chord) in Forward Flight.

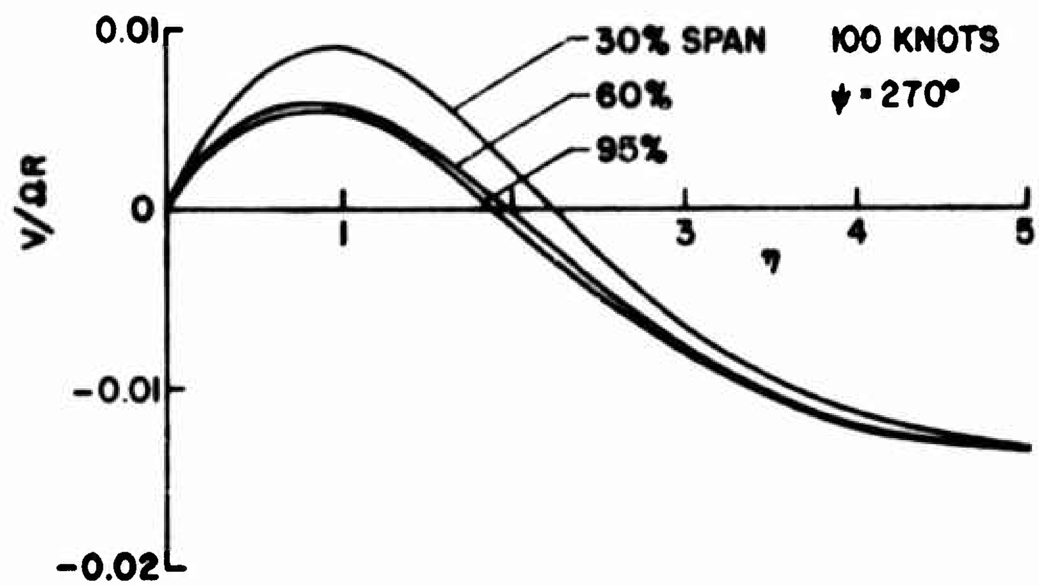

Figure 59. The Spanwise Velocity Profile for the 40-Foot Rotor (at Zero Degrees Blade Angle of Attack and 30% Chord) in Forward Flight.

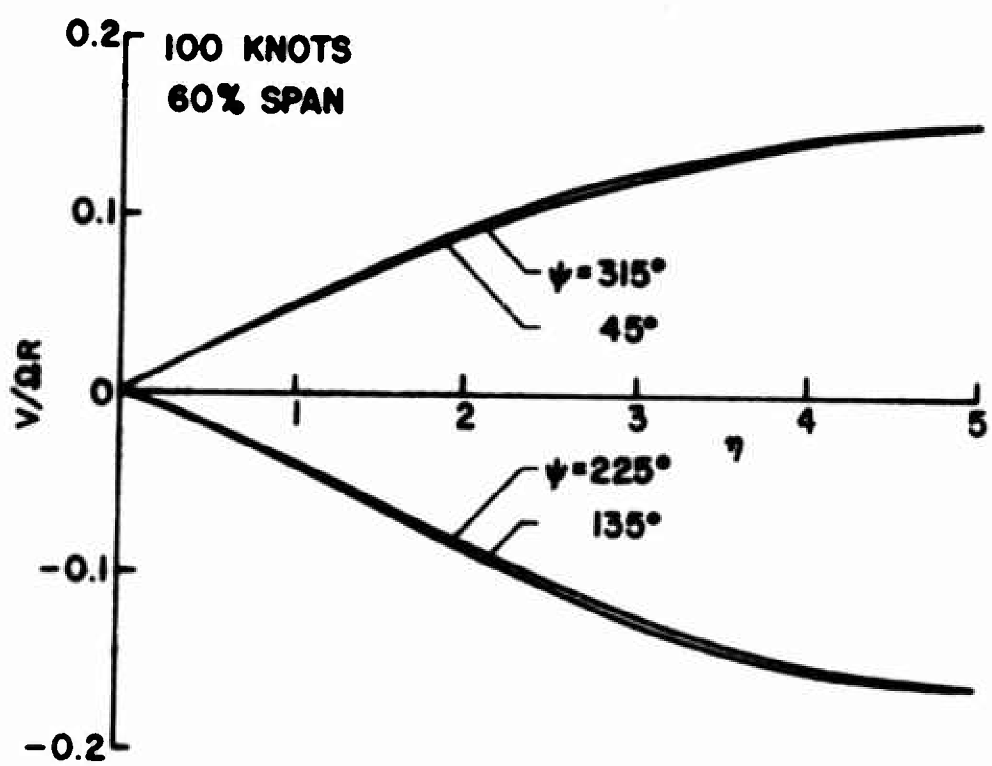

Figure 60. The Spanwise Velocity Profile for the 24-Foot Rotor (at 8000 lbf and 10% Chord) in Forward Flight.

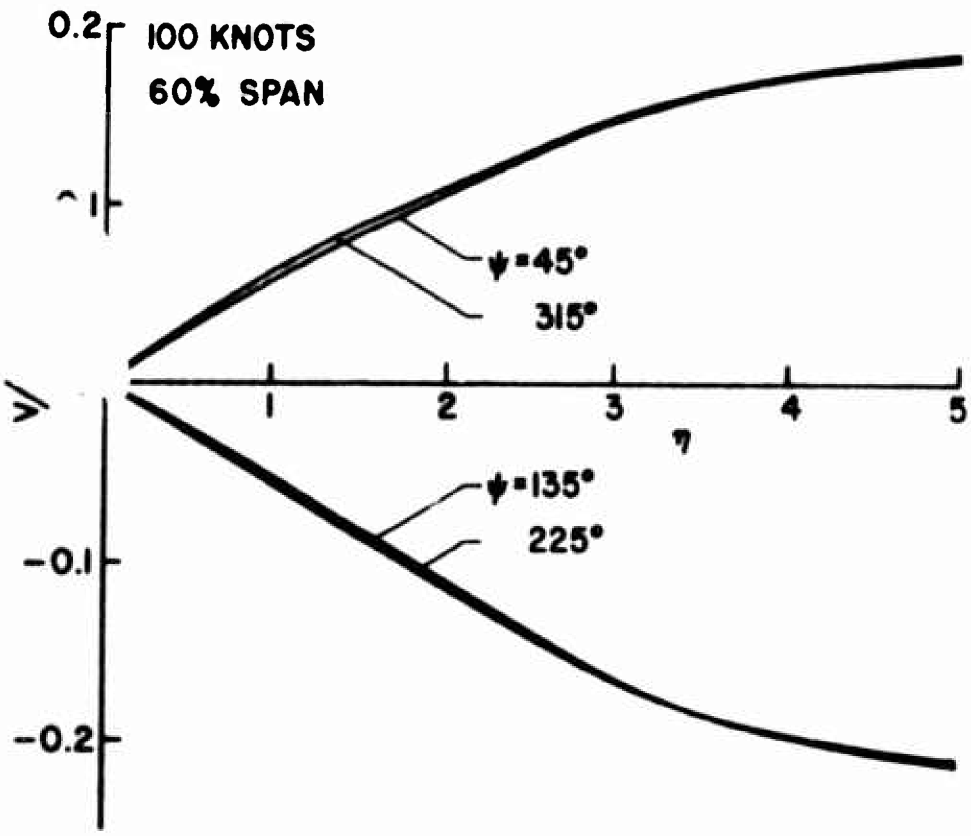

Figure 61. The Spanwise Velocity Profile for the 40-Foot Rotor (at Zero Degrees Blade Angle of Attack and 30% Chord) in Forward Flight.

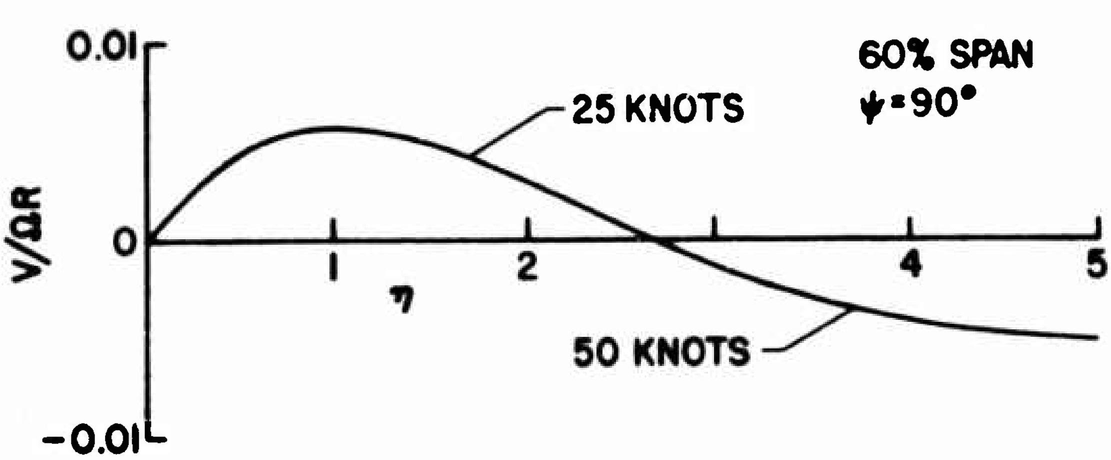

Figure 62. The Spanwise Velocity Profile for the 24-Foot Rotor (at 8000 lbf, 60% Span, and 10% Chord) in Forward Flight.

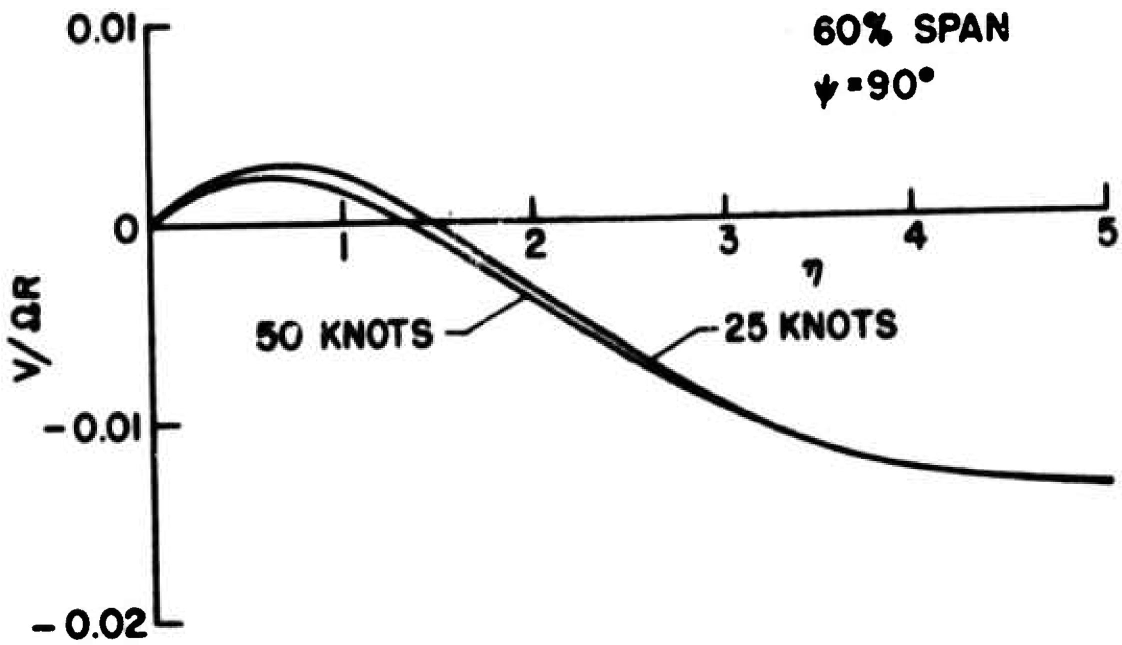

Figure 63. The Spanwise Velocity Profile for the 40-Foot Rotor (at Zero Degrees Blade Angle of Attack, 60% Span, and 30% Chord) in Forward Flight.

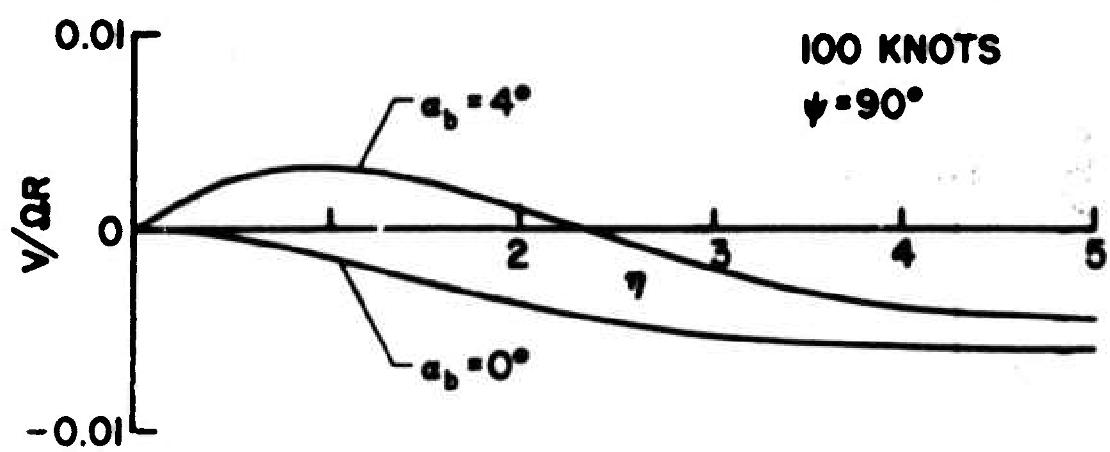

Figure 64. The Spanwise Velocity Profile for the 40-Foot Rotor (at 10% Chord and 60% Span) in Forward Flight.

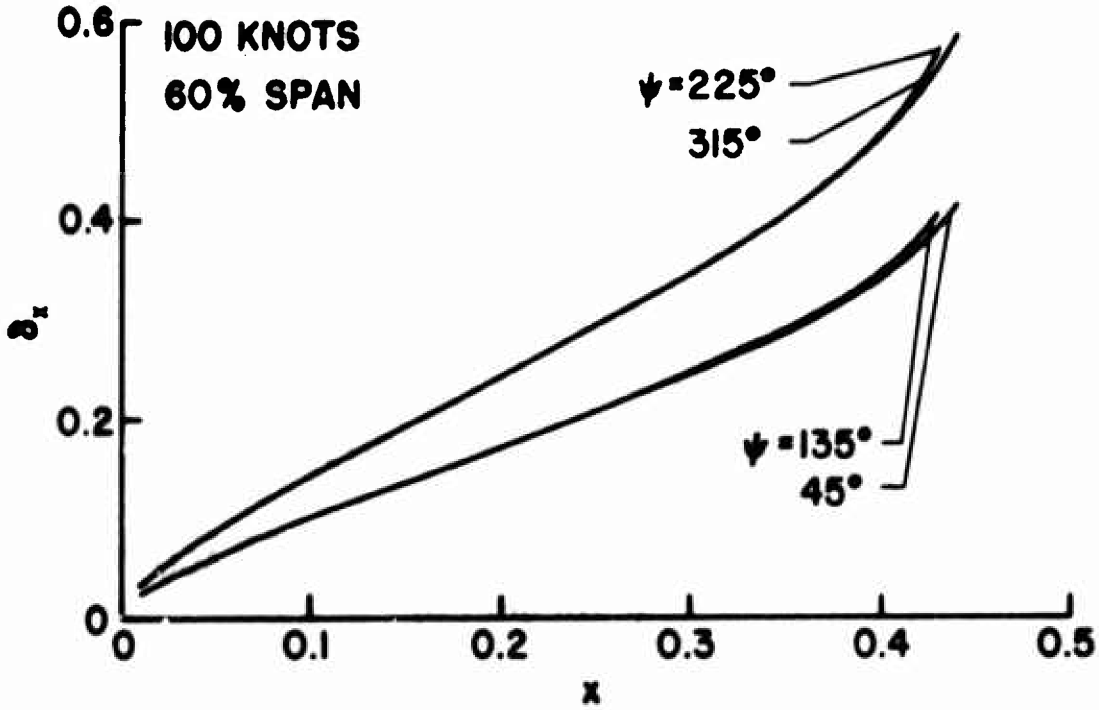

Figure 65. The Chordwise Displacement Thickness for the 40-Foot Rotor (at Zero Degrees Blade Angle of Attack and 60% Span) in Forward Flight.

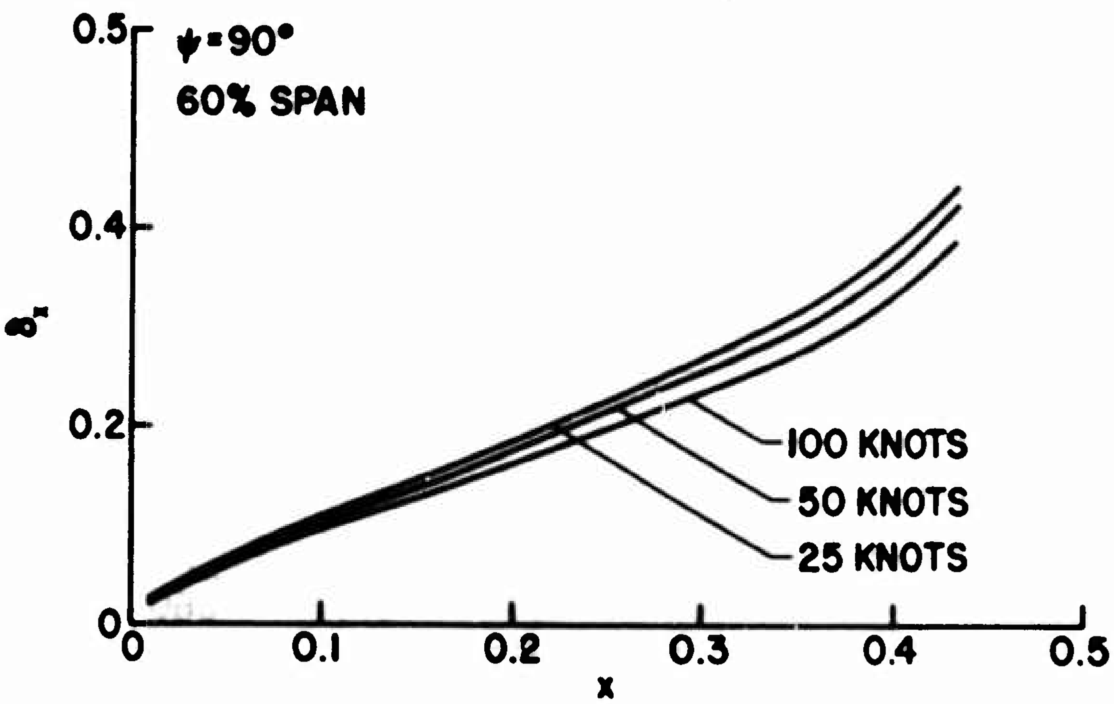

Figure 66. The Chordwise Displacement Thickness for the 40-Foot Rotor (at Zero Degrees Blade Angle of Attack) in Forward Flight.

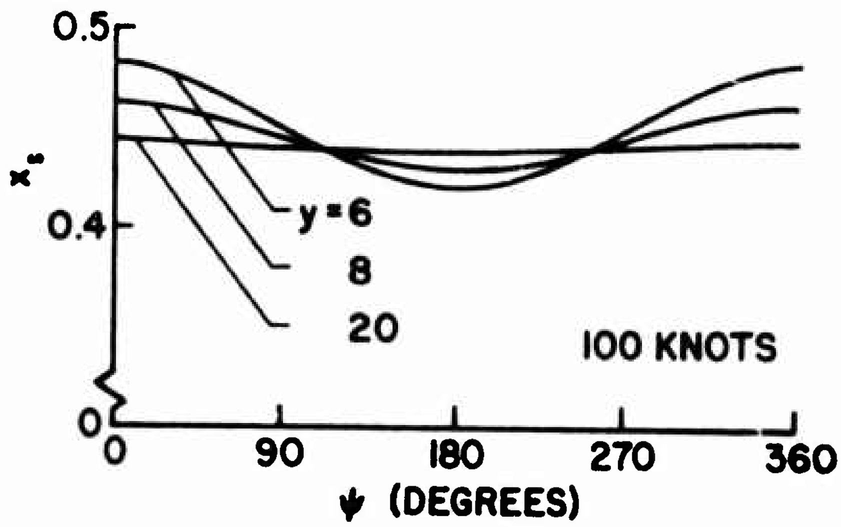

Figure 67. The Separation Line for the 40-Foot Rotor at Zero Degrees Blade Angle of Attack and 100 Knots Forward Flight Speed.

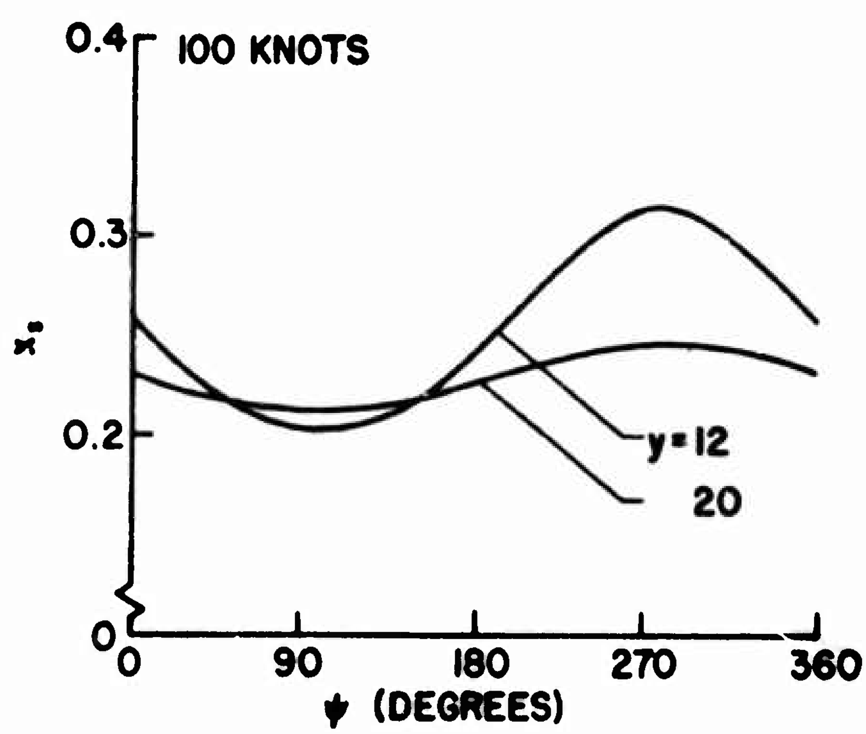

Figure 68. The Separation Line for the 40-Foot Rotor at 4 Degrees Blade Angle of Attack and 100 Knots Forward Flight Speed.

Figure 69 shows this effect more explicitly when there is no inflow. For no inflow, the curve has symmetry about the line $\psi = 180°$, so the mean curve coincides with the line marked $\psi = 90°, 270°$. With inflow, the curves are no longer symmetric. Figures 70 and 71 show that the delay in separation at 270° is greater than the advance at 90°. Figures 72 and 73 emphasize the difference the inflow makes. For no inflow (Figure 72), the dependence on forward flight is eliminated at $\psi = 90°$. With inflow the separation line actually advances with increased forward flight speed, as shown in Figure 73. This is misleading; Figure 74 gives a better understanding of the situation. The separation line will be advanced or delayed according to the azimuthal angle chosen. The effect of forward flight speed, span, and azimuthal angle should not be examined without consideration of Equation (75).

In Figure 75, the thrust dependence appears to contradict a previous result: the increase of angle of attack reduces the time dependent effects. However, the increase of inflow tends to increase time dependence, so there is no contradiction. The increase in thrust causes an increase in both angle of attack and inflow, and the inflow increase is the more important. A better view of the mean separation line, and its relation to separation on an airfoil in two-dimensional flow, can be found in Figures 76 and 77. The aerodynamic angle of attack variation decreases with span because only the change due to the time dependence of the chordwise component of forward flight is considered. When the angle of attack decreases, the separation line retreats toward the trailing edge with very nearly a linear dependence on angle of attack. As the angle of attack begins to increase, the response of the separation line lags. The separation line may even retreat for a time. As the angle of attack increases further, the separation line moves forward more rapidly than it moves back. It moves forward past the two-dimensional separation line but stops its advance as soon as the angle of attack ceases to increase.

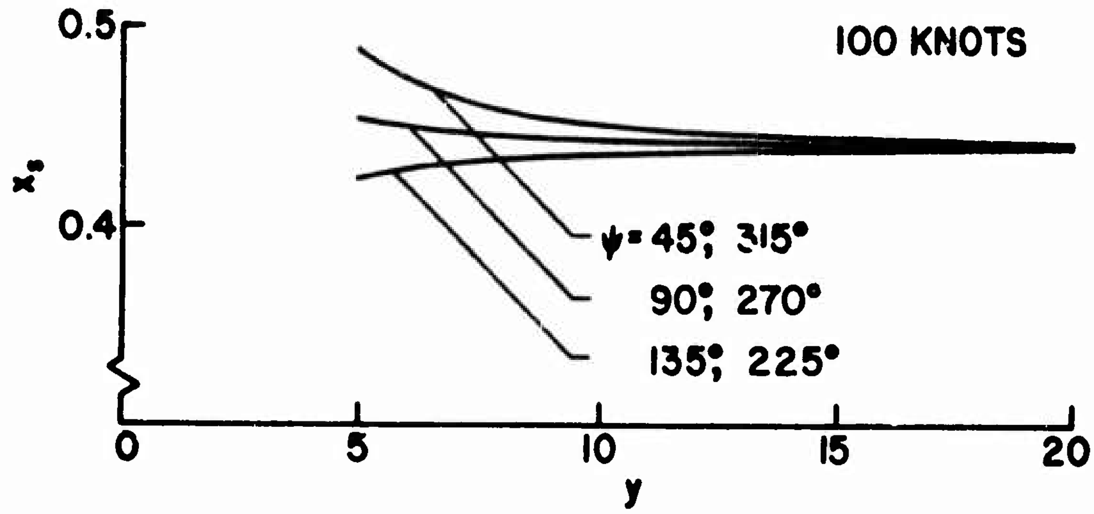

Figure 69. The Separation Line for the 40-Foot Rotor at Zero Degrees Blade Angle of Attack in Forward Flight.

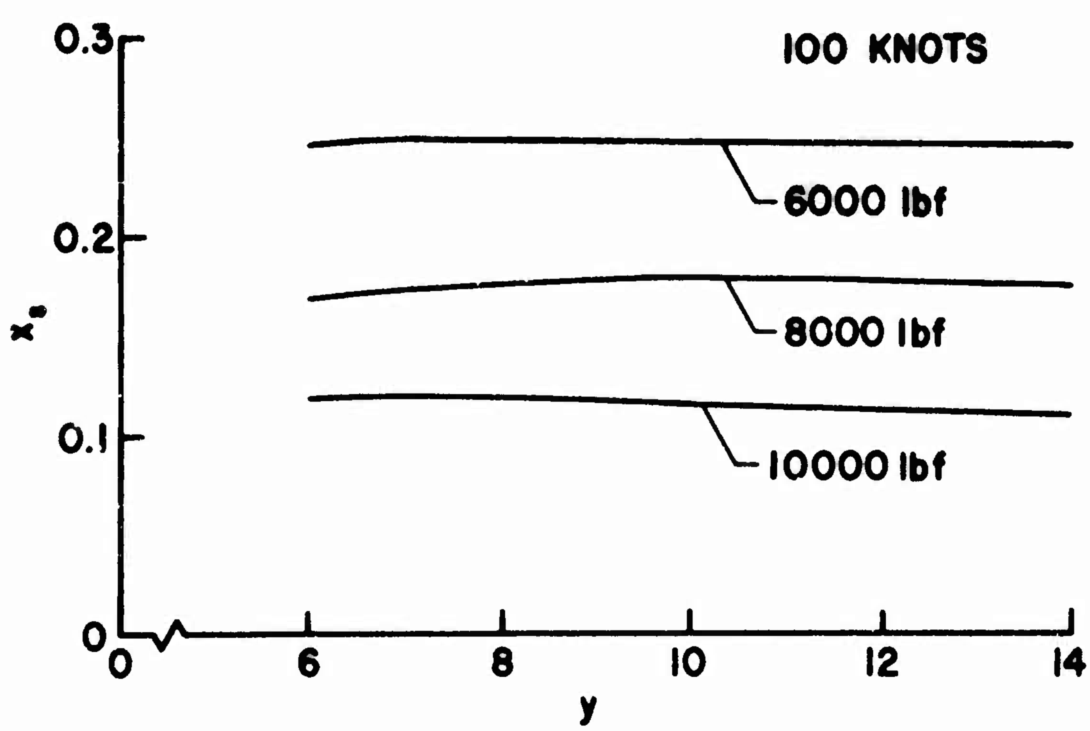

Figure 70. The Separation Line for the 24-Foot Rotor at 100 Knots and 90° Azimuthal Angle.

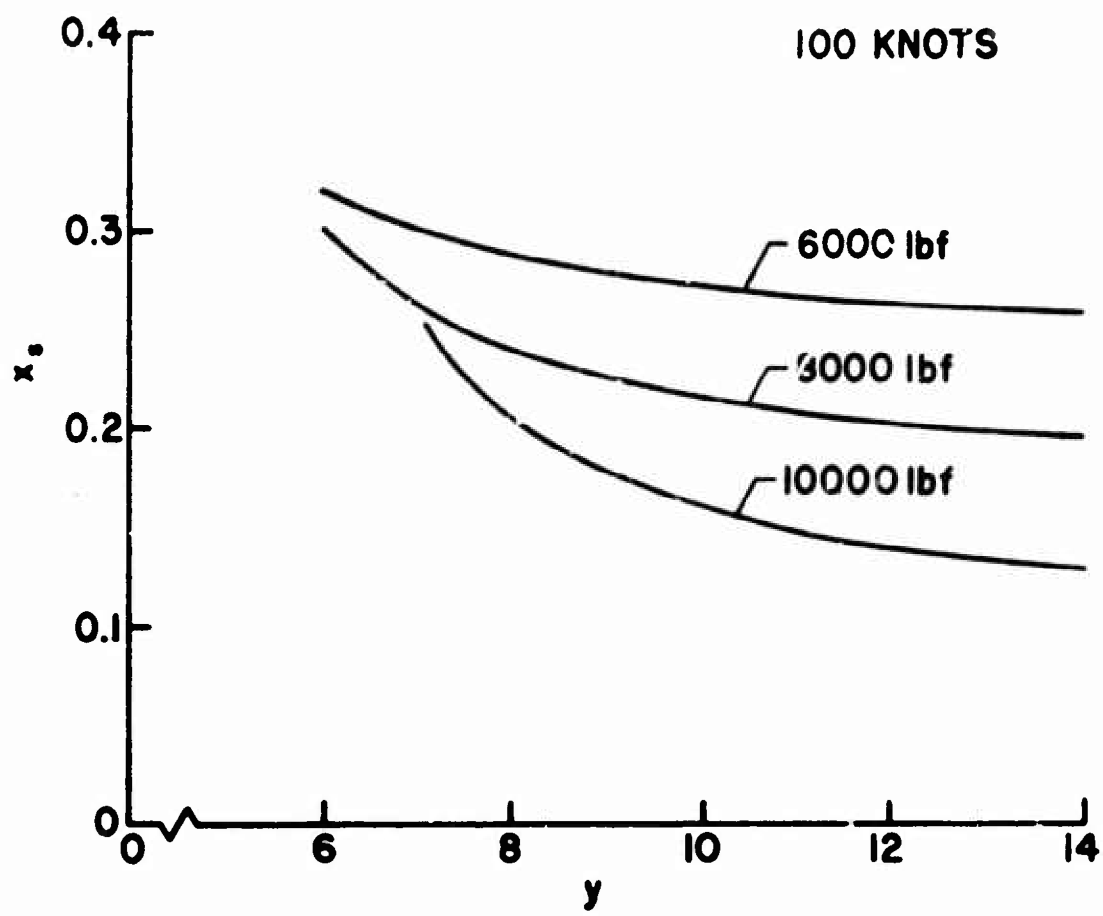

Figure 71. The Separation Line for the 24-Foot Rotor at 100 Knots and 270° Azimuthal Angle.

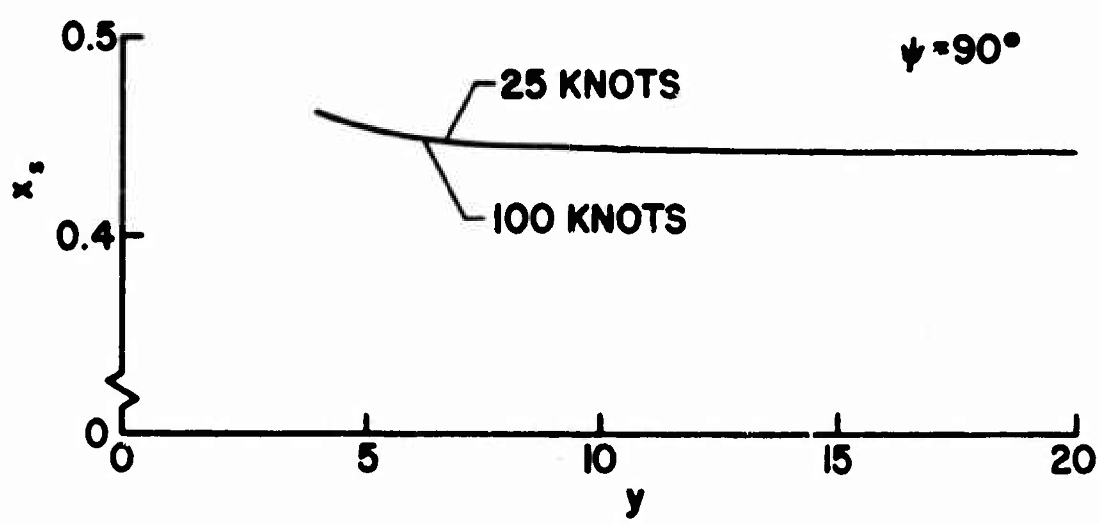

Figure 72. The Separation Line for the 40-Foot Rotor at Zero Degrees Blade Angle of Attack and 90° Azimuthal Angle.

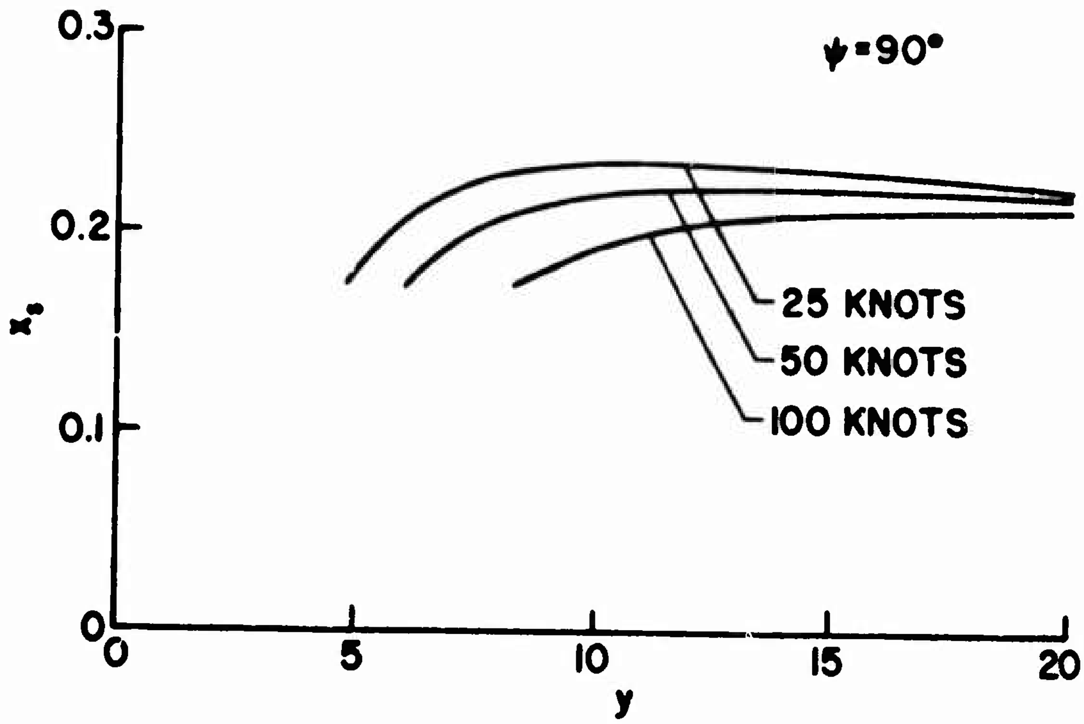

Figure 73. The Separation Line for the 40-Foot Rotor at 4 Degrees Blade Angle of Attack.

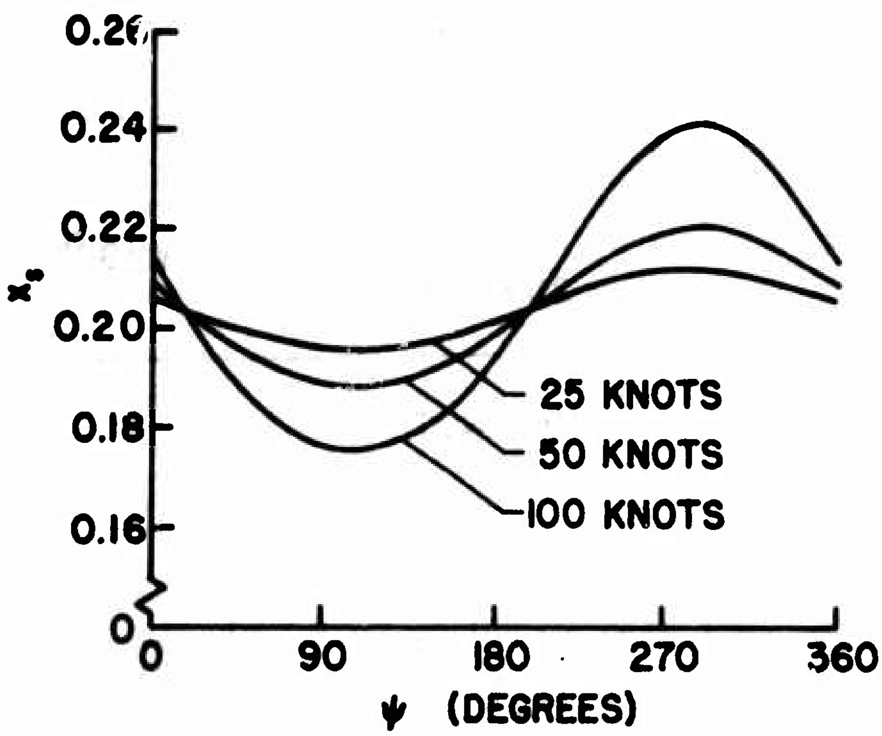

Figure 74. The Separation Line for the 24-Foot Rotor at 8000 lbf and 8 Chord Lengths From the Axis of Rotation.

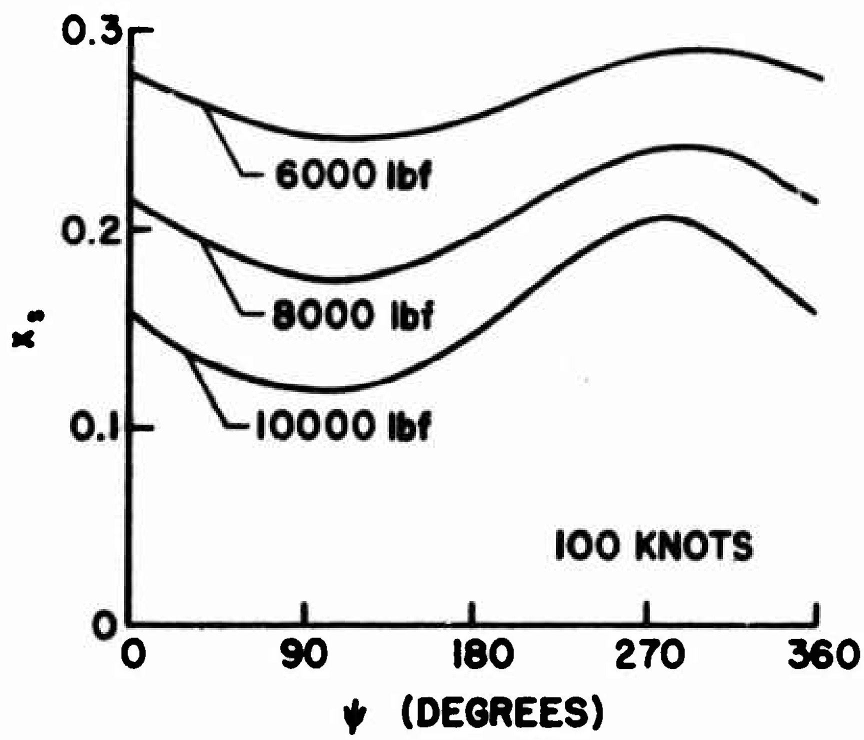

Figure 75. The Separation Line for the 24-Foot Rotor at 100 Knots and 8 Chord Lengths From the Axis of Rotation.

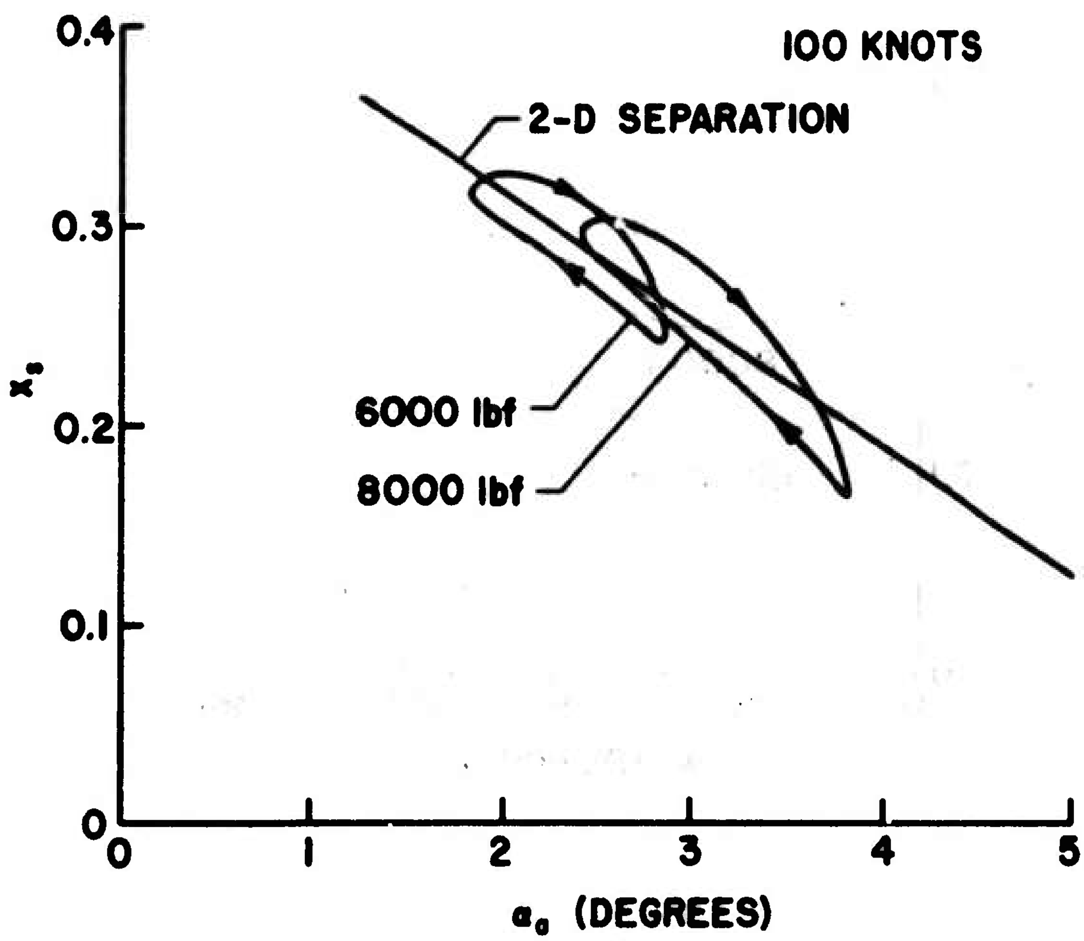

Figure 76. The Separation Line for the 24-Foot Rotor at 6 Chord Lengths From the Axis of Rotation.

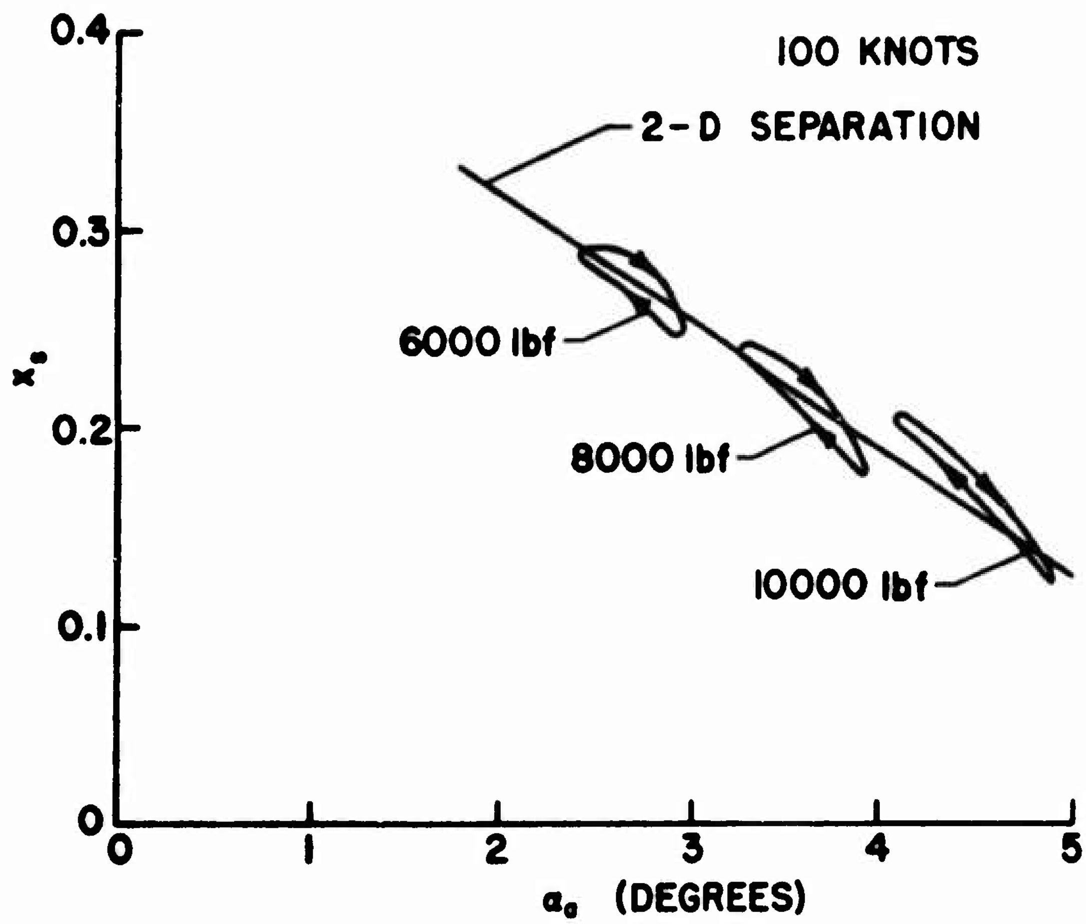

Figure 77. The Separation Line for the 40-Foot Rotor at 8 Chord Lengths From the Axis of Rotation.

SUMMARY

A solution has been obtained for the laminar boundary layer on a rotating blade that includes the effects of lift and forward flight, but does not include tip effects, cyclic pitch, or flapping. The results are primarily applicable to a rotating blade that is part of a system of rotors. The entire rotor disk induces an inflow velocity that is proportional to span in the part of the analysis called the hover case. In the forward flight case, the induced velocity is a constant v_a and the speed of forward flight is s_H. Either s_H or v_a, or both, may be eliminated from consideration since they appear explicitly in the equations for velocity and separation. In all calculations, it is implicit that the axis of rotation is located at the quarter-chord point and that the blade is a symmetrical, 11.9-percent-thick Joukowski airfoil. The geometric blade angle of attack must be known before calculations are made. In the hover case, the constant of proportionality between the inflow and the span must also be known.

For both cases, the chordwise dimension is transformed so that in the transformed coordinates, the distance from the stagnation point to the separation point is independent of span and time. Time is more conveniently thought of as the angle through which the blade has rotated, the azimuthal angle ψ. In the transformed coordinates, the velocities are expanded in an asymptotic series in the span. The use of transformed coordinates makes it possible to approach the separation point. The first term in the series for the chordwise velocity satisfies the two-dimensional boundary layer equations at the geometric angle of attack. Higher terms in the asymptotic series are given by linear equations, allowing the time dependence to be removed by applying the principle of superposition. The accuracy of the asymptotic series cannot be easily estimated, but the hover case seems to be accurate for y greater than about 2. The forward flight case, with $s_H = 0$, depends strongly on the value of v_a. For $v_a = .1$, there may be sufficient accuracy for values of span greater than 3 or 4. For forward flight, $y + T_2$, as well as y, must be large. The asymptotic series is useful for relatively small deviations from the solution at large span. The most practicable criterion for accuracy is that the higher terms be small compared to the first term in the series. By this criterion, the solution well fulfills its purpose. Since most helicopter blades have aspect ratios greater than 10 or 12, the solution is able to assess the importance of each effect over most of the blade.

Many of the effects seen in the results have been described in previous work. The asymptotic solutions at large span showed that the chordwise flow approaches the two-dimensional flow over an airfoil. At smaller values of span, separation is delayed by rotational effects. Rotational effects cause an S-shaped velocity profile in the spanwise flow. The potential flow generally causes flow toward the axis of rotation, but rotational effects which become important near the surface cause outward

flow. Rotation, by itself, has little influence on the separation line except for the region close to the axis of rotation.

In forward flight, the spanwise flow is much larger than in the hover case. The rotational effects are still present, but the spanwise flow due to yaw is dominant. Through the effect of changes in the yaw angle, the chordwise flow becomes time dependent. Although the present solution cannot account for flapping or feathering, it is clear that time-dependent effects in the forward flight case are much larger than the effects of rotation in the hover case. The aerodynamic angle of attack, which changes with time, is an important influence on the chordwise flow, and the time derivative of the chordwise flow is also important. The time dependence decreases as span increases, and its effect seems to diminish as angle of attack increases, provided the inflow is held constant.

The time dependence can best be assessed by examining the displacement thicknesses or the separation line, instead of the velocity profiles. Much of the spanwise dependence and time dependence of the velocity has been accounted for by nondimensionalizing by u_δ and by transforming the dimensional normal to the surface by a Falkner-Skan transformation.

The separation line oscillates due to forward flight. The maximum delay occurs at an azimuthal angle that seems to depend primarily on the aerodynamic angle of attack and secondarily on the time derivative of the chordwise flow. In hover, separation depends almost entirely on the aerodynamic angle of attack. In forward flight, even for small oscillations of the angle of attack, there is a lag in the response of the separation line to increases in the angle of attack.

The rotor blade under consideration is part of a rotor disk which generates thrust. The values of angle of attack, thrust, and inflow were chosen to be representative of two specific helicopters. As thrust increases, both angle of attack and inflow increase. In hover, separation is closely correlated to the aerodynamic angle of attack. The form or magnitude of inflow, thrust or geometric angle of attack was unimportant except for its influence on aerodynamic angle of attack. In forward flight, the situation is much more complex. At constant angle of attack, increased inflow delays separation and increases time dependence. For no inflow, time dependence decreases as angle of attack increases, but for large inflow the opposite is true. Inflow also shifts the phase angle of the separation line through its influence on the aerodynamic angle of attack. When the dependence of the separation line on thrust is considered, the magnitude of the oscillations increases as thrust increases, and for normal values of thrust, inflow is the primary influence on the phase angle of the separation line.

CONCLUSIONS

As a result of the present study, certain conclusions can be made regarding the effects of rotation, forward flight speed and inflow on the laminar boundary layer development and laminar separation line on a rotating helicopter blade. The analysis is limited in that such effects as lead-lag, flapping, feathering, and reverse flow must be excluded at this time due to the mathematical complexity involved in including these effects. Within the framework of the present analysis, it is concluded that:

1. The technique of scaling the chordwise coordinate so that separation always occurs at the same location in the scaled coordinate offers an excellent method for studying three-dimensional time-dependent boundary layers where the separation line varies with spanwise location and time.

2. The normal delay of the separation line near the axis of rotation due to blade rotation is obtained. This effect has been previously obtained by a number of investigators and is well known. As usual, the chordwise flow asymptotically approached the two-dimensional flow over the blade at large span.

3. In the hover case, two solutions have been obtained: the normal hover case with a linear variation of inflow, and in the forward flight solution, the limiting case of zero forward flight speed in which the inflow is constant. In each case the delay in separation due to rotation is still present, but the main effect of the inflow is to change the aerodynamic angle of attack. Compared at the same span and aerodynamic angle of attack, neither the form of the inflow (constant or variable along the span) nor its magnitude has a significant effect on the separation point. As in two-dimensional flow, increasing the aerodynamic angle of attack moves separation forward on the blade.

   The main effect of thrust level is to change the aerodynamic angle of attack, by altering both the geometric angle of attack and the inflow velocity. As the thrust level is increased, the geometric angle of attack, the inflow velocity, and the aerodynamic angle of attack are all increased. In general, then, increasing the thrust level moves the separation line forward on the blade. However, increasing the thrust level decreases the spanwise variation of the separation line.

4. At normal helicopter forward flight speeds, the dominant spanwise flow is the time-dependent flow due to the angle of yaw. This, together with the time-dependent chordwise flow

due to changing yaw angle, causes a time-dependent separation line oscillating about the no-forward-flight separation line. Both the average delay in separation and the oscillations are diminished as the angle of attack of the blade increases (if inflow is held constant).

The simultaneous action of inflow and forward flight speed causes the magnitude of the oscillations of the separation line to increase, for a given geometric angle of attack. When the inflow is zero, the time dependence of the separation line is dominated by the time derivative of the chordwise flow. It is most favorable to delayed separation at the extreme downstream position of the blade. This makes the maximum delay in separation occur at $\psi = 360°$. Inflow causes the aerodynamic angle of attack to vary with time so that it is smallest at $\psi = 270°$. The combination of inflow and forward flight shifts the maximum delay of the separation line into the fourth quadrant.

In the forward flight case, increasing the thrust level moves the separation line forward at all values of ψ and increases the magnitude of the oscillations of the separation line.

5. Increases in forward flight speed cause the magnitude of oscillations of the separation line to increase.

6. When plotted as a function of angle of attack, the separation line in forward flight, for fixed span, describes a loop (for normal thrust levels). This indicates that the oscillations of the separation line are not correlated with angle of attack alone, as in the hover case. This indicates that other nonsteady effects, in addition to the time varying angle of attack, are important in determining the separation line.

7. When the inflow is zero, the phase advance angle (the angle between the maximum of the shear stress at the wall and the maximum of the velocity at the edge of the boundary layer) agrees qualitatively with the solution of Lighthill.[18]

RECOMMENDATIONS

1. The technique of scaling the chordwise coordinate so that separation always occurs at the same location in the scaled coordinate offers an effective method for attacking the more realistic problem of turbulent boundary layers on rotating blades. It is recommended, therefore, that this method be employed in a study of the turbulent boundary layer on a rotating helicopter blade.

2. Additional studies should be conducted to isolate and determine more clearly the true nature of the unsteady boundary layer effects on the separation line on a helicopter blade. A first step would be to eliminate the effects of rotation and study the nonsteady boundary layer effects alone on an airfoil blade.

3. Additional work must be done to include the effects of lead-lag, feathering, cyclic pitch, and flapping, which occur in real helicopter blade motions, into the analysis of the boundary layer on rotating blades. It is recommended that a continuing effort be made to develop techniques which will allow the incorporation of these effects into the boundary layer analysis.

LITERATURE CITED

1. Harris, F. D., and Pruyn, R. R., BLADE STALL-HALF FACT, HALF FICTION, American Helicopter Society Twenty-third National Forum Report 101, Washington, D. C., May 1967.

2. Sweet, G. E., Jenkins, J. L., Jr., and Winston, M. M., WIND-TUNNEL MEASUREMENTS ON A LIFTING ROTOR AT HIGH THRUST COEFFICIENTS AND HIGH TIP-SPEED RATIOS, NASA Technical Note TN-D-2462, National Aeronautics and Space Administration, Langley Research Center, Hampton, Virginia, September 1964.

3. Harris, F. D., SPANWISE FLOW EFFECTS ON ROTOR PERFORMANCE, CAL/USAAVLABS Symposium Proceedings, Volume III, Buffalo, New York, June 1966.

4. Liiva, Jaan, and Davenport, F. J., DYNAMIC STALL OF AIRFOIL SECTIONS FOR HIGH-SPEED ROTORS, Journal of the American Helicopter Society, Vol. 14, April 1969, pp. 26-33.

5. Velkoff, H. R., Blaser, D. A., and Jones, K. M., BOUNDARY LAYER DISCONTINUITY ON A HELICOPTER ROTOR BLADE IN HOVERING, AIAA Paper 69-197, American Institute of Aeronautics and Astronautics, New York, 1969.

6. Dwyer, H. A., and McCroskey, W. J., CROSSFLOW AND UNSTEADY BOUNDARY-LAYER EFFECTS ON ROTATING BLADES, AIAA Paper 70-50, AIAA Eighth Aerospace Sciences Meeting, New York, January 1970.

7. Sears, W. R., POTENTIAL FLOW AROUND A ROTATING CYLINDRICAL BLADE, Journal of Aeronautical Science, Vol. 17, 1950, pp. 183-184.

8. Rott, N., and Smith, W. C., SOME EXAMPLES OF LAMINAR BOUNDARY LAYER FLOW ON ROTATING BLADES, Journal of the Aerospace Sciences, Vol. 23, 1956, pp. 991-996.

9. McCroskey, W. J., and Yaggy, P. F., LAMINAR BOUNDARY LAYERS ON HELICOPTER ROTORS IN FORWARD FLIGHT, AIAA Journal, Vol. 6, 1968, pp. 1919-1926.

10. Liu, S. W., THE LAMINAR BOUNDARY LAYER FLOW ON ROTATING CYLINDERS, AFOSR TN 57-298, Armed Services Technical Information Agency, Arlington, Virginia, June 1957, AD 132369.

11. Young, W. H., Jr., and Williams, J. C., III, THE BOUNDARY LAYER ON ROTATING BLADES IN FORWARD FLIGHT, AIAA Paper 70-49, AIAA Eighth Aerospace Sciences Meeting, New York, January 1970.

12. Sears, W. R., and Fogarty, L. E., POTENTIAL FLOW AROUND A ROTATING ADVANCING CYLINDRICAL BLADE, Journal of Aeronautical Sciences, Vol. 17, 1950, p. 599.

13. Smith, A. M. O., and Clutter, D. W., SOLUTION OF THE INCOMPRESSIBLE LAMINAR BOUNDARY-LAYER EQUATIONS, AIAA Journal, Vol. 1, 1963, pp. 2062-2071.

14. Hildebrand, F. B., INTRODUCTION TO NUMERICAL ANALYSIS, New York, McGraw-Hill Book Company, 1956, p. 236.

15. Lew, H. G., METHOD OF ACCELERATED SUCCESSIVE REPLACEMENT APPLIED TO BOUNDARY LAYER EQUATIONS, AIAA Journal, Vol. 6, 1968, pp. 929-931.

16. Young, W. H., Jr., LAMINAR BOUNDARY LAYER ON A LIFTING ROTOR IN FORWARD FLIGHT, North Carolina State University, Ph.D. Dissertation, University Microfilms, Inc., Ann Arbor, Michigan, 1970.

17. Moore, F. K., ed., THEORY OF LAMINAR FLOWS, Princeton, N. J., Princeton University Press, 1964, pp. 388-390.

18. Lighthill, M. J., THE RESPONSE OF LAMINAR SKIN FRICTION AND HEAT TRANSFER TO FLUCTUATIONS IN THE STREAM VELOCITY, Proceedings of the Royal Society, Vol. A224, 1954, pp. 1-23.

19. Gessow, Alfred, and Myers, G. C., Jr., AERODYNAMICS OF THE HELICOPTER, New York, The MacMillan Company, 1952.

20. Mil', M. L., HELICOPTERS: CALCULATION AND DESIGN, NASA TT F-494, National Aeronautics and Space Administration, Washington, D. C., September 1967.

APPENDIX I
THRUST CALCULATIONS

In order to calculate the boundary layer development on a rotating blade, it is necessary first to determine the inviscid flow over the blade. In practice, this inviscid flow depends on such factors as the geometry of the blade (airfoil section), the geometric angle of attack of the blade, the forward flight speed, and the inflow velocity due to the blade system. In the design of a real helicopter, these factors are not independent and therefore cannot be chosen arbitrarily. The inflow, for example, depends upon the airfoil section, the geometric angle of attack, and the forward flight speed, as well as on the number of blades in the helicopter rotor N_b, the radius (span) of the blade system R, the thrust level T, the rotational speed Ω, and the blade chord c. It is not possible, therefore, to assign values to each of these parameters independently. In order to obtain a reasonably consistent set of parameters required to determine the potential flow, calculations were made for two helicopters for which some of the above parameters were specified in the contractual arrangement for the present work. The remaining parameters were then calculated using simple momentum theory and blade element theory. The calculations required to obtain the above parameters are outlined herein.

In the present work, the potential flow calculations were made for two helicopters. The first was a helicopter with a two bladed rotor of 24-foot radius, a blade chord of 21 inches with the rotor rotational velocity of 295 revolutions per minute, and blade loadings corresponding to vehicle gross weights of 6,000, 8,000, and 10,000 pounds. The second helicopter was to have six blades of 40-foot radius and 24-inch chord, with a rotational velocity of 143.3 revolutions per minute and blade geometric angles of attack of 0 and 4 or 6 degrees. In each case the blade airfoil section was a 11.9%-thick symmetrical Joukowski airfoil and the blades were assumed to operate in an atmosphere of density 0.0765 lbm/ft^3 and with a speed of sound of 1117 ft/sec. These operating conditions are summarized in Table III, together with several parameters which characterize the airfoil aerodynamics.

It is also necessary, in the forward flight case, to prescribe the forward flight speed. In order to compare the two helicopters on the same basis, the speed calculations were made for both helicopters at forward flight speeds of 25, 50 and 100 knots. This corresponds to values of s_H of 0.7807, 1.5613 and 3.1226 for the 24-foot rotor and to values of 1.406, 2.812 and 5.625 for the 40-foot rotor.

These prescribed values are still not sufficient for the calculation of the potential flow over the blade section. For the helicopter with the 24-foot rotor, it will be necessary to determine the geometric angle of attack and the inflow velocity; for the helicopter with the 40-foot rotor, it will be necessary to determine the thrust level and the inflow velocity.

TABLE III. CHARACTERISTICS OF TWO HELICOPTERS			
Symbol	Dimensions	24-Foot Rotor	40-Foot Rotor
R	ft	24	40
Ω	RPM	295	143.3
c	ft	1.75	2.00
N_b	-	2	6
A_R	-	13.71	20.00
T	lb	6,000	-
		8,000	-
		10,000	-
α_b	deg	-	0
		-	4 or 6
Ωc	ft/sec	54.06	30.01
σ_r	-	0.04642	0.09549
M_t	-	0.665	0.6884
$\pi\rho\Omega^2R^4$	lb^f	2.360×10^6	4.302×10^6

The calculations required to obtain these additional parameters were based on momentum theory and blade element theory. For clarity and convenience, the simplest form of each theory will be used and all variables will be written in nondimensional form. Both of these theories are available in texts on helicopter aerodynamics.[19,20]

The starting point for each of these theories is the thrust coefficient defined by

$$c_T = \frac{T}{\pi \rho R^2 (\Omega R)^2} \tag{85}$$

The simple or classical momentum theory relates an element of thrust dc_T to the downflow velocity v_i in an annulus of radius y and width dy by

$$d\ c_T = -\ S_s\ (2\ v_i)\ \frac{2}{A_R^4}\ y\ dy \tag{86}$$

where $S_s = \sqrt{s_H^2 + v_i^2}$. The thrust coefficient is found by integration over the span and azimuthal angle:

$$c_T = \int_0^{A_R} \int_0^{2\pi} d\ c_T\ d\ \psi\ dy \tag{87}$$

For the hover case, the forward flight speed is zero, and the inflow velocity is taken herein to have the form $v_i = -\omega_i y$. This yields

$$c_T = \omega_i^2 \tag{88}$$

For the forward flight case, the inflow is taken herein to be constant, *i.e.*, $v_i = -$[illegible]. Integration of Equation (87) for this case yields

$$C_T = 2\sqrt{s_H^2 + v_a^2}\ \frac{v_a}{A_R^2} \tag{89}$$

In either case, then, the momentum theory yields a relation between thrust coefficient and inflow velocity.

The simplest blade element theory calculates the lift from the slope of the two-dimensional lift curve a_0. It is assumed that the angle of attack and inflow are small so that $\tan \alpha_b \doteq \alpha_b$ and $\tan (v_i\ /\ \bar{U}_0) \doteq v_i\ /\ \bar{U}_0$. The velocity relative to the blade in the chordwise direction consists of the inflow in the z direction and $\bar{U}_0$ in the plane of rotation. Further $\bar{U}_0$ contains two components: one due to the rotation and the other due to forward flight. An element of one blade of length dy then produces an element of thrust of

$$d\ C_t = \frac{a_0}{2\pi\ A_R^4}\ (\alpha_b\ \bar{U}_0^2 + \bar{U}_0\ v_i)\ dy$$

where

a_0 is the slope of the lift curve (taken as 6.016 per radian, corresponding to an NACA 0012 airfoil)

$\bar{U}_0 = y + s_H \sin \psi$

For the hover case ($s_H = 0$, $v_i = -\omega_i y$),

$$C_t = a_0 \sigma_r (\alpha_b - \omega_i) / 6$$

where

$$\sigma_r = N_b c / \pi R$$

The number of blades in the helicopter rotor has been incorporated into the solidity of the rotor σ_r. For the forward flight case ($v_i = -v_a$),

$$c_t = a_0 \sigma_r \left(\frac{\alpha_b}{6} + \frac{\alpha_b}{4} \left(\frac{s_H}{A_R}\right)^2 - \frac{v_a}{4A_R}\right)$$

The blade element theory relates the thrust coefficient to the geometric angle of attack and the inflow. When the results of blade element theory are combined with the results of momentum theory, one has two relations between the thrust coefficient, the geometric angle of attack and the inflow. If any one of these is given, the other two are then uniquely determined.

The aerodynamic angle of attack is also necessary in the calculation of the potential flow. Once the geometric angle of attack is known, the aerodynamic angle of attack is easily computed from the simple geometric relationship

$$\alpha_a = \alpha_b - \arctan \frac{v_i}{\bar{U}_0}$$

These relations have been utilized to obtain the additional information necessary for the potential flow calculations in the present analysis. In the case of the 24-foot rotor system, they are used to obtain the blade geometric angle, the inflow constant, and the aerodynamic angle of attack. In the case of the 40-foot blade system, they are used to obtain the inflow, the aerodynamic angle of attack, and the thrust. The thrust level for the 40-foot rotor sysem is not used directly in the calculations but is obtained as a matter of interest. The results of these calculations are presented in Table IV for the hover case and in Table V for the forward flight case. In Table IV, the aerodynamic angle of attack corresponds to the presented values of geometric angle of attack α_b and inflow constant ω_i. In the case of forward flight, the aerodynamic angle of attack varies with azimuthal angle and therefore is not presented.

TABLE IV. THRUST CALCULATIONS IN HOVER

Rotor Span (ft)	Aerodynamic Angle of Attack (deg)	Thrust (lb^f)	Geometric Angle of Attack (deg)	Inflow Constant
24	3.12	6,000	6.01	0.0504
24	4.16	8,000	7.50	0.0582
24	5.21	10,000	8.94	0.0651
40	0	0	0	0
40	2.38	17,140	6.00	0.0631

TABLE V. THRUST CALCULATIONS FOR A FORWARD FLIGHT SPEED OF 100 KNOTS

Rotor Span (ft)	Thrust (lb^f)	Geometric Angle of Attack (deg)	Inflow Constant
24	6,000	3.349	0.0765
24	8,000	4.465	0.1020
24	10,000	5.581	0.1274
40	0	0	0
40	25,600	4.000	0.2117

The information given in Tables IV and V, together with that given in Table III, is sufficient to make the calculations of the inviscid flow over the blade.

APPENDIX II
COMPUTER PROGRAMS

Separate computer programs were used for the hover case and the forward flight case. In "Method of Solution," the more important features of these programs were discussed. The programs themselves have been well annotated by comment cards, and a brief list of the correspondence between the variable names used in the report and the FORTRAN names is presented in Table VI. The listing of the programs follows. The subroutine RK1 is omitted from the forward flight program because it is shown in the hover program.

TABLE VI. FORTRAN NOMENCLATURE

Name Used in the Report	FORTRAN Name
F''_0, G''_0, G''_{01}, etc.	DVDZ
F'_0, G'_0, G'_{01}, etc.	VEL
m_{10}	XM10
x	X
Δx	DX
ξ	XI
$\Delta\xi$	DXI
α_b (degrees)	ALPHB
α_b (radians)	AB
ε	EPS
δ	DELTA, DEP, DET
δ_I	DEI
σ	T
σ_I	SI
η	Z
$\Delta\eta$	DZ

```
C  A FORTRAN PROGRAM  FOR A ROTATING, HOVERING, SYMMETRIC AIRFOIL WITH
C  LIFT ; INFLCW=TR*SPAN
C      PROGRAM SIZE: 97880 BYTES IN FORTRAN IV-G,LEVEL1,MOD3,RELEASE15
C      LESS THAN 100 PAGES ARE PRINTED
C      RUN TIME (CPU) IN MINUTES=5+.4*(KMAX-34) WHERE KMAX IS THE VALUE
C      CF K AT THE LAST STATION AND MACHINE IS IBM 360/75 AT TUCC
       IMPLICIT REAL*8 (A-H,O-Z)
       CCMMON/BIJ/EPS,SGN,B1,B2,B3,B4,B5,B6,B7,B8,B9,B10
C      THIS DIMENSION STMT ASSUMES K<46,IBLUP<61,M<4,J<6,L<73,I<5,ITER<10
       DIMENSION X(45),DX(45),XI(45),DXI(45),BP(20),NBLUP(60),V(3,5),
      1 DD(3,5),Y(3,5,72,4),ST(6),U(3,5),ERR(9),DVZ(5,9),ITERKP(5),
      2 HIS(9),VINF(5),Z(72),DZ(72),A(3,5,72),S(4)   ,THT(5),XD2(5)
       DIMENSION PCC(50),UTIL(5C),VDEL(50),TK(6),E(4),UP(75),VP(75),
      D ILIM(4,4)
       EXTERNAL DSDX
C      ACCURACY IS CONTROLLED BY THE VALUES OF ERRMAX,ZMAX,DXI(K),JS,
C      DZ(L),IMAX
C      ERRMAX SEEMS TO HAVE LITTLE EFFECT ON ACCURACY,BUT IF IT IS TOO
C      SMALL THE VALUE CF THE 2NC DERIVATIVE OF THE STREAM FUNCTION WRT
C      ETA (DVDZ) CANNOT BE FOUND TO SUFFICIENT ACCURACY AT THE WALL TC
C      CONVERGE THE EQUATION.
C      ZMAX MUST BE LARGE ENOUGH SO THAT DVDZ IS LESS THAN ABOUT .001
C      AT ZMAX; IF IT IS LARGER THAN NECESSARY SPEED AND CONVERGENCE
C      WILL SUFFER. THE LARGER ZMAX IS, THE MORE AN ERROR IN DVDZ AT THE
C      WALL WILL AFFECT THE ERROR IN VELOCITY AT ZMAX, ESPECIALLY NEAR
C      SEPARATICN.
C      THE EFFECT OF DXI(K) IS  DESCRIBED AT LENGTH IN THE AIAA JOURNAL,
C      VCL. 1, P.2062, 1963, ANC IN PREVIOUS WORK BY A.M.O. SMITH
C      THE ERRCR IN THE RUNGE KUTTA INTEGRATION IS PROPORTIONAL TO DZ**4
C      THE ERROR IN RK3 IS PROPORTIONAL TO H**4, H IS DETERMINED BY JS
C      IMAX-1 MAY NOT BE LARGER THAN THE NO. OF PREVIOUS K STATIONS
C      KNOWN. FCR K>=8 (K STARTS AT 5)  IMAX=3 MAY GIVE SUFFICIENT
C      ACCURACY FOR THE  XI  CERIVATIVES.
C      BEGIN SECTION 1
C     PARAMETERS FOR VELOCITY ECNS
       LMAXU=69
       LMAX=40
       JCIM=5
C      JCIM IS THE NO. CF EQNS;IT IS THE MAXIMUM VALUE OF J
       DO 67 I=1,4
   67  S(I)=0.D0
       DO 1480 J=1,5
C      JCIM<=5 REQUIRED
       VINF(J)=0.D0
       DO 1480 M=1,3
       DO 1480 L=1,LMAXU
       DO 1480 I=1,4
 1480  Y(M,J,L,I)=0.D0
       VINF(1)=1.D0
C      IN THE LOCAL IMPLEMENTATION AT TRIANGLE UNIVERSITIES COMPUTING
C      CENTER (TUCC), FILE 1 IS THE DATA CARDS AT THE END OF THIS DECK,
C      FILE 2 IS THE CARD PUNCH, FILE 3 IS AN 133 SPACE/LINE PRINTER
C      THE FIRST DATA CARD HAS,IN FORMAT(5F15.10) THE INITIAL ESTIMATES
C      CF DVZ FCR THE 5 EQNS.
C      THE  2ND  DATA CARD CONTAINS,IN FORMAT(F10.7,F10.4,2F10.7,F20.16,
C      F10.7) THE VALUES OF:
C      1  XO: THE PCSITION OF AXIS CF ROTATION ALONG THE CHCRD;XO=.25 IS
C              25% CHORD
C      2  AR: THE ASPECT RATIO; IT IS USED ONLY IN STMT 8189
C      3  ALPHB: THE GEOMETRIC ANGLE OF ATTACK OF THE BLADE IN DEGREES
C      4  TR: THE NONDIMENSIONAL INDUCED VELOCITY=TR*(SPAN/CHORD)
C              IT IS OF THE ORDER OF THE SQUARE ROOT OF THE COEFFICIENT
```

```
C             OF THRUST
C       5  XIINF: THE POSITION OF THE STAGNATION POINT IN BODY COORDINATES
C                  IT IS NORMALLY NEGATIVE,I.E. ON THE BOTTOM SURFACE OF
C                  THE AIRFOIL.IF IT IS NOT KNOWN, READ IN A VALUE OF 14.D0
C                  AND THE PROGRAM WILL CALCULATE A CORRECT VALUE
C       6  RK2: THIS IS THE CONSTANT K2 IN THE EQN FOR LOWER CASE Q. IF IT
C               IS NOT KNOWN,PUT IN AN ESTIMATE(SAY .1) AND AFTER THE PGM
C               RUNS IT MAY BE FOUND BY EXTRAPOLATING -F2C"/F2K" TO THE
C               SEPARATION POINT XIS.  XIS IS THE VALUE OF XI AT WHICH FO"
C               AT THE WALL (Y(3,I,2,1)) GOES TO ZERO. SINCE THE 1ST EQN
C               (FOR FO) WILL NOT CONVERGE FOR FO" AT WALL < .06 TO .04,
C               XIS IS FOUND BY EXTRAPOLATION.
      READ(1,1481) (DVZ(J,1), J=1,JDIM)
 1481 FORMAT(5F15.10)
C     THIS WRITE STMT IS FOR CHECKOUT PURPOSES
      WRITE(3,2001) (DVZ(J,1), J=1,JDIM)
 2001 FORMAT( ' DVZ=',6D18.9   )
      DO 1399 IS=1,5
 1399 HIS(IS)=.5D0*(IS/3+IS/5)
      DO 1485 M=1,3
 1485 U(M,1)=0.D0
      DVZINC=.005D0
      ERRMAX=2.D-5
      WRITE(3,152) JDIM,LMAX,ERRMAX
  152 FORMAT(/' NO. EQNS=',I2,5X,'LMAX MUST BE <',I3,5X,'MAX ERROR IN VE
     FLOCITY AT MAX ETA=',D12.5/)
      DZST=.1D0
      ZMAX=5.5
      Z(2)=0.D0
      DZ(1)=.1
      Z(1)=-.1
C     FIX STEP SIZE IN ETA (Z) AND INCREMENT OF ETA (DZ)
      DF=0
      DO 1484 L=2,LMAXU
      Z(L)=(L-2)*DZST
      IF( Z(L) .LT. ZMAX   ) LLL=L
 1484 DZ(L)=Z(L)-Z(L-1)
      ZMAX=Z(LLL-1)
      DZST=DZ(LLL)
      N=0
      DO 954 L=LLL,LMAXU
      DZE=2.D0*DZ(L-1)-DZ(L-2)
      D12=1.D0/DZST+ZMAX-Z(L-1)-DZE/4.D0
      DZ(L)=(1.D0+ZMAX**2+Z(L-1)*(Z(L-1)-2.D0*ZMAX) )/D12
      IF( DZ(L) .GT. .4D0) N=1
      IF(N.EQ. 1) DZ(L)=.4D0
  954 Z(L)=Z(L-1)+DZ(L)
      WRITE(3,1482) (L ,Z(L),DZ(L),L=1,LMAXU)
 1482 FORMAT(/ '    L',6X,'Z',9X,'DZ',6X,'L',6X,'Z',9X,'DZ',6X,'L',6X,'Z'
     1,9X,'DZ',6X,'L',6X,'Z',9X,'DZ',6X,'L',6X,'Z',9X,'DZ'/ (I4,2F10.6,
     2';',I4,2F10.6,';',I4,2F10.6,';',I4,2F10.6,';',I4,2F10.6))
C     INITIALIZATION FOR "VELOCITY PROFILES AT SELECTED CHORDWISE
C     POSITIONS" & MAY BE REMOVED IF THAT SECTION IS DELETED
      DO 8025 IYP=1,4
      DO 8025 IXP=1,4
 8025 ILIM(IXP,IYP)=0.D0
      PCNS=50.D0
C END INITIALIZATION FOR "VELOCITY PROFILES AT SELECTED CHORDWISE
C ENDPARAMETERS FOR VELOCITY EQNS
C     END OF SECTION 1
C     BEGIN SECTION 2
C     PARAMETERS FOR POTENTIAL FLOW
```

```
C  THRUST(LBF)  6000     8000     10C00     .18         17140
C  TR           .0504    .0582    .0651     .000C2057   .C63115
C  AB(RADIANS)  .1050    .1310    .1561     .C00207     .1C48
C  ALPHB(DEG.)  6.01     7.50     8.94      .0118379    6.C0
C  XIS          .256     .188      .123     .460        .30
C  RK2          .365     .226     .081      .898        .45C
C  RCTCR(FEET)  24       24       24        4C
      READ(1,246) XO,AR    ,ALPHB,TR,XIINF,RK2
  246 FCRMAT(F1C.7,F10.4,2F10.7,F2C.16,F10.7)
C     TAB-TR>DSCRT(2.D0*DSTRT) IS NECESSARY TO AVOID OVERFLOW
      EPS=9.2D-2
C     EPS DETERMINES THICKNESS OF JOUKOWSKI AIRFOIF
C     XO IS POSITICN ALONG THE CHORD OF THE AXIS OF ROTATION; .25 IS 25%
C     CHORD
C     AR IS THE ASPECT RATIO;IT IS USED ONLY IN 'VELOCITY PROFILES AT
C     SELECTEC CHCRDWISE POSITIONS'
C     ALPHB IS GEOMETRIC ANGLE OF ATTACK
C     THE NONDIMESIONALIZED INDUCED VELOCITY=TR*(SPAN/CHORD)
C     XIINF IS THE CHORDWISE PCSITION OF THE STAGNATICN POINT. IT IS IN
C     BCDY COCRDINATES ANC IS NORMALLY A NEGATIVE NUMBER.
C     RK2 IS THE CCNSTANT K2 IN  Q=1-K2/YY**2;YY=SPAN/CHORD
      AB=ALPHB/57.29578
      TAB=DTAN(AB)
      WRITE(3,400) XO,AR    ,ALPHB,TR,XIINF,RK2,EPS,TAB
  400 FORMAT(// ' THE POSITICN OF THE AXIS OF RCTATICN IS',F8.4,'CHORD'/
     1' ASPECT RATIO=',F8.4/' GEOMETRIC ANGLE OF ATTACK=',F12.8,'DEG.'/
     2' COEFFICIENT OF INDUCED VELCCITY=TR=',F12.8/' PCSIITION OF THE ST
     3AGNATICN POINT IN BODY CCORDINATES:  XIINF=',D15.8/' K2=',F8.4/
     4' THE THICKNESS CF THE AIRFOIL IS CONTROLLED BY THE PARAMETER EPS'
     5,' ;EPS=',F12.8,/' TANGENT OF AOA=',D15.8//)
      FBS=DSIN(AB)
      FBR=-DCCS(AB)
      FAS=-FBR+TR*FBS
      FAR=FBS+TR*FBR
      FI=-(1.D0+TR*TAB)/(TAB-TR)
      SGN=1.D0
      DEI=2.D0/(1.D0+FI*FI)
C     DE IS THE PARAMETER DELTA;IT APPEARS IN THE PARAMETRIC EQNS FOR
C     A JOUKOWSKI AIRFCIL. AS DE VARIES FROM  0 TO 2, %CHORD GOES FROM
C     0 TC 100%
C     DEI IS DE AT THE STAGNATICN POINT.
      SI=DEI-1.D0
      JS=1200
      H=1.D-3/JS
      DSTRT=1.D-20
      XSTRT=EPS*DSCRT(2.D0*DSTRT)/(1.D0+EPS)
      IF( XIINF .GT. 13.D0) IBLUP=2C7C
      IF( IBLUP .NE. 2070) GO TO 819C
      DEP=1.D-3*DEI
      CALL RK3(DSDX,H,XSTRT,DSTRT,3.D0,DEP,XIINT,DV,IER)
      H=.1D0/JS
      CALL RK3(DSDX,H,XIINT,DEP,3.DC,DEI,XIINF,DV,IER)
C     DSDX  CALCULATES THE DERIVATIVE OF DE (OR S ,SINCE S=DE-1)
 8190 CONTINUE
      IF( FI    .LT. 0.D0 ) SGN=-1.DC
C     SGN =1.D0 FOR THE TOP(ABOVE THE CHORD LINE) OF THE AIRFCIL;
C     SGN=-1.D0 FCR THE BOTTOM
      IF( IBLUP .EC. 2070 ) XIINF=XIINF*SGN
      IBLUP=0
      WRITE(3,401) SI,XIINF,DEI,FI
  401 FORMAT(     ' SI,XIINF,DEI,FI      ',6D18.10 ///)
      DUMMY=13.D0
```

```
      B99=DSDX(DUMMY,DEI)
C     DSDX WILL CALCULATE XR (THE POSITION ALONG THE CHORD,MEASURED FROM
C     THE AXIS OF ROTATION) AND ZR (ONE-HALF THE AIRFOIL THICKNESS) AND
C     THEIR DERIVATIVES WITH RESPECT TO DE (B2 THRU B10)
      B10I=B10
      DXI(4)=1.2D-6
      DELX=2.5D-3
      XI(4)=0.D0
      X(4)=XIINF
      DE=DEI
      T=SI
      NTX=0
C END PARAMETERS FOR POTENTIAL FLOW
C     END OF SECTION 2
C BEGIN  K LOOP IN XI
C     K IS THE INDEX FOR XI ; DXI(K)=XI(K)-XI(K-1)
      DO 30 K=5,45
C     BEGIN SECTION 3
C     THE OPTIMUM XI SPACING DEPENDS ON ALPHB AND TR;THE SPACINGS USED
C     FOR VARIOUS COMBINATIONS OF THE TWO ARE GIVEN:
C     FOR ALPHB=6.01; TR=.0504
      DXI(K)=DELX*(1+K/23+2*(K/33)+4*(K/40) )
C     FOR ALPHB=  .50; TR=.0582
C     DXI(K)=DELX*(1+K/23+2*(K/33)+2*(K/40) )
C     FOR  ALPHB=8.94; TR=.0651
C     DXI(K)=DELX*(1+K/23+2*(K/33))
C     FOR  ALPHB=6.00; TR=.0631
C     DXI(K)=DELX*(1+K/23-K/46+2*(K/33)+2*(K/40)+6*(K/44))
C     FOR  ALPHB=.0118379; TR=.0002057
C     DXI(K)=DELX*(2+K/13-K/26+K/21+8*(K/22)+ 5*(K/29))
  153 XI(K)=XI(K-1)+DXI(K)
      X(K)=XI(K)+XIINF
      DX(K)=DXI(K)
      IMAX=4
      IF(K .LT. 7) GO TO 516
      DO 1489 J=1,JDIM
 1489 DVZ(J,1)=(Y(3,J,2,2)*(X(K)-X(K-2))-Y(3,J,2,3)*DX(K))/DX(K-1)
      IF(K .LE. 7) GO TO 516
C     K>=8
      S(1)=XI(K)*(1.D0/(X(K)-X(K-3))+1.D0/(DX(K)+DX(K-1))+1.D0/DX(K) )
      S(2)=-XI(K)*(X(K)-X(K-3))*(DX(K)+DX(K-1))/( (DX(K-1)+DX(K-2))*
     2 DX(K-1)*DX(K) )
      S(3)=XI(K)*(X(K)-X(K-3))*DX(K)/(DX(K-2)*DX(K-1)*(DX(K)+DX(K-1)) )
      S(4)=-XI(K)*(DX(K)+DX(K-1))*DX(K)/( DX(K-2)*(DX(K-1)+DX(K-2))*
     4   (X(K)-X(K-3)) )
C     S(I) IS THE COEFFICIENT OF THE VALUE AT THE POINT K-I+1 IN FORMING
C     THE DERIVATIVE  XI*(DERIVATIVE WRT XI)
C     IMAX IS THE MAX VALUE OF I
      DO 1437 J=1,JDIM
 1437 DVZ(J,1)=DVZ(J,1)+DX(K)*(X(K)-X(K-2))*( Y(3,J,2,3)*(X(K-1)-X(K-3))
     D -Y(3,J,2,4)*DX(K-1)-Y(3,J,2,2)*DX(K-2) )/(DX(K-1)*DX(K-2))
  516 IF(K-6) 518,519,520
  518 XI(5)=DXI(4)
      DXI(K)=XI(K)-XI(K-1)
      IMAX=2
      GO TO 521
  519 CONTINUE
      XI(6)=.5D-3
C     K=6
      S(1)=1.D0
      S(2)=-1.D0
      DXI(K)=XI(K)-XI(K-1)
```

```
      IMAX=2
      DO 1490 J=1,JDIM
 1490 DVZ(J,1)=Y(3,J,2,2)*(1.D0-1.5D0*DVZINC)*.8
      GO TO 521
  520 IF(K .GT. 7) GO TO 521
C     K=7
      XI(7)=DXI(7)
      DXI(K)=XI(K)-XI(K-1)
      DX(K)=DXI(K)
      X(K)=XI(K)+XIINF
      S(1)=(1.D0/DX(K)+1.D0/(DX(K)+DX(K-1)))*XI(K)
      S(2)=-(DX(K)+DX(K-1))/(DX(K)*DX(K-1)) *XI(K)
      S(3)=DX(K)/((DX(K)+DX(K-1))*DX(K-1))
      S(3)=S(3)*XI(K)
      IMAX=3
  521 CONTINUE
      X(K)=XI(K)+XIINF
      DX(K)=DXI(K)
      SGN=1.D0
      IF(X(K) .LT. 0.D0) SGN=-1.D0
      JS=15000*25/(K*K)+1000
      H=(X(K)-X(K-1))/JS
      H=10.D0*H
      DEP=DE
C     END OF SECTION 3
C     BEGIN SECTION 4
C BEGIN CALCULATION OF THE FUNCTIONS OF XI THAT APPEAR IN B.C. AND EQNS.
      IF(X(K)*X(K-1)) 3314,1405,3315
 3314 H=.01D0*H
C     THE VALUE OF DE IS FOUND BY INTEGRATING DSDX TO X(K) FROM XSTRT
      CALL RK3(DSDX,H,XSTRT,DSTRT,X(K),27.D0,XF,DE,IER)
      GO TO 320
C     THE VALUE OF DE IS FOUND BY INTEGRATING DSDX TO X(K) FROM X(K-1)
 3315 CALL RK3(DSDX,H,X(K-1),DEP,X(K),27.D0,XF,DE,IER)
  320 CONTINUE
      T=DE-1.D0
      DUMMY=13.D0*SGN
  319 B99=DSDX(DUMMY,DE)
      WRITE(3,450) K,XI(K),IER,DXI(K),DE,SGN,X(K)
  450 FORMAT(' K=',I3,5X,'XI(K)=',D19.11,10X,'IER=',I5 / ' DXI(K)=',
     1D19.11,5X,'DE=',D19.11,5X,'SGN=',F5.2,5X,'X(K)=',D19.11)
      B11=2.D0*(B2*B4+B3*B5)
      B12=2.D0*(B4*B4+B2*B6+B5*B5+B3*B7)
      XR=(1.D0+EPS)*(T-EPS)*(1.D0+((1.D0-EPS)**2)/B1)/4.D0
      XR=XR+(1.D0+EPS*EPS)/2.D0-X0
      ZR=.25D0*(1.D0+EPS)*DSQRT(DE*(1.D0-T))*(1.D0-(1.D0-EPS)**2/B1)*SGN
      WRITE(3,451) XR,B2,B4,B6,ZR,B3,B5,B7,B1,B10,B11,B12
  451 FORMAT( ' XR,B2,B4,B6,ZR/B3,B5,B7,B1,B10,B11,B12',5D16.9 /7D18.10)
      DES=DSQRT(DE)
      OMSS=DSQRT(1.D0-T)
C     PS1 IS 1ST DERIVATIVE OF THE POTENTIAL, SUBSCRIPT SIGMA, WRT SIGMA
C     PR3 IS 3RD DERIVATIVE OF THE POTENTIAL, SUBSCRIPT RHO, WRT SIGMA
      PS0=(1.D0+EPS)*T/2.D0
      PR0=(1.D0+EPS)*(SGN*DES*OMSS-DATAN(SGN*DES*OMSS/T))/2.D0
      PS1=(1.D0+EPS)/2.D0
      PS2=0.D0
      PS3=0.D0
      PR1=SGN*PS1*OMSS/DES
      PR2=-SGN*PS1/(OMSS*(DES**3))
      PR3= SGN*PS1*(1.D0-2.D0*T)/((OMSS**3)*(DES**5))
      BP(1)=B10
      DO 317 I=2,10
```

```
  317 BP(I)=BP(I-1)*B10
C     US0 IS 1ST (0+1)DERIVATIVE OF POTENTIAL,SUBSCRIPT SIGMA, WRT XI
C     UR2 IS 3RD (2+1)DERIVATIVE OF POTENTIAL,SUBSCRIPT RHO, WRT XI
      US0=PS1/B10
      UR0=PR1/B10
      US1=-.5D0*B11/BP(4)
      UR1=US1*PR1+PR2/BP(2)
      US1=US1*PS1
      US2=-.5D0*B12/BP(5)+B11*B11/BP(7)
      UR2=US2*PR1-PR2*1.5D0*B11/BP(5)+PR3/BP(3)
      US2=US2*PS1
C     PHIA IS PHI,SUBCRIPT A.  UA0 IS THE FIRST DERIVATIVE OF PHIA WRT X
C     UA1 IS THE SECOND DERIVATIVE....ETC.
      PHIA=FAS*PS0+FAR*PR0
      UA0=FAS*US0+FAR*UR0
      UA1=FAS*US1+FAR*UR1
      UA2=FAS*US2+FAR*UR2
      WRITE(3,459) PR0,PR1,PR2,PR3,PS0,PS1,PS2,PS3, US0,US1,US2,UR0,
     W UR1,UR2, PHIA,UA0,UA1,UA2
  459 FORMAT( ' PR0,PR1,PR2,PR3/PS0,PS1,PS2,PS3 ',4D20.11/4D20.11,
     F ' US0,US1,US2,UR0,UR1,UR2'/6D20.11/' PHIA,UA0,UA1,UA2 ',4D20.11 )
C     ALPHA IS THE ANGLE BETWEEN THE NORMAL TO THE SURFACE OF THE
C     AIRFOIL AND THE UPWARD NORMAL TO THE CHORD LINE
      ALPHA=DATAN(B3/B2)
      IF(SGN .LT. 0.D0 ) ALPHA= 3.1415926536 +ALPHA
      ADEG=57.2958*ALPHA
      CC=2.D0*DCOS(ALPHA-AB)/UA0
C     VDELTA IS THE FIRST TERM IN THE EXPANSION FOR THE SPANWISE
C     POTENTIAL FLOW, WHICH= VDELTA+VDEL2/YY**2
      VDELTA=PHIA+XR*(FBR-FAS)-ZR*(FBS+FAR)
      P0=XI(K)/UA0
      H0=XI(K)*UA0
C     XM0 IS M,SUBSCRIPT 0 . XM2K IS M,SUBSCRIPT 2K
      XM0=P0*UA1
      RM=(XM0+1.D0)/2.D0
      XM2K=XM0*(1.D0-XM0)+XI(K)*XI(K)*UA2/UA0
      DCDXA=(B4-B2*B11/(2.D0*B10*B10))/(B10*B10)
      DSDXA=(B5-B3*B11/(2.D0*B10*B10))/(B10*B10)
      DCDX=DCDXA*DCOS(AB)+DSDXA*DSIN(AB)
      DSWX=DSDXA*DCOS(AB)-DCDXA*DSIN(AB)
      CS=TR*XI(K)*DSIN(ALPHA-AB)
      CS2=RK2*(CS+TR*XI(K)*XI(K)*DSWX)
      CC2=RK2*(-XM0*CC+2.D0*P0*DCDX)
      RL2=2.D0*RK2
      P2=RK2*P0*(1.D0-XM0)
      VDEL2=RK2 *(H0*(1.D0-CC)+CS)
      H2=RK2*H0*(1.D0+XM0)
C     PCC IS %CHORD; PCNS IS %CHORD NEAR SEPARATION
      PCC(K)=100.D0*(XR+X0)
      UTIL(K)=UA0
      VDEL(K)=VDELTA
C     THIS WRITE STMT IS FOR CHECKOUT PURPOSES
C     WRITE(3,166) ALPHA,AB,DCDXA,DSDXA,DCDX,DSWX
C 166 FORMAT(     ' ALPHA,AB,DCDXA,DSDXA,DCDX,DSWX ',2D18.10,4D16.7 )
C     VINF(J) IS THE B.C. ON THE VELOCITY IN THE JTH ECN.
      VINF(5)=VDEL2
      VINF(2)=VDELTA
      WRITE(3,471) XR,ZR,PCC(K),ADEG,CC,CC2,H0,H2,PC,P2,UA0,VDELTA,VDEL2
     W,CS,CS2,     XM0,XM2K
  471 FORMAT( ' THE POINT HAS COORDINATES XR=',D17.10,1X,
     1'AND ZR=',D17.10,5X,' %CHORD(AT INFINITE SPAN)=',D17.10/
     2' THE ANGLE BETWEEN NORMAL TO SURFACE AND NORMAL TO CHORD=',D17.10
```

```
     3,'DEG',5X,'CC=',D17.10,5X,'CC2=',D17.10/  ' HO=',D17.10,5X,
     4 'H2=',D17.10,5X,'PO=',D17.10,5X,'P2=',D17.10,5X,'UAO=',D17.10/
     5 ' VDELTA=',D17.10,5X,'VDEL2=',D17.10,5X,' CS=',D17.10,5X,'CS2=',
     6 D17.10,5X,    /            ' XMO=',D17.10,5X,'XM2K=',D17.10 )
      ZMAX=5.4D0+11.D0*XI(K)
C     ZMAX IS THE VALUE OF ETA TO WHICH THE SOLUTIONS ARE TAKEN.  FOR
C     GOOD ACCURACY, ZMAX SHOULD BE CHOSEN SO THAT THE 2ND DERIVATIVE
C     OF THE STREAM FUNCTION WRT ETA (DVDZ) IS <=.001
C     SPEED AND CONVERGENCE ARE IMPROVED IF LMAX (WHERE Z(LMAX))=ZMAX)
C     IS AS SMALL AS POSSIBLE
C  END  CALCULATION OF THE FUNCTIONS OF XI THAT APPEAR IN B.C. AND EQNS.
C     END OF SECTION 4
 1345 DO 979 L=LMAX,LMAXU
      IF(Z(L) .LE.  ZMAX) GO TO 979
      LMAX=L
      GO TO 980
  979 CONTINUE
      LMAX=LMAXU-1
  980 IF( LMAX .GT. LMAXU-1) LMAX=LMAXU-1
      WRITE(3,148) LMAX,ZMAX,Z(LMAX),H,DCDX,ALPHA
  148 FORMAT(  '   LMAX,ZMAX,Z(LMAX),H,DCDX,ALPHA ',I5,3D14.6,2D20.12 )
      WRITE(3,149) IMAX,(S(I),I=1,4)
  149 FORMAT( ' IMAX=',I3,'     S(I)=',4D20.10   )
C     BEGIN SECTION 5
C BEGIN J LOOP TO CHOOSE VARIABLE
C     WHEN J=IS        1   2    3  4 4     5
C     STREAM FUNC IS   FO  GO   F2K  F2C  G2
C     M DENOTES NO. PRIMES+1
      DO 1500 J=1,JDIM
      IF(J .EQ. 2) LMAX=LMAX-1
      IF( J .EQ. 3) LMAX=LMAX+1
C     LMAX<LMAXU IS REQUIRED
      DVZINC=.005D0
      IF(J.EQ. 1 .AND. K .GE. 8) DVZINC=1.D-9
C     ERRMAX MAY BE REDIFINED HERE
      Y(2,J,LMAX,1)=VINF(J)
C     Y(M,J,L,I) IS THE (M-1)DERIVATIVE OF THE STREAM FUNCTION OF THE
C     JTH VARIABLE AT ETA=Z(L) AND  XI=XI(K-I+1)
C     FOR EXAMPLE,IF K CURRENTLY=12, Y(2,5,37,3) IS G2' AT ETA=Z(37) AND
C     XI=XI(10)
C     A(M,J,L)+S(1)*Y(M,J,L,1)=XI*(DERIVATIVE OF Y(M,J,L,1) WRT XI)
      DO 1491 L=1,LMAXU
      DO 1491 M=1,3
      A(M,J,L)=0.D0
      DO 1491 I=2,IMAX
 1491 A(M,J,L)=A(M,J,L)+S(I)*Y(M,J,L,I)
      NBLUP(J)=0
C
C BEGIN ITERATIONS ON B.C. ON VELUCITY AT EDGE OF B.L.
C     ONCE THE RUNGE-KUTTA SCHEME HAS INTEGRATED THE JTH EQN FROM ETA=0
C     TO ETA=Z(LMAX-1),THE ERROR IN VELOCITY (Y(2,J,LMAX-1,1)-VINF(J))
C     AT Z(LMAX-1) IS STORED IN ERR(ITER). THE SECOND DERIVATIVE AT THE
C     WALL (DVZ(J,ITER)) IS CHANGED AND ITER INCREMENTED, THIS CONTINUES
C      UNTIL ITER=6 (EQN PRESUMABLY NOT CONVERGENT) OR ERR(ITER)<ERRMAX
C     THE RUNGE-KUTTA SCHEME USED IS  DESCRIBED IN "INTRODUCTION TO
C     NUMERICAL ANALYSIS" ,F.B. HILDEBRAND,MCGRAW-HILL,1956,PAGE237
      DO 1400 ITER=1,6
      IBLUP=0
      WAYN=0.D0
      WAYP=0.D0
      ERRN=0.D0
      ERRP=0.D0
```

```
      LLM=LMAX*.9+K/5+K/12
 2848 Y(3,J,2,1)=DVZ(J,ITER)
      STIRL=0.DO
      LLL=LMAX-2
C
C BEGIN L LOOP IN ETA (I.E. IN Z)
      DO 1300 L=2,LLL
      ST(1)=-.125DO*(DZ(L+1)**2)/((DZ(L+1)+DZ(L))*DZ(L))
      ST(2)      =-.125DO*DZ(L+1)*(DZ(L)-DZ(L+1)-DZ(L+2))/((DZ(L+1)
     2 +DZ(L+2))*DZ(L))
      ST(3)      =-.125DO*DZ(L+1)*(DZ(L+2)-DZ(L+1)-DZ(L))/((DZ(L+1)
     3 +DZ(L))*DZ(L+2))
      ST(4)      =-.125DO*(DZ(L+1)**2)/((DZ(L+1)+DZ(L+2))*DZ(L+2))
      N=0
C BEGIN ITERATIONS FOR RUNGE KUTTA
      DO 1200 IS=2,5
      JM1=J-1
      IF(  (IS-3)*(2-L) .GT. 0 .OR.  IS .EQ. 4 ) GO TO 1527
      IF( (IS-3)*(IS-4) .EQ. 0) GO TO 176
      DO 1492 JT=1,JM1
      DO 1492 M=1,3
C     V(M,J) IS THE Y(M,J,L,1) EVALUATED AT THE VALUE OF Z REQUIRED BY
C     STEP "IS" OF THE RUNGE KUTTA SCHEME
      V(M,JT)=Y(M,JT,L+N,1)
 1492 DD(M,JT)=S(1)*Y(M,JT,L+N,1)+A(M,JT,L+N)
      DO 1493 M=1,2
 1493 DD(M,J)=A(M,J,L+N)
      GO TO 1527
  176 DO 1593 M=1,3
      DD(M,J)=.5DO*(A(M,J,L)  +A(M,J,L+1)   )
      IF(J-1) 1692,1692,1693
 1693 DO 1592 JT=1,JM1
      V(M,JT)=.5DO*(Y(M,JT,L,1)+Y(M,JT,L+1,1) )
      DD(M,JT)=.5DO*(S(1)*(Y(M,JT,L,1)+  Y(M,JT,L+1,1))+ A(M,JT,L)+
     D A(M,JT,L+1) )
      DO 1592 IST=1,4
      V(M,JT)=V(M,JT)+STIRL*ST(IST)*Y(M,JT,L-2+IST,1)
 1592 DD(M,JT)=DD(M,JT)+STIRL*ST(IST)*(S(1)*Y(M,JT,L-2+IST,1)+
     D A(M,JT,L-2+IST) )
 1692 CONTINUE
      DO 1593 IST=1,4
 1593 DD(M,J)=DD(M,J)+STIRL*ST(IST)*A(M,J,L-2+IST)
 1527 N=1
      DO 2732 M=1,3
 2732 V(M,J)=Y(M,J,L,1)+HIS(IS)*U(M,IS-1)
C     U(M,IS) IS DZ(L+1)*(DERIVATIVE OF Y(M,J, ,1)) EVALUATED AT THE
C     VALUE OF ETA CALLED FOR BY IS.  FOR IS=2,ETA=Z(L); FOR IS=3&4,ETA=
C     =(Z(L)+Z(L+1))/2; FOR IS=5,ETA=Z(L+1)
      U(2,IS)=DZ(L+1)*(Y(3,J,L,1)+HIS(IS)*U(3,IS-1))
      U(1,IS)=DZ(L+1)*(Y(2,J,L,1)+HIS(IS)*U(2,IS-1))
      GO TO (1,2,3,4,5),J
    1 CONTINUE
C     EQN 1    J=1    Y(2,J,L,1)=FO'
      U(3,IS)=XMO*V(2,J)**2-RM*V(1,J)*V(3,J)-XMO+V(2,J)*(S(1)*V(2,J)+
     1 DD(2,1))-V(3,J)*(S(1)*V(1,J)+DD(1,1))
      GO TO 1200
    2 CONTINUE
C     EQN 2    J=2    Y(2,J,L,1)=GO'
      U(3,IS)=-(RM*V(1,1)+DD(1,1))*V(3,J)+V(2,1)*(S(1)*V(2,J)
     2 +DD(2,2)) -HO*(1.DO-CC*V(2,1))-CS
      GO TO 1200
    3 CONTINUE
```

```
C      EQN 3    J=3    Y(2,J,L,1)=F2K'
       U(3,IS)=-(RM*V(1,1)+DD(1,1))*V(3,J)+(XMO*V(2,1)+DD(2,1))*V(2,J)
     3 +(XMO-1.DO)*.5DO*V(3,1)*V(1,J)+V(2,1)*(S(1)*V(2,J)+DD(2,J))
     3 -V(3,1)*(S(1)*V(1,J)+DD(1,J))
     3 +XM2K*UAO*(V(2,1)**2-.5DO*V(3,1)*V(1,1)-1.DO)
       GO TO 1200
     4 CONTINUE
C      EQN 4    J=4    Y(2,J,L,1)=F2C'
       U(3,IS)=-(RM*V(1,1)+DD(1,1))*V(3,J)+(XMO*V(2,1)+DD(2,1))*V(2,J)
     4 +(XMO-1.DO)*.5DO*V(3,1)*V(1,J)+V(2,1)*(S(1)*V(2,J)+DD(2,J))
     4 -V(3,1)*(S(1)*V(1,J)+DD(1,J))
     4+XI(K)*(V(2,2)*V(2,1)+.5*V(3,1)*V(1,2)+CC*(VDELTA-V(2,2))-VDELTA)
       GO TO 1200
     5 CONTINUE
C      EQN 5    J=5    Y(2,J,L,1)=G2'
C      RK2 IS USED IN THIS EQN
       U(3,IS)=-(RM*V(1,1)+DD(1,1))*V(3,J)+V(2,1)*(S(1)*V(2,J)+DD(2,J))
     5+RK2*(-((1.DO-XMO)*.5DO*V(1,3)/UAO+PO*DD(1,3)/XI(K)+V(1,1)*XM2K*
     5 .5DO)*V(3,2)+PO*V(2,3)*DD(2,2)/XI(K)-(1.DO-CC*V(2,1))*H2/RK2
     5 +HO*V(2,1)*CC2/RK2 +XI(K)*CC*V(2,3)-CS2/RK2 )
     5-((1.DO-XMO)*.5DO*V(1,4)/UAO+PO*DD(1,4)/XI(K)+.5*PO*V(1,2))*V(3,2)
     5 +PO*V(2,4)*DD(2,2)/XI(K)+XI(K)*CC*V(2,4)
 1200 U(3,IS)=U(3,IS)*DZ(L+1)
C END   ITERATIONS FOR RUNGE KUTTA
       DO 1201 M=1,3
C      THE VALUES AT Z(L+1) ARE EVALUATED
 1201 Y(M,J,L+1,1)=Y(M,J,L,1)+(U(M,2)+2.DO*(U(M,3)+U(M,4))+U(M,5))/6.DO
C      IF THE VELOCITY IS TOO LARGE OR SMALL,THE RUNGE-KUTTA INTEGRATION
C      IS STOPPED AND THE VALUE OF DVZ(J,ITER) IS ADJUSTED AND THE
C      PROGRAM RETURNS TO STMT 2848.'AFTER 50 ADJUSTMENTS(IBLUP=50),THE
C      PROGRAM WILL CALL EXIT (I.E. STOP)  AT STMT 1405
       IF( Y(2,1,L+1,1) .LT. 0 .OR.  Y(2,1,L+1,1) .GT.1.8) GO TO 1299
       IF(DABS(Y(2,J,L+1,1)) .LT. 1.D6 )    GO TO 1300
 1299 IBLUP= IBLUP+1
       NBLUP(J)=NBLUP(J)+1
       IF(IBLUP .GT. 40)
      IWRITE(3,2849) IBLUP,J,L,ITER,DVZ(J,ITER),Y(2,J,L+1,1),Y(3,J,L+1,1)
 2849 FORMAT( I4,' TH BLOWUP; J=',I3,'  L=',I3,' ITER=',  I4,' DVZ=',
     F D20.13, '  VEL=',D15.6,  ' DVDZ=',D15.6)
       IWAY=Y(2,J,L+1,1)/DABS(Y(2,J,L+1,1))
       IF(IWAY .GT. 0 ) WAYP=DVZ(J,ITER)
       IF(IWAY .LT. 0 ) WAYN=DVZ(J,ITER)
       IF( IWAY .GT. 0 .AND. L .GT. LLM) ERRP=Y(2,J,LLM,1)-VINF(J)
       IF( IWAY .LT. 0 .AND. L .GT. LLM) ERRN=Y(2,J,LLM,1)-VINF(J)
       IF(WAYN*WAYP)-2219,1218,2219
 2219 DVZ(J,ITER)=(WAYN+WAYP)*.5DO
       IF(ERRP*ERRN .NE.0.DO) DVZ(J,ITER)=(WAYN*ERRP-WAYP*ERRN)/(ERRP
     D -ERRN)
       GO TO 2220
 1218 DVZ(J,ITER)=DVZ(J,ITER)*(1.DO-IBLUP*IWAY* .1DO   *DVZ(J,ITER)/
     I DABS(DVZ(J,ITER)) )
       IF(WAYN*WAYP+(IBLUP/10-1).NE.0 .AND.DABS(DVZ(J,ITER)).LT. 1.D-10)
     I DVZ(J,ITER)=DVZ(J,ITER)-IWAY*.001
 2220 IF(IBLUP .GT. 50) GO TO 1405
       GO TO 2848
 1300 STIRL=1.DO
C END   L LOOP IN ETA (I.E. IN Z)
       ERR(ITER)=Y(2,J,LLL+1,1) -VINF(J)
C      THE ERROR IN MATCHING THE B.C. ON VELOCITY AT THE EDGE OF THE
C      BOUNDARY LAYER ( ERR(ITTER)) IS USED TO FIND A BETTER VALUE FOR
C      THE SECOND DERIVATIVE OF THE STREAM FUNCTION AT THE WALL (DVZ(J,IT
C      (DVZ(J,ITER)) UNTIL ERR(ITER)<ERRMAX
```

```
      IF(ITER .GT.3 )
C     THIS WRITE STMT IS FOR CHECKOUT PURPOSES
     1WRITE(3,965) K,J,ITER,L,IS,DVZ(J,ITER),ERR(ITER)
  965 FORMAT(    '  K,J,ITER,L,IS,DVZ,ERR',5I5,3D15.6)
      IF(DABS(ERR(ITER)) .LT. ERRMAX) GO TO 1401
      IF(ITER-2) 81,82,83
C    ERRMAX& DVZINC CAN BE FUNCTIONS OF J
   81 DVZ(J,2)=DVZ(J,1)*(1.D0-DVZINC)
      GO TO 1400
   82 DVZ(J,3)=(ERR(2)*DVZ(J,1)-ERR(1)*DVZ(J,2))/(ERR(2)-ERR(1))
      GO TO 1400
   83 D12=(DVZ(J,ITER-1)-DVZ(J,ITER-2))/(ERR(ITER-1)-ERR(ITER-2))
      D23=(DVZ(J,ITER)  -DVZ(J,ITER-1))/(ERR(ITER)  -ERR(ITER-1))
      D123=(D23-D12)/(ERR(ITER)-ERR(ITER-2))
      DVZ(J,ITER+1)=DVZ(J,ITER)-ERR(ITER)*(D23-ERR(ITER-1)*D123)
 1400 CONTINUE
C END   ITERATIONS ON B.C. ON VELOCITY AT EDGE OF B.L.
 1405 WRITE(3,1403) J
 1403 FORMAT(' EQN NO.',I2,' FAILS TO CONVERGE BECAUSE' )
      IF(IBLUP .GT. 50) WRITE(3,8186) ITER,Z(L)
 8186 FORMAT(' FOR ITER=',I2,', THE VELOCITY BECAME TOO LARGE OR TOO',
     1'SMALL FOR ETA=',D15.6 / ' THE VELOCITIES ARE CHECKED FOR SIZE',
     2'AFTER STMT 1201')
      IF( ITER .GE. 6) WRITE(3,8187) (ERR(I),DVZ(J,I),I,I=1,6)
 8187 FORMAT(' THE B.C. AT Z(LMAX) WERE NOT MATCHED AFTER 6 ITERATIONS,'
     F'ON THE SECOND DERIVATIVE OF STREAM FUNCTION AT WALL (DVDZ) '//
     2'  THE ERROR IN MATCHING B.C.       DVDZ AT THE WALL    ITERATION'/
     3 ( 8X,D14.7,8X,D22.15,5X,I2) )
      CALL EXIT
 1401 CONTINUE
      ITERKP(J)=ITER
      DO 2324 L=LMAX,LMAXU
C     THE STREAM FUNCTIONS (Y(1,J,L,I)),"VELOCITIES"(Y(2,J,L,I)), AND
C     "SHEAR RATE",(Y(3,J,L,I)) ARE CALCULATED UP TO Z(LMAXU) IN CASE
C     LMAX INCREASES AT THE NEXT XI(K) STATION
      Y(1,J,L,1)=Y(1,J,LLL+1,1)+VINF(J)*(Z(L)-Z(LLL+1))
      Y(3,J,L,1)=Y(3,J,LLL+1,1)
 2324 Y(2,J,L,1)=VINF(J)
 1500 CONTINUE
C END   J LOOP TO CHOOSE VARIABLE
C     END OF SECTION 5
C     BEGIN SECTION 6
      DO 157 J=1,JDIM
  157 IF(DABS(Y(3,J,LLL+1,1)) .GT. 1.D-3)  N=27
      WRITE(3,8183) (J,J=1,JDIM)
 8183 FORMAT(/' CONVERGENCE ACHIEVED  FOR  J=   ',5X,6(I3,11X))
      WRITE(3,8184) (NBLUP(J),J=1,JDIM)
 8184 FORMAT( ' NO. ITERATIONS TO REACH Z(LMAX)',5X,6(I3,11X))
      WRITE(3,8185) (ITERKP(J),J=1,JDIM)
 8185 FORMAT( ' NO. ITERATIONS TO MATCH B.C.    ',5X,6(I3,11X))
      IF(N .EQ. 27) WRITE(3,158) (Y(3,J,LLL+1,1),J=1,JDIM)
  158 FORMAT( ' ZMAX TOO SMALL; DVDZ(J) AT ZMAX=', 6D14.5)
      WRITE(3,144)
  144 FORMAT(/ '       Z     L       ' ,  T25,'F0',T43,'G0', T61,'F2K',
     F  T79,'F2C', T97,'G2'     )
      JM1=LMAX/4
      DO 861 L=2,LMAX
C     VELOCITY OR VEL IS ACTUALLY THE FIRST DERIVATIVE WRT ETA OF THE
C     STREAM FUNCTION OR Y(2,J,L,I). THE 2ND DERIVATIVE IS CALLED DVDZ
C     OR DVZ (WHEN EVALUATED AT THE WALL)
      IF((L/2)*2.NE.L .AND. L.GT.10 .AND. L.LT.LMAX-2) GO TO 861
      WRITE(3,142) Z(L),L, (Y(2,J,L,1),J=1,JDIM)
```

```
      IF(L .GT. 10 .AND. L .LT. LMAX-2 .AND. L .NE. (L/JM1)*JM1)GOTO 861
      WRITE(3,143) (Y(3,J,L,1),J=1,JDIM)
  861 CONTINUE
      WRITE(3,161) (Y(1,J,LMAX,1),J=1,JDIM)
  161 FORMAT( ' STREAM FUNCTION '  ,6D18.9 )
      WRITE(3,147) (VINF(J),J=1,JDIM)
  147 FORMAT(' VELOCITY AT ZMAX' ,6D18.9)
  142 FORMAT( F8.4,I4,' VEL ', 6D18.9 )
  143  FORMAT(  13X,'DVOZ ',6D18.9)
C     END OF SECTION 6
C     BEGIN SECTION 7
C      CHECK OF X DERIVATIVES            AF
C     THIS SECTION MAY BE REMOVED IF DESIRED
      IF(K.LT. 7) GO TO 7139
      DK=DX(K)
      DP=DX(K-1)
      L=LMAXU-3
      DO 7138 J=1,JDIM
      A(3,J,5)=-DK*Y(2,J,10,3)/((DK+DP)*DP)+(DK-DP)*Y(2,J,10,2)/(DK*DP)
     5 +DP*Y(2,J,10,1)/((DK+DP)*DK)
      A(3,J,5)=A(3,J,5)*XI(K-1)
 7138 CONTINUE
C     THIS IS THE VALUE OF XI*(DERIVATIVE OF Y(2,J.10.2) WRT XI) USED IN
C     CALCULATIONS AT K-1
      WRITE(3,7140) (XD2(J)   ,J=1,JDIM)
C     THIS IS THE VALUE OF XI*(DERIVATIIVE OF Y(2,J,10,2) WRT XI ) AT
C     XI=XI(K-1) FOUND FROM VALUES AT K,K-1,&K-2.  THE DIFFERENCE IN
C     THESE TWO IS A MEASURE OF THE ERROR. REDUCTION OF THE XI SPACING
C     WILL REDUCE ERROR BUT ALSO SLOW CONVERGENCE.
      WRITE(3,7140) (A(3,J,5),J=1,JDIM)
 7140 FORMAT( ' XI DERIVATIVES '     ,6D18.9)
 7139 DO 7136 J=1,JDIM
 7136 XD2(J)   =A(2,J,10)+S(1)*Y(2,J,10,1)
C     THIS SECTION MAY BE REMOVED IF DESIRED
C END  CHECK OF X DERIVATIVES            AFTER 1428
C     END OF SECTION 7
C     BEGIN SECTION 8
C     DISPLACEMENT THICKNESS,SHAPE FACTOR & SKEW ANGLE    AFTER 143
C     THIS SECTION MAY BE REMOVED IF DESIRED
      IF(K .LT. 8 .OR. JDIM .LT. 5 ) GO TO 8090
      DO 8040 IYP=1,4
      YP=(.3D0*IYP-.25D0*(IYP/4))*AR
      XP=XI(K)/(1.D0-RK2/YP**2)+XIINF
      E(1)=(XP-X(K-1))*(XP-X(K-2))/( (X(K)-X(K-1))*(X(K)  -X(K-2)) )
      E(2)=(XP-X(K)   )*(XP-X(K-2))/( (X(K-1)-X(K))*(X(K-1)-X(K-2)) )
      E(3)=(XP-X(K)   )*(XP-X(K-1))/( (X(K-2)-X(K))*(X(K-2)-X(K-1)) )
      PCCP=0.D0
      UTILP=0.D0
      VDELP=0.D0
      DVAR=UAO*YP*YP
      DO 8020 I=1,3
      PCCP=PCCP+E(I)*PCC(K-I+1)
      UTILP=UTILP+E(I)*UTIL(K-I+1)
 8020 VDELP=VDELP+E(I)*VDEL(K-I+1)
      VDELS=VDELTA+VDEL2/YP**2
C     RK2 IS USED IN THIS EQN
      TK(3)=Y(1,1,LLL,1)+(RK2*Y(1,3,LLL,1)+Y(1,4,LLL,1))/DVAR
      TK(4)=Y(1,2,LLL,1)+Y(1,5,LLL,1)/(YP*YP)
      TK(1)=Z(LLL)-TK(3)
      TK(2)=Z(LLL)-TK(4)/VDELP
      UP(2)=0.D0
      VP(2)=0.D0
```

```
      CC 8030 L=3,LLL
C     RK2 IS USED IN THIS EQN
      UP(L)=(Y(2,1,L,1)+(RK2*Y(2,3,L,1)+Y(2,4,L,1))/DVAR)**2
      VP(L)=(Y(2,2,L,1)+Y(2,5,L,1)/(YP*YP))**2
 8030 VP(L)=VP(L)/VDELS
      CC 8031 L=4,LLL,2
      TK(3)=TK(3)-CZ(L)*(UP(L-2)+4.CO*UP(L-1)+UP(L))/3.DO
      TK(4)=TK(4)-CZ(L)*(VP(L-2)+4.CO*VP(L-1)+VP(L))/3.CC
      LST=L
      IF(CZ(L+2) .NE. CZ(3)) GO TO 8033
 8031 CONTINUE
 8033 DC 8032 L=LST,LLL
      TK(3)=TK(3)-CZ(L)*(UP(L)+UP(L-1))*.5DC
 8032 TK(4)=TK(4)-CZ(L)*(VP(L)+VP(L-1))*.5DC
      DVAR=DSQRT(DABS((XP-XIINF)/(YP*UTILP)))
      CC 8016 I=1,4
 8016 TK(I)=TK(I)*DVAR
      TK(3)=TK(1)/TK(3)
      TK(4)=TK(2)*VDELP/TK(4)
C     RK2 IS USED IN THIS EQN
      DVAR=YP+UTILP*(Y(3,1,2,1)+(RK2*Y(3,3,2,1)+Y(3,4,2,1))/(LAG*YP*YP))
     C  /(Y(3,2,2,1)+Y(3,5,2,1)/(YP*YP))
      DVAR=1.DO/DVAR
      BETA=DATAN(DVAR)*57.29578DO
      WRITE(3,8015)
 8015 FORMAT(/8X,'X',8X,'  X DISPLACEMENT ','  Y DISPLACEMENT ',
     1' X SHAPE FACTOR  ',' Y SHAPE FACTOR  ', '  SKEW  ANGLE   ',
     2'  ASPECT RATIO  ' ,'  SPAN/CHORD '   /  19X,'   THICKNESS     ',
     3'    THICKNESS    ',  T86,'IN DEGREES' )
      WRITE(3,8014) XP,(TK(I),I=1,4),BETA,AR,YP
 8014 FORMAT(5D17.10,2D16.9,D15.8)
 804C CONTINUE
C     THIS SECTION MAY BE REMOVED IF DESIRED
C END DISPLACEMENT THICKNESS,SHAPE FACTOR & SKEW ANGLE    AFTER 143
C     END OF SECTION 8
      IF(JOIN .LT. 4 ) GO TO 1428
      RK2A=-Y(3,4,2,1)/     Y(3,3,2,1)
      WRITE(3,146) RK2A
  146 FORMAT( ' -F2C"/F2K"=',D2C.9 )
 1428 CONTINUE
C     BEGIN SECTION 9
C     VELOCITY PROFILES AT SELECTED CHORDWISE POSITIONS
C     THIS SECTION MAY BE REMOVED IF DESIRED
      IF(Y(3,1,2,1) .LT..0885) PCNS=PCC(K)  -1.1
      CC 8080 IXP=1,4
      GC TO (8C71,8072,8072,8073) ,IXP
 8071 PCCP=60.CO
      GC TC 8074
 8072 PCCP=10.CO+20.CO*(IXP-2)
      GC TO 8074
 8073 PCCP=PCNS
 8074 IF(PCCP .GT. PCC(K) .OR. PCCP .LT. PCC(K-2)) GO TO 8C8C
      E(1)=(PCCP-PCC(K-1))*(PCCP-PCC(K-2))/((PCC(K)-PCC(K-1))*(PCC(K)-
     1PCC(K-2)))
      E(2)=(PCCP-PCC(K))*(PCCP-PCC(K-2))/((PCC(K-1)-PCC(K))*(PCC(K-1)-
     2 PCC(K-2)))
      E(3)=(PCCP-PCC(K))*(PCCP-PCC(K-1))/((PCC(K-2)-PCC(K))*(PCC(K-2)-
     3PCC(K-1)))
      XP=E(1)*X(K)+E(2)*X(K-1)+E(3)*X(K-2)
C     IF XP BE FOUND FOR EACH PCCP, ABOVE XP&E NEEDED ONLY FOR PCNS
      CC 8084 IYP=1,4
      YP=(.3DO*IYP-.25DO*(IYP/4))*AR
```

```
      IF(ILIM(IXP,IYP) .GT. 0) GO TO 8084
C     RK2 IS USED IN THIS EQN
      XIP=( XP-XIINF)*(1.D0-RK2/YP**2)
      IF( XI(K) .LT. XIP ) GO TO 8084
      ILIM(IXP,IYP)=1.D0
      E(1)=(XIP-XI(K-1))*(XIP-XI(K-2))/((XI(K)-XI(K-1))*(XI(K)-XI(K-2)))
      E(2)=(XIP-XI(K))*(XIP-XI(K-2))/((XI(K-1)-XI(K))*(XI(K-1)-XI(K-2)))
      E(3)=(XIP-XI(K))*(XIP-XI(K-1))/((XI(K-2)-XI(K))*(XI(K-2)-XI(K-1)))
      DVAR=YP*YP*(E(1)*UTIL(K)+E(2)*UTIL(K-1)+E(3)*UTIL(K-2) )
      DO 8083 L=2,LMAX
      UP(L)=0.D0
      VP(L)=0.D0
      DO 8083  I=1,3
C     RK2 IS USED IN THIS EQN
      UP(L)=UP(L)+E(I)*(Y(2,1,L,I)+(RK2*Y(2,3,L,I)+Y(2,4,L,I))/DVAR)
 8083 VP(L)=VP(L)+E(I)*(Y(2,2,L,I)+Y(2,5,L,I)/ (YP*YP))
      WRITE(3,8091) PCCP,YP,XP,XIP
 8091 FORMAT(//' %CHORD=',F10.6,5X,'SPAN/CHORD=',F12.8,5X'X=',F15.10,5X,
     F 'XI=',F15.10 )
      WRITE(3,8093) (UP(L),L=2,LMAX)
 8093 FORMAT(' CHORDWISE VELOCITIES' /( 1X,10F8.4))
      WRITE(3,8092) (VP(L),L=2,LMAX)
 8092 FORMAT(/' SPANWISE VELOCITIES' /( 1X,10F8.4))
 8084 CONTINUE
 8080 CONTINUE
C     THIS SECTION MAY BE REMOVED IF DESIRED
C END VELOCITY PROFILES AT SELECTED CHORDWISE POSITIONS
C     END OF SECTION 9
 8090 CONTINUE
      WRITE(3,872) K
  872 FORMAT('  END OF K=',I5 ///)
C     UPDATE MATRIX FOR NEW VALUE OFK
      DO 1429 IT=1,3
      DO 1429 L=1,LMAXU
       DO 1429 J=1,JOIM
      DO 1429 M=1,3
 1429 Y(M,J,L,5-IT)=Y(M,J,L,4-IT)
   30 CONTINUE
C END    K LOOP IN XI
C
      CALL EXIT
      END
      REAL FUNCTION DSDX*8(DUMMY,DE)
      IMPLICIT REAL*8 (A-H,O-Z)
      COMMON/BIJ/EPS,SGN,B1,B2,B3,B4,B5,B6,B7,B8,B9,B10
      IF(SGN) 85,85,75
   85 IF( DUMMY .GT. 0.D0) SGN=1.D0
   75 S=DE-1.D0
      OMS2=DE*(1.D0-S)
      IF(DABS(OMS2) .LT. 1.D-50)   WRITE(3,401) DE,SGN,OMS2,DUMMY
      IF(DABS(OMS2) .LT. 1.D-50) OMS2=1.D-50
      BA=(1.D0-EPS)**2
      BB=1.D0-EPS*EPS
      BC=1.D0+EPS
      B1=1.D0+EPS*EPS-2.D0*EPS*S
      B2=BC*(1.D0+BA*BB/(B1*B1))/4.D0
      B3=SGN*BC*(-S*(1.D0-BA/B1)-OMS2*2.D0*EPS*BA/B1**2)/(4.D0*
     3 DSQRT(OMS2))
      IF( DABS(DUMMY*SGN-13.D0)  .GT. 1.D-4) GO TO 18
      BD=EPS*BC*BA/(2.D0*B1*DSQRT(OMS2))
      B4=BC*BA*BB*EPS/B1**3
      BE=B1*B1
```

```
      B5=SGN*BD*(-1.D0/(BA*DE)+2.D0*S/B1-4.D0*EPS*OMS2/BE)
      B6=6.D0*EPS*B4/B1
      BF=1.D0/(CE*CE*BA)+2.D0/B1+12. *EPS*S/BE-16.D0*EPS*EPS*OMS2/B1**3
      B7=B5*(2.D0*EPS/B1+S/OMS2)+SGN*BD*BF
  401 FORMAT(     ' B2,B3,DE,SGN,OMS2,DUMMY   ',6D16.7   )
   18 B10=DSQRT(B2*B2+B3*B3)*SGN
C    ,IF(DABS(DUMMY).LT.1.D-6)WRITE(3,401)B2,B3,DE,SGN,OMS2,DUMMY
      DSDX=1.D0/B10
      RETURN
      END
      SUBROUTINE RK3(FUN,HI,XI,YI,XF,YF,ANSX,ANSY,IER)
C     RK3 IS THE DOUBLE PRECISION VERSION OF THE PROGRAM RK1 DOCUMENTED
C     IN THE IBM MANUAL H20-0205-3 "SYSTEM/360 SCIENTIFIC SUBROUTINE
C     PACKAGE-PROGRAMMERS MANUAL" PAGE 331
      DOUBLE PRECISION HI,XI,YI,XF,YF,ANSX,ANSY,H,XN,YN,HNEW,XN1,YN1,    RK1  580
     1                 XX,YY,XNEW,YNEW,H2,T1,T2,T3,T4,FUN                RK1  590
       IER = 0                                                           RK1  705
      IF(XF-XI) 11,11,12                                                 RK1  710
   11 ANSX=XI                                                            RK1  720
      ANSY=YI                                                            RK1  730
      RETURN                                                             RK1  740
C     TEST INTERVAL VALUE                                                RK1  760
   12 H=HI                                                               RK1  780
      IF(HI) 16,14,20                                                    RK1  790
   14 IER=1                                                              RK1  800
      ANSX=XI                                                            RK1  810
      ANSY=0.0                                                           RK1  820
      RETURN                                                             RK1  830
   16 H=-HI                                                              RK1  840
C     SET XN=INITIAL X,YN=INITIAL Y                                      RK1  860
   20 XN=XI                                                              RK1  880
      YN=YI                                                              RK1  890
C     INTEGRATE ONE TIME STEP                                            RK1  910
      HNEW=H                                                             RK1  930
      JUMP=1                                                             RK1  940
      GO TO 170                                                          RK1  950
   25 XN1=XX                                                             RK1  960
      YN1=YY                                                             RK1  970
C     COMPARE XN1 (=X(N+1)) TO X FINAL AND BRANCH ACCORDINGLY            RK1  990
      IF(XN1-XF)50,30,40                                                 RK1 1010
C     XN1=XF, RETURN (XF,YN1) AS ANSWER                                  RK1 1030
   30 ANSX=XF                                                            RK1 1050
      ANSY=YN1                                                           RK1 1060
      GO TO 160                                                          RK1 1070
C     XN1 GREATER THAN XF, SET NEW STEP SIZE AND INTEGRATE ONE STEP      RK1 1090
C     RETURN RESULTS OF INTEGRATION AS ANSWER                            RK1 1100
   40 HNEW=XF-XN                                                         RK1 1120
      JUMP=2                                                             RK1 1130
      GO TO 170                                                          RK1 1140
   45 ANSX=XX                                                            RK1 1150
      ANSY=YY                                                            RK1 1160
      GO TO 160                                                          RK1 1170
C     XN1 LESS THAN X FINAL, CHECK IF (YN,YN1) SPAN Y FINAL              RK1 1190
   50 IF((YN1-YF)*(YF-YN))60,70,110                                      RK1 1220
C     YN1 AND YN DO NOT SPAN YF. SET (XN,YN) AS (XN1,YN1) AND REPEAT     RK1 1240
   60 YN=YN1                                                             RK1 1260
      XN=XN1                                                             RK1 1270
      GO TO 170                                                          RK1 1280
C     EITHER YN OR YN1 =YF. CHECK WHICH AND SET PROPER (X,Y) AS ANSWER   RK1 1300
   70 IF(YN1-YF)80,100,80                                                RK1 1320
   80 ANSY=YN                                                            RK1 1330
      ANSX=XN                                                            RK1 1340
```

```
      GC TO 160                                                         RK1 1350
  100 ANSY=YN1                                                          RK1 1360
      ANSX=XN1                                                          RK1 1370
      GC TO 160                                                         RK1 1380
C     YN AND YN1 SPAN YF. TRY TO FIND X VALUE ASSOCIATED WITH YF        RK1 1400
  110 CC 140 I=1,10                                                     RK1 1420
C     INTERPOLATE TO FIND NEW TIME STEP AND INTEGRATE ONE STEP          RK1 1440
C     TRY TEN INTERPOLATIONS AT MOST                                    RK1 1450
      HNEW=((YF-YN )/(YN1-YN))*(XN1-XN)                                 RK1 1470
      JUMP=3                                                            RK1 1480
      GC TO 170                                                         RK1 1490
  115 XNEW=XX                                                           RK1 1500
      YNEW=YY                                                           RK1 1510
C     COMPARE COMPUTED Y VALUE WITH YF AND BRANCH                       RK1 1530
      IF(YNEW-YF)120,150,130                                            RK1 1550
C     ADVANCE, YF IS BETWEEN YNEW AND YN1                               RK1 1570
  120 YN=YNEW                                                           RK1 1590
      XN=XNEW                                                           RK1 1600
      GC TO 140                                                         RK1 1610
C     ADVANCE, YF IS BETWEEN YN ANC YNEW                                RK1 1630
  130 YN1=YNEW                                                          RK1 1650
      XN1=XNEW                                                          RK1 1660
  140 CONTINUE                                                          RK1 1670
C     RETURN (XNEW,YF) AS ANSWER                                        RK1 1690
  150 ANSX=XNEW                                                         RK1 1710
      ANSY=YF                                                           RK1 1720
  160 RETURN                                                            RK1 1730
  170 H2=HNEW/2.0                                                       RK1 1750
      T1=HNEW*FUN(XN,YN)                                                RK1 1760
      T2=HNEW*FUN(XN+H2,YN+T1/2.0)                                      RK1 1770
      T3=HNEW*FUN(XN+H2,YN+T2/2.0)                                      RK1 1780
      T4=HNEW*FUN(XN+HNEW,YN+T3)                                        RK1 1790
      YY=YN+(T1+2.0*T2+2.0*T3+T4)/6.0                                   RK1 1800
      XX=XN+HNEW                                                        R-1 1810
      GC TO (25,45,115), JUMP
      END                                                               RK1 1840
```

```
C
C
C
      IMPLICIT REAL*8 (A-H,O-Z)
C     A FORTRAN PROGRAM FOR A ROTOR BLADE IN FORWARD FLIGHT  WITH LIFT
C     THE PROGRAM OCCUPIES LESS THAN 200,000 BYTES IN FORTRAN IV-G,
C     LEVEL 1, MOD 3
      COMMON/BIJ/EPS,SGN,B1,B2,B3,B4,B5,B6,B7,B8,B9,B10
      DIMENSION X(80),DX(80),XI(80),DXI(80),BP(4),Y(3,12,75,4),
     1 A(2,12,75), S(4), ST(4), ERROR(12),BC(12),BCL(12),LMAXR(12),
     2 OMEGA(12),ITERK(12), Z(75),DZ(75),DN(75),EN(75),
     3 SDZ(75),EY(75),DUMV(75),DT(75), EYK(450),EBC(12),RHSF(75)
     4 , XDC(12),XDP(12),PCE(12),RKJ(12),IKERR(80)
      DIMENSION SHV(20),PSIV(20),VAV(20),ARV(20),PCCV(20),SHT(20),
     D PSIT(20),VAT(20),ART(20), RHS(12,75),DT2(75),PCC(80),UAPK(80),
     D UCPK(80),E(3)
     V, ILIM(20,4),RNUK(80),TK(6),UP(75),VP(75)
C     THIS DIMENSION STMT IS FOR:K<=80,M<=3,J<=12,L<=75,I<=4,NGT&NGVEL<61
      EXTERNAL DSDX
C     SYMMETRIC,LIFTING ROTOR UNDERGOING FORWARD FLIGHT
      JDIM=5
C     JDIM IS THE NO. OF EQUATIONS TO BE SOLVED; IT IS THE MAXIMUM
C     VALUE OF J
C       IF JDIM=5 THE PGM ASSUMES THAT K10 IS TO BE FOUND
C       IF JDIM=9 THE PGM ASSUMES THAT K20R,K20,K21,&K22 ARE TO BE FOUND
C     AND THE VALUE OF K10 (RK10) THAT WAS READ IN IS CORRECT
C     IF JDIM>9 THE PGM ASSUMES THAT K10,K20R,K20,K21 & K22 ARE KNOWN
C     AND HAVE BEEN READ IN CORRECTLY
C
C  SECTION 1: INPUT VALUES NEEDED FOR THE POTENTIAL FLOW SOLUTION
C      READ(1,XXXX) DENOTES THE DATA CARDS AT THE END OF THE DECK;
C     WRITE(2,XXXX) DENOTES THE CARD PUNCH; WRITE(3,XXXX) DENOTES A
C     133 SPACE/LINE PRINTER
C     PARAMETERS FOR POTENTIAL FLOW
C      EPS(EPSILON) OF .092 GIVES AN 11.9% THICK AIRFOIL
      EPS=9.2D-2
C     LESS THAN 160 PAGES ARE NORMALLY PRINTED.
C     ON IBM MODEL 360/75 A CPU TIME OF 9 MINUTES IS ALWAYS ADEQUATE.
C     IF NEITHER K10 NOR THE POSITION OF THE STAGNATION POINT (XIINF) IS
C     KNOWN, SET JDIM=5 AND PUT XIINF=14. ON THE FIRST DATA CARD.
C     ONCE THE VALUE OF K10 HAS BEEN FOUND ( BY EXTRAPOLATING
C     F10C*/F1K*@WALL TO SEPARATION VALUE OF XI, XIS),THEN JDIM SHOULD
C     BE SET TO 9 AND THE PROGRAM RERUN. VALUES OF K20R,K20,K21, AND
C     K22 ARE FOUND BY EXTRAPOLATING THE VALUES OF -DVD7/F2K* TO XIS.
C     ONCE THE CORRECT VALUES OF THE K2'S HAVE BEEN ENTERED ON THE
C     SECOND DATA CARD, SET JDIM TO 12 AND RERUN THE PROGRAM. THE
C     SUCCEEDING DATA CARDS WILL BE USED TO SPECIFY THE NUMBER OF
C     VELOCITY PROFILES      DISPLACEMENT THICKNESSES,AND MOMENTUM
C     THICKNESS DESIRED.
C        SUMMARY
C     1ST DATA CARD:FORMAT(F10.6,F10.7,F20.16,3F10.7) XO,ALPHB,XIINF,
C     XIS,RK10
C     SUCCEEDING DATA CARDS ARE NOT READ IF JDIM<10
C     2ND DATA CARD:FORMAT(8F10.5) RK20R,RK20,RK21,RK22
C     3RD DATA CARD:FORMAT(I5) NGVEL ( NO. VEL. PROFILES TO BE FOUND)
C     NEXT NGVEL CARDS:FORMAT(8F10.5) SH,PSI,VA,AR,PCC
C     (NGVEL+4)TH CARD:FORMAT(I5) NGT (NO. THICKNESSES TO BE FOUND)
C     NEXT NGT CARDS:  FORMAT(8F10.5) SH,PSI,VA,AR
C      XO IS THE POSITION OF THE AXIS OF ROTATION ALONG THE CHORD.
C      ALPHB IS THE BLADE ANGLE OF ATTACK IN DEGREES
C      XIINF IS THE POSITION OF THE STAGNATION POINT AT LARGE SPAN. IF
C     IT IS UNKOWN,SET IT EQUAL TO 14. AND THE PROGRAM WILL CALCULATE IT
```

```
C      RK10 IS THE CONSTANT K10 IN THE EQUATION FOR Q. IF IT IS UNKNOWN,
C      SET JDIM=5 AND PUT SOME VALUE, SAY 10., ON THE DATA CARD.
C      XIS IS THE VALUE OF XIS AT SEPARATION. IT IS FOUND BY EXTRAPOLATNG
C      FO" (Y(3,1,L,1) OR DVDZ AT Z=0 FOR J=1)
       READ(1,482) XO,ALPHB,XIINF,XIS,RK10
  482 FORMAT(F10.6,F10.7,F20.16,3F10.7 )
      AB=ALPHB/57.29578
      TAB=DTAN(AB)
      SAB=DSIN(AB)
      CAB=DCOS(AB)
      WRITE(3,400) XO,ALPHB,XIINF,XIS,RK10,F/S
  400 FORMAT(/' INPUT VALUES '/' AXIS OF RO ATION IS AT',F7.4, 'CHORD'/
     1 ' ANGLE OF ATTACK IS',F9.6,'DEGREES',' STAGNATION POINT AT INFINI
     2TE SPAN IS',D20.14/ ' ESTIMATED SEPARATION POINT IS',F12.7/
     3 ' RK10=',F10.6/' PARAMETER EPS FOR MAX. THICKNESS OF AIRFOIL=',
     4 F12.7/ )
C
C  SECTION 2: INPUT NEEDED IN SECTIONS 15 AND 16
      IF(JDIM .LT. 10) GO TO 4412
       READ(1,4404) RK20R,RK20,RK21,RK22
      WRITE(3,4039) RK20R,RK20,RK21,RK22
 4039 FORMAT(//' IN ORDER TO CALCULATE VELOCITIES: RK2CR=',F9.4,5X,
     F 'RK20=',F9.4,5X,'RK21=',F9.4,5X,'RK22=',F9.4//)
       READ(1,7056) NGVEL
 7056 FORMAT(I5)
      WRITE(3,4400) NGVEL
 4400 FORMAT( I5,' NO. CONDS. TO CALCULATE VELOCITY' )
      IF(NGVEL) 4401,4401,4402
 4402 WRITE(3,4405)
 4405 FORMAT(/'    VELOCITY PROFILES WILL BE FOUND FOR:' /
     1'  SPEED RATIO    AZIMUTH ANGLE    INDUCED VEL    ASPECT RATIC
     2%CHORD')
      DO 4403 NG=1,NGVEL
      DO 4760 IYP=1,4
 4760 ILIM(NG,IYP)=0
 4404 FORMAT(8F10.5)
       READ(1,4404) SHV(NG),PSIV(NG),VAV(NG),ARV(NG),PCCV(NG)
C      SH IS  A SPEED OF FORWARD FLIGHT (LIKE ALL VELOCITIES,IT IS
C      NON-DIMENSIONALIZED WRT CHORD TIMES ROTATIONAL VELOCITY)
C      PSI IS THE AZIMUTHAL ANGLE IN DEGREES
C      VA IS THE DOWNFLOW
C      AR IS THE ASPECT RATIO OF THE BLADE. POINTS WILL BE TAKEN AT 30%,
C      60%,90% AND 95% OF SPAN.
C      PCC IS THE PER CENT CHORD
C      FOR EACH SET OF CONDITIONS (SH,PSI,VA,AR,&PCC) BOTH THE CHORDWISE
C      AND SPANWISE VELOCITY PROFILES WILL BE CALCULATED.
 4403 WRITE(3,4406) SHV(NG),PSIV(NG),VAV(NG),ARV(NG),PCCV(NG)
 4406 FORMAT(5F15.5)
 4401  READ(1,7056) NGT
      WRITE(3,4410) NGT
 4410 FORMAT(I5,'STATIONS TO CALCULATE THICKNESSES ')
      IF(NGT ) 4412,4412,4411
 4411 WRITE(3,4413)
 4413 FORMAT(/' THICKNESSES WILL BE FOUND FOR:'/ '  SPEED RATIO    ',
     1' AZIMUTH ANGLE    INDUCED VEL    ASPECT RATIO  ')
      DO 4414 NG=1,NGT
      READ(1,4404) SHT(NG),PSIT(NG),VAT(NG),ART(NG)
C      FOR EACH SET OF CONDITIONS (SH,PSI,VA,AR) THE B.L. THICKNESSES
C      WILL BE CALCULATED FOR K>8
 4414 WRITE(3,4406)SHT(NG),PSIT(NG),VAT(NG),ART(NG)
 4412 CONTINUE
C
```

```
C  SECTION 3: SOLUTION FOR THE STAGNATION POINT
      WRITE(3,7048) AB,TAB,CAB,SAB
 7048 FORMAT(/' AB=',D20.13,'RADIANS;    TAN(AB)=',D20.12,';  COS(AB)=',
     8 D20.13,';    SIN(AB)=',D20.13/)
      SGN=1.D0
      DEI=2.D0*SAB*SAB
C      DEI IS THE VALUE OF DELTA AT THE STAGNATION POINT. DELTA IS 1-SIGMA.
      SI=DEI-1.D0
      HST=.5D-3
      DET=.12121277151 5D-6
      XIINT=.41493299383D-4
      H=.5D-4*HST
C      H IS THE SPACING IN RK3 SUBROUTINE
      DSTRT=1.D-20
      XSTRT=EPS*DSQRT(2.D0*DSTRT)/(1.D0+EPS)
C      SINCE DSDX BLOWS UP AT(DELTA=0,X=0); RK3 BEGINS INTEGRATING AT
C     DELTA=DSTRT,X=XSTRT
      DEP=1.D-5*DEI
C      RK3 INTEGRATES FIRST FROM DSTRT TO DEP. THEN H IS INCREASED AND
C     INTEGRATION GOES FROM DEP TO DEI. IF THERE IS AN ABNORMAL
C     CONDITION IN RK3 (IER .NE. 0) SEE THE WRITE UP ON THE RK1 SUB-
C     ROUTINE IN THE IBM 360 SCIENTIFIC SUBROUTINE PACKAGE.
C      SGN=-1.D0 DENOTES THE UNDERSIDE OF THE AIRFOIL; +1 IS UPPER SIDE
      J=0
      IF(XIINF .GT. 13.D0) J=2070
      IF(J .NE. 2070) GO TO 397
      CALL RK3(DSDX,H,XSTRT,DSTRT,3.D0,DEP,XIINT,DET,IER)
      WRITE(3,435) XIINT,DET,XSTRT,DSTRT,IER,H
  435 FORMAT(/' RK3 FINDS X=',D19.12,2X,'AT DELTA=',D19.12/5X,'BY INTEGR
     1ATING FROM X=',D19.12,2X,'AND DELTA=',D19.12/' THE NUMBER OF ABNOR
     2MAL CONDITIONS ENCOUNTERED BY RK3 IS',I3,8X,'THE SPACING IN X IS',
     3 D15.6 /)
      H=.01D0*HST
      CALL RK3(DSDX,H,XIINT,DET,3.D0,DEI,XIINF,DV,IER)
      IF(TAB .GT. 0.D0) SGN=-1.D0
      XIINF=XIINF*SGN
C      XIINF (ALSO CALLED CHI0) IS THE VALUE OF X AT THE STAGNATION
C     POINT AT  Y=INFINITY. NORMALLY IT IS A NEGATIVE NUMBER
      WRITE(3,435) XIINF,DV,XIINT,DEP,IER,H
  397 IF(TAB .GT. 0.D0) SGN=-1.D0
      WRITE(3,401) XIINF,DEI
  401 FORMAT(/' XIINF=',D22.15,' IS THE VALUE OF X, AND DEI=',D22.14,
     F' IS THE VALUE OF DELTA, AT THE STAGNATION POINT'/)
      IF(JDIM .EQ. 5) WRITE(2,246) X0,ALPHB,XIINF
  246 FORMAT(F10.6,F10.7,F20.16,30X,'EXTRASTAFF' )
      DV=SGN*13.D0
      B99=DSDX(DV,DEI)
C     DSDX WILL CALCULATE XR AND ZR AND THEIR DERIVATIVES WRT DELTA (OR
C     SIGMA)
      B11=2.D0*(B2*B4+B3*B5)
      WRITE(3,436) B1,B2,B3,B4,B5,B6,B7,B8,B9,B10,B11
  436 FORMAT(     ' B1,B2,B3,B4,B5/B6,B7,B8,B9,B10,B11',5D18.10/6D18.10)
      CHI0=XIINF
      CHI10=-4.D0*B10*CAB*SAB
      CHI20=(B11/B10)*4.D0*(CAB*SAB)**2+2.D0*B10*(     CAB**2-SAB**2)
      CHI22=-CHI10
      WRITE(3,434)CHI0,CHI10,CHI20,CHI22
  434 FORMAT(/ ' THE COEFFICIENTS IN THE SERIES FOR STAGNATION POINT'/
     1' CHI0=',D15.8,5X'CHI10=',D15.8,5X,'CHI20=',D15.8,5X,'CHI22=',
     2D15.8 /)
C END PARAMETERS FOR POTENTIAL FLOW
C
```

```
C   SECTION 4: PARAMETERS AND FUNCTIONS OF Z FOR LEW'S METHOD
C        PARAMETERS FOR SOLUTION BY LEW'S METHOD
      DELX=2.5D-3
C       THE INCREMENT OF XI IS PROPORTIONAL TO DELX. FOR REASONS BEYOND
C       RECALL THE STAGNATION POINT (XI=0,X=-XIINF) IS TAKEN AT K=4, WHERE
C       K IS THE SUBSCRIPT FOR XI.
      XI(4)=0.D0
      X(4)=XIINF
      DE=DEI
      T=SI
C        DELTA (DE) AND SIGMA (T) ARE SET TO STAGNATION POINT VALUES.
      ERRORR=.5D-6
      OMEGAR=1.7D0
C        ERROR AND OMEGA ARE THE PARAMETERS THAT H.G. LEW CALLS EPSILON
C       AND OMEGA. ERROR AND OMEGA ARE PROPORTIONAL TO ERRORR & OMEGAR.
C       SEE STMT 528
      LMAXU=75
C        L IS THE SUBSCRIPT FOR Z (ETA); FOR EACH J AND K, A VALUE OF LMAX
C       WILL BE FOUND; L WILL BE <=LMAX AND LMAX WILL BE <=LMAXU. SEE THE
C       DIMENSION STMT.
      KMAX=70
C        K WILL BE <=KMAX.  IF K=KMAX BEFORE FO" REACHES .05 OR .04, THEN
C       EITHER DXI(K) MUST BE INCREASED (SEE DELX) OR KMAX INCREASED (SEE
C       DIMENSION STMT).
      LST=55
      ITERM=450
C        ITERM IS MAXIMUM NO. OF ITERATIONS BEFORE LEW'S METHOD IS
C       DECLARED NON-CONVERGENT. COMPARE IT TO VALUES OF ITER (SEE
C       WRITE(3,474))
      DZST=.1D0
C        CALCULATE Z(L) & RELATED FUNCTIONS
      DO 521 L=1,LST
      DZ(L)=DZST
  521 Z(L)=DZST*(L-1)
      DO 522 L=LST,LMAXU
C        OMISSION OF THIS DO LOOP AND SETTING LST=LMAXU WILL MAKE DZ(L)
C       CONSTANT
      DZ(L)=DZST*(2.D0**(Z(L-1)-Z(LST)+DZST))
      IF( DZ(L) .GT. .4D0) DZ(L)=.4D0
  522 Z(L)=Z(L-1)+DZ(L)
      WRITE(3,1482) (L ,Z(L),DZ(L),L=1,LMAXU)
 1482 FORMAT(/ '   L',6X,'Z',9X,'DZ',6X,'L',6X,'Z',9X,'DZ',6X,'L',6X,'Z'
     1,9X,'DZ',6X,'L',6X,'Z',9X,'DZ',6X,'L',6X,'Z',9X,'DZ'/ (I4,2F10.6,
     2';',I4,2F10.6,';',I4,2F10.6,';',I4,2F10.6,';',I4,2F10.6))
      LMM1=LMAXU-1
      DO 523 L=1,LMM1
C       DN,EN AND SDZ ARE USED RIGHT AFTER  "DO 1300" TO FIND THE STREAM
C       FUNCTION (FO,GO,ETC), THE SECOND DERIVATIVE OF THE STREAM FUNCTION
C       (FO",GO",ETC), AND  THE THIRD DERIVATIVE (FO"',ETC).
      DN(L)=1.D0/DZ(L+1)-1.D0/DZ(L)
      EN(L)=1.D0/DZ(L+1)+1.D0/DZ(L)
  523 SDZ(L)=2.D0/(DZ(L)+DZ(L+1))
      WRITE(3,440) DZST,LST,LMAXU,OMEGAR,ERRORR,DELX,JDIM
  440 FORMAT(/ ' THE ETA SPACING IS',F6.4,' UP TO L=',I3,'; IT GRADUALLY
     1 INCREASES UP TO THE MAXIMUM OF L=',I3// ' THE SPEED OF CONVERGENC
     2E IN ETA DEPENDS ON OMEGAR=',F8.4/
     3' SUCCESSIVE ITERATIONS MUST MATCH VELOCITY WITHIN AN ERROR THAT',
     4' DEPENDS ON ERRORR=',D12.5//' THE X SPACING DEPENDS ON DELX=',
     5 F12.8//' THE NO. OF EQUATIONS IS',I3// ' BEGIN SOLUTION'///  )
C END  CALCULATE Z(L) & RELATED FUNCTIONS
C
C   SECTION 5: STARTING VALUES
```

```
C       FIX STARTING VALUES
C      J=1 DENOTES F0,F0,F0" OR F0"';J=2 IS G03,G03',ETC;J=3 IS G01;
C      J=6 IS F20R;J=7 IS F20C;8 IS'F210;9 IS F220;10 IS G10;11 IS G11;
C      12 IS G12;IF JDIM<=5 THEN J=4 IS F1K AND J=5 IS F10C ; IF JDIM>=6
C      THEN J=4 IS F10 (F10=F10C+K10*F1K) AND J=5 IS F2K.
       DO 525 J=1,JDIM
       BC(J)=0.D0
C      BC(J) IS THE VALUE OF THE J'TH VEL (VEL IS F0',G00',G01',ETC AND
C      DVDZ IS F0",G03",ETC) AT ZMAX (AT ETA=INFINITY)
       EBC(J)=0.D0
       LMAXR(J)=0
       DO 525 L=1,LMAXU
       RHS(J,L)=0.D0
       A(1,J,L)=0.D0
       A(2,J,L)=0.D0
       DO 525 M=1,3
       DO 525 I=1,4
  525  Y(M,J,L,I)=0.D0
       DO 526 I=1,4
       ST(I)=0.D0
  526  S(I)=0.D0
C       THESE MATRICES (EBC,RHS,A,Y,S,AND ST) WILL BE REDEFINED AS NEEDED
       BC(1)=1.D0
       BC(3)=1.D0
C       BC(2) AND BC(4) WILL BE REDEFINED LATER.
       DO 527 L=1,LMAXU
C       THIS IS THE INITIAL ESTIMATE FOR THE VELOCITY PROFILES.
       Y(2,1,L,1)=1.D0-DEXP(-Z(L))
       DO 546 J=2,JDIM
  546  Y(2,J,L,1)=Y(2,1,L,1)
  527  CONTINUE
       Y(3,1,1,2)=1.2D0
C END   FIX STARTING VALUES
C END   PARAMETERS FOR SOLUTION BY LEW'S METHOD
C BEGIN  K LOOP IN XI
C       K IS THE SUBSCRIPT FOR XI,DXI,X AND DX
       DO 30 K=5,KMAX
       DXI(K)=DELX*(1+K/23+2*(K/33)+2*(K/40))
C
C  SECTION 6: VALUES OF XI AND X AT K'TH CHORDWISE STATION
C       THESE VALUES FOR THE INCREMENTS OF XI (DXI) HAVE PROVED BOTH
C      ACCURATE AND REASONABLE FAST. IF DIFFERENT VALUES OF ALPHB ARE
C      NEEDED, DXI(K) NEAR SEPARATION CAN BE ADJUSTED SO THAT F0" (DVDZ
C      FOR J=1) IS < ABOUT .05 AT THE FINAL VALUE OF XI(K).
       IF(DABS(ALPHB) .LT. 2.D-2) DXI(K) =DELX*(2+K/13-K/26+K/21
     C +4*(K/22)-3*(K/38))
C      IF(ALPHB .GE. 1.D0) DXI(K)=DELX*(1.5D0+.5D0*(K/23)+2*(K/27)
C    1 +4*(K/31))
       IF(DABS(ALPHB-2.D0) .LT. 2.D-2) DXI(K)=DELX*(1+.6D0*(K/19-K/38-K/
     2 57) +.8D0*(K/29-K/58) +1.6D0*(K/39)+2*(K/50)-K/62)
       IF(DABS(ALPHB-3.349D0) .LT. 2.D-2) DXI(K)=.8D0*DELX*(1+(K/27-K/34)
     4*.5D0+(K/37)*.5D0+K/44+K/51)
       IF(DABS(ALPHB-4.000D0) .LT. 2.D-2) DXI(K)=.8D0*DELX*(1+(K/27-K/34)
     4*.5D0+(K/37)*.5D0+K/44+K/51)
       IF(DABS(ALPHB-4.465D0) .LT. 2.D-2) DXI(K)=.8D0*DELX*(1+(K/27-K/34)
     4*.5D0+(K/37)*.5D0+K/44 )
       IF(DABS(ALPHB-5.581D0) .LT. 2.D-2) DXI(K)=.8D0*DELX*(1+(K/27-K/34)
     4*.5D0+(K/37)*.5D0)
       IF(K .GE. 8) GO TO 513
       IF(K-6) 502,503,504
C         K=5
  502  XI(5)=.5D-3*DELX
```

```
      IMAX=2
      DXI(5)=XI(5)
      GO TO 520
  503 XI(6)=.20D0*CELX
C        K=6
      S(1)=1.D0
      S(2)=-1.D0
      DXI(K)=XI(K)-XI(K-1)
      GO TO 520
  504 XI(7)=DXI(7)
C        K=7
      S(1)=(1.D0/DXI(K)+1.D0/(DXI(K-1)+DXI(K)))*XI(K)
      S(2)=-XI(K)*(DXI(K)+DXI(K-1))/(DXI(K)*DXI(K-1))
      S(3)=XI(K)*DXI(K)/((DXI(K)+DXI(K-1))*DXI(K-1))
C     XI*(DERIVATIVE OF Y(M,J,L,1) WRT XI)= SUM OF S(I)*Y(M,J,L,I) FOR
C     I=1 TO IMAX
      IMAX=3
      DXI(K)=XI(K)-XI(K-1)
      GO TO 512
  513 XI(K)=XI(K-1)+DXI(K)
C        K>=8
      S(1)=(1.D0/(XI(K)-XI(K-3))+1.D0/(XI(K)-XI(K-2))+1.D0/DXI(K))*XI(K)
      S(2)=-XI(K)*(XI(K)-XI(K-3))*(XI(K)-XI(K-2))/(DXI(K)*DXI(K-1)*
     2 (XI(K-1)-XI(K-3)))
      S(3)=XI(K)*(XI(K)-XI(K-3))*DXI(K)/(DXI(K-2)*(XI(K)-XI(K-2))*
     3 DXI(K-1))
      S(4)=-XI(K)*(XI(K)-XI(K-2))*DXI(K)/(DXI(K-2)*(XI(K-1)-XI(K-3))*
     4 (XI(K)-XI(K-3)))
C     IF ALL DXI ARE EQUAL; S1=11/6, S2=-3, S3=1.5, S4=-1/3
      IMAX=4
  512 CONTINUE
  520 X(K)=XI(K)+XIINF
C        K>=7
      DX(K)=DXI(K)
C
C  SECTION 7: FUNCTIONS OF XI FOUND FROM POTENTIAL FLOW
C      CALCULATIONS FOR POTENTIAL FLOW
      SGN=1.D0
      IF(X(K) .LT. 0.D0) SGN=-1.D0
      H=.1D0*HST
      IF(DABS(X(K)) .LT. 1.D-3) H=.05D0*HST
      IF(X(K) .GT. 0.D0 .AND. X(K) .LT. 3.D-2) H=.03D0*HST
      IF(X(K) .GT. .06D0) H=.2D0*HST
      IF(H .GT. 1.D-2*DXI(K)) H=1.D-2*DXI(K)
      DEP=DE
      IF(X(K)*X(K-1)) 3314,1405,3315
 3314 H=1.D-2*HST
      IF(X(K) .LT. XIINT) GO TO 1405
      CALL RK3(DSDX,H,XIINT,DET,X(K),27.D0,XF,DE,IER)
      WRITE(3,435) XF,DE,XIINT,DET,IER,H
      GO TO 320
 3315 CALL RK3(DSDX,H,X(K-1),DEP,X(K),27.D0,XF,DE,IER)
C     RK3 INTEGRATES DSDX TO FIND THE VALUE OF SIGMA(NOW CALLED T) AT
C     X(K).
  320 CONTINUE
      T=DE-1.D0
      DUMMY=13.D0*SGN
  319 P99=DSDX(DUMMY,DE)
      WRITE(3,450) K,XI(K),IER,DXI(K),DE,SGN,X(K)
  450 FORMAT(' K=',I3,5X,'XI(K)=',D19.11,10X,'IER=',I5 / ' DXI(K)=',
     1D19.11,5X,'DE=',D19.11,5X,'SGN=',F5.2,5X,'X(K)=',D19.11)
C      P2=DERIV. OF XR WRT SIGMA (OR DELTA,WHERE DELTA=1+SIGMA);
```

```
C       B3=DERIV. OF ZR WRT SIGMA; B4=DERIV. OF B2 WRT SIGMA; B5=DERIV. OF
C       B3 WRT SIGMA; AND SO ON UP TO B9=DERIV. OF B7 WRT SIGMA.
C        B10= DERIV. OF X WRT SIGMA =SGN*DSQRT(B2*B2+B3*B3);
C       B11= DERIV. OF B10**2 WRT SIGMA; B12=DERIV. B11; B13= DERIV. B12
C       B20 AND B21 ARE DEFINED FOR CONVENIENCE, AS ARE BC,BD,ETC.
        B11=2.D0*(B2*B4+B3*B5)
        B12=2.D0*(B4*B4+B2*B6+B5*B5+B3*B7)
        B13=2.D0*(3.D0*(B4*B6+B5*B7)+B2*B8+B3*B9)
        B20=(B11/B10)/(B10*B10)
        B21=(B12/B10)/(B10**4)
        XR=(1.D0+EPS)*(T-EPS)*(1.D0+((1.DC-EPS)**2)/B1)/4.DC
        XR=XR+(1.D0+EPS*EPS)/2.DC-XC
        ZR=.25D0*(1.D0+EPS)*DSQRT(DE*(1.DC-T))*(1.D0-(1.DC-EPS)**2/B1)*SGN
C        XR IS CAPITAL X(SUBSCRIPT R); ZR IS CAP Z(SUB R)
        WRITE(3,479) B1,B10,B11,B12,B13
  479 FORMAT(     ' B1,B10,B11,B12,B13 ',5D22.14 )
        DES=DSQRT(DE)
        OMSS=DSQRT(1.DC-T)
C        PSO IS PHI(SUBSCRIPT SIGMA); PRO IS PHI(SUBSCRIPT RHO);
C       PS1 IS THE FIRST DERIV. OF PSO WRT SIGMA; PR2 IS 2ND DERIV. OF PRO
C       AND SO ON.
        PSO=(1.D0+EPS)*T/2.D0
        PRO=(1.D0+EPS)*(SGN*DES*OMSS-DATAN(SGN*DES*OMSS/T))/2.DC
        PS1=(1.D0+EPS)/2.D0
        PS2=0.D0
        PS3=0.D0
        PR1=SGN*PS1*OMSS/DES
        PR2=-SGN*PS1/(OMSS*(DES**3))
        PR3= SGN*PS1*(1.D0-2.D0*T)/((OMSS**3)*(DES**5))
        PR4=-SGN*PS1*3.D0*(1.DC-2.D0*(1.DC-T)*T)/((OMSS**5)*(DES**7))
        BP(1)=B10
        DO 317 I=2,4
  317 BP(I)=BP(I-1)*B10
C        USO IS U(SUPERSCRIPT TILDA,SUBSCRIPT SIGMA); URO IS U(SUPERSCRIPT
C       TILDA,SUB RHO); US1 IS FIRST DERIV. OF USO WRT X, ETC.
        USO=PS1/B10
        URO=PR1/B10
        US1=-.5DC*B11/BP(4)
        UR1=US1*PR1+PR2/BP(2)
        US1=US1*PS1
        US2=B20*B20/B10-.5D0*B21
        UR2=US2*PR1-PR2*1.5DC*B2C/BP(2)+PR3/BP(3)
        US2=US2*PS1
        US3= B20*(3.25D0*B21-3.50D0*B2C*B20/B1C)- .5DC*B13/(BP(3)**2)
        UR3= US3*PR1+(4.75DC*B2C*B2C/B1C-2.DC*B21)*PR2/B10
     3 -3.D0*B2C*PR3/BP(3)+PR4/BP(4)
        US3=US3*PS1
C        PHIA IS  PHI(SUB A) ; UAO IS U(SUPER TILDA,SUB A) ; UA1 IS FIRST
C       DERIV. OF UAO WRT X, AND SO ON.
        PHIA=CAB*PSO+SAB*PRO
        UAO= CAB*USO+SAB*URO
        UA1= CAB*US1+SAB*UR1
        UA2= CAB*US2+SAB*UR2
        UA3= CAB*US3+SAB*UR3
        PHIC=SAB*PSO-CAB*PRO
        UCO =SAB*USO-CAB*URO
        UC1 =SAB*US1-CAB*UR1
        UC2 =SAB*US2-CAB*UR2
        UC3 =SAB*US3-CAB*UR3
C        UAPK,UCPK,PCC, AND RNUK STORE VALUES FOR LATER USE TO INTERPOLATE
C       FOR VELOCITY PROFILES AND THICKNESSES
        PCC(K)=(XR+XO)*1.D2
```

```
      UAPK(K)=UAO
      UCPK(K)=UCO
      WRITE(3,490)
  490 FORMAT('  PSO,PS1...PS4  |PRO,PR1...PR4  |PSC,USC...US3  |PRO,URO'
     F ,'...UR3  |PHIA,UAO...UA3 |PHIC,UCO...UC3 |XR,B2,B4,B6,B8 |'
     F ,'ZR,B3,B5,B7,B9'  )
      WRITE(3,492) PSO,PRO,PSO,PRO,PHIA,PHIC,XR,ZR, PS1,PR1,USO,URO,UAO,
     1UCO,B2,B3,PS2,PR2,US1,UR1,UA1,UC1,B4,B5,  PS2,PR3,US2,UR2,UA2,UC2,
     2B6,B7, PS2,PR4,US3,UR3,UA3,UC3,B8,B9
  492 FORMAT( ( ' ', 8D16.8 ))
      ALPHA=DATAN(B3/B2)
      IF(SGN .LT. 0.D0 ) ALPHA= 3.1415926536 +ALPHA
      ADEG=57.2958*ALPHA
      PO=XI(K)/UAO
      XMO=PO*UA1
C      XMO IS M(SUB O);XMIK IS M(SUB 1K); RNUO IS NU(SUB O)
      RM=(XMO+1.D0)/2.D0
C      RM,RN,RMS ARE DEFINED FOR CONVENIENCE
      RN=(XMO-1.D0)/2.D0
      RMS=RM+S(1)
      RNUO=PHIA-2.D0*(XR*CAB+ZR*SAB)
      RNUK(K)=RNUO
      CO=2.D0*(CAB*B2+SAB*B3)/B10
C     PARAMETERS NEEDED FOR F10
      XM1K=XI(K)*UA2+UA1*(1.D0-XMO)
      XM10C=CHI10*UA2+UC1-(CHI10*UA1+UCO)*UA1/UAO
      WRITE(3,430) XMO,PO,CO,RM,ALPHA,H,ADEG
  430 FORMAT(    ' XMO,PO,CO,RM,ALPHA,H,ADEG     ',7D14.6)
      WRITE(3,431) XMO,XM1K,XM1CC,RNUC
  431 FORMAT(    ' XMO,XM1K,XM1CC,RNUC            '   ,6D15.7)
C       END PARAMETERS FOR F1
      IF(JDIM .LE. 5) GO TO 8632
C     PARAMETERS NEEDED FOR G1
      DCDXA=(B4-B2*B11/(2.D0*B10*B10))/(B10*B1C)
      DSDXA=(B5-B3*B11/(2.D0*B1C*B1C))/(B1C*B1C)
      DCDX=DCDXA*DCOS(AB)+DSDXA*DSIN(AB)
C     RK10 MUST BE DEFINED HERE
      XM10=XM1K*RK10+XM10C
       CPK=CHI10+XI(K)*RK10
      RMUA10=CPK*UA1
C      RMUA10 IS MU(SUPER A,SUB 10), UD10 IS U(SUPER DELTA,SUB 10)
      RNU10=CPK*(UAO-CO)
      C10=CPK*2.D0*DCDX
      UD10=CPK*UA1+UCO
      UD12=UAO
C     PARAMETERS NEEDED FOR F2
      XM2K=XM1K
      XM22C=( CPK+CHI22)*(UA2-UA1*UA1/UAO)+RK1C*UA1
      XM20C=(CHI20+XI(K)*RK10**2)*(UA2-UA1*UA1/UAO)+(UA3-UA1*UA2/UAO)*
     X .5D0*CPK*CPK +CPK*(UC2+RK10*UA2-UA1*UC1/UAO)+RK10*(UC1+RK1C*UA1)
      WRITE(3,432) XMO,XM10,XM2CC,XM22C,RK1C,CPK
  432 FORMAT(    ' XMO,XM10,XM2CC,XM22C,RK1C,CPK '     ,6D16.8)
      WRITE(3,433) C10,RNU10,UD10,DCDX
  433 FORMAT(    ' C10,RNU10,UD10,DCDX            '            ,5D17.9)
C  J=1  2   3   4   5   6   7   8   9   10  11  12
C    FO G00 G01 F10 F2K F20R F2CC F21C F22C G10 G11 G12
      PC(10)=RNU10
C     END PARAMETERS FOR G1 &F2
 8632 CONTINUE
C END  CALCULATIONS FOR POTENTIAL FLOW
C
C  SECTION 8: PARAMETERS FOR LEW'S METHOD AND A GUESS AT NEW VELOCITY
```

```
C            PROFILE BY EXTRAPOLATICN
C       FIX BC,PARAMETERS, AND VELOCITIES IN NEW X  STATION
      BC(2)=RNUO
      CC 528 J=1,JDIM
      LMAXT=LMAXU+(8.DO+1/J)*XI(K)/XIS-10/J-10
      IF(JDIM .GT. 5 .AND. J .GT. 3) LMAXT=LMAXT-1
      IF(LMAXT .GT. LMAXR(J)) LMAXR(J)=LMAXT
      IF(DABS(EBC(J)) .GT. 0.DC) LMAXR(J)=LMAXR(J)+DABS(EBC(J)/1.D-3)
C       EBC IS DVDZ( 2ND DERIV. OF STREAM FUNC. WRT ETA) AT Z(LMAXR(J))
C       EACH STREAM FUNCTION IS INTEGRATED TO ITS OWN MAX VALUE OF ETA,
      WHICH IS GIVEN BY Z(LMAXR(J))
      IF(LMAXR(J) .GT. LMAXU-1) LMAXR(J)=LMAXU-1
      CMEGA(J)=OMEGAR +.020C*(J-1)
  528 ERROR(J)=ERRCRR*( 1.D-1 +CABS(EC(J))+ .5C-2*Y(2,J,15,1)**2+J/5)
      IF(Y(3,1,1,2) .LT. .12CO ) ERROR(1)=ERROR(1)*2.CC
C       NEW VELOCITIES BY INTERPOLATION
      IF(K-8) 543,543,542
  542 ST(2)=(XI(K)-XI(K-2))*(XI(K)-XI(K-3))/(DXI(K-1)*(XI(K-1)-XI(K-3)))
      ST(3)=-DXI(K)*(XI(K)-XI(K-3))/(DXI(K-1)*DXI(K-2))
      ST(4)=CXI(K)*(XI(K)-XI(K-2))/((XI(K-1)-XI(K-3))*DXI(K-2))
      CC 544 J=1,JCIM
      DC 544 L=2,LMAXU
  544 Y(2,J,L,1)=ST(2)*Y(2,J,L,2)+ST(3)*Y(2,J,L,3)+ST(4)*Y(2,J,L,4)
  543 CONTINUE
      WRITE(3,481) (S(I),I=1,4),(ST(I),I=2,4)
  481 FORMAT( ' S(I)= ',4F15.10, 1CX, 'ST(I)=',3F15.1C)
C END   NEW VELOCITIES BY INTERPOLATICN
C END   FIX BC,PARAMETERS, AND VELOCITIES IN NEW X  STATICN
C       CHCOSE VARIABLE TO BE SCLVED FOR          DO 15CC J
      CC 1500 J=1,JDIM

C   SECTION 9: FIX UP ESTIMATED PRCFILE TO MATCH BOUNDARY CCNDITICNS
      LMAX=LMAXR(J)
      LMM1=LMAX-1
C       CORRECT VELCCITIES TC MATCH BC & CALCULATE A'S
C         IF BC(J) CHANGES WITH X (OR XI), THEN A NEW PRCFILE FCR VELCCITY
C       (ACTUALLY DERIV. OF STREAM FUNC. WRT ETA) MUST BE FCUND. STMT 549
C       IS NECESSARY TC BE SURE TC AVOID DIVISION BY ZERO
      IF(DABS(BC(J)-Y(2,J,LMAX,1)) -1.D-14) 547,547,549
  549 IF(DABS(Y(2,J,LMAX,1)) -1.D-10) 551,545,545
  545 BCO=BC(J)/Y(2,J,LMAX,1)
      CC 531 L=2,LMAX
  531 Y(2,J,L,1)=Y(2,J,L,1)*BCC
      GC TO 547
  551 BCO=(BC(J)-Y(2,J,LMAX,1))/Z(LMAX)
      DO 548 L=2,LMAX
  548 Y(2,J,L,1)=Y(2,J,L,1)+BCC*Z(L)
  547 CC 532 M=1,2
      CC 532 L=1,LMAXU
      A(M,J,L)=0.DO
      DC 532 I=2,IMAX
  532 A(M,J,L)=A(M,J,L)+S(I)*Y(M,J,L,I)
C       AT THIS POINT, A(M,J,L)=SUM CF S(I)*Y(M,J,L,I) FROM I=2 TC IMAX,
C       CR XI*DERIV. OF Y(M,J,L,1) WRT XI MINUS S(1)*Y(M,J,L,I). AS SCCN
C       AS Y(M,J,L,1) IS KNCWN, IT WILL BE ACCED IN SO A CAN BE USED FCR
C       SUBSEQUENT VALVES OF J TO REPRESENT ALL THE DERIVATIVE
C END   CORRECT VELCCITIES TC MATCH BC & CALCULATE A'S
C
C   SECTICN 10: SOLUTION OF DE'S BY LEW'S METHOD
C       BEGIN ITERATICN CN LEW'S SUCCESSIVE REPLACEMENTS      DO 14CC ITER
      CC 1400 ITER=1,ITERM
C       BEGIN MARCHING IN Z DIRECTICN      DO 13CC L
```

```
      DO 1300 L=2,LMM1
C       DEFINE VEL,DVDZ & STREAM FUNCTION
      YT=Y(2,J,L,1)
      Y(1,J,L,1)=Y(1,J,L-1,1)+DZ(L)*(Y(2,J,L-1,1)+YT)/2.D0
      Y(3,J,L,1)=(Y(2,J,L+1,1)/DZ(L+1)-DN(L)*YT-Y(2,J,L-1,1)/DZ(L))*.5D0
      YP=SDZ(L)*(Y(2,J,L+1,1)/DZ(L+1)-EN(L)*YT+Y(2,J,L-1,1)/DZ(L))
C       YP IS 2ND DERIVATIVE OF VELOCITY
C       YP IS USED INSTEAD OF Y(4,J,L,1) TO DECREASE STORAGE.
C  J=1  2   3   4   5
C     FO G00 G01 F1K F10C
      GO TO (1,2,3,4,5,6,6,6,6,10,10,10),J
C       THIS STMT CHOOSES THE EQUATION TO BE SOLVED. IF TIME IS NOT
C      IMPORTANT A FUNCTION SUBROUTINE TO CALCULATE FN AND FNN (THE
C      DERIV. OF FN WRT YT) COULD BE USED. THE 6,6,6,6 OCCURS BECAUSE
C      FOUR EQNS ARE IDENTICAL EXCEPT FOR RHS. RHS CONTAINS NO YT SO IT
C      CAN BE CALCULATED JUST ONCE AND SAVE TIME(SEE DO LOOP FOR STMT
C      NO. 8220)
C                   YT=FO'
    1 FN=-YP-Y(3,J,L,1)*(RMS       *Y(1,J,L,1)+A(1,J,L)   )+YT*((XMC+S(1))
     1 *YT+A(2,J,L)   )-XMO
      FNN= EN(L)*SDZ(L)+.5D0*DN(L)*(RMS       *Y(1,J,L,1)+A(1,J,L))
     1-Y(3,J,L,1)*RMS       *.5CO*DZ(L)+YT*2.D0*(XMC+S(1))+A(2,J,L)
      GO TO 117
C                   YT=G00'
    2 FN=-YP-DUMV(L)*Y(3,J,L,1)+Y(2,1,L,1)*(S(1)*YT+A(2,J,L)   )
     2 +XI(K)*(CO*Y(2,1,L,1)-UAO)
      FNN=EN(L)*SDZ(L)+DUMV(L)*.5D0*DN(L)+Y(2,1,L,1)*S(1)
      GO TO 117
C                   YT=G01'
    3 FN=-YP-DUMV(L)*Y(3,J,L,1)+Y(2,1,L,1)*(S(1)*YT+A(2,J,L)   )
      FNN=EN(L)*SDZ(L)+DUMV(L)*.5DO*DN(L)+Y(2,1,L,1)*S(1)
      GO TO 117
    4 IF(JDIM-5) 8720,8720,8721
C                   YT=F1K'   J=4         JDIM<=5
 8720 FN=-YP-DUMV(L)*Y(3,J,L,1)+(DT(L)+XMC*Y(2,1,L,1))*YT+
     1 Y(2,1,L,1)*A(2,J,L)-Y(3,1,L,1)*(RMS       *Y(1,J,L,1)+A(1,J,L))
     2 +PO*RHSF(L)*XM1K
      GO TO 8722
C                   YT=F10'   J=4         JDIM>=6
 8721 FN=-YP-DUMV(L)*Y(3,J,L,1)+(DT(L)+XMO*Y(2,1,L,1))*YT+
     1 Y(2,1,L,1)*A(2,J,L)-Y(3,1,L,1)*(RMS       *Y(1,J,L,1)+A(1,J,L))
     2 +PO*RHSF(L)*XM10
 8722 FNN=SDZ(L)*EN(L)+DUMV(L)*DN(L)*.5CO+ DT(L)+XMC*Y(2,1,L,1)
     1 -Y(3,1,L,1)*RMS       *DZ(L)*.5DO
      GO TO 117
    5 IF(JDIM-5) 8726,8726,8724
C                   YT=F10C'  J=5         JDIM<=5
 8726 FN=-YP-DUMV(L)*Y(3,J,L,1)+(DT(L)+XMO*Y(2,1,L,1))*YT+
     1 Y(2,1,L,1)*A(2,J,L)-Y(3,1,L,1)*(RMS       *Y(1,J,L,1)+A(1,J,L))
     2 +PO*RHSF(L)*XM10C
      FNN=SDZ(L)*EN(L)+DUMV(L)*DN(L)*.5CO+ DT(L)+XMC*Y(2,1,L,1)
     1 -Y(3,1,L,1)*RMS       *DZ(L)*.5CO
      GO TO 117
C                   YT=F2K'   J=5         JDIM>=6
 8724 FN=-YP-DUMV(L)*Y(3,J,L,1)+DT(L)*YT+DT2(L)*Y(1,J,L,1)+Y(2,1,L,1)*
     1 A(2,J,L)-Y(3,1,L,1)*A(1,J,L)
     5 +XI(K)*XM2K*RHSF(L)
      FNN=SDZ(L)*EN(L)+DUMV(L)*DN(L)*.5CO+DT(L)+DT2(L)*DZ(L)*.5DC
      GO TO 117
C                   YT=F20K'  J=6
    6 FN=-YP-DUMV(L)*Y(3,J,L,1)+DT(L)*YT+DT2(L)*Y(1,J,L,1)+Y(2,1,L,1)*
     1 A(2,J,L)-Y(3,1,L,1)*A(1,J,L)   +RHS(J,L)
```

```
      FNN=SDZ(L)*EN(L)+DUMV(L)*CN(L)*.5C0+DT(L)+DT2(L)*DZ(L)*.5D0
      GC TO 117
C                     YT=F20C'  J=7
C                     YT=F21C'  J=8
C                     YT=F22C'  J=9
   10 FN=-YP-DUMV(L)*Y(3,J,L,1)+Y(2,1,L,1)*(S(1)*YT+A(2,J,L))+RHS(J,L)
     ' FNN=SDZ(L)*EN(L)+DUMV(L)*CN(L)*.5C0+Y(2,1,L,1)*S(1)
C                     YT=G11'   J=11
C                     YT=G12'   J=12
  117 EY(L)=-OMEGA(J)*FN/FNN
C     CALCULATE NEW VALUES FOR Y(2,J,L,1)
      Y(2,J,L,1)=YT+EY(L)
 1300 CONTINUE
C END  BEGIN MARCHING IN Z DIRECTION     DO 13CC L
      DC 536 L=2,LMM1
      IF(DABS(EY(L))-ERROR(J)) 536,535,535
C      THE CHANGE IN Y(2,J,L,1) SINCE THE LAST PASS THRU THE L LOOP IS
C     COMPARED TO ERROR (LEW CALLS IT EPSILON)
  536 CONTINUE
      GO TO 14C1
  535 CONTINUE
      EYK(ITER)=EY(10)
C     IT IS NOT NECESSARY TO STORE A VALUE OF EY IF EYK IS REMOVED FROM
C   . WRITE(3,462) IN SECTION 11.
 1400 CONTINUE
C END  BEGIN ITERATION ON LEW'S SUCCESSIVE REPLACEMENTS     DC 14CC ITER
C
C  SECTION 11: TIDY UP Y AND A MATRICES
      WRITE(3,462) J
      WRITE(3,462) J,K,ITER,LMAX,(EYK(I),I=1,ITER)
  462 FORMAT(' ITER FAILS ',4I5/(6D18.9))
      GC TO 1405
 1401 ITERK(J)=ITER
C      LEW'S METHOD HAS NOW CONVERGED.
  463 FORMAT( ' J,ITER=', 2I5/(10D13.5))
C      THE VALUE OF Y(3,J,1,1) (I.E. DVDZ AT Z=0) IS CALCULATED. THIS
C     FORMULA IS GOOD ONLY IF  DZ(5)=DZ(4)=...DZ(2)  .
      Y(3,J,1,1)=( -25.D0*Y(2,J,1,1)+48.D0*Y(2,J,2,1)-36.DC*Y(2,J,3,1)
    * Y +16.D0*Y(2,J,4,1)-3.C0*Y(2,J,5,1) )/(12.DC*DZ(3) )
      CC 537 L=LMAX,LMAXU
      Y(2,J,L,1)=BC(J)
C      THIS DO LOOP EXTENDS THE SOLUTION FROM LMAX TO LMAXU
      Y(1,J,L,1)=Y(1,J,LMM1,1)+(Z(L)-Z(LMM1))*BC(J)
      Y(3,J,L,1)=Y(3,J,LMM1,1)*DEXP((Z(LMM1)-Z(L))/DZST)
  537 CONTINUE
      DC 538 L=1,LMAXU
      DC 538 M=1,2
C   .  THE ADDITIONAL TERM FOR A (SEE SEC 9) IS ADDED IN
  538 A(M,J,L)=A(M,J,L)+S(1)*Y(M,J,L,1)
C END  DEFINE VEL,DVDZ & STREAM FUNCTION
C
C  SECTION 12: FUNCTIONS OF ETA USED IN DE
      IF(JDIM .LE. 5 .OR. J .NE. 5) GO TO 633
      DO 8220 L=1,LMAXU
C      TERMS THAT INVOLVE FUNCTIONS OF Z (ETA) BUT DO NOT CONTAIN YT
C     WHEN LEW'S METHOD IS APPLIED, ARE BEST CALCULATED HERE AND STORED.
C     THIS AVOIDS DOING THE CALCULATION ITERK(J) TIMES. RHS(J,L) IS NOT
C     USED FOR THE FIRST 5 EQUATIONS (GIVEN BY STMTS 1 TO 5). DUMV,RHSF,
C     DT2 AND DT ARE DEFINED FOR CONVENIENCE.
  626 RHS(6,L)=XI(K)*(Y(2,1,L,1)*Y(2,2,L,1)-RNUC+.5DC*Y(3,1,L,1)
    6 *Y(1,2,L,1) ) +PO*CO*(RNUO-Y(2,2,L,1))
  627 RHS(7,L)=UAO*(-RM*Y(1,4,L,1)*Y(3,4,L,1)+XMO*Y(2,4,L,1)**2
```

```
      7 +Y(2,4,L,1)*A(2,4,L)-Y(3,4,L,1)*A(1,4,L))
      7 +XI(K)*XM10*(2.D0*Y(2,1,L,1)*Y(2,4,L,1)-.5D0*Y(3,1,L,1)*
      7 Y(1,4,L,1)-.5D0*Y(1,1,L,1)*Y(3,4,L,1) ) + XI(K)*(XM20C-XM10*UD10
      7 /UA0) * RHSF(L)
  628 RHS(8,L)=XI(K)*(Y(2,1,L,1)-2.D0+.5D0*Y(3,1,L,1)*(Y(1,3,L,1)+Z(L))+
      8 Y(2,1,L,1)*Y(2,3,L,1) ) +P0*C0*(1.D0-Y(2,3,L,1) )
  629 RHS(9,L)=XI(K)*(XM22C-XM1C*UD12/UA0)*RHSF(L)
      IF( JDIM .LT. 10 ) GO TO 8220
      RHS(10,L)=-(RM*Y(1,4,L,1)+A(1,4,L)+.5D0*P0*XM10*Y(1,1,L,1))*
      C Y(3,2,L,1)  +Y(2,4,L,1)*A(2,2,L)   +XI(K)*( C0*Y(2,4,L,1)-RMUA10
      0 +Y(2,1,L,1)*C10+RK10*(Y(2,1,L,1)*C0-UA0))
      RHS(11,L)=-(RM*Y(1,4,L,1)+A(1,4,L)+.5D0*P0*XM10*Y(1,1,L,1))*
      1 Y(3,3,L,1)  +Y(2,4,L,1)*A(2,3,L)
      RHS(12,L)=P0*(1.D0-Y(2,3,L,1))
 8220 CONTINUE
  633 CONTINUE
      IF(J-1) 539,539,1500
  539 DO 540 L=1,LMAXU
      CUMV(L)=RM*Y(1,1,L,1)+A(1,1,L)
      RHSF(L)=Y(2,1,L,1)**2-.5D0*Y(3,1,L,1)*Y(1,1,L,1)-1.D0
      CT2(L)= (RN-S(1))*Y(3,1,L,1)
  540 CT(L)=(XM0     +S(1))*Y(2,1,L,1)+A(2,1,L)
 1500 CONTINUE
C END  CHOOSE VARIABLE TO BE SOLVED FOR          DO 1500 J
C
C  SECTION 13: WRITE UP OF RESULTS
      WRITE(3,4628)
 4628 FORMAT(1X,  T22,'J=1',T35,'J=2',T46,'J=3',T57,'J=4',T66,'J=5',T76,
      8 'J=6',T86,'J=7',T94,'J=8',T103,'J=9',T113,'J=10',T121,'J=11',T128
      8 ,'J=12')
      IF(JDIM .LE. 5) WRITE(3,4640)
 4640 FORMAT(   '    Z        L         ',  T23,'F0',T35,'G00',T46,'G01',T57,
      1 'F1K',T67,'F10C' )
      IF(JDIM .GT. 5) WRITE(3,464)
  464 FORMAT(   '    Z        L         ',  T23,'F0',T35,'G00',T46,'G01',T57,
      1'F10',T66,'F2K', T76,'F2CR',T86,'F2CC',T94,'F21C',T103,'F22C',T113
      2,     'G10',T121,'G11',T128,'G12' )
  465 FORMAT(1X,F7.4,I4,'VEL ',     F12.8,2F11.7,2F10.6,F9.6,F9.3, F9.5,
      5 F9.4,F9.5,F8.4,F9.5 )
  466 FORMAT(10X, ' DVDZ ',         F12.8,2F11.7,2F10.6,F9.6,F9.3, F9.6,
      5 F9.5,F9.6,F8.4,F9.5)
  467 FORMAT(' B.C. AT Z=INF.  ',  F12.8,2F11.7,2F10.7,5F9.6,2F8.5 )
  468 FORMAT(' MAX ERROR IN VEL',  F12.8,2F11.7,2F10.7,5F9.6,2F8.5 )
  469 FORMAT(' OMEGA-FINAL VAL'   ,F12.8,2F11.7,2F10.7,5F9.6,2F8.5 )
  470 FORMAT(' STREAM FUN@LMAXU'  ,F12.8,2F11.7,F10.6,F10.7,5F9.4,2F8.3)
  473 FORMAT(' MAX VALUE OF L  '   I7,2I11,2I10,5I9,2I8 )
  474 FORMAT(' NO OF ITERATIONS',  I5,2I11,2I10,5I9,2I8 )
  475 FORMAT(' DVDZ TOO BIG@LMX'  ,F12.8,2F11.7,2F10.7,5F9.6,2F8.5 )
      NTEST=0
      LMIN=LMAXU
      LMAX=1
      DO 552 J=1,JDIM
      IF(LMAXR(J) .LT. LMIN) LMIN =LMAXR(J)
      IF(LMAXR(J) .GT. LMAX) LMAX=LMAXR(J)
C      IF DVDZ IS NOT SMALL (LESS THAN SAY 1.D-3) AT Z(LMAXR(J)) THEN
C     THE B.C. AT EDGE OF BOUNDARY LAYER IS NOT CORRECTLY SATISFIED.
C     THIS MEANS THAT Z(LMAXR(J)) ( THE MAX. VALUE OF ETA FOR EQN. NO.J)
C     IS NOT LARGE ENOUGH. LMAXR(J) SHOULD BE INCREASED.
C      THIS DO LOOP CHECKS DVDZ AT Z(LMAXR(J)) . LMIN AND LMAX ARE JUST
C     USED FOR WRITE(3,465) AND WRITE(3,466).
      IF(DABS(Y(3,J,LMAXR(J),1))-1.D-3) 600,600,601
  601 ERC(J)=Y(3,J,LMAXR(J),1)
```

```
      NTEST=1
      GO TO 552
  600 EBC(J)=0.D0
  552 CONTINUE
      IF(LMAX .GT. LMAXU) GO TO 1405
      JM1=LMAX/5
      DO 861 L=1,LMAX
      IF((L/2)*2.EQ. L .AND. L .GT. 8 .AND. L .LT. LMAX-2) GO TO 861
      WRITE(3,465) Z(L),L,(Y(2,J,L,1),J=1,JDIM)
      IF(L.GT. 10 .AND.L.LT.LMIN-2 .AND.L.NE.(L/JM1)*JM1) GO TO 861
      WRITE(3,466) (Y(3,J,L,1),J=1,JDIM)
  861 CONTINUE
      WRITE(3,467) (     PC(J),J=1,JDIM)
      WRITE(3,468) ( ERROR(J),J=1,JDIM)
      WRITE(3,469) ( OMEGA(J),J=1,JDIM)
      WRITE(3,473) ( LMAXR(J),J=1,JDIM)
      WRITE(3,474) ( ITERK(J),J=1,JDIM)
      WRITE(3,470) (Y(1,J,LMAXU,1),J=1,JDIM)
      IF(NTEST .GT. 0) WRITE(3,475) (EBC(J),J=1,JDIM)
C END WRITE STMTS
C
C  SECTION 14: CHECK OF CHORDWISE DERIVATIVES (OPTIONAL)
C       THIS SECTION CAN BE OMITTED IF DESIRED. THIS CHECK CONSIDERABLY
C      OVERESTIMATES THE ERROR, ESPECIALLY IF THE FUNCTION IS DECREASING
C      IN MAGNITUDE.
      DP=DX(K-1)
      DK=DX(K)
      IERRXD=0
      IF(K .LT. 9) GO TO 7140
      DO 7138 J=1,JDIM
      XDC(J)=XI(K-1)*( -DK*Y(2,J,10,3)/((DK+DP)*DP)+(DK-DP)*Y(2,J,10,2)
     1 /(DK*DP)+DP*Y(2,J,10,1)/((DK+DP)*DK) )
C       XDC IS A CENTRAL DIFFERENCE AT THE (K-1) POINT. XDP IS THE BACK-
C      WARD DIFFERENCE USED AT (K-1)
      PCE(J)=XDC(J)-XDP(J)
      IF(DABS(PCE(J))-1.D-2-1.D-3*Y(2,15,J,1)**2) 7138,7138,7137
 7137 IF(DABS(PCE(J)/XDC(J)).GT. 5.D-2) IERRXD=J
 7138 CONTINUE
      IKERR(K-1) =IERRXD
 7140 DO 7141 J=1,JDIM
 7141 XDP(J)=A(2,J,10)
      IF(IERRXD .GT. 0) WRITE(3,476)(PCE(J),J=1#JDIM)
  476 FORMAT('  ERROR X DERIV. '  ,F12.7,2F11.6,2F10.5,5F9.4,2F8.3 )
      IF(IERRXD .GT. 0) WRITE(3,477)(XDC(J),J=1,JDIM)
  477 FORMAT(' VELOC. X DERIV. '  ,F12.7,2F11.6,2F10.5.5F9.4,2F8.3 )
C END  CHECK OF X DERIVATIVES     AFTER WRITE STATEMENTS
C
C  SECTION 15: B.L. THICKNESSES (OPTIONAL,SEE SECTIONS 2 AND 16)
C BEGIN CALCULATION OF THICKNESSES
C       THIS SECTION CAN BE OMITTED IF DESIRED. FOR GIVEN VALUES OF
C      FORWARD FLIGHT SPEED (SHT), AZIMUTHAL ANGLE (PSIT), (DOWNFLOW( VAT)
C      SPAN/CHORD (YP,FOUND FROM THE ASPECT RATIO,ART) AND FOR THE
C      CURRENT VALUE OF XI (XI(K) THE VALUE OF X (XP) IS CALCULATED. BY
C      INTERPOLATION, UAO (UAP), UCO(UCP),PER CENT CHORD(PCCP),AND
C      NL(RNUP) ARE FOUND AT XP. DISPLACEMNT AND MOMENTUM THICKNESS ARE
C      CALCULATED AND WRITTEN.
      IF( K .LT. 8 .OR. JDIM .LT. 10 .OR. NGT .EQ. 0) GO TO 5050
      DO  5040 NG=1,NGT
      T1     =SHT(NG)*DCOS(PSIT(NG)/57.29578DO)
      T2     =SHT(NG)*DSIN(PSIT(NG)/57.29578DO)
      VA2=VAT(NG)**2
      WRITE(3,5036) PSIT(NG),VAT(NG),SHT(NG),ART(NG)
```

```
 5036 FORMAT(/ ' AZIMUTH ANGLE=',F6.1,5X,'INDUCED VEL=',F9.6,5X,'SPEED R
     1ATIO=',F9.5,5X,'ASPECT RATIO=',F7.3 /
     2 ' SPAN/CHORD',4X,' X',4X,'  %CHORD  ',' X DISPMENT THK ',' Y DIS
     3PENT THK ','     X MOM THK    ','     Y MOM THK    ',
     4'     XI     ','     Q ' )
      DO 5040 IYP=1,4
      YP=(.3D0*IYP-.25D0*(IYP/4))*ART(NG)
      IF(YP+T2 .LT. 0) GO TO 5038
      QP=1.D0-VAT(NG)*RK10/YP-(RK20R+RK20*VA2+RK21*T1+RK22*T2*VAT(NG))/
     C(YP*YP)
      IF(QP .LT. .3D0 .OR. QP.GT. 2.D0) GO TO 5038
      XIIP=       CHI0+VAT(NG)*(CHI10+(VAT(NG)*CHI20+T2*CHI22)/YP)/YP
      XP=XI(K)/QP + XIIP
      CALL COEX(E,X(K),X(K-1),X(K-2),XP)
C       SUBROUTINE COEX JUST CALCULATES INTERPOLATION CONSTANTS FOR 3
C     POINT LANGRANGIAN INTERPOLATION.
      PCCP=0.D0
      UAP=0.D0
      UCP=0.D0
      RNUP=0.D0
      DO 5020 I=1,3
      PCCP=PCCP+ E(I)*PCC(K-I+1)
      UAP=UAP+E(I)*UAPK(K)
      UCP=UCP+E(I)*UCPK(K)
 5020 RNUP=RNUP+E(I)*RNUK(K)
      RNUP=RNUP+T1
      DVAR=     (XP-XIIP)/((YP+T2)*UAP+VAT(NG)*UCP)
      IF(DVAR) 4740,4740,4741
 4740 WRITE(3,4742) YP,XP,QP,UAP,UCP,DVAR
C       IF Q<.3 OR>2,THEN SERIES IN SPAN IS PROBABLY INACCURATE.
 4742 FORMAT(1X,2F10.6,'DVAR<0;YP+T2 TOO SMALL  QP=',F10.6,' UAP=',
     F F10.6,' UCP=',F10.6, ' DVAR=',D11.4  )
      GO TO 5040
 4741 DVAR=DSQRT(DVAR)
      CON0=1.D0/(UA0*YP*YP)
      CON1=VAT(NG)/YP
      CON2=(VAT(NG)**2)*CON0
      CON3=T1*CON0
      CON4=VAT(NG)*T2*CON0
      CON5=VAT(NG)*T1/YP
      DO 4750 L=1,LMAXU
      UP(L)=Y(2,1,L,1)+CON1*Y(2,4,L,1)+CON0*(Y(2,6,L,1)+RK20R*Y(2,5,L,1)
     1) +CON2*(Y(2,7,L,1)+RK20*Y(2,5,L,1))+ CON3*(Y(2,8,L,1)+RK21*
     2 Y(2,5,L,1))+ CON4*(Y(2,9,L,1)+RK22*Y(2,5,L,1))
      VP(L)=Y(2,2,L,1)+T1*Y(2,3,L,1)+CON1*Y(2,10,L,1)+CON5*Y(2,11,L,1)
     V +T2*Y(2,12,L,1)/YP
      UP(L)=UP(L)*UP(L)
 4750 VP(L)=VP(L)*VP(L)/RNUP
      L=LMAXU
      TK(3)=Y(1,1,L,1)+CON1*Y(1,4,L,1)+CON0*(Y(1,6,L,1)+RK20R*Y(1,5,L,1)
     1) +CON2*(Y(1,7,L,1)+RK20*Y(1,5,L,1))+CON3*(Y(1,8,L,1)+RK21*
     2 Y(1,5,L,1))+ CON4*(Y(1,9,L,1)+RK22*Y(1,5,L,1))
      TK(4)=Y(1,2,L,1)+T1*Y(1,3,L,1)+CON1*Y(1,10,L,1)+CON5*Y(1,11,L,1)
     V +T2*Y(1,12,L,1)/YP
      TK(1)=DVAR*(Z(LMAXU)-TK(3))
      TK(2)=DVAR*(Z(LMAXU)-TK(4)/RNUP)
      DO 4751 L=3,LMAXU,2
      TK(3)=TK(3)-DZ(L)*(UP(L-2)+4.D0*UP(L-1)+UP(L))/3.D0
      TK(4)=TK(4)-DZ(L)*(VP(L-2)+4.D0*VP(L-1)+VP(L))/3.D0
      LST=L+1
      IF(DZ(L+2) .NE. DZ(3)) GOTO 4755
 4751 CONTINUE
```

```
4755 CO 4756 L=LST,LMAXU
     TK(3)=TK(3)-CZ(L)*(UP(L)+UP(L-1))*.5DC
4756 TK(4)=TK(4)-CZ(L)*(VP(L)+VP(L-1))*.5DC
     TK(3)=DVAR*TK(3)
     TK(4)=TK(4)*CVAR/RNUP
     WRITE(3,5035) YP,XP,PCCP,(TK(I),I=1,4),XIIP,QP
5035 FCRMAT( 1X,3F10.6,4F16.1C,      2F1C.7 )
     GC TC 5040
5038 WRITE(3,5034) YP,T2,QP,PSIT(NG)
5034 FCRMAT( ' EITHER YP=',F10.6,' IS < T2=',F10.6,6X'OR QP=',F1C.6,
    F ' IS <.3 OR > 2. ',5X,'PSI=',F7.2/'%CHORD=',F6.2, 'SPEED RATIO=',
    3 F7.3/)
5040 CONTINUE
5050 CCNTINUE
C    END CALCULATICN CF THICKNESSES
C
C    SECTION 16: VELCCITY PROFILES(OPTICNAL,SEE SECTICNS 2 AND 15)
C       THIS SECTION CAN BE OMITTED IF DESIRED. VELCCITY PRCFILES ARE
C       FCUND AT A GIVEN PER CENT CHCRD (WHICH GIVES A VALUE OF X). THUS
C       XI MUST BE FCUND (XIP). SINCE FO',GOO',ETC ARE KNOWN ONLY AT THE
C       PCINTS XI(K),THEY MUST BE INTERPOLATED TO XIP.
C BEGIN CALCULATICN CF VELCCITY PRCFILES
     IF(NGVEL .EC. C .OR. JCIP .LT. 10 .OR. K .LT. 8) GC TQ 5C8C
     DC 5076 NG=1,NGVEL
     IF(PCCV(NG) .GT. 3.LO*PCC(K)) GO TO 5C76
     CALL COEX(E,PCC(K),PCC(K-1),PCC(K-2),PCCV(NG))
     XP=E(1)*X(K)+E(2)*X(K-1)+E(3)*X(K-2)
     T1=SHV(NG)*DCOS(PSIV(NG)/57.29578)
     T2=SHV(NG)*DSIN(PSIV(NG)/57.29578)
     VA =VAV(NC)
     VA2=VA*VA
     DC 5075 IYP=1,4
     YP=(.300*IYP-.25C0*(IYP/4))*ARV(NG)
     IF(ILIM(NG,IYP) .GT. 0 ) GO TO 5C75
     IF(YP+T2 .LT. 0) GO TO 5C73
     QP=1.DC-VA*RK10/YP-(RK20R+RK20*VA2+RK21*T1+RK22*VA*T2)/(YP*YP)
     IF(QP .LT. .300 .OR. QP .GT. 2) GO TO 5073
     XIIP=CHI0+VA*(CHI10+(VA*CHI2C+T2*CHI22)/YP)/YP
     XIP=QP*(XP-XIIP)
     IF(XIP .GT. XI(K) ) GC TC  5075
     ILIM(NG,IYP)=K
     CALL COEX(E,XI(K),XI(K-1),XI(K-2),XIP)
     DVAR=YP*YP*(E(1)*UAPK(K)+E(2)*UAPK(K-1)+E(3)*UAPK(K-2))
     DC 5070 L=1,LMAXU
     UP(L)=0.CO
     VP(L)=0.CC
     DC 5069 I=1,3
     UP(L)=UP(L)+E(I)*(  Y(2,1,L,I)+VA*Y(2,4,L,I)/YP+( Y(2,6,L,I)+
    1 RK20R*Y(2,5,L,I)+VA2*(Y(2,7,L,I)+RK2C*Y(2,5,L,I)) +T1*(Y(2,8,L,I)
    2 + RK21*Y(2,5,L,I))+VA*T2*(Y(2,9,L,I)+RK22*Y(2,5,L,I)) )/DVAR   )
5069 VP(L)=VP(L)+E(I)*(  Y(2,2,L,I)+T1*Y(2,3,L,I)+( VA*(Y(2,10,L,I)+
    1 T1*Y(2,11,L,I))+T2*Y(2,12,L,I) )/YP   )
5070 VP(L)=VP(L)/ARV(NG)
     IF(IYP.EC.1) GO TO 5060
     WRITE(3,5062) PSIV(NG),PCCV(NG),XP,SHV(NG),VAV(NG),ARV(NG)
5062 FCRMAT(//' AZIMUTH ANGLE=',F6.1,4X,'%CHORD=',F8.5,4X,'X=',F12.8,
    1 4X,'SPEEC RATIO=',F9.5,4X,'INDUCED VEL',F7.3,4X,'ASPECT RATIC',
    2F7.3 )
5060 WRITE(3,5059) YP
     WRITE(3,5064) (L,Z(L),UP(L),L=1,LMAXU)
5064 FCRMAT(     1X,I2,F7.3,F8.4,4X,I2,F7.3,F8.4,4X,I2,F7.3,F8.4,4X,I2,
    1 F7.3,F8.4,4X,I2,F7.3,F8.4 )
```

```
      WRITE(3,5065) QP,XIIP,XIP,DVAR
5065  FORMAT( ' QP=',D15.5,'XIIP,XIP,DVAR=',3D15.6 )
      WRITE(3,5066)
5066  FORMAT(/ 1X,5(' L      Z    V/R*OMEGA  ')  )
      WRITE(3,5064) (L,Z(L),VP(L),L=1,LMAXU)
      GO TO 5075
5073  WRITE(3,5034) YP,T2,QP,PSIV(NG),PCCV(NG),SHV(NG)
5075  CONTINUE
5059  FORMAT(/' VELOCITY PROFILES FOR SPAN/CHORD=',F8.5/1X,
     1 5(' L     Z    U/UDELTA     ' ))
5076  CONTINUE
5080  CONTINUE
C   END  CALCULATION OF VELOCITY PROFILES

C   SECTION 17: VALUES OF XIS AND K'S
      IF(JDIM-5) 566,567,566
C      FO"3WALL IS EXTRAPOLATED TO ZERO TO FIND XIS. THEN K10 IS THE
C     VALUE OF -F10C/F1K3WALL EXTRAPOLATED TO XIS.
 567  RK10TE =-Y(3,5,1,1)/Y(3,4,1,1)
      WRITE(3,489) RK10TE,Y(3,1,1,1)
 489  FORMAT('  -F10C"/F1K"3WALL= ' ,D20.12,10X,' FO"3WALL=',D20.10)
 566  CONTINUE
      IF(K .LT. 15) GO TO 568
      IF(JDIM-9) 568,569,568
 569  DO 570 J=6,9
 570  RKJ(J)=-Y(3,J,1,1)/Y(3,5,1,1)
C      RKJ(6)...RKJ(9) ARE EXTRAPOLATED TO XIS TO FIND K2CR,K20,K21,K22.
      WRITE(3,571) RKJ(6),RKJ(8),RKJ(7),RKJ(9)
 571  FORMAT(' -DVCZ3WALL/F2K" '  ,52X,D13.6,5X,D13.6 /80X,D13.6,5X,
     1 D13.6)
 568  CONTINUE

C   SECTION 18: UPDATE VELOCITIES
C      UPDATE VELOCITIES FOR NEW X STATION
C      THE VALUE OF K WILL BE INCREMENTED SOON. SINCE I=1 DENOTES THE
C     CURRENT VALUE OF K, Y(M,J,L,I) MUST BE UPDATED. THESE DO LOOPS
C     SET Y(M,J,L,IMAX)=Y(M,J,L,IMAX-1)...Y(M,J,L,2)=Y(M,J,L,1). AFTER
C     K IS INCREMENTED (BY DO 30 K=1,KMAX) Y(M,J,L,1) BECOMES THE
C     VARIABLE TO BE SOLVED FOR.
      DO 1429 IT=1,3
      DO 1429 L=1,LMAXU
      DO 1429 J=1,JDIM
      DO 1429 M=1,3
1429  Y(M,J,L,5-IT) =Y(M,J,L,4-IT)
C   END  UPDATE VELOCITIES FOR NEW X STATION
8723  CONTINUE
      WRITE(3,872) K,PCC(K)
 872  FORMAT('  END OF K=',I5,10X,' PER CENT CHORD AT INFINITE SPAN=',
     F F12.8,'%'///)
      GO TO 30

C   SECTION 19: DIAGNOSTIC WRITE STMTS AND TERMINATION
C      THESE WRITE STMTS GIVE SOME INFORMATION ON WHY THE PGM STOPPED.
1405  IF(X(K) .LT. XIINT.AND.X(K)*X(K-1).LT.0.D0)WRITE(3,480) X(K)
 480  FORMAT(/' AT STMT 3314 X(K)  (=',D20.12,')  IS < XIINT'/' CHANGE
     1DXI(K)      ' /)
      IF(LMAX .GT. LMAXU) WRITE(3,7040) LMAX
7040  FORMAT(/' AT STMT 552, LMAXU<LMAX, WHICH=',I5 )
      IF(ITER .GE. ITERM) WRITE(3,7041)J,LMAX,ITER,(Y(2,J,L,1),L=1,LMAX)
7041  FORMAT(/' SUCCESSIVE REPLACEMENTS DIVERGE FOR J=',I3/' LMAX=',
     1 I3/' ITER=',I4//' Y(2,J,L,1)='/( 1X,10D13.5))
      IF(ITER .GE. ITERM .AND. K .GT. 15 .AND. Y(3,1,1,1) .LT. .09D0)
```

```
      WRITE(3,7044) Y(3,1,1,1),XI(K)
 7044 FORMAT(/' FO" AT Z=0 IS',D15.7,'; LEW'S METHOD WILL NOT CONVERGE
     1FOR FO" < .03 OR .04' // ' IF THE CURRENT VALUE OF XI (',D15.7,
     2') SEEMS LIKELY TO GIVE FO" TOO SMALL, THIS IS PROBABLY A NORMAL
     3TERMINATION ' )
C     THE FINAL VALUE OF XI SHOULD BE CHOSEN (BY TRIAL AND ERROR) TC
C     GIVE FO" BETWEEN .06 AND .04
      IF(X(K)*X(K-1) .EQ. 0.D0) WRITE(3,7042) X(K)
 7042 FORMAT(/' AT STMT 3314 X(K)=',D20.10/ ' CHANGE DXI(K) ' /)
      KM=K-2
      DO 7051 I=9,KM
 7051 IF(IKERR(I).GT.0 .AND. KM  .GT.9) WRITE(3,7052) I,IKERR(I)
 7052 FORMAT(' X DERIVATIVES MAY BE INACCURATE AT K=',I3,'  FOR J=',I3)
 9996 WRITE(3,7043) K
 7043 FORMAT(/' EXIT CALLED AT STMT 1405 FOR K=',I5)
      IF(J .EQ. 1) CALL EXIT
      JDIM=J-1
      IF( ITER .EQ. ITERM ) GO TO 1401
      CALL EXIT
   30 CONTINUE
C END     K LOOP IN XI
      WRITE(3,7055)
 7055 FORMAT( '   PGM STOPS BECAUSE KMAX IS TOO SMALL ' )
      CALL EXIT
      END


      SUBROUTINE COEX(E,A,B,C,D)
      IMPLICIT REAL*8 (A-H,O-Z)
C     COEX PROVIDES COEFFICIENTS FOR 3 POINT LANGRANGIAN INTERPOLATION.
C     IT IS USED IN SECTIONS 15 AND 16.
      DIMENSION E(3)
      E(1)=(D-B)*(D-C)/( (A-B)*(A-C) )
      E(2)=(D-A)*(D-C)/( (B-A)*(B-C) )
      E(3)=(D-A)*(D-B)/( (C-A)*(C-B) )
C     F(D)=E(1)*F(A)+E(2)*F(B)+E(3)*F(C), WHERE F IS SOME FUNCTION
      RETURN
      END


      REAL FUNCTION DSDX*8(DUMMY,DE)
      IMPLICIT REAL*8 (A-H,O-Z)
C     DSDX CALCULATES THE VALUES OF B1....B1C NEEDED TO FIND THE
C     POTENTIAL FLOW AND TO RELATE X AND SIGMA.
      COMMON/BIJ/EPS,SGN,B1,B2,B3,B4,B5,B6,B7,B8,B9,B10
      IF(SGN) 85,85,75
   85 IF(DUMMY) 75,75,74
   74 SGN=1.D0
      WRITE(3,401) DE,SGN,SGN,DUMMY
   75 S=DE-1.D0
      OMS2=DE*(1.D0-S)
      IF(DABS(OMS2) .LT. 1.D-50)   WRITE(3,401) DE,SGN,OMS2,DUMMY
      IF(DABS(OMS2) .LT. 1.D-50) OMS2=1.D-50
      BA=(1.D0-EPS)**2
      BB=1.D0-EPS*EPS
      BC=1.D0+EPS
```

```
      B1=1.DO+EPS*EPS-2.DO*EPS*S
      B2=BC*(1.DO+BA*BB/(B1*B1))/4.DO
      B3=SGN*BC*(-S*(1.DO-BA/B1)-OMS2*2.DO*EPS*BA/B1**2)/(4.DO*
     3 DSQRT(OMS2))
      IF( DABS(DUMMY*SGN-13.CO)  .GT. 1.D-4) GO TO 18
      BD=EPS*BC*BA/(2.CO*B1*DSQRT(OMS2))
      B4=BC*BA*BB*EPS/B1**3
      BE=B1*B1
      B5=SGN*BD*(-1.CO/(BA*BE)+2.DO*S/B1-4.DO*EPS*OMS2/BE)
      B6=6.DO*EPS*B4/B1
      B8=8.DO*EPS*B6/B1
      BG=2.DO*EPS/B1+S/OMS2
      BF=1.DO/(BE*BE*BA)+2.CO/B1+12. *EPS*S/BE-16.DC*EPS*EPS*OMS2/B1**3
      B7=B5*BG+SGN*BC*BF
      B9=BG*B7+(4.CO*EPS*EPS/BE+(1.CO+2.*S*S/OMS2)/OMS2)*B5+SGN*BD*BF*BG
     9 +SGN*BD*(-2.DO/(BA*BE**3)+16.DO*EPS/BE+80.DO*EPS*EPS*S/(BE*B1)
     9 -96.DO*(EPS**3)*OMS2/(BE*BE) )
  401 FCRMAT(     ' B2,B3,DE,SGN,OMS2,CUMMY   ',6D16.7   )
   18 B10=DSQRT(B2*B2+B3*B3)*SGN
      IF(DABS(DUMMY).LT.1.D-6)WRITE(3,401)B2,B3,DE,SGN,OMS2,DUMMY
      DSDX=1.DO/B10
      RETURN
      END
```

```
                                   CATA CARDS
                    SAMPLE CATA CARCS FCR ALPHB = .CO5
.25        0.005      -.000016128455600C7  .44C       7.18              EXTRASTAFF
.795       -55.05     .423       -7.19                          RK2 FCR .005 DEG
  10
5.625      90.        0.         20.        10.        .CC5
5.625      90.        0.         2C.        30.        .CC5
5.625      270.       0.         20.        10.        .CC5
5.625      270.       0.         20.        30.        .CO5
2.812      90.        0.         20.        30.        .CO5
1.406      90.        0.         20.        30.        .CC5
5.625      45.        0.         20.        30.        .CC5
5.625      135.       0.         20.        30.        .CO5
5.625      225.       0.         20.        30.        .CC5
5.625      315.       0.         20.        30.        .CC5
  7
5.625      90.        0.         2C.                   .CO5
2.812      90.        0.         20.                   .CC5
1.406      90.        0.         20.                   .CC5
5.625      45.        0.         20.                   .CC5
5.625      135.       0.         20.                   .CO5
5.625      225.       0.         20.                   .CC5
5.625      315.       0.         2C.                   .CC5
                    SAMPLE DATA CARDS FOR ALPHB = 2.
 0.250000 2.0000000 -0.0059944141423240 .323           10.4             EXTRASTAFF
.485       -122.4     .596       -10.46                         RK2 FOR 2 DEG
                    SAMPLE CATA CARCS FOR ALPHB = 3.349
 0.250000 3.3490000 -0.01036290782202279 .244          15.01            EXTRASTAFF
.329       -252.6     .703       -15.C5                6K
  1
3.1226     90.        .07650     13.71      10.        6K
  1
3.1226     90.        .07650     13.71                 6K
```

```
                 SAMPLE DATA CARDS FOR ALPHB = 4.
 0.250000 4.0000000 -0.0126237115182189 .201      18.8                   EXTRASTAFF
.246      -368.7    .728      -18.82                           RK2 FOR 4 DEG
   1
[illegible].625     90.       .2117     20.       10.       4 DEG
   0
                 SAMPLE DATA CARDS FOR ALPHB = 4.465
.25       4.465    -.01431093492            .170      22.15                 EXTRASTAFF
.178      -447.5    .709      -22.15                           RK2 FOR 4.465 DEG
  10
3.1226    90.       .10198    13.71     10.       8K
3.1226    90.       .10198    13.71     12.       8K
3.1226    270.      .10198    13.71     10.       8K
3.1226    270.      .10198    13.71     12.       8K
1.5613    90.       .10198    13.71     10.       8K
.7807     90.       .10198    13.71     10.       8K
3.1226    45.       .10198    13.71     10.       8K
3.1226    135.      .10198    13.71     10.       8K
3.1226    225.      .10198    13.71     10.       8K
3.1226    315.      .10198    13.71     10.       8K
   7
3.1226    90.       .10198    13.71               8K
1.5613    90.       .10198    13.71               8K
.7807     90.       .10198    13.71               8K
3.1226    45.       .10198    13.71               8K
3.1226    135.      .10198    13.71               8K
3.1226    225.      .10198    13.71               8K
3.1226    315.      .10198    13.71               8K
                 SAMPLE DATA CARDS FOR ALPHB = 5.581
 0.250000 5.5810000 -0.0186346963551100 .106      24.22                  EXTRASTAFF
.048      -86.      .450      -24.13              RK2 FOR 5.581 DEG.
   1
3.1226    90.       .12743    13.71     10.       10K
   1
3.1226    90.       .12743    13.71               10K
```

Unclassified

Security Classification

DOCUMENT CONTROL DATA - R & D

(Security classification of title, body of abstract and indexing annotation must be entered when the overall report is classified)

1. ORIGINATING ACTIVITY (Corporate author) Department of Mechanical and Aerospace Engineering North Carolina State University Raleight, North Carolina	2a. REPORT SECURITY CLASSIFICATION Unclassified 2b. GROUP
3. REPORT TITLE THE LAMINAR BOUNDARY LAYER ON A ROTATING BLADE OF SYMMETRICAL AIRFOIL SHAPE	
4. DESCRIPTIVE NOTES (Type of report and inclusive dates) Final Report	
5. AUTHOR(S) (First name, middle initial, last name) James C. Williams, III Warren H. Young, Jr.	

6. REPORT DATE December 1970	7a. TOTAL NO. OF PAGES 155	7b. NO. OF REFS 20
8a. CONTRACT OR GRANT NO. DAAJ02-69-C-0086 b. PROJECT NO. c. Task 1F162204A13903 d.	9a. ORIGINATOR'S REPORT NUMBER(S) USAAVLABS Technical Report 70-64 9b. OTHER REPORT NO(S) (Any other numbers that may be assigned this report)	

10. DISTRIBUTION STATEMENT

This document is subject to special export controls, and each transmittal to foreign governments or foreign nationals may be made only with prior approval of Eustis Directorate, U. S. Army Air Mobility R&D Laboratory, Fort Eustis, VA 23604.

11. SUPPLEMENTARY NOTES	12. SPONSORING MILITARY ACTIVITY Eustis Directorate U.S. Army Air Mobility R&D Laboratory Fort Eustis, Virginia

13. ABSTRACT

A theoretical study has been conducted to determine the effects of rotation, inflow, and forward flight on the development of the laminar boundary layer on a helicopter blade. Particular emphasis was placed on the determination of the separation line. In order to facilitate the computation of the inviscid flow about the blade, an 11.9%-thick symmetrical Joukowski airfoil was used. The essential feature of the analysis was the scaling of the chordwise coordinate so that the separation line is invariant with span and time in the transformed coordinate system. The transformed boundary layer equations were expanded in an asymptotic series in span, and the resulting equations were solved ~~by the method of Smith and Clutter.~~

The major effect of rotation is a delay in separation. The separation line delay is most pronounced near the axis of rotation. Forward flight causes an oscillation about this separation line, so that the delay is greatest in the first and fourth quadrants. The oscillations are affected by the blade angle of attack and the inflow due to lift. The phase advance between the wall shear and the free-stream velocity is in qualitative agreement with the results of Lighthill.

Rotation alone does not influence the separation line greatly. However, its combination with forward flight and inflow contribute, at least in part, to the increase in maximum lift observed on helicopter blades.

DD FORM 1 NOV 65 1473 REPLACES DD FORM 1473, 1 JAN 64, WHICH IS OBSOLETE FOR ARMY USE.

Unclassified

Security Classification

Unclassified

Security Classification

14. KEY WORDS	LINK A ROLE	LINK A WT	LINK B ROLE	LINK B WT	LINK C ROLE	LINK C WT
Helicopter rotors						
Helicopter blades						
Boundary layer						

Unclassified

Security Classification

10440-70